

**Investigation on the biosynthesis of polyketides in  
two *Penicillium* strains**

**Untersuchung zur Biosynthese von Polyketiden in  
zwei *Penicillium*-Stämmen**

Dissertation

zur Erlangung des Doktorgrades  
der Naturwissenschaften  
(Dr. rer. nat.)

dem Fachbereich Pharmazie  
der Philipps-Universität Marburg

vorgelegt von

**Pan Xiang**

aus Taoyuan, China

Marburg/Lahn **2022**

Erstgutachter: **Prof. Dr. Shu-Ming Li**

Zweitgutachter: **Prof. Dr. Michael Keusgen**

Eingereicht am **14. Oktober 2022**

Tag der mündlichen Prüfung am **25. November 2022**

Hochschulkennziffer: 1180

**Dedicated to my family**





## TABLE OF CONTENTS

---

### Table of contents

List of publications .....	III
Abbreviations .....	VII
Summary .....	1
Zusammenfassung .....	3
1 Introduction .....	5
1.1 Filamentous fungi as sources of natural products .....	5
1.2 The fungal genus <i>Penicillium</i> .....	8
1.2.1 <i>Penicillium crustosum</i> and its secondary metabolites.....	8
1.2.2 <i>Penicillium roqueforti</i> and its secondary metabolites .....	9
1.3 Biosynthesis of natural products in fungi.....	10
1.3.1 Genome mining for fungal natural product discovery.....	11
1.3.2 Heterologous expression .....	13
1.3.2.1 Hosts for heterologous gene expression.....	14
1.3.2.2 Promoters for heterologous gene expression.....	16
1.4 Polyketide synthases.....	17
1.4.1 Type I polyketide synthases .....	18
1.4.2 Type II polyketide synthases .....	21
1.4.3 Type III polyketide synthases .....	21
1.5 Tailoring enzymes .....	22
2 Aims of this thesis .....	25
3 Results and discussion.....	29
3.1 Formation of isocoumarin by heterologous gene expression and modifications by host enzymes .....	29
3.2 Formation of 3-orsellinoxipropanoic acid in <i>Penicillium crustosum</i> .....	32
3.3 Biosynthesis of annullatin D in <i>Penicillium roqueforti</i> requires a BBE-like enzyme for the five-member lactone ring formation .....	37
4 Publications.....	43
4.1 Isocoumarin formation by heterologous gene expression and modification by host enzymes .....	43

## TABLE OF CONTENTS

---

4.2 Formation of 3-orsellinoxypyranoic acid in <i>Penicillium crustosum</i> is catalyzed by a bifunctional nonreducing polyketide synthase .....	59
4.3 Biosynthesis of annullatin D in <i>Penicillium roqueforti</i> implies oxidative lactonization between two hydroxyl groups catalyzed by a BBE-like enzyme .....	91
5 Conclusions and future prospects .....	171
6 References .....	173
Statutory Declaration.....	189
Acknowledgements .....	191
Curriculum Vitae .....	193

**List of publications**

1. **Pan Xiang**, Lena Ludwig-Radtke, Wen-Bing Yin, and Shu-Ming Li (2020). Isocoumarin formation by heterologous gene expression and modification by host enzymes. *Organic and Biomolecular Chemistry*, 18, 4946–4948, DOI: 10.1039/D0OB00989J.
2. **Pan Xiang** and Shu-Ming Li (2022). Formation of 3-orsellinoxipropanoic acid in *Penicillium crustosum* is catalyzed by a bifunctional nonreducing polyketide synthase. *Organic Letters*, 24 (1), 462–466, DOI: 10.1021/acs.orglett.1c04189.
3. **Pan Xiang**,\* Bastian Kemmerich,\* Li Yang, and Shu-Ming Li (2022). Biosynthesis of annullatin D in *Penicillium roqueforti* implies oxidative lactonization between two hydroxyl groups catalyzed by a BBE-like enzyme. *Organic Letters*, 24 (32), 6072–6077, DOI: 10.1021/acs.orglett.2c02438. (\*equal contribution)



## Erklärung zum Eigenanteil

Titel der Publikation und <b>Journal incl. Jahr, Heft, Seitzahl + doi</b>	Autoren	geschätzter Eigenanteil in %	<u>Bitte</u> <u>angeben:</u> angenommen /eingereicht
<b>O: Originalarbeit</b> <b>Ü: Übersichtartikel/Review</b>  Isocoumarin formation by heterologous gene expression and modification by host enzymes. <a href="#">Organic and Biomolecular Chemistry, 2020, 18, 4946–4948</a> <a href="#">DOI: 10.1039/D0OB00989J</a> <b>Originalarbeit</b>	<b>Pan Xiang</b> , Lena Ludwig-Radtke, Wen-Bing Yin, and Shu-Ming Li	65	angenommen
Formation of 3-orsellinoxypropanoic acid in <i>Penicillium crustosum</i> is catalyzed by a bifunctional nonreducing polyketide synthase. <a href="#">Organic Letters, 2022, 24 (1), 462–466</a> <a href="#">DOI: 10.1021/acs.orglett.1c04189</a> <b>Originalarbeit</b>	<b>Pan Xiang</b> and Shu-Ming Li	75	angenommen
Biosynthesis of annullatin D in <i>Penicillium roqueforti</i> implies oxidative lactonization between two hydroxyl groups catalyzed by a BBE-like enzyme. <a href="#">Organic Letters, 2022, 24 (32), 6072–6077</a> <a href="#">DOI: 10.1021/acs.orglett.2c02438</a> <b>Originalarbeit</b>	<b>Pan Xiang</b> ,* Bastian Kemmerich,* Li Yang, and Shu-Ming Li	35	angenommen

\*: These authors contributed equally to this work.

-----  
**Kandidat(in)**

-----  
**Unterschrift Betreuer(in)**



## Abbreviations

The international system of units and units derived thereof have been used.

[M+H] <sup>+</sup>	molecular ion plus proton
[M-H] <sup>-</sup>	molecular ion minus proton
[M+Na] <sup>+</sup>	molecular ion plus sodium
× <i>g</i>	gravitational acceleration
2-OG	2-oxoglutarate
6-MSA	6-methylsalicylic acid
aa	amino acid
A domain	adenylation domain
ACP domain	acyl carrier protein domain
<i>anu</i> cluster	<u>ann</u> ullatin cluster
AT domain	acyltransferase domain
<i>A. fumigatus</i>	<i>Aspergillus fumigatus</i>
<i>A. glaucus</i>	<i>Aspergillus glaucus</i>
<i>A. nidulans</i>	<i>Aspergillus nidulans</i>
<i>A. niger</i>	<i>Aspergillus niger</i>
<i>A. oryzae</i>	<i>Aspergillus oryzae</i>
<i>A. ruber</i>	<i>Aspergillus ruber</i>
<i>A. terreus</i>	<i>Aspergillus terreus</i>
bp	base pair
br	broad (NMR signal)
BGC	biosynthetic gene cluster
C domain	condensation domain
CD <sub>3</sub> OD	deuterated methanol
CDCl <sub>3</sub>	deuterated chloroform
CDP	cyclic dipeptide
cDNA	copy deoxyribonucleic acid
CoA	coenzyme A
COSY	correlation spectroscopy
d	doublet
D <sub>2</sub> O	deuterium oxide

## ABBREVIATIONS

---

Da	dalton
dd	double doublet
DEBS	6-deoxyerythronolide B synthase
DH domain	dehydratase domain
DMA	dimethylallyl
DMAPP	dimethylallyl diphosphate
DMATS	dimethylallyltryptophan synthase
DMSO- <i>d</i> <sub>6</sub>	deuterated dimethyl sulfoxide
DNA	deoxyribonucleic acid
dt	double triplet
DTT	dithiothreitol
<i>E. coli</i>	<i>Escherichia coli</i>
E domain	epimerization domain
<i>e.g.</i>	exempli gratia
EIC	extracted ion chromatogram
ER domain	enoyl reductase domain
ESI	electrospray ionization
EtOAc	ethyl acetate
FAD	flavin adenine dinucleotide
<i>fog</i> cluster	<u>flavogl</u> aucin cluster
FPP	farnesyl diphosphate
gDNA	genomic deoxyribonucleic acid
GGPP	geranylgeranyl diphosphate
GMM	glucose minimal medium
GPP	geranyl diphosphate
HE	heterologous expression
His <sub>6</sub>	hexahistidine
HMBC	heteronuclear multiple bond correlation
HPLC	high performance liquid chromatography
HR-MS	high resolution-mass spectrometry
HRPKS	highly reducing polyketide synthase
HSQC	heteronuclear single quantum coherence



## ABBREVIATIONS

---

Hz	hertz
<i>i.e.</i>	id est
IPP	isopentenyl diphosphate
<i>J</i>	coupling constant
kbp	kilo base pairs
$k_{cat}$	turnover number
kDa	kilodalton
$K_M$	Michaelis-Menten constant
KR domain	ketoreductase domain
KS domain	ketosynthase domain
LCMS	liquid chromatography mass spectrometry
m	multiplet
$m/z$	mass-to-charge ratio
mAU	milliabsorbance unit
Mbp	mega base pairs
MeOH	methanol
MeT domain	methyltransferase domain
MHz	mega hertz
mRNA	messenger ribonucleic acid
MS	mass spectroscopy
multi	multiplicity
NADH	nicotinamide adenine dinucleotide (reduced form)
NADPH	nicotinamide adenine dinucleotide phosphate (reduced form)
NMR	nuclear magnetic resonance
NP	natural product
NRPKS	nonreducing polyketide synthase
NRPS	nonribosomal peptide synthetase
OSMAC	one strain many compounds
P450	cytochrome P450
<i>P. camemberti</i>	<i>Penicillium camemberti</i>
<i>P. crustosum</i>	<i>Penicillium crustosum</i>
<i>P. roqueforti</i>	<i>Penicillium roqueforti</i>

## ABBREVIATIONS

---

<i>P. rubens</i>	<i>Penicillium rubens</i>
PCP domain	peptidyl carrier protein domain
PCR	polymerase chain reaction
PD	potato dextrose
PDB	potato dextrose broth
PEG	polyethylene glycol
PKS	polyketide synthase
PKS-NRPS	polyketide synthase-nonribosomal peptide synthetase
PPi	pyrophosphate
ppm	parts per million
PRPKS	partially reducing polyketide synthase
PT	prenyltransferase
PT domain	product template domain
q	quartet
R domain	reductase domain
RNA	ribonucleic acid
rpm	revolutions per minute
s	singlet
SAM	S-adenosyl-L-methionine
SAT domain	starter unit acyltransferase domain
<i>S. cerevisiae</i>	<i>Saccharomyces cerevisiae</i>
SDS-PAGE	sodium dodecyl sulfate polyacrylamide gel electrophoresis
SM	secondary metabolite
t	triplet
TC	terpene cyclase
T domain	thiolation domain
TB	terrific broth
td	triple doublet
TE domain	thioesterase domain
Tris	tris(hydroxymethyl)aminomethane
UV	ultraviolet
v/v	volume per volume

## ABBREVIATIONS

---

$w/v$	weight per volume
WT	wild-type
$\delta_C$	chemical shift of $^{13}\text{C}$
$\delta_H$	chemical shift of $^1\text{H}$



## Summary

Secondary metabolites, a special class of natural products, generally display significant biological activities in organisms, especially those from plants, bacteria, and fungi. For example, diverse natural products with remarkable structures have been found in fungi. Most of these compounds can be further categorized into four main classes based on their biosynthetic origins: polyketides, peptides, alkaloids, and terpenoids. Polyketide natural products have revolutionized medicine and drastically improved our lives by providing such important active substances as drugs to fight cancer, pathogens, and autoimmune diseases. Advances in sequencing technologies and bioinformatic analysis have facilitated the elucidation of the biosynthesis of these natural products. Their structural divergence begins with the formation of the initial skeletons by different backbone enzymes using fundamental metabolic building blocks derived from primary metabolism. For example, the carbon backbone for polyketides is derived from acyl-CoA and constructed by the core enzymes polyketide synthases (PKSs), which belong to one of the most studied enzyme classes in the last decades. The fungal aromatic polyketides are mainly synthesized by nonreducing polyketide synthases (NRPKSs), in which no reduction is employed during the elongation of the polyketide chain. Subsequent modifications of the backbone structures are catalyzed by tailoring enzymes, such as transferases and oxidoreductases, to form diverse and complex pathway products.

In this thesis, two NRPKS genes were identified in *Penicillium crustosum* and functionally confirmed by heterologous expression, domain deletion and recombination, as well as by feeding experiments. Expression of the NRPKS gene *pcr9304* in the established and frequently used host *Aspergillus nidulans* led to the accumulation of three isocoumarins, proving its function as an isocoumarin synthase. Precursor feeding experiments revealed that the endogenous enzymes from *A. nidulans* can modify the initial PKS product by hydroxylation and methylation. These results provided one additional example that unexpected further modifications can take place in a heterologous host. Heterologous expression of another NRPKS gene, *oesA* from *P. crustosum*, led to the identification of 3-orsellinoxipropanoic acid. Domain deletion and recombination demonstrated that OesA with a domain structure of SAT-KS-AT-PT-ACP1-ACP2-TE catalyzed not only the formation of orsellinic acid, but also its transfer to 3-hydroxypropanoic acid, proving its role as a bifunctional enzyme, *i.e.* orsellinic acid synthase and transferase. Both ACP domains contribute independently and complementarily to the product formation. Isotopic labelling experiments proved that only the orsellinyl residue of 3-orsellinoxipropanoic acid is derived from acetate.

In cooperation with Bastian Kemmerich, the biosynthetic pathway of annulatins in *Penicillium roqueforti* was elucidated. An eleven-gene *anu* cluster was identified in *P. roqueforti* by genome mining. The involvement of the *anu* cluster in the biosynthesis of annulatin D with a fused dihydrobenzofuran lactone ring system and its derivatives was confirmed by heterologous expression of the whole cluster in *A. nidulans*. A combinational approach of *in vitro* enzymatic studies and heterologous expression

## SUMMARY

---

was used to understand the formation of the five-member lactone ring in annullatin D. The aromatic backbone is assembled by a cooperation of the highly reducing polyketide synthase AnuA, together with two additional enzymes AnuBC. Then, the polyketide core structure is consecutively modified by hydroxylation at the C<sub>5</sub> alkyl chain with the cytochrome P450 AnuE. The prenyltransferase AnuH subsequently installs one isoprenyl group at the benzene ring. Afterward, enzymatic or non-enzymatic dihydrobenzofuran ring formation between the prenyl and the phenolic hydroxyl groups in the prenylated product results in two diastereomers. Among them, the (2*S*, 9*S*)-configured isomer is converted to annullatin D by the BBE-like enzyme AnuG for the five-member lactone ring formation. The (2*R*, 9*S*)-isomer is likely very instable and immediately oxidized by the short-chain dehydrogenase/reductase AnuF to annullatin F. This study demonstrated a highly programmed and efficient biosynthetic pathway for annullatins. Despite the intriguing structural features and biological activities, biosynthetic studies on annullatins, especially on the formation of the lactone ring in annullatin D have not been reported prior to our study. Furthermore, we identified a new BBE-like enzyme for oxidative lactonization between two hydroxyl groups.

### Zusammenfassung

Sekundärmetabolite, eine spezielle Gruppe von Naturstoffen, besitzen wichtige biologische Aktivitäten in Organismen, besonders jene aus Pflanzen, Bakterien und Pilzen. Bisher wurden verschiedenste Naturstoffe mit außergewöhnlichen Strukturen aus Pilzen isoliert. Diese meisten dieser Substanzen können anhand ihrer biosynthetischen Herkunft in vier Hauptklassen unterteilt werden: Polyketide, Peptide, Alkaloide und Terpenoide. Polyketide haben nicht nur die Medizin revolutioniert, sondern auch unser Leben drastisch verbessert, da aus dieser Klasse wichtige Arzneistoffe gegen Krebs, pathogene Organismen und Autoimmunerkrankungen hervorgingen. Fortschritte bei Sequenzierungstechnologien und der Bioinformatik haben die Aufklärung von Biosynthesewegen in Pilzen ermöglicht. Die strukturelle Vielfalt der Naturstoffe beginnt mit der Bildung der jeweiligen Grundgerüste, die durch verschiedene sogenannte Backbone-Enzyme unter Verwendung von Bausteinen aus dem Primärmetabolismus hergestellt werden. Das Kohlenstoff-Grundgerüst der Polyketide wird beispielsweise von Polyketid-Synthasen (PKSs) aus Acetyl-Coenzym A aufgebaut. Bei der Biosynthese der Grundgerüste folgen PKSs einer einfachen Abfolge und stellen eine der am meisten untersuchten Enzymklassen der letzten Jahrzehnte dar. Pilzliche aromatische Polyketide werden hauptsächlich von nicht-reduzierenden Polyketid-Synthasen (NRPKSs) gebildet, die keine reduktiven Domänen besitzen. Nachfolgende Veränderungen der Grundstrukturen werden von modifizierenden Enzymen, z.B. Transferasen oder Oxidoreduktasen katalysiert, was zu stark unterschiedlichen und komplexen Endprodukten führt.

In der vorliegenden Arbeit wurden zwei NRPKS-Gene aus *Penicillium crustosum* identifiziert und deren Funktion mittels heterologer Expression, Deletion, Austausch von Domänen in Enzymen und Fütterungsversuche aufgeklärt. Expression des NRPKS-Gens *pcr9304* in dem etablierten und häufig verwendeten Stamm *Aspergillus nidulans* führte zur Produktion von drei Isocumarin-Analoga, welches dessen Funktion als Isocumarin-Synthase bewies. Durch Zufütterung von Vorstufen konnte nachgewiesen werden, dass endogene Enzyme aus *A. nidulans* das PK-Grundgerüst weiter mittels Hydroxylierung und Methylierung modifizieren. Diese Beobachtungen bestätigten, dass unvorhergesehene Modifikationen durch den heterologen Expressionsstamm auftreten können.

Heterologe Expression des zweiten NRPKS-Gens *oesA* aus *P. crustosum* führte zur Identifizierung von 3-Orsellinoxypfansäure. Deletion und Rekombination von Domänen bestätigten, dass OesA, mit einer SAT-KS-AT-ACP1-ACP2-TE Domänenstruktur, nicht nur die Entstehung von Orsellinsäure, sondern auch den Transfer der 3-Hydroxypropansäure katalysiert. Dies bewies dessen Rolle als ein bi-funktionelles Enzym, nämlich als Orsellinsäure-Synthase und -Transferase. Beide ACP-Domänen tragen unabhängig voneinander und komplementär zur Produktsynthese bei. Durch Isotopenmarkierung konnte bewiesen werden, dass nur der Orsellinyl-Rest der 3-Orsellinoxypfansäure aus Acetat stammt.

## ZUSAMMENFASSUNG

---

In Kooperation mit Bastian Kemmerich wurde die Biosynthese der Annullatine in *Penicillium roqueforti* aufgeklärt. Das *anu* Cluster mit elf Genen wurde durch genome mining in *P. roqueforti* identifiziert. Die Beteiligung des *anu* Clusters an der Biosynthese von Annullatin D, welches ein Dihydrobenzofuran-Lacton Grundgerüst besitzt, sowie dessen Derivaten wurde durch heterologe Expression des kompletten Clusters in *A. nidulans* bestätigt. Eine Kombination aus enzymatischen Untersuchungen *in vitro* und heterologer Expression wurde durchgeführt, um die Entstehung des fünfgliedrigen Lactonrings in Annullatin D aufzuklären. Das aromatische Grundgerüst wird durch die vollständig reduzierende Polyketid-Synthase AnuA unter Beteiligung von zwei weiteren Enzymen, AnuBC, gebildet. Danach wird das Polyketid durch das Cytochrom P450 AnuE an der C<sub>5</sub>-Alkylkette hydroxyliert. Die Prenyltransferase AnuH installiert anschließend eine Isoprenyl-Gruppe am Benzolring. Enzymatischer oder nicht-enzymatischer Dihydrobenzofuran-Ringschluss zwischen der Prenyl- und der phenolischen Hydroxylgruppe führt zu zwei Diastereomeren. Das (2*S*, 9*S*)-Isomer wird im Anschluss daran durch das BBE-ähnliche Enzym AnuG zu Annullatin D umgewandelt, welches den Ringschluss des fünfgliedrigen Lactonrings katalysiert. Das (2*R*, 9*S*)-Isomer ist höchstwahrscheinlich instabil und wird vermutlich direkt durch die kurzkettige Dehydrogenase/Reduktase AnuF zu Annullatin F oxidiert. Diese Arbeit zeigt somit einen hoch effizienten und programmierten Biosyntheseweg für die Annullatine. Trotz der faszinierenden Strukturen und den biologischen Aktivitäten wurden bisher keine biosynthetischen Studien zu Annullatinen, vor allem im Hinblick auf die Entstehung des Lactonrings des Annullatin D, berichtet. Darüber hinaus wurde ein neues, BBE-ähnliches Enzym identifiziert, welches die oxidative Lactonbildung zwischen zwei Hydroxylgruppen katalysiert.



## 1 Introduction

### 1.1 Filamentous fungi as sources of natural products

Secondary metabolites (SMs), or natural products (NPs), refer to specialized low-molecule-weight compounds derived from a natural source. NPs have been evolutionarily crafted over millions of years to possess merits of structural diversity, steric complexity, multiple chiral centers and modes of action. Some of the NPs have been served as excellent drugs/drug leads, or molecular probes to influence processes across the biomedical spectrum, especially in the therapeutic treatment of infectious diseases and cancers.<sup>1-4</sup> Infectious diseases like COVID-19 have suddenly spread all over the world since 2020, which caused huge economic losses and even millions of deaths. Discovering potential effective drugs is an important solution for humans to fight against the virus.

Plants, insects, and microorganisms including ascomycetes and actinobacteria are major sources of biologically active NPs.<sup>5-7</sup> Among them, filamentous fungi are prolific producers of diverse NPs. Fungi are widely spread in nature and are capable of surviving in diverse environments. Filamentous fungi reproduce either by the formation of conidia, which are borne on specialized stalks known as conidiophores, or by the formation of ascospores, which are produced in specialized tube- or sac-like cells termed asci.<sup>8, 9</sup> *Aspergillus*, *Penicillium*, and *Fusarium* are typical members of filamentous fungi growing in a polar fashion, extending in one direction, by elongation at the apex of the hypha, the so-called mycelium.<sup>10</sup> Fungi can interact human life in many aspects. In a negative way, fungi can spoil our foods and food grains, blight cultivated plants and cause health hazards. However, we also have taken benefits from fungi by applying them in food and enzyme production, as well as in chemical and pharmaceutical industries.<sup>3, 5, 11</sup> The development of synthetic biology, genetics, bioinformatics, and NP chemistry has greatly enhanced our ability to efficiently mine their genomes for the discovery of novel molecules.<sup>11-14</sup>

Since the discovery of the first broad-spectrum antibiotic penicillin G in 1928, most of the bioactive SMs derived from ascomycetes have intrigued chemists and biochemists.<sup>5</sup> Tremendous progress has been achieved in isolation and chemical characterization of a multitude of fungal SMs over the past decades.<sup>15-17</sup> Up to the year 2022, over 328,000 natural products were listed in the *Dictionary of Natural Products* (<http://dnp.chemnetbase.com>). Among them, about 45 % of microbial metabolites are produced by various fungi.<sup>5</sup> Based on the primary metabolism, the majority of so far discovered fungal NPs belongs to four categories: polyketides, peptides, terpenoids, and alkaloids (**Figure 1**). Furthermore, hybrid products of two or more main classes have also been found in fungi, such as hybrid polyketide-nonribosomal peptides and hybrid polyketide-terpenes.<sup>18</sup>

Polyketides constitute a large class of NPs with widely varying structures and biological functions. These compounds are usually biosynthesized by successive Claisen condensations between an acyl starter and a malonate derivative.<sup>19</sup> Representatives of polyketides are shown in **Figure 1**. Among

## INTRODUCTION

---

them, patulin is a well-studied mycotoxin produced by a variety of molds and induces immunological, neurological, and gastrointestinal effects.<sup>20, 21</sup> The biosynthetic precursor of patulin is 6-methylsalicylic acid (6-MSA), a well-characterized polyketide mainly found in *Penicillium* species.<sup>22</sup> Orsellinic acid is also an acetate-derived tetraketide similar to 6-MSA, but it harbors an additional hydroxyl group. Citrinin is a potent mycotoxin with nephrotoxic activity and was firstly isolated from a culture of *Penicillium citrinum*.<sup>23, 24</sup> Interestingly, sepedonin shares similar biosynthetic precursors with citrinin, but different subsequent modifications lead to the distinct structures.<sup>25</sup> Other prominent representatives are lovastatin, produced by *Aspergillus terreus*, which is used as a cholesterol-lowering drug,<sup>26</sup> and aflatoxin B<sub>1</sub>,<sup>27, 28</sup> isolated from *Aspergillus flavus* and *Aspergillus parasiticus*, exhibiting highly hepatotoxic activity. In addition, griseofulvin as an antifungal drug was isolated from *Penicillium* species<sup>29</sup> and zearalenone is an anabolic agent from *Fusarium* species.

Another important group of fungal NPs belongs to nonribosomal peptides with large structural and functional diversities (**Figure 1**). Similar to polyketides, many nonribosomal peptides have also been used as clinical drugs. The characteristics of nonribosomal peptides are amino acids instead of acyl-CoA as building blocks and elongation by C-N rather than C-C bond formation during their biosynthesis.<sup>30</sup> The representative  $\beta$ -lactam antibiotic penicillin G from *Penicillium* species is applied to the treatment of bacterial infections. Diverse penicillin derivatives have significantly expanded the spectrum of antibiotics.<sup>31, 32</sup> Cephalosporin C is another  $\beta$ -lactam antibiotic isolated from *Cephalosporium acremonium*.<sup>33</sup> Gliotoxin from *Aspergillus fumigatus* belonging to epipolythiodioxopiperazines contains a characteristic internal sulfur bridge.<sup>34, 35</sup> The well-known antifungal agent echinocandin B from *Aspergillus nidulans* is a cyclic hexapeptide with a linoleoyl side chain<sup>36</sup> and the immunosuppressant drug cyclosporin A from *Tolypocladium inflatum* is a cyclic peptide which consists of eleven amino acids.<sup>37</sup>

The third major group of fungal metabolites are undoubtedly terpenoids, also known as isoprenoids (**Figure 1**). Despite the structural diversity, terpenoids are biosynthesized from two C<sub>5</sub> units: dimethylallyl diphosphate (DMAPP) and isopentenyl diphosphate (IPP), *via* elongation by head-to-tail and occasionally tail-to-tail condensations. The subsequent products can be classified as monoterpenes (C<sub>10</sub>), sesquiterpenes (C<sub>15</sub>), diterpenes (C<sub>20</sub>), and triterpenes (C<sub>30</sub>).<sup>38, 39</sup> (+)-Aristolochene is a bicyclic sesquiterpene produced by *Penicillium roqueforti* and provides a biosynthetic scaffold for a number of toxins.<sup>40</sup> Gibberellin A3 as a typical example of oxygenated tetracyclic diterpenoids is a plant growth hormone with positive effects on plant development.<sup>41</sup> The typical fungal triterpenoid fusidic acid isolated from *Fusidium coccineum* acts as an oral antistaphylococcal antibiotic by preventing the turnover of elongation factor G from the ribosome.<sup>42</sup>

## INTRODUCTION

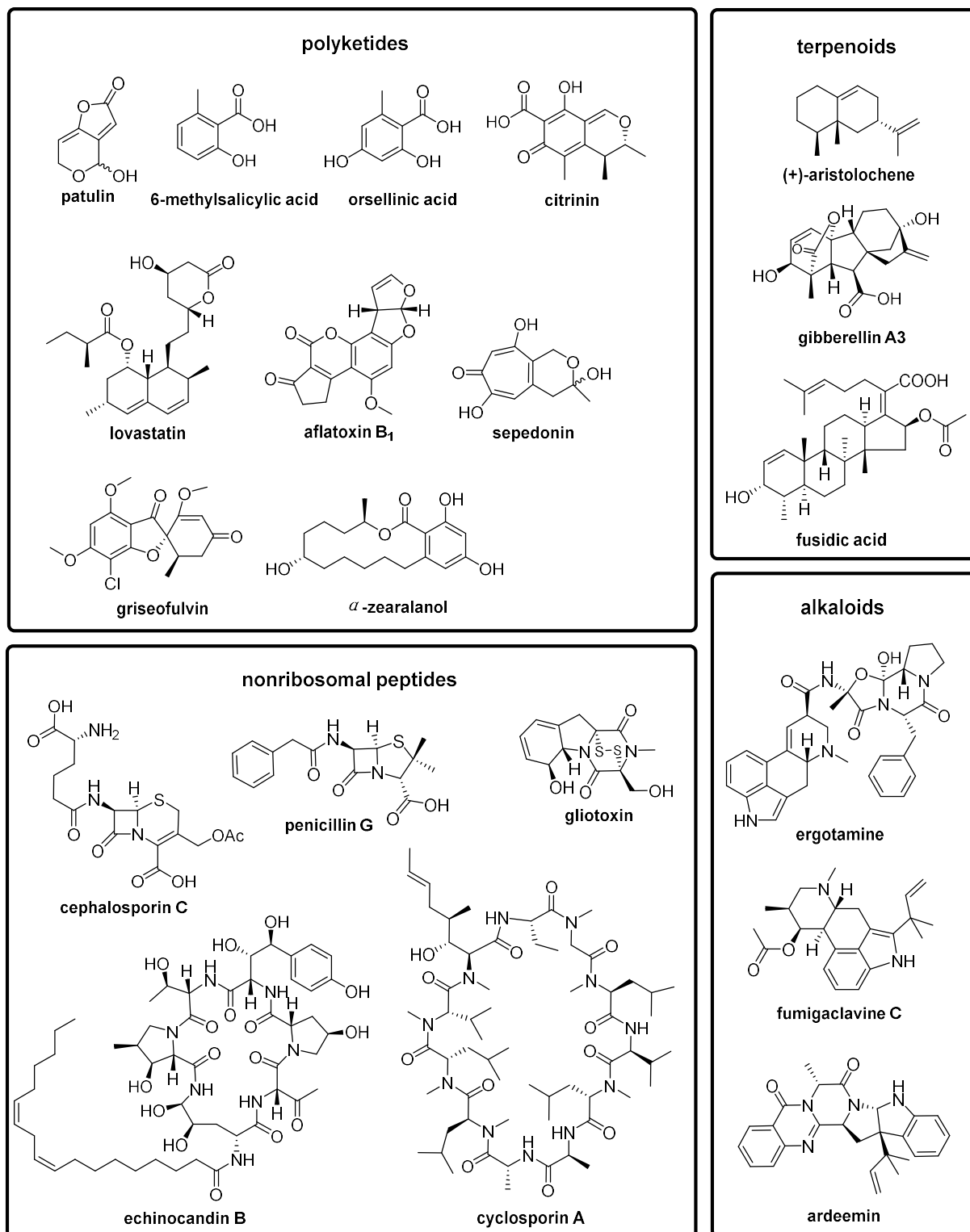


**Figure 1.** Representatives of fungal natural products.

In addition, alkaloids represent one of the largest classes of nitrogen-containing SMs in fungi (**Figure**

1).<sup>43, 44</sup> Ergotamine, the first isolated alkaloid from the cereal crop-related fungus *Claviceps purpurea* was responsible for the clinical effects in the treatment of migraines and cluster headaches.<sup>45</sup> Fumigaclavine C produced by *Aspergillus fumigatus* has significant anti-inflammatory activity and shows substantial inhibition of colitis.<sup>46, 47</sup> The hexacyclic peptidyl alkaloid ardeemin from *Aspergillus fischeri* exhibits antitumor activity.<sup>48</sup>

Overall, filamentous fungi are notable for producing plentiful SMs including clinically used drugs. Although a wide variety of NPs have been isolated and identified from fungi to date, there is still a large part of the NP treasure to be discovered. Advances in microbiology, biochemistry, sequencing technologies and bioinformatics provide greater possibilities to continue the discovery of new NPs and expand our knowledge of chemical logic and enzymatic machinery of NP biosynthesis, which benefits the mankind in all aspects.

## 1.2 The fungal genus *Penicillium*

As aforementioned, filamentous fungi produce a variety of SMs. Since the discovery of penicillin produced in *Penicillium notatum*,<sup>49</sup> the genus *Penicillium* has been extensively studied for its capacity to produce a wide range of NPs with biotechnological and pharmaceutical applications.<sup>50, 51</sup> *Penicillium* is a genus of ascomycete fungi belonging to the class Eurotiomycetes, family *Aspergillaceae*, and occurs in a diverse range of habitats, from soil to vegetation to air, indoor environments and various food products.<sup>52</sup> Some *Penicillium* species have been used for centuries in certain aspects. These include *Penicillium camemberti* and *Penicillium roqueforti* for cheese production,<sup>53, 54</sup> *Penicillium citrinum* for the production of the cholesterol-lowering drug mevastatin.<sup>55</sup> On the other hand, most species of *Penicillium* are regarded as spoilage and mycotoxin-producing organisms. For example, *Penicillium expansum*, *Penicillium digitatum*, and *Penicillium italicum* are postharvest pathogens in citrus fruits, stored grains, and other cereal crops.<sup>56-58</sup>

*Penicillium* species are known to produce SMs of various classes of chemical compounds, e.g., ergot alkaloids, diketopiperazines, benzodiazepines, quinolines, quinazolines, and polyketides.<sup>51</sup> So far, genome sequences of 298 *Penicillium* species are available in the public databases, e.g., NCBI database (<https://www.ncbi.nlm.nih.gov/data-hub/taxonomy/5073/>). Since the large biosynthetic potential in this genus has not been fully explored yet, it is of great significance to use *Penicillium* as research objective for NP discovery.

### 1.2.1 *Penicillium crustosum* and its secondary metabolites

*Penicillium crustosum* occurs on feed and on recycled food used as animal feed.<sup>59</sup> The conidia of *P. crustosum* are globose to subglobose, usually 3 – 4 µm, with dull green to grey green or blue green at the colony margin.<sup>52</sup> Phylogenetic analysis shows that *P. crustosum* is close to *Penicillium expansum*, *Penicillium commune*, and *Penicillium palitans*.<sup>52</sup> *P. crustosum* is a promising source of bioactive

## INTRODUCTION

compounds with diverse structures.<sup>51</sup> A wide range of SMs have been isolated and identified from *P. crustosum* including penitrem A – F,<sup>60</sup> alkaloids,<sup>61</sup> diketopiperazines,<sup>62</sup> and polyketides.<sup>63-65</sup>

The strain *Penicillium crustosum* PRB-2 was isolated from a deep-sea sediment collected in Prydz Bay (–526 m) and is able to produce abundant SMs, especially some novel polyketides including penilactones A and B, peniphenone D, and crustosumin A (**Figure 2**).<sup>63, 66</sup>

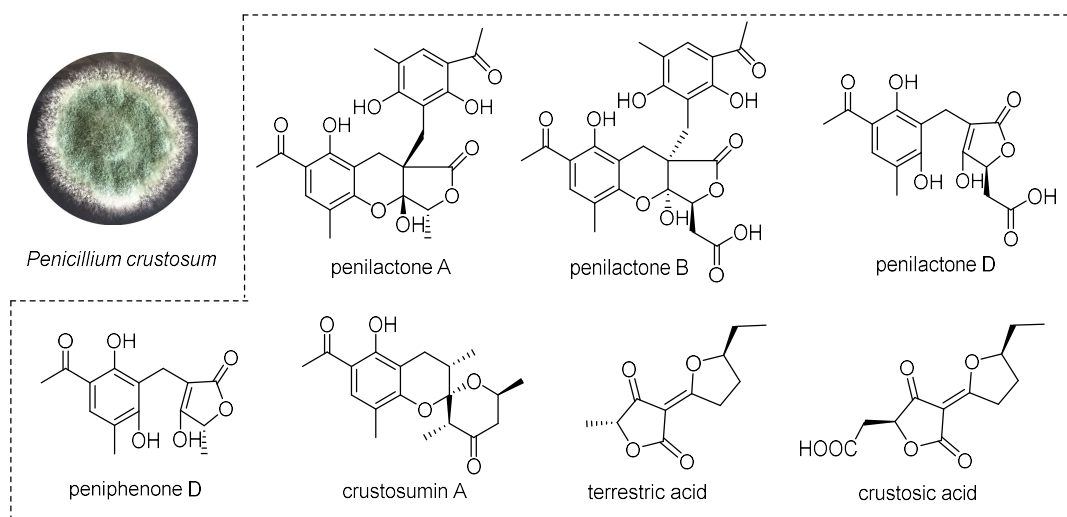


**Figure 2.** *Penicillium crustosum* and its known secondary metabolites.

In 2019, this strain was sequenced and a total of 31.3 Mbp length scaffolds were assembled.<sup>67</sup> Bioinformatic analysis revealed the presence of more than 56 BGCs for SMs. Twenty-two of these BGCs contain genes coding for PKSs. Previous biosynthetic studies reported investigations on three BGCs and a melanin pigment gene in *P. crustosum* PRB-2.<sup>67, 68</sup> In this thesis, this PhD candidate mainly focused on the PKSs in *P. crustosum* PRB-2 and elucidated the biosynthetic pathways of two polyketides.

### 1.2.2 *Penicillium roqueforti* and its secondary metabolites

*Penicillium roqueforti* is a saprophytic fungus that is commonly found in nature and can be isolated from soil or from decaying organic matter. As indicated above, *P. roqueforti* predominates in the fungal biota of traditional blue-veined cheeses such as Gorgonzola, Roquefort, and Stilton.<sup>69, 70</sup> *P. roqueforti* belongs to the *Roquefortorum* section that also includes *P. carneum*, *P. paneum*, *P. psychrosexualis*, and *P. mediterraneum*.<sup>69</sup>

*P. roqueforti* is a rapidly growing fungus and produces low and velutinous dark green colonies, which can reach 40 – 70 mm in diameter on malt extract agar media. These colonies are characterized by moderate to heavy conidial production with a typical blue-green or dull green color.<sup>52, 70</sup> *P. roqueforti* appears to have the lowest oxygen requirements for growth of any *Penicillium* species and can grow

## INTRODUCTION

in the pH range of 3 – 10. Moreover, *P. roqueforti* is a psychrophile and grows vigorously at temperatures between 4 – 35 °C. This tolerance makes the fungus a common cause of spoilage in cool-stored preserved commercial and domestic foods.<sup>69-71</sup> *P. roqueforti* is also well known for its ability to produce a wide range of SMs including roquefortine C, PR-toxin, andrastin A, mycophenolic acid, eremefortin C, and citreoisocoumarin (**Figure 3**).<sup>72, 73</sup> So far, several BGCs were identified including those for roquefortine C, mycophenolic acid, andrastin A, and PR-toxin.<sup>69, 74</sup>

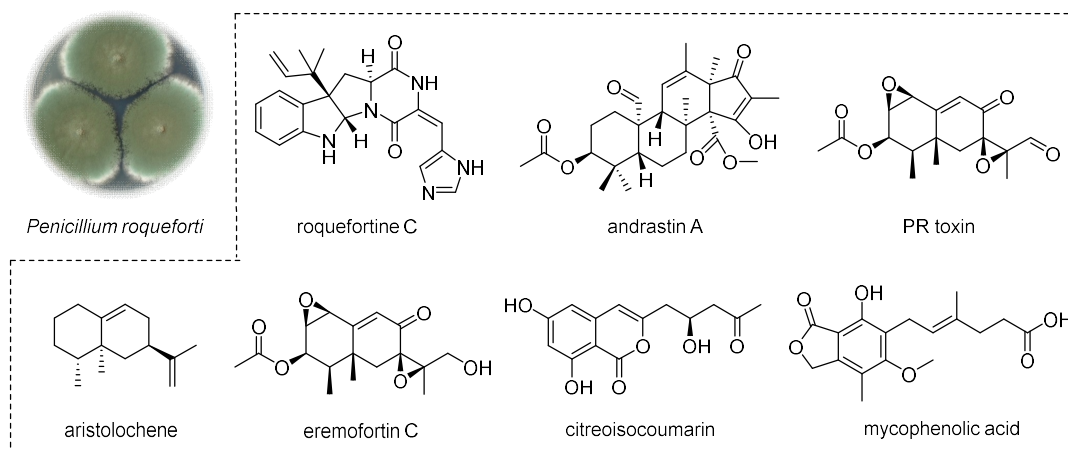


**Figure 3.** *Penicillium roqueforti* and its known secondary metabolites.

The whole genome sequence of *Penicillium roqueforti* FM164 used in this thesis was first published in 2013 (GenBank assembly accession: GCA\_000513255.1), which assembled a total of 26.9 Mbp length scaffolds.<sup>75</sup> Bioinformatic analysis revealed the presence of 33 BGCs of SMs and 12 of them contain genes coding for PKs. Although such BGCs have been identified in *P. roqueforti* FM164, there is still limited information on the biosynthesis of SMs in *P. roqueforti*. In this thesis, this PhD candidate mainly focused on the investigation of a cryptic BGC and elucidated SMs encoded by the biosynthetic pathway.

### 1.3 Biosynthesis of natural products in fungi

NPs from fungi represent an important source of biologically active metabolites notably for therapeutic agent development.<sup>29, 76</sup> Importantly, as mentioned in section 1.1, some of these fungal NPs have been developed into drugs and are used widely for human health.<sup>77</sup> The structural diversity of NPs arises from their biosynthetic classification. It has been demonstrated that the genes coding for enzymes of a given biosynthetic pathway are often co-regulated and located adjacent in the fungal genome, forming so-called biosynthetic gene clusters (BGCs).<sup>78-80</sup>

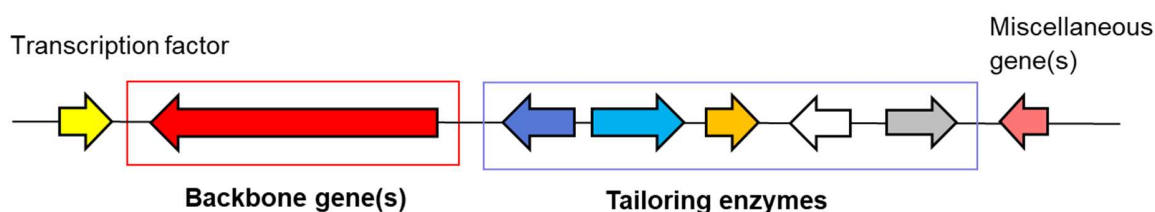


**Figure 4.** Schematic representation of fungal biosynthetic gene clusters.

Typical fungal BGCs share a common set-up, usually consisting of one or more genes for backbone enzymes, which catalyze the synthesis of the skeleton of the metabolite. Examples for backbone enzymes include polyketide synthases (PKSs), nonribosomal peptide synthetases (NRPSs), terpene synthases, and hybrid polyketide synthase-nonribosomal peptides synthetases (hybrid PKS-NRPSs). The surrounding genes usually code for tailoring enzymes, such as oxidoreductases and transferases, which modify the backbone scaffold in multiple biosynthetic steps to produce the final product. In addition, genes for regulation of the whole gene cluster or transporters for secretion of the products or uptake of special substrates can also be included in the BGCs (**Figure 4**).<sup>80, 81</sup> Therefore, SMs often feature more chiral centers and increased steric complexity than synthetic molecules. For instance, lovastatin was biosynthesized in *Aspergillus terreus* by an 18-gene BGC containing two multifunctional PKSs (LovB and LovF) and several decoration enzymes.<sup>19, 82</sup>

### 1.3.1 Genome mining for fungal natural product discovery

Genome mining refers to the utilization of genomic information for novel processes, target, and product discovery. It includes bioinformatic analysis and identification of unknown BGCs in the target genomes, sequence analysis of the genes, and the experimental identification of the products synthesized by these BGCs. Currently, around 120,000 species of fungi have been described<sup>83</sup> and over 1,000 fungal genome sequences are available through the JGI 1000 Fungal Genomes Project. Traditionally, NPs were identified through screening fungal cultural extracts for biologically active compounds. Genome mining has the potential to increase the chance to find novel molecules and biosynthetic pathways. With increasing technological improvements in genome sequencing, a range of computational approaches has been developed to automatically identify the sets of genes that code for specialized metabolic enzymes across genome sequences.<sup>84</sup> The specialized softwares for the prediction of fungal BGCs include Antibiotics and Secondary Metabolite Analysis Shell (antiSMASH), Secondary Metabolite Unknown Regions Finder (SMURF), and the annotated database Minimum Information about a Biosynthetic Gene cluster (MIBiG). Prediction with these tools revealed that most filamentous fungi contain dozens of BGCs in their genomes, revealing their potential ability to produce many SMs.<sup>85, 86</sup>

## INTRODUCTION

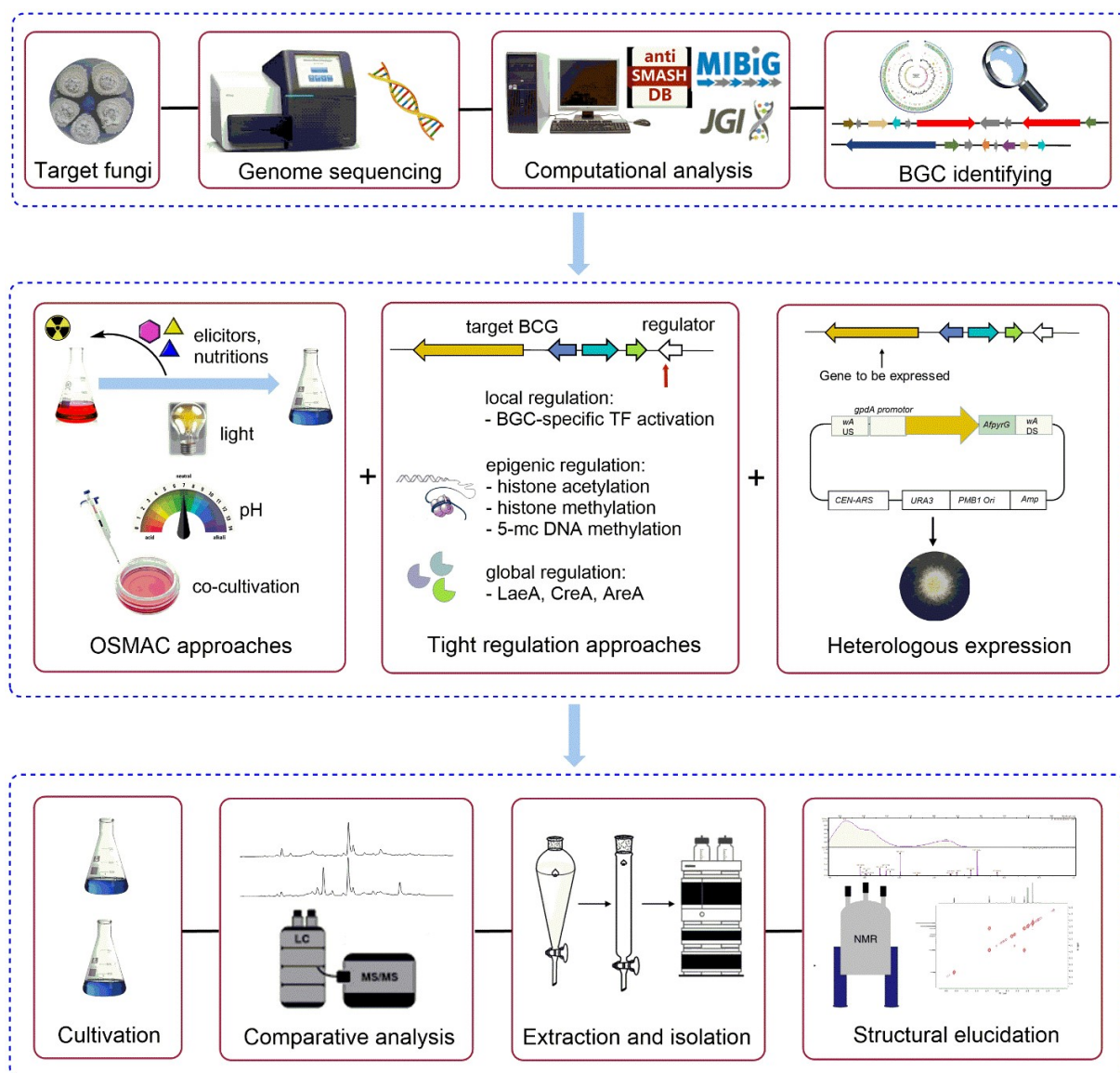


**Figure 5.** Genome mining approach for natural product discovery in fungi.

It is worth noting that a large number of BGCs identified in one particular fungal genome far exceeds the SMs that have been detected under standard laboratory culture conditions.<sup>85, 87</sup> This indicates the presence of a large number of cryptic BGCs in fungi. For the vast majority of these BGCs, external and/or internal signals that trigger their expression remain largely unknown. In the post-genomic era, numerous efforts have been done for development of strategies for activating these silent gene clusters or for fungi that are difficult to be cultivated.<sup>2, 88-90</sup> The strategies for engineering fungal NP biosynthesis<sup>91</sup> can be divided into four broad categories as shown in **Figure 5**: (i) optimization of the cultivation conditions, also known as OSMAC (One Strain, Many Compounds) approach, e.g., media composition, cultivation time or temperature, pH values, and co-cultivation.<sup>92-94</sup> (ii) Induction of global transcriptional changes, e.g., through epigenetic modifications<sup>95-97</sup> or overexpression of global



transcriptional regulators,<sup>98-105</sup> can effectively 'awaken' the biosynthetic machinery, but often affects multiple pathways resulting in the production of a variety of NPs, which is unpredictable and difficult to control. (iii) Manipulating of specific biosynthetic pathways either in the native host or in a heterologous host<sup>106-109</sup> is more targeted and enabled thorough understanding of the function of each gene and may lead to the discovery of unprecedented enzyme classes/ functions, but it is often substantially more labor intensive. (iv) Specific engineering of enzymes to synthesize novel NPs *in vivo* or *in vitro*, which may be adapted as biocatalysts or used in chemoenzymatic synthesis. The subsequent work flow to explore SMs from fungi includes extraction of the cultures by using solvents with different polarities, separation of the crude extracts by using column chromatography, as well as structural elucidation of the purified compounds by NMR and LCMS analyses (**Figure 5**).

Advances in the identification and engineering of fungal BGCs provide a toolbox of methods for the discovery and improved production of numerous novel NPs. In the last ten years, the CRISPR-Cas9 (Clustered regularly interspaced short palindromic repeats-CRISPR-associated protein) technologies with a broad host range has been developed as a novel approach to efficiently manipulate genes in a complex microbiome.<sup>110</sup> Considering the efficiency and breadth of new strategies for genome mining and the increased extent of resources available for mining, it should be noted that the most suitable strategies depend on the research objective. Taken together, many new sources, enzymes, and metabolites are expected to be discovered in the coming years.

### 1.3.2 Heterologous expression

In order to activate cryptic SM production, heterologous expression strategy can be applied, especially for clusters of interest from strains that are difficult to be manipulated genetically.<sup>85, 111, 112</sup> The typical workflow of heterologous expression usually includes steps as shown in **Figure 6**: identification of targeted SM biosynthetic gene or BGC from the sequenced genomes using bioinformatic tools; selection of an appropriate heterologous host; cloning the gene or BGC into a suitable vector with appropriate promoter, transferring it into the heterologous hosts, and product characterization.

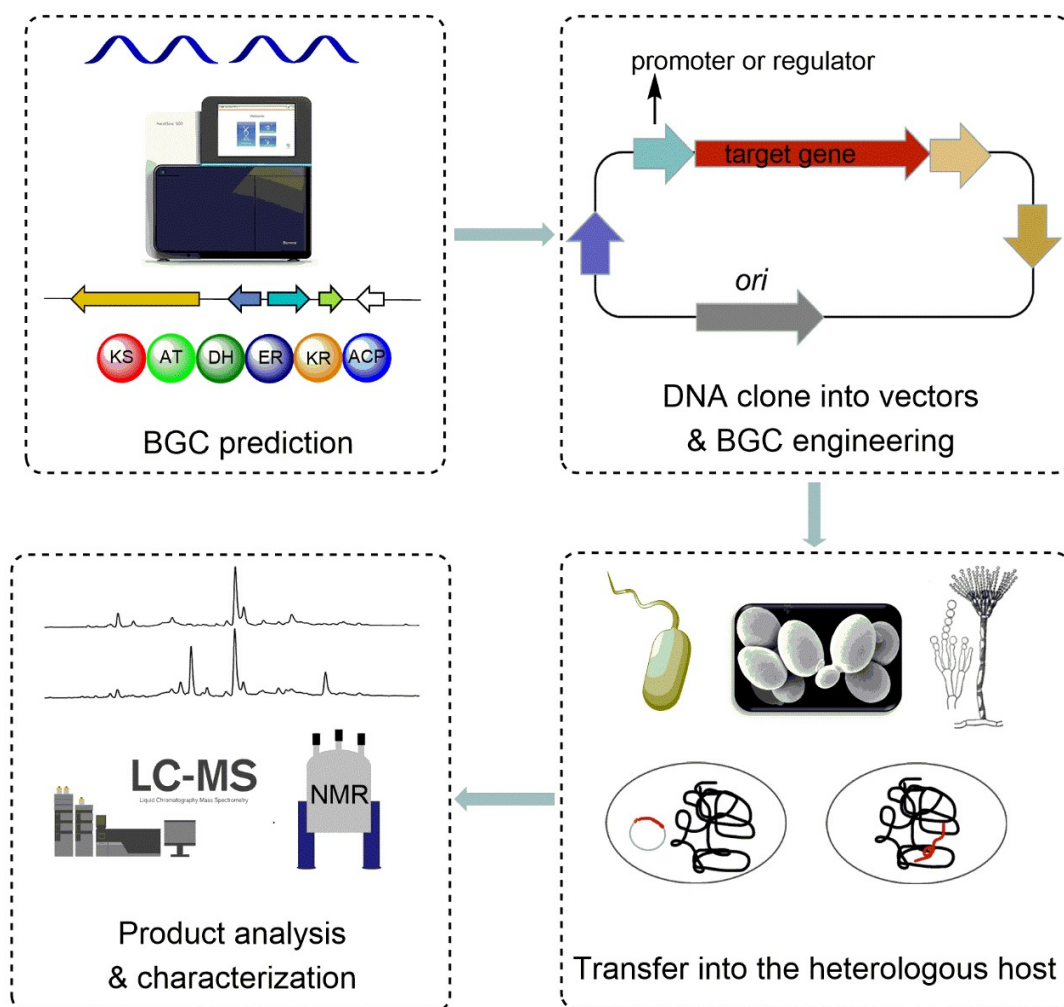


**Figure 6.** Workflow for heterologous expression of gene or gene clusters.

### 1.3.2.1 Hosts for heterologous gene expression

Selecting a suitable host is the first thing to be considered for heterologous expression. This choice depends on several factors, such as convenience, the chemical background and the toxicity of the compound, as well as the availability of genetic manipulation tools for the host. Generally, the more phylogenetically close to the native producer, the higher efficient expression can be expected, because of the functionality of native transcriptional elements of the gene cluster with high similarity. Transcriptional elements or parameters include promoters, regulatory elements, codon bias, ribosome binding sites, and RNA maturation including intron splicing.<sup>85, 113</sup> Different organisms have been developed and utilized as heterologous hosts, such as *Escherichia coli*,<sup>114</sup> actinomycetes,<sup>113</sup> yeast,<sup>115</sup> filamentous fungi,<sup>116</sup> plants<sup>117</sup> and animal cells.<sup>118</sup>

*E. coli* is widely used as a prokaryotic host due to a number of advantages including strong engineering toolbox, easy cultivation, fast and robust growth, and a well-understood primary metabolism.<sup>119</sup> An

## INTRODUCTION

---

early successful example is the expression the 6-methylsalicylic acid synthase (6-MSAS) gene from *Penicillium patulum* in *E. coli*, which thereby produced 6-methylsalicylic acid (6-MSA).<sup>120</sup> In a more recent study, *pks4* from *Gibberella fujikuroi* was expressed in *E. coli*, and its product was verified as SMA76a.<sup>121</sup> Similarly, eleven sesquiterpene synthetase genes from *Omphalotus olearus* were expressed in *E. coli* and the products were identified directly.<sup>122</sup> In addition, *E. coli* is widely and continuously used as a protein overproduction host for *in vitro* functional characterization of accessory enzymes in fungal BGCs. Zabala *et al.* purified an FAD-dependent monooxygenase AzaH and verified its function in azaphilone biosynthesis *via in vitro* protein assays.<sup>123</sup> In spite of its widespread use in fungal BGC enzyme characterization, *E. coli* has apparent limitations as a heterologous host for the reconstitution of full pathways of fungal NPs.

Yeast, in particular *Saccharomyces cerevisiae*, is a fast growing unicellular eukaryotic model microorganism. It is widely used as heterologous expression host for polyketide- and nonribosomal peptide-related genes.<sup>111, 124</sup> Besides, versatile genetic manipulation tools have been developed in *S. cerevisiae* to facilitate the BGC assembly and metabolic engineering. Homologous recombination is very efficient in *S. cerevisiae* and has been frequently employed for *in vivo* BGC assembly.<sup>125, 126</sup> It is worth mentioning that when yeast or *E. coli* are used as expression hosts for eukaryotic SM biosynthetic genes, the introns in the target genes have to be removed first, and the 4-phosphopantetheinyl transferase (PPTase) needs to be integrated into the yeast genome before, especially for PKSs and NRPSs expression.<sup>127</sup> The above mentioned 6-MSAS from *P. patulum* was also expressed in a *S. cerevisiae* strain with a heterologous PPTase, and successfully produced much higher amount of 6-MSA than in both the native species and *E. coli*.<sup>120</sup> An engineered *S. cerevisiae* strain with *matB* (malonyl-CoA synthetase) and *npgA* (a PPTase) was successfully used for expression of a cassette of five PKSs and one NRPS.<sup>126</sup>

In addition to single synthase genes, whole gene clusters have also been expressed in *S. cerevisiae*. For instance, three biosynthetic genes from *Fusarium graminearum* together with the heterologous *npgA* gene from *A. fumigatus* were co-expressed and resulted in the production of rubrofusarin.<sup>128</sup> Very recently, the Heterologous EXpression (HEX) platform was developed in *S. cerevisiae* for fast and scalable expression of fungal biosynthetic genes and their encoded metabolites.<sup>109</sup> Furthermore, 41 unique BGCs were selected and transformed in *S. cerevisiae*, and more than half (22/41) of these BGCs produced different SMs. Similar to *E. coli*, using *S. cerevisiae* as a heterologous host displays additional advantages including highly efficient homologous recombination, limited native secondary metabolism, sufficient supply of building blocks and cofactors, and self-supported correct folding.<sup>112</sup> Although yeast has been extensively used for heterologous expression of fungal BGCs, some issues also need to be considered for NP biosynthesis, *i.e.* lack of endogenous secondary metabolism, insufficient precursors and building blocks specific activation, and the toxicity of the produced compounds.

Apart from *E. coli* and yeast, filamentous fungi are efficient and preferred hosts for exploration and production of fungal NPs.<sup>85</sup> First of all, the genetic systems of fungi are generally compatible for correct translation folding and post-translational modifying, thus fungal BGCs can be used without codon optimization and introns-removal in advance. Secondly, filamentous fungi possess endogenous PPTases for PKS and NRPS modification. Additionally, they can utilize relatively cheap non-food biomass as carbon source to achieve a high level of gene expression. In addition to diverse filamentous fungal hosts including *Neurospora crassa*, *Penicillium* and *Fusarium* species, *Aspergillus* species, especially *A. oryzae*, *A. nidulans*, and *A. niger* have become the most widely used heterologous hosts for NP production.<sup>85, 129</sup>

*A. nidulans*, the well-known model organism used for the exploration of many fungal BGCs, possesses the distinct advantage of easy genetic manipulation.<sup>116, 130, 131</sup> Recently, an engineered strain *A. nidulans* LO8030 with deletion of eight SM clusters has been used for the reconstitution of fungal BGCs of unknown biosynthetic pathways and for studying the mechanisms of key biosynthetic enzymes.<sup>132</sup> Besides, the lower SM background of LO8030 made it an excellent host for easy detection of compounds produced by the genes or BGCs of interest.

*A. oryzae* is a filamentous fungus extensively used for the industrial production of enzymes and traditional fermented food. Due to its clean SM background and well-developed genetic manipulation tools, it is also frequently used as a heterologous host for the production and elucidation of biosynthetic pathways of NPs.<sup>116, 133</sup> Nowadays, several *A. oryzae* strains have been developed. For example, the engineered *A. oryzae* NSAR1 strain with five expression vectors (pTAex3, pUSA, pAdeA, pPTR1, pUNA) was used for reconstructing terpenoid biosynthetic pathway.<sup>134</sup> The NSAR1 strain was further modified recently by deletion of the FAD-dependent oxidoreductase gene *kojA* controlling kojic acid biosynthesis, thus making it as a more appropriate heterologous host.<sup>135</sup> Another widely used *Aspergillus* host is *A. niger*, which has been applied in producing sake, miso, soy sauce, industrial enzymes, and citric acid.<sup>116</sup>

### 1.3.2.2 Promoters for heterologous gene expression

The second aspect to be considered for heterologous expression is the promoter selection for the expression construct. The heterologous host normally cannot use the endogenous promoters of the genes in BGCs, unless their taxonomic relationship for transcription initiation and regulation is close enough.<sup>136, 137</sup> Therefore, the promoters need to be replaced for a genetically distant host. To achieve concurrent high-yield production or to control the initial synthesis of NPs at the appropriate time, a large set of efficient promoters are required for heterologous expression of BGCs. Generally, constitutive promoters are believed to result in stable expression under varying conditions, whereas inducible promoters induce dramatic changes in expression levels in response to environmental stimuli.<sup>85</sup> A diversity of constitutive promoters or inducible promoters are frequently used to activate the expression of BGC genes for high-yield production of proteins in the existing heterologous

expression systems.<sup>138</sup> Representative constitutive promoters include those for glyceraldehyde-3-phosphate dehydrogenase (*gpdA*), 3-phosphoglycerate kinase (*pgkA*), and translation-elongation factor EF-1  $\alpha$  (*tef1*). Examples of typical inducible promoters are alcohol dehydrogenase promoters (*adhA* and *alcA*), amylase promoters (*amyA* and *amyB*), glucoamylase promoter (*glaA*), and xylose-inducible promoter (*xyIP*). Although both constitutive and inducible promoters can directly affect the transcription level, it is better to select inducible promoters when the expression system may produce harmful products. In addition, the auto-inducible promoters (*ADH2* and *ADH2*-like) are frequently used for producing desired compounds with titers of up to 100-fold compared to those obtained using constitutive promoters.<sup>109</sup> Despite the above mentioned natural promoters, synthetic promoters were also found to be useful for NP biosynthesis, such as the bacterial-fungal hybrid Tet-on promoter, which can be used for the establishment of conditional overexpression mutants.<sup>139</sup>

Over the past decades, heterologous expression has long been used with significant successes as a robust tool for activating cryptic or silent SM BGCs and elucidating biosynthetic pathways. Nowadays, with the comprehensive development of functional characterizations, bioinformatics, and biotechnological tools, heterologous expression is promising to produce diverse bioactive fungal NPs.

## 1.4 Polyketide synthases

As aforementioned, polyketides constitute one of the major classes of NPs, which comprise an enormous structural diversity and a wide range of biological activities. The formation of the carbon backbone in polyketides is catalyzed by polyketide synthases (PKSs), which share similar logic and enzyme machinery as fatty acid biosynthesis.<sup>1, 140</sup>

The fundamental chemical aspect in the biosynthesis of polyketide backbone is achieved by the utilization of different starter and extender units. The starter units include acetyl-CoA, malonyl-CoA, methylmalonyl-CoA, propionyl-CoA, benzoyl-CoA, and 4-coumaroyl-CoA. Examples of common extender units are malonyl-CoA, (2*S*)-methylmalonyl-CoA, (2*S*)-ethylmalonyl-CoA and chloroethylmalonyl-CoA.<sup>141, 142</sup> It is worth mentioning that the isotopic building blocks such as [1-<sup>13</sup>C]-, [1,2-<sup>13</sup>C<sub>2</sub>]-, [1-<sup>13</sup>C, <sup>18</sup>O<sub>2</sub>]-acetate, and [2-<sup>13</sup>C]-malonic acid have been commonly applied to confirm the biosynthetic origin and to identify the enzymatic logic for the complicated synthetic mechanism.<sup>143, 144</sup>

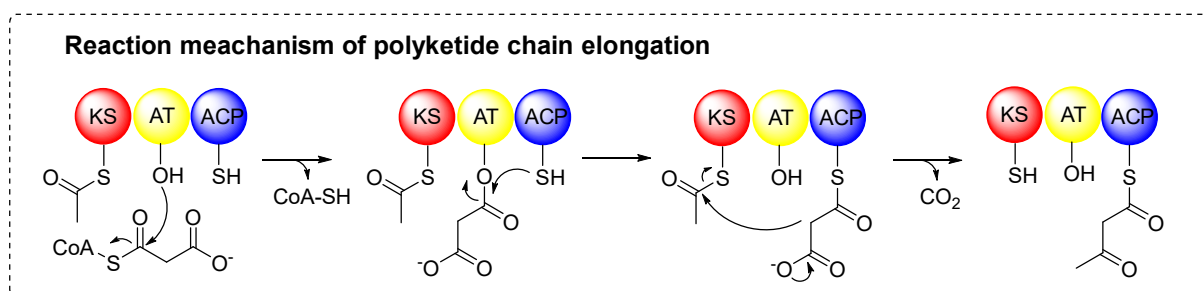


**Figure 7.** Reaction mechanism of polyketide chain elongation.

The biosynthesis of polyketides proceeds in three basic phases, *i.e.* starter unit loading, chain elongation and reduction, and polyketide cyclization and release (**Figure 7**).<sup>1, 145</sup>

Generally, polyketide elongation requires three basic domains including ketosynthase (KS), acyltransferase (AT), and acyl carrier protein (ACP) domains. KS domain normally catalyzes the decarboxylative Claisen condensation of the extender unit to an acyl starter substrate to extend the polyketide chain. AT domain is responsible for recognizing the starter or extender unit and catalyzes its transfer to the phosphopantetheine arm of ACP domain, which serves as a covalent binding site for the intermediate formed during biosynthesis. In addition, the resulting moiety can be further processed by accessory domains for polyketide chain modification. These include ketoreductase (KR) domain for optional reduction of the  $\beta$ -keto group to a hydroxyl group, dehydratase (DH) domain catalyzing dehydration to generate an  $\alpha,\beta$ -unsaturated thioester, enoylreductase (ER) domain that further reduces the double bond to a saturated moiety, and methyl transferase (MeT) domain that catalyzes the transfer of methyl groups from S-adenosylmethionine (SAM) to the  $\beta$ -carbon of the growing polyketide chain, as well as product template (PT) domain.<sup>146, 147</sup> The reductive step can be partly or fully omitted before the next condensation step and leads to a complex functionalization pattern at the  $\beta$ -position. Additionally, structural modifications, such as alkylations, hydroxylations, glycosylations, and heterocyclizations, which are often crucial for the biological activities of the final polyketides, may occur during chain elongation.<sup>140, 148, 149</sup> Lastly, the elongated polyketide chain is released from the PKS assembly line by the thioesterase (TE) domain, leading to the end product.<sup>150</sup>

Based on the architecture and mode of action of the enzymatic assembly lines, PKSs are generally classified into three distinct types. Type I PKSs are multifunctional enzymes that are organized structurally into modules.<sup>151</sup> Type II PKSs consist of a dissociable complex of subunits such as KS, chain-length factor, and ACP.<sup>152</sup> Type III PKSs are KS homodimers.<sup>153</sup>

### 1.4.1 Type I polyketide synthases

Type I PKSs have been discovered in both bacteria and fungi. They can be basically classified into iterative type I PKSs and modular type I PKSs.<sup>141, 154</sup> In modular type I PKSs, which are commonly found in bacteria, domains with defined functions are separated by short spacer regions and organized into several modules. A single module is constituted of KS, AT, and ACP domains, as well as optional  $\beta$ -keto processing domains, and generally catalyzes one step of condensation. The number of the modules thus correlates with the number of extension cycles executed by the PKS. The presence of KR, DH, and ER domains defines the degree of  $\beta$ -keto processing.<sup>155</sup> One of the best-studied example of modular type I PKSs is the giant multimodular megasynthase 6-deoxyerythronolide synthase (DEBS) from *Saccharopolyspora erythraea*, which assembles the macrolide scaffold 6-deoxyerythronolide B in the biosynthesis of erythromycin A (**Figure 8A**).<sup>156</sup> Modular type I PKSs can be further divided into *cis*-AT PKSs and *trans*-AT PKSs based on their AT architecture. Distinct to the standard *cis*-AT PKS, the ACPs of the *trans*-AT PKS are loaded by stand-alone ATs.<sup>157, 158</sup>

## INTRODUCTION

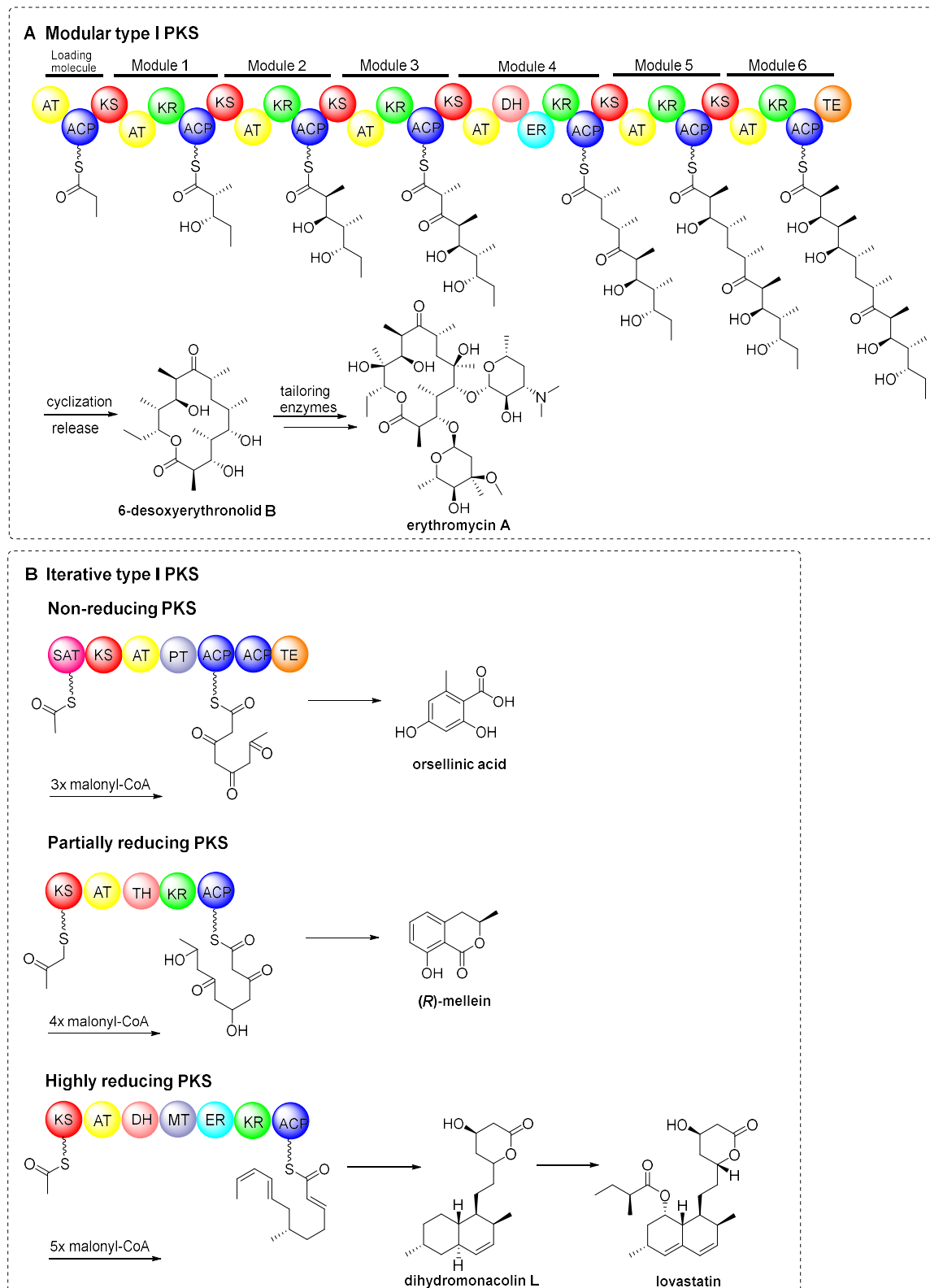


**Figure 8.** Representatives of the modular (A) and iterative (B) type I PKSs involved in the secondary metabolite biosynthesis.

In comparison, domains in iterative type I PKSs are clustered in a single module, which are used repeatedly to catalyze multiple rounds of elongation for polyketide formation (**Figure 8B**).<sup>145, 151, 159</sup> In most cases, fungal polyketides are products of iterative type I PKSs. According to the extent of  $\beta$ -keto reduction, iterative type I PKSs can be functionally grouped into three major classes, *i.e.* nonreducing PKSs (NRPKSs), partially reducing PKSs (PRPKSs), and highly reducing PKSs (HRPKSs).

Fungal NRPKSs are usually responsible for the production of aromatic polyketides. In addition to the minimal PKS domains (KS, AT, and ACP domains), there are functional domains that are unique to the NRPKSs, *e.g.*, the starter unit acyl transferase (SAT) domain, the product template (PT) domain, and the C-terminus thioesterase/Claisen-like-cyclase (TE/CLC) domain.<sup>160</sup> In most cases, the SAT domain is selective for acetyl-CoA, a fundamental metabolic building block.<sup>142, 161</sup> However, in the biosynthetic pathway of aflatoxin B1, the SAT domain of PksA accepts a hexanoyl starter unit.<sup>162</sup> Cyclizations are generally catalyzed by the PT domain with a poly- $\beta$ -ketone backbone as the substrate. For example, the simplest NRPKS OrsA from *Aspergillus nidulans* utilizes acetyl-CoA as starter unit by the SAT domain and elongates with three malonyl-CoA catalyzed by KS, AT, and ACP domains to form the polyketide chain. Cyclization of the intermediate is catalyzed by the PT domain and the aromatic intermediate is released by the TE domain to form the end product orsellinic acid (**Figure 8B**).<sup>163</sup> In some cases, NRPKSs contain a reductase (R) domain instead of the TE domain at the C-terminus as the release domain,<sup>159</sup> such as 3-methylorcinolaldehyde synthase (MOS) with a SAT-KS-MAT-PT-ACP-CMeT-R domain structure.<sup>164</sup> Notably, some PKSs do not carry such a releasing domain and have co-evolved with other enzymes, like  $\beta$ -lactamases and hydrolases, to release the polyketide chain.<sup>148</sup>

In contrast to NRPKSs, the HRPKSs exhibit a much higher degree of complexity in their biosynthetic programming. Besides the common domains that control chain extension and release, the HRPKSs contain three  $\beta$ -keto processing domains (DH, ER, and KR domains) that could selectively catalyze ketoreduction, dehydration and enoylreduction during each extension cycle.<sup>151, 159</sup> Thus, the HRPKS can produce complex, highly reduced compounds such as lovastatin, T-toxin, fumonisin B1, and squalenol.<sup>159</sup> In addition, many HRPKSs also possess a C-methyltransferase (CMeT) domain for methylation of the  $\alpha$ -carbon on the extended polyketide chain.<sup>165</sup> For instance, in the biosynthesis of lovastatin, the elongation intermediate was methylated by the SAM-dependent CMeT domain and subsequently reduced by the KR domain to form a hydroxyl group. Further reduction steps are achieved by the DH domain and the NADPH-dependent *trans*-ER domain, consequently leading to a fully saturated product (**Figure 8B**).<sup>166, 167</sup>

Unlike the HRPKSs, product release of PRPKSs differ from the fully reduction mechanism due to the absence of ER domain. In the biosynthesis of (*R*)-mellein, the KR domain selectively reduces the keto groups. The pentaketide intermediate subsequently undergoes an aldol cyclization to furnish the aromatic structure through dehydration, and the TH (thioester hydrolase) domain catalyzes the release of (*R*)-mellein *via* a stereospecific cyclization process (**Figure 8B**).<sup>168</sup>



### 1.4.2 Type II polyketide synthases

Bacterial aromatic polyketides such as tetracyclines and actinorhodin are polycyclic compounds that are assembled by type II PKSs.<sup>169</sup> Type II PKSs are dissociable multi-enzyme complexes that have sets of iteratively used individual proteins. They typically produce polycyclic aromatic compounds by catalyzing iterative Claisen condensation reactions using acetate as the starter unit.<sup>152, 169, 170</sup>

A minimal set of type II PKS consists of the ketoacyl synthase ( $KS_{\alpha}$ ), the chain length factor (CLF, also referred as  $KS_{\beta}$ ) and the ACP subunit. The  $KS_{\alpha}$  and  $KS_{\beta}$  form a strongly associated heterodimer and catalyze the Claisen-like condensation of acetyl- and malonyl-CoA units in an iterative fashion. The biosynthetic reaction typically includes the following steps: firstly, the acetate precursor is loaded onto ACP and give rise to acyl-ACP. Subsequently, the acyl-ACP is transferred to the  $KS_{\alpha}$  subunit and iteratively elongated with the extender unit malonyl-CoA to form the poly- $\beta$ -keto chain. Afterwards, the polyketone chain is further modified by aromatases (AROs) and oxygenases to afford the aromatic polyketide core *via* cyclization and/or aromatization. Additional PKS subunits such as KRs, cyclases or AROs define the folding pattern of the polyketone intermediate and further post-PKS modifications, such as oxidations, reductions or glycosylations are added to the polyketide.<sup>152, 171</sup>

On the basis of the polyphenolic ring system and their biosynthetic pathways, representative metabolites produced by type II PKSs range from anthracyclines, angucyclines, aureolic acids, tetracyclines, tetracenomycins, pradimicin-type polyphenols, to benzoisochromanequinones.<sup>152</sup> A well-studied example of type II PKS is TcmKLM, which is involved in the biosynthesis of the antibiotic tetracenomycin C (**Figure 9**).<sup>172</sup>

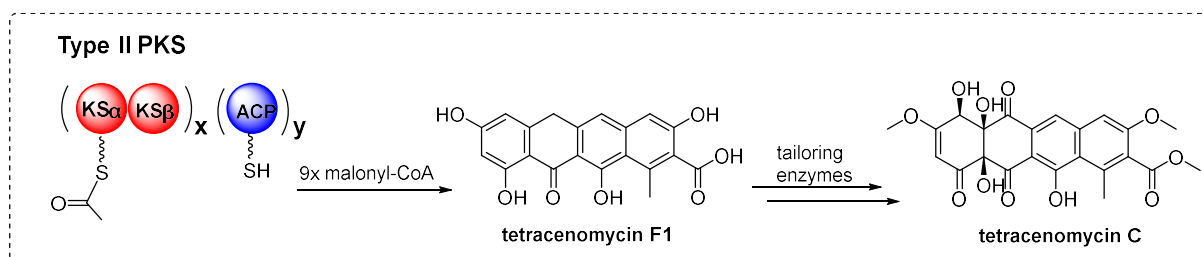


**Figure 9.** Representative of the type II PKS involved in the secondary metabolite biosynthesis.

### 1.4.3 Type III polyketide synthases

Different from above-mentioned type I and type II PKSs, type III PKSs are simple homodimeric ketosynthases (KS) that mainly catalyze the formation of pyrone- and resorcinol-type aromatic polyketides (**Figure 10**).<sup>153</sup> Type III PKSs are mainly found in plants, but are also present in bacteria<sup>173</sup> and fungi.<sup>174</sup> They are essentially condensing enzymes that lack ACP domains and act directly on acyl-CoA substrates.<sup>175</sup> Type III PKSs synthesize a wide variety of products and they differ from each other in terms of the preference of starter and extender units (ranging from short to long linear or cyclic

acyl-CoA), the number of condensation steps, and the mechanism of intramolecular cyclization of poly- $\beta$ -keto intermediates.<sup>140</sup>

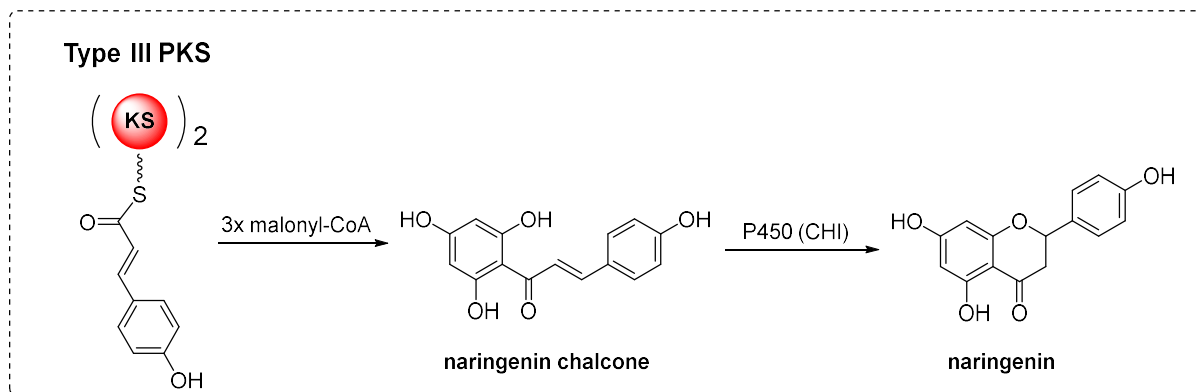


**Figure 10.** Representative of the type III PKS involved in the secondary metabolite biosynthesis.

The well-studied family of type III PKSs are plant chalcone/stilbene synthases (CHS/STS) which produce compounds like naringenin chalcone (**Figure 10**).<sup>176</sup> The CHS uses a single KS-like active site to catalyze the repetitive condensation of acetate units to a CoA-derived starter molecule, typically yielding mono- and bi-cyclic aromatic products.<sup>177</sup>

As described in this chapter, all PKS types contribute significantly to the diversity of NPs. Based on the growing knowledge about structural functionality in the fields of starter/extender unit selection, cyclization and release reactions, as well as domain structure-function relationships, approaches for PKS engineering will increase polyketide product diversification and fulfill the strong demand for a highly detailed structural and biochemical characterization of PKSs.

## 1.5 Tailoring enzymes

As introduced in section 1.3, the backbone genes in fungal BGCs are usually surrounded by several genes coding for post-modification enzymes, the so-called tailoring enzymes, including prenyltransferases (PTs), acyltransferases, oxidoreductases, and cyclases.<sup>159, 178</sup> In the biosynthesis of the most NPs, backbone enzymes are responsible for scaffold complexity of SMs. Further processing of the nascent scaffolds can occur in a set of post-assembly enzymatic tailoring steps, which contribute to the formation of diverse and sophisticated SMs.<sup>179, 180</sup> Moreover, for the biosynthesis of a complex polyketide, different enzymes participate in the polyketide biosynthetic pathway and catalyze specific reactions in a highly organized and coordinated manner.<sup>91</sup>

PTs serve as remarkable modification enzymes during numerous metabolite post-assembly lines to produce key intermediates or final products. Many prenylated NPs have shown to exhibit various biological activities.<sup>181</sup> PTs catalyze the prenyl transfer reaction from different prenyl donors, *e.g.*, dimethylallyl diphosphate (DMAPP, C<sub>5</sub>), geranyl diphosphate (GPP, C<sub>10</sub>) or farnesyl diphosphate (FPP,

C<sub>15</sub>) to various acceptors including nucleic acids and proteins, as well as aliphatic and aromatic small molecules.<sup>182</sup> PTs for small aromatic compounds are generally classified into membrane-embedded UbiA-type, bacterial and fungal ABBA-type including the fungal dimethylallyltryptophan synthase (DMATS)-type.<sup>183, 184</sup> PTs belonging to the DMATS superfamily mainly catalyze the prenylation of indole derivatives, either at the first pathway-specific step or at the later tailoring steps.<sup>183, 185</sup> DMATS PTs are also metal-independent enzymes, while in several cases, the addition of metal ions such as Ca<sup>2+</sup> and Mg<sup>2+</sup> enhances their activities.<sup>183</sup> So far, the DMATS enzymes that catalyze prenylation at all positions of the indole ring have been identified (N-1, C-2, C-3, C-4, C-5, C-6, and C-7 prenylating PTs).<sup>186, 187</sup> Structural analysis of the DMATS enzyme FgaPT2 identified in *Aspergillus fumigatus* revealed the overall structure of αββα PT folds.<sup>188</sup> In many cases, DMATS enzymes show a broad substrate flexibility towards aromatic substrates, while they exhibit a narrow specificity toward the length of prenyl donors.<sup>183, 185, 186</sup>

Oxidoreductases can catalyze different chemical reactions, e.g., hydroxylations, epoxidations, anthrone oxidations and oxidative rearrangements, which lead to enormous structural diversity.<sup>171</sup> Cytochrome P450 enzymes (P450s) are the most common biocatalysts in NP biosynthesis. Generally, P450s are a superfamily of heme-containing monooxygenases and catalyze hydroxylation and epoxidation steps.<sup>189</sup> The currently accepted catalytic mechanism for P450s employs a sophisticated, multi-step catalytic cycle involving a range of transient intermediates.<sup>190</sup> There are two major types of P450 redox systems: (i) two-component system comprising of a flavin adenine dinucleotide (FAD)-containing reductase (FdR) and an iron-sulfur containing ferredoxin (Fdx) reductase, which are usually present in most bacterial and mitochondrial P450s. (ii) One-component system including a single FAD- and flavin mononucleotide (FMN)-containing reductase, referred to cytochrome P450 reductase (CPR), as redox partner, which are mainly found in eukaryotic organisms.<sup>191</sup> Recently, despite the common transformations mediated by P450s like C-H, C-N hydroxylation and C=C double bond epoxidation, increasing cases demonstrated other intriguing P450s functions, e.g., C-C bond coupling, cleavage, and migration.<sup>192</sup> In fungi, numerous P450s are involved in the biosynthesis of a wide range of metabolites and catalyze extremely diverse oxidations.<sup>193-195</sup> The P450 enzyme VdoD from *Penicillium palitans* is responsible for the *meta* hydroxylation of cyclopenin.<sup>196</sup> KtnC from *Aspergillus niger* catalyzes the coupling of the monomeric coumarin 7-demethylsiderin both regio- and stereoselectively to the 8-8' dimer *P*-orlandin.<sup>197</sup>

Berberine bridge enzyme-like (BBE-like) proteins are a subgroup of the superfamily of FAD-linked oxidases and structurally characterized by a typical fold observed initially for vanillyl alcohol oxidase (VAO).<sup>198, 199</sup> Characteristic structural features of this family are an FAD binding domain that is formed by the N- and C-terminal parts of the protein, and a substrate binding domain, together with the isoalloxazine ring of FAD for efficient substrate binding and oxidation.<sup>200, 201</sup> While BBE-like proteins share a similar overall fold to that of other prototypic members of this superfamily, a specific structural feature, Y/FxN motif, in the N-terminal part of the FAD-binding site distinguishes the BBE family from

## INTRODUCTION

---

other FAD-linked oxidases.<sup>201, 202</sup> The representative functional example is found in the biosynthesis of isoquinoline alkaloids, where a BBE-like enzyme catalyzes the oxidative cyclization of (S)-reticuline to (S)-scoulerine to form the C-C bond.<sup>203</sup> BBE-like enzymes catalyze a broad range of reactions such as two-electron oxidations as reported for AtBBE-like protein 15<sup>204</sup> or four-electron oxidations for Dbv29.<sup>205</sup> More complex oxidations and ring closure reactions were discovered in the biosynthesis of the ergot alkaloid intermediate chanoclavine I and the indole alkaloid communesin.<sup>206, 207</sup> More recently, AsmF from *Streptomyces seoulensis* dictated the formation of the naphthalenic hydroxyl group in the ansaseomycin biosynthesis.<sup>208</sup> In another case, AspoA catalyzes an unusual protonation driven double bond isomerization in the biosynthesis of aspochalasin family compounds.<sup>209</sup>

Short-chain dehydrogenases/reductases (SDRs) constitute one of the largest and oldest protein superfamilies, which are widely present in archaea, eukaryotes, prokaryotes and viruses.<sup>210-212</sup> Their structures consist typically of Rossmann folds with a central  $\beta$ -sheet of 6–7 strands sandwiched between three  $\alpha$ -helices on both sides.<sup>213</sup> The conserved sequences of SDR contain typically around 250 amino acid residues. However, there are also SDRs with an additional 100-residue subunit in the C-terminal region.<sup>214</sup> The active site is formed by a catalytic tetrad of Asn Ser, Tyr, and Lys.<sup>213</sup> In contrast to other dehydrogenase superfamilies, no metal is required in SDRs at the active site. They utilize NAD(H) or NADP(H) as cofactors and the coenzyme-binding site is located at the N-terminal region.<sup>210</sup> Most of the SDR members are medium or long-chain dehydrogenase families and show diverse substrate spectra, including steroids, alcohols, sugars, aromatic compounds, and xenobiotics.<sup>215</sup> They play diverse roles in core metabolism and specific metabolism pathways such as steroidal metabolism, detoxification and drug resistance.<sup>216-218</sup>

To summarize, NPs have drastically improved our lives by providing an excellent source of molecules benefiting humans in various fields. All the above-mentioned studies undoubtedly expand the spectrum of NP biosynthetic pathways. Further accumulation of knowledge should be useful for engineering biosynthetic pathways to create novel bioactive NP derivatives.

## 2 Aims of this thesis

In this thesis, the following issues have been addressed:

### **Identification of a NRPKS as an isocoumarin synthase and demonstration of further conversions of the products by host enzymes**

NPs and derivatives contribute significantly to drug discovery and development.<sup>219</sup> Bioinformatic analysis and prediction of the putative genes or BGCs in the genome sequences have shown that most of these genes are silent or expressed only at a low level in the native producer under standard laboratory conditions.<sup>220</sup> For example, only four of the 56 putative gene clusters from *Penicillium crustosum* PRB-2 are expressed and their products were detected by LCMS analysis.<sup>67, 68, 221</sup> To exploit the genetic potential hidden in microbial genomes, different strategies have been developed to reactivate the silent clusters, *i.e.* by co-cultivation, media composition, optimization of the cultivation conditions, as well as manipulation of global regulators and transcription factors.<sup>222</sup> So far, heterologous expression represents a very mature and promising method for the identification of new NPs of cryptic or silent genes hidden in the genome sequences.<sup>111</sup> In this study, the silent NRPKS gene *pcr9304* from *P. crustosum* PRB-2 was heterologously expressed in an appropriate host. The following experiments were carried out:

- Bioinformatic analysis and identification of the NRPKS gene *pcr9304* from the sequenced genomes
- Assembly of the overexpression construct of *pcr9304* by homologous recombination in *E. coli*
- Generating the heterologous expression strain *A. nidulans* PX001 by introduction of the obtained expression construct into *A. nidulans* LO8030
- Cultivation of PX001 and LCMS analysis
- Isolation and structural elucidation of three isocoumarin derivatives from PX001
- Feeding experiments proved that the uncharacterized endogenous enzymes from the host *A. nidulans* were able to modify the initial polyketide product

### **Biosynthesis of 3-orsellinoxypropanoic acid in *Penicillium crustosum* requires a bifunctional NRPKS**

Polyketide NPs are structurally diverse and biologically active SMs produced by plants, bacteria, and fungi.<sup>223</sup> Their backbones are biosynthesized by PKSs which can be modified by multiple tailoring enzymes.<sup>176</sup> Among them, nonreducing fungal PKSs are usually responsible for the formation of aromatic acids like the archetypal phenolic polyketide orsellinic acid (OA) by orsellinic acid synthases (OSASs).<sup>224</sup> Until now, a large number of OSASs have been identified in bacteria and fungi. For example, the distinguished example OrsA (AN7909) from *Aspergillus nidulans* with two ACP domains catalyzes not only the formation of OA but also its dimerization. The domain structure and its function

for dimerization raised our interest in studying its homologues. In this study, a putative NRPKS OesA from *P. crustosum* PRB-2 was identified and successfully expressed in *A. nidulans* LO8030, leading to the identification of 3-orsellinoxipropanoic acid as its product. The ester bond formation in 3-orsellinoxipropanoic acid is likely an enzymatic or nonenzymatic transfer of the orsellinyl residue from OesA to the hydroxyl group of 3-hydroxypropionic acid (3-HP). Besides, it is also interesting to investigate the mechanism for the enzymatic transesterification which could be catalyzed either by the TE domain of OesA, as reported for other PKSs, or by an unknown host enzyme from *A. nidulans*. To understand the ester bond formation, the following experiments were carried out:

- Bioinformatic analysis of *P. crustosum* and further identification of the putative NRPKS OesA by sequence comparison with OrsA
- Heterologous expression of the NRPKS genes *oesA* and *orsA* in *A. nidulans* LO8030
- Large-scale fermentation of the respective heterologous expression transformants for isolation and structure elucidation of the secondary metabolites
- Deletion of the two ACP domains in the *oesA* overexpression strain
- Construction of the hybrid gene expression transformants with different domain combinations between *oesA* and *orsA*
- Elucidation of the origin of 3-orsellinoxipropanoic acid by feeding with different isotopic precursors
- Quantification of 3-orsellinoxipropanoic acid and OA in different transformants

#### **Biosynthesis of annullatin D in *Penicillium roqueforti* and the oxidative lactonization between two hydroxyl groups is catalyzed by a BBE-like enzyme**

NPs of HRPKSs are of great importance by exhibiting a broad range of biological activities. Iterative fungal HRPKSs together with additional enzymes like short-chain dehydrogenases were reported to synthesize alkylated salicylaldehyde or derivatives thereof. Despite the abundant SMs from *Penicillium roqueforti*, biosynthesis of only few natural products was reported. To strengthen our understanding on alkylated salicylaldehydes or derivatives, we used the *fog* gene cluster from *Aspergillus ruber*<sup>225</sup> as a probe for searching homologues in the genome of *Penicillium roqueforti* FM164 and identified a putative eleven-gene (*anu*) cluster with four genes of more than 40% identity to those of the *fog* cluster on the amino acid level. To identify the biosynthetic pathway of annullatins in *P. roqueforti*, the following experiments were carried out in cooperation with Bastian Kemmerich:

- Genome mining for annullatin biosynthetic gene cluster in *P. roqueforti*
- Heterologous expression of the whole *anu* cluster in *A. nidulans* LO8030
- Large-scale fermentation of the *anu* cluster expression strain for isolation and structure elucidation of the SMs

## AIMS OF THIS THESIS

---

- Functional proof of the genes from the *anu* cluster by gene deletion and pathway intermediate analysis *via* LCMS and NMR analyses
- *In vitro* characterization of the prenyltransferase AnuH with recombinant purified protein
- Verification of the functions of *anuE* and *anuG* by heterologous expression in *A. nidulans* and feeding experiments





### 3 Results and discussion

#### 3.1 Formation of isocoumarin by heterologous gene expression and modifications by host enzymes

Diverse NPs contribute significantly to drug discovery and development. Most of such so-called SMs are produced by actinobacteria or ascomycetous fungi from the genera *Penicillium* and *Aspergillus*.<sup>226-229</sup> The frequent occurrence of polyketides in bacteria, fungi, and plants makes them one of the most abundant and sophisticated SM groups.<sup>159, 230, 231</sup> Polyketides are generally synthesized by PKSs and then modified by diverse tailoring enzymes. As mentioned in section 1.3.1, most of the genes or BGCs for SMs are silent or only expressed at a low level under standard laboratory cultivation conditions. Therefore, different strategies have been developed to exploit these potentials.<sup>112</sup> A particularly mature and promising approach is heterologous expression.<sup>111</sup> In our previous study, only four of the 56 putative gene clusters from *Penicillium crustosum* PRB-2 are expressed and their products could be detected by LCMS analysis. Among them, three genes or gene clusters were activated after heterologous expression in *Aspergillus nidulans*.<sup>67, 68, 221</sup> Following this work, we analyzed the genome sequence of *P. crustosum* PRB-2 and selected a silent NRPKS gene *pcr9304* to prove its function.

Based on the bioinformatics analysis, *pcr9304* comprises nine exons of 1263, 354, 579, 24, 119, 85, 1623, 2346, and 51 bps, interrupted by eight introns of 54, 58, 58, 55, 53, 59, 65, and 75 bps, respectively. The coding sequence of *pcr9304* consists of 2147 amino acids and has a SAT-KS-AT-PT-ACP-ACP-TE domain structure. In addition, gene deletion did not lead to detectable SM changes in the  $\Delta$ *pcr9304* mutant compared with the wild type PRB-2, indicating that *pcr9304* was not expressed under our cultivation conditions. Therefore, we changed our strategy to heterologous expression in *A. nidulans*. For this purpose, the whole genomic sequence of *pcr9304* including its downstream region was amplified by PCR from genomic DNA of *P. crustosum*. Subsequently, the PCR fragment and linearized vector pYH-wA-pyrG<sup>232</sup> were mixed and transformed into *E. coli* DH5 $\alpha$  for homologous recombination. The assembled plasmid pPX001 was confirmed by enzyme restriction and then introduced into *A. nidulans* LO8030 by PEG-mediated protoplast transformation.<sup>232</sup> After selection by uridine and uracil autotrophy and subsequent confirmation by PCR amplification, the correct integration transformant *A. nidulans* PX001 was cultivated on rice medium for 14 days.

HPLC analysis of the EtOAc extract of the transformant culture showed that three additional peaks **1–3** were detected in comparison to the negative control strain (**Figure 11**). Subsequent isolation and structure elucidation by interpretation of their <sup>1</sup>H NMR spectra proved **1**, **2**, and **3** to be 6,8-dihydroxy-3-methylisocoumarin (**1**), 6,8-dihydroxy-3-hydroxymethylisocoumarin (**2**), and 6-methoxy-8-hydroxy-3-methylisocoumarin (**3**), respectively. All three compounds have been isolated from a number of fungal and bacteria strains including *Aspergillus terreus*.<sup>233, 234</sup> For example, together with its acidic form, **1** has been obtained from the heterologous expression *A. nidulans* transformant harboring the

## RESULTS AND DISCUSSION

NRPKS gene ATEG\_00145.1.<sup>106</sup> Another PKS gene *lcmM* from *Streptomyces* sp. MBT76 was also verified to be responsible for the formation of **1**.<sup>234</sup> However, Pcr9304 shares only 19 and 41 % sequence identities with *lcmM* and ATEG\_00145.1 on the amino acid level, respectively.

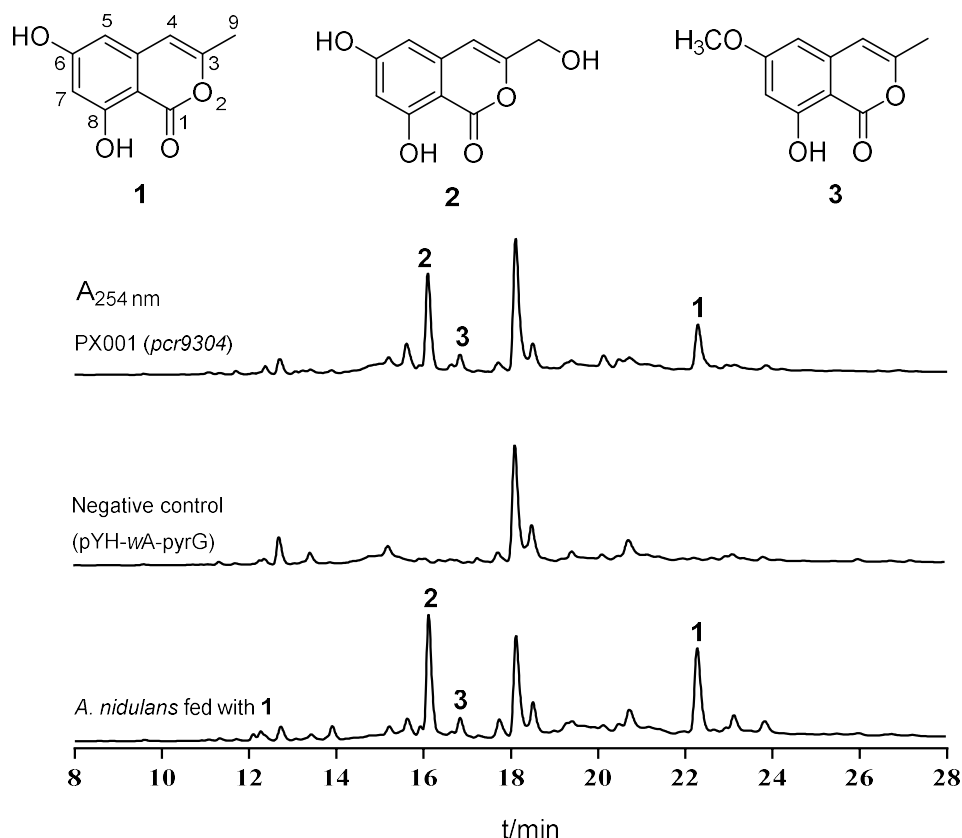


**Figure 11.** HPLC analysis of the secondary metabolites in 14 day-old *A. nidulans* strains with and without feeding.

Compounds **2** and **3** were unexpectedly accumulated as hydroxylated and methylated derivatives of **1**. This prompted us to investigate the origin of the hydroxylation and methylation activities, because no ketoreductase or methyltransferase domain was predicted in Pcr9304. It was reported that the heterologous host *A. nidulans* has the capability of hydroxylation activity at the benzene ring.<sup>225</sup> Therefore, we proposed that the endogenous enzymes from *A. nidulans* were responsible for the conversion of **1** to its hydroxylated product **2** and methylated product **3**. To verify this hypothesis, we synthesized **1**<sup>235</sup> and used it for feeding experiments in *A. nidulans* LO8030. LCMS analysis of the culture extract clearly showed the presence of **2** and **3** in the control strain without *pcr9304* after feeding with **1** (**Figure 11**). The integrity of the products was confirmed by comparison of their retention times, UV spectra and mass data including MS<sup>2</sup> fragmentation patterns.<sup>236</sup> The results proved that the host *A. nidulans* is able to modify the initial polyketide product **1** by hydroxylation at the methyl and

methylation of the 6-hydroxyl group. Unfortunately, no candidate enzymes from *A. nidulans* could be predicted for these two reactions.

In summary, we successfully expressed the NRPKS gene *pcr9304* from *P. crustosum* in *A. nidulans*, which led to the accumulation of three isocoumarins **1–3**, and proved its function as an isocoumarin synthase. Furthermore, feeding experiments revealed that the PKS product **1** can be converted by the uncharacterized endogenous host enzymes to its hydroxylated (**2**) and methylated (**3**) derivatives (**Figure 12**). Our results, thus, provide one additional example that unexpected further modifications of an enzyme product can take place in a heterologous host, which should always be taken in consideration for the interpretation of gene/cluster function.

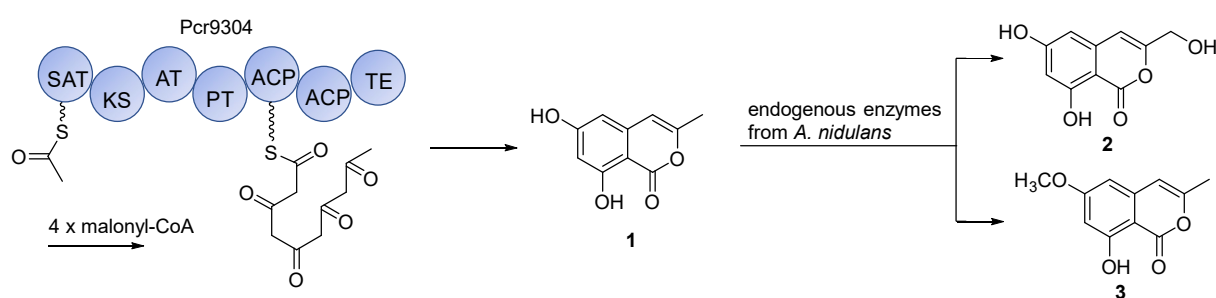


**Figure 12.** Formation of **1** and its conversion to **2** and **3** in *A. nidulans* LO8030.

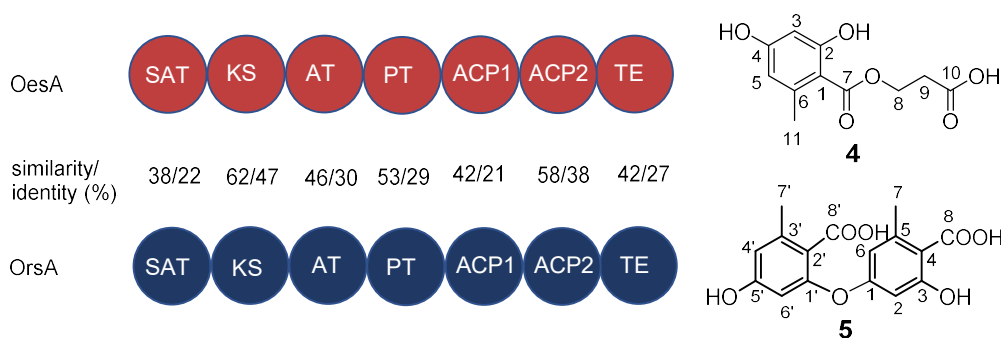
For details on this work, please see the publication (section 4.1)

**Pan Xiang**, Lena Ludwig-Radtke, Wen-Bing Yin, and Shu-Ming Li (2020). Isocoumarin formation by heterologous gene expression and modification by host enzymes. *Organic and Biomolecular Chemistry*, 18, 4946–4948, DOI: 10.1039/D0OB00989J.

### 3.2 Formation of 3-orsellinoxipropanoic acid in *Penicillium crustosum*

Polyketide NPs are a remarkable class of compounds with diverse structures and important biological activities. As mentioned in section 1.4.1, the fungal NRPKSs are usually responsible for the production of aromatic polyketides. Orsellinic acid (OA) is a representative simple archetypal phenolic polyketide formed through stepwise condensations of acetyl-CoA with three units of malonyl-CoA.<sup>163</sup> More than 200 OA derivatives, including monomers and polymers, have been identified in different species.<sup>237</sup> Until now, a large number of orsellinic acid synthases (OSAs) have been identified in bacteria and fungi. For example, OrsA (AN7909) from *Aspergillus nidulans* with two ACP domains catalyzes not only the OA formation, but also its dimerization.<sup>163, 238</sup> The domain structure and its function for dimerization raised our curiosity to study its homologues. In this study, the investigation on the PKS genes in *Penicillium crustosum* PRB-2 was continued and led to the identification of a putative NRPKS Pcr7502, termed OesA hereafter, in the genome of *P. crustosum*.

OesA comprises seven exons of 287, 286, 618, 933, 207, 3873, and 63 bps, interrupted by six introns of 56, 58, 61, 60, 60, and 73 bps, respectively. The deduced polypeptide of the coding sequence of *oesA* consists of 2088 amino acids. Bioinformatic analysis revealed that OesA has a similar domain architecture as OrsA, *i.e.* SAT-KS-AT-PT-ACP1-ACP2-TE and shares 32.2% sequence identity with OrsA on the amino acid level with each other (**Figure 13**). Identities of the four corresponding domains between the two proteins are less than 30%. No SM changes were detected in the *oesA* deletion mutant in comparison to the wild type. This suggests that *oesA* is probably a silent gene and not expressed under our cultivation conditions.



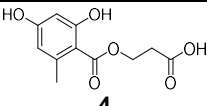
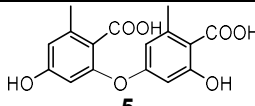
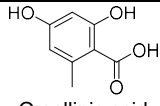










**Figure 13.** Domains structures of OesA and OrsA with their main products.

To investigate its function, the whole sequence of *oesA* including the terminator region of 517 bp was amplified from genomic DNA of *P. crustosum* PRB-2 and subsequently inserted into the expression vector pYH-wA-pyrG by homologous recombination in *Saccharomyces cerevisiae*. The obtained construct pPX15 was afterward heterologously expressed in *Aspergillus nidulans* LO8030,<sup>132</sup> resulting in the transformant *A. nidulans* PX15. LCMS analysis of the EtOAc extract of PX15 revealed the presence of an additional peak with a  $[M + Na]^+$  ion at  $m/z$  263.0522 for a deduced molecular formula

## RESULTS AND DISCUSSION

of C<sub>11</sub>H<sub>12</sub>O<sub>6</sub> compared to that of the negative control strain (**Table 1**). Detailed 1D and 2D NMR analyses revealed the accumulated product was an OA derivative and further determined as 3-orsellinoxypropanoic acid (**4**).

**Table 1.** Overview of the secondary metabolite profile of *A. nidulans* strains. Domains in OesA and OrsA are highlighted in red and blue, respectively.

Strains	 <b>4</b>	 <b>5</b>	 Orsellinic acid
<i>A. nidulans</i> (isogenic control)	–	–	–
PX15 	✓	–	–
PX26 	–	✓	–
PX29 	✓	–	–
PX30 	✓	–	–
PX31 	–	–	–
PX32 	✓	–	–
PX34 	–	–	–
PX35 	–	–	–
PX36 	–	–	–
PX37 	–	–	–

As aforementioned, OA can be modified by hydroxylation and methoxylation, as well as dimerization.<sup>239-242</sup> The ester bond formation in **4** is likely an enzymatic or nonenzymatic transfer of the orsellinyl residue from OesA to the hydroxyl group of 3-hydroxypropionic acid (3-HP), as observed for the precursor of ustethylin A.<sup>243</sup> The enzymatic transesterification could be catalyzed by the TE domain of OesA as reported for other PKSs<sup>244</sup> or by an unknown host enzyme from *A. nidulans*. To

## RESULTS AND DISCUSSION

understand the ester bond formation, *orsA* was also heterologously expressed in LO8030. LCMS analysis of the crude extracts of the *orsA* expression strain *A. nidulans* PX26 produced a sole product (**5**) in comparison to the negative control (**Table 1**). Detailed UV, MS, and  $^1\text{H}$  NMR data of **5** are consistent with those published previously.<sup>242</sup> Compound **5** was afterward identified as the OA dimer, diorcinolic acid (**5**). These results suggest that the enzymatic events were involved and also ruled out the involvement of host enzymes in the formation of **4**. Differing from OrsA with a dimerization activity for OA, OesA catalyzes the ester formation of OA with 3-HP.

After identification of OesA as an OA synthase, we focused on the functions of the two ACP and TE domains for detailed investigation. Feng et al. reported that both ACP domains in OrsA are involved in the OA dimerization.<sup>242</sup> We therefore deleted both ACPs in PX15 separately. As shown in **Table 1**, both deletion mutants, PX29 without ACP1 and PX30 lacking ACP2, can still produce **4**. These results demonstrated that both ACP1 and ACP2 contribute independently to the OA formation, as reported for other PKSs.<sup>242, 245, 246</sup>

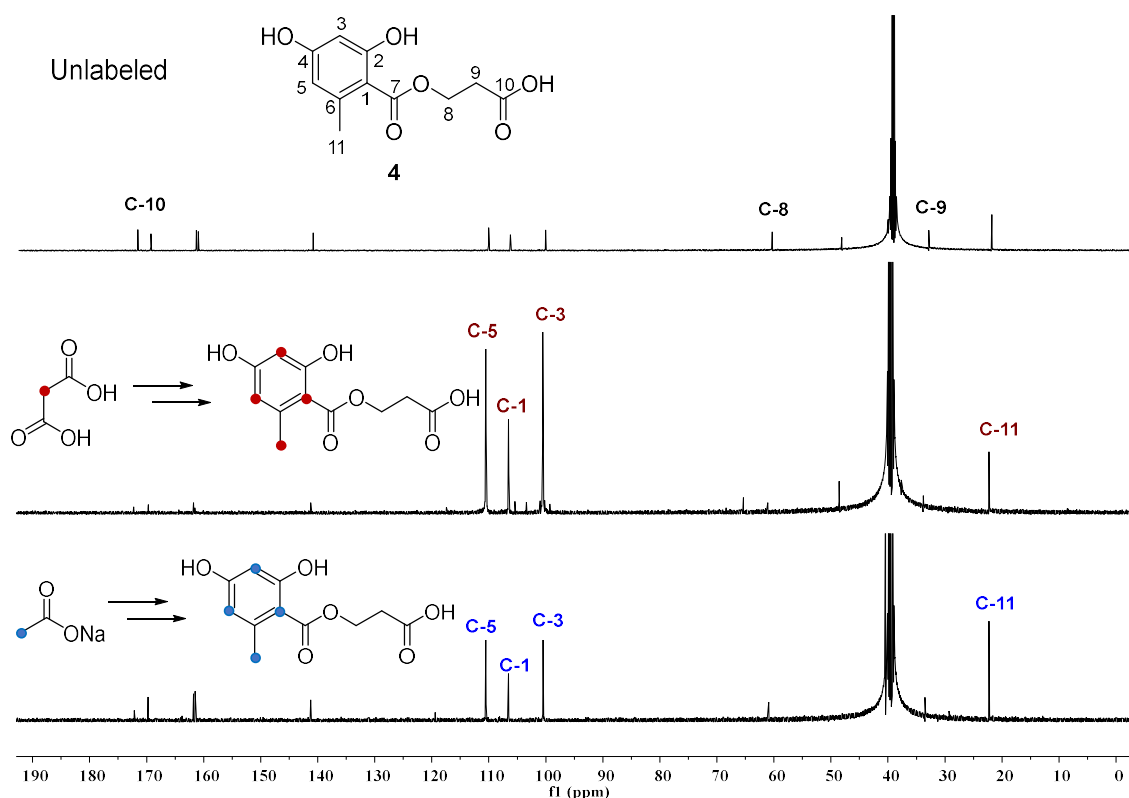


**Figure 14.**  $^{13}\text{C}$  NMR spectra of the unlabeled and labeled **4** after feeding with different precursors.

After identification of the functions of both ACPs in OesA, we then constructed several constructs with hybrid genes in pYH-wA-pyrG partially containing domains of *oesA* and *orsA*, resulting in different heterologous expression transformants (**Table 1**). LCMS analysis revealed that PX31, which contains the SAT-KS-AT-PT domains of OesA and the ACP1-ACP2-TE domains of OrsA, produced neither **4**

## RESULTS AND DISCUSSION

nor **5**, while PX32 which contains the SAT-KS-AT-PT domains of OrsA and the ACP1-ACP2-TE domains of OesA can still produce **4**. PX34 with the SAT-KS-AT-PT-ACP1 domains of OesA and the ACP2-TE domains of OrsA, and PX36 with the SAT-KS-AT-PT-ACP1-ACP2 domains of OesA and the TE domain of OrsA did not show any detectable SM changes, compared to the isogenic control. Similar negative results were obtained for PX35 with the SAT-KS-AT-PT-ACP1 domains of OrsA and the ACP2-TE domains of OesA as well as PX37, the SAT-KS-AT-PT-ACP1-ACP2 domains of OrsA with the TE domain of OesA (**Table 1**). These results proved that the ACP1-ACP2-TE domains of OesA are necessary for the ester bond formation in **4**. They can cooperate with SAT-KS-AT-PT domains of OrsA, but not *vice versa*. Notably, no OA was accumulated in the transformants PX34–PX37, indicating no gene expression, functional protein or product release from the PKS template.

To elucidate the origin of **4**, we carried out feeding experiments with sodium [2-<sup>13</sup>C] acetate and [2-<sup>13</sup>C] malonic acid in PX15. The <sup>13</sup>C NMR results provided direct evidence that C-1, C-3, C-5, and C-11 of the OA moiety of **4** are from four intact units of acetate or malonate (**Figure 14**). Besides, no enrichment was observed for the carbons in the 3-HP moiety, indicating that it is not originated from acetate or malonate. In view of the 3-HP metabolic pathways, we speculated that the 3-HP moiety could be derived from fumaric acid during the tricarboxylic acid cycle (TCA cycle).<sup>247, 248</sup>

Based on the above results, we speculated a formation mechanism for **4** in *Penicillium crustosum* (**Figure 15**). One acetyl-CoA condenses with three malonyl-CoA molecules on the OesA assembly line. The finished orsellinyl moiety is attached to ACP1 or ACP2. The TE domain catalyzes the transfer of the OA residue from both ACPs to 3-HP to form **4**.<sup>244, 249</sup>

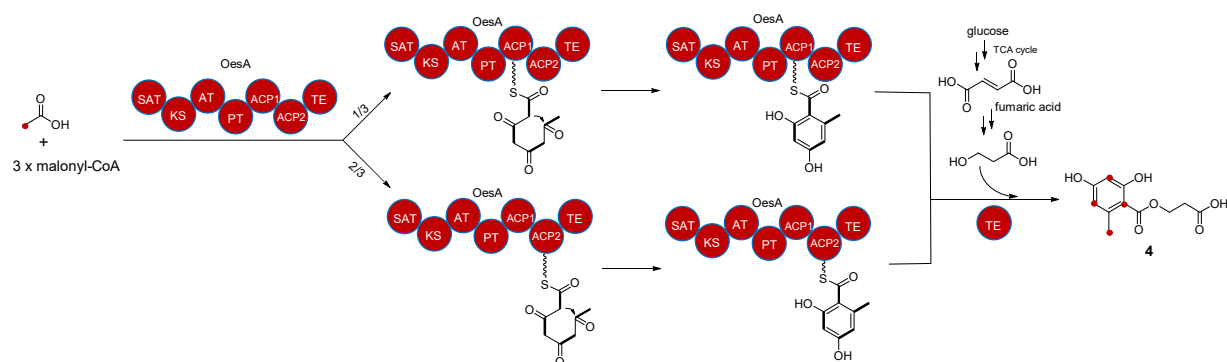


**Figure 15.** Proposed biosynthetic mechanism of 3-orsellinoxypropanoic acid.

Having proven the domain function of OesA, we also conducted a quantitative experiment to monitor the production of **4** and **5** in the producing strains. The accumulated **4** and **5** were quantified by LCMS. As shown in **Figure 16A**, after 10 days cultivation, the product yields reached their maximal values in the strains producing **4**. The sum of the two strains with ACP deletion, *i.e.* PX29 with ACP1 deletion ( $2.2 \pm 0.19$  mg/L) and PX30 with ACP2 deletion ( $1.1 \pm 0.04$  mg/L), is almost the same of PX15 without deletion ( $3.3 \pm 0.1$  mg/L). This suggests the independent and complementary contribution of both

ACPs for ester formation with 3-HP. On the other hand, the productivity of PX32 with the SAT-KS-AT-PT of OrsA at  $5.3 \pm 0.16$  mg/L is approximate 1.6-fold of that of PX15 with the intact OesA. This indicates that the SAT-KS-AT-PT domains of OrsA have a higher efficiency for assembling the orsellinyl residue than those of OesA and corresponds to the high product yield of the strain PX26 with OrsA ( $47.4 \pm 5.4$  mg/L) (**Figure 16B**). Meanwhile, these results suggest that the PKS-assembled orsellinyl moiety determined the yield of the final product.

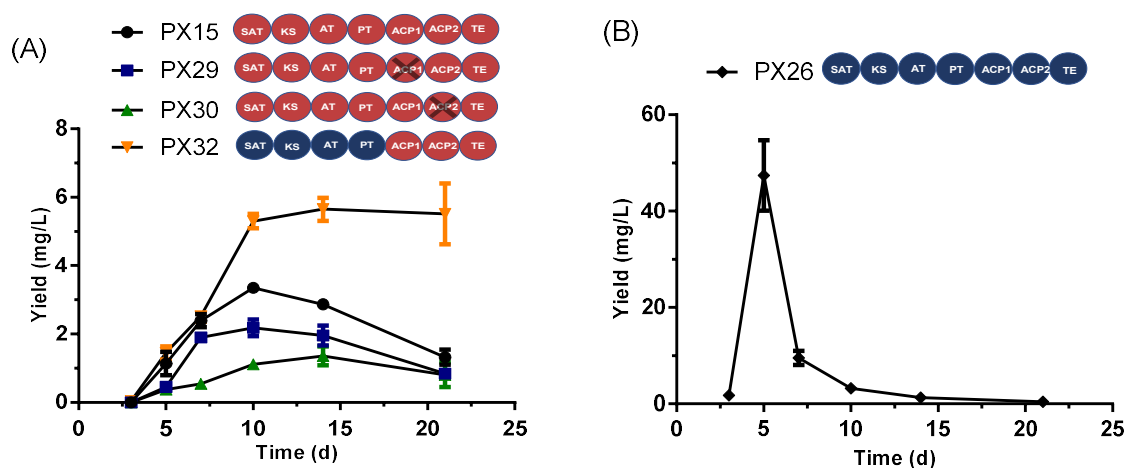


**Figure 16.** Dependence of (A) **4** and (B) **5** formation in *A. nidulans* on different cultivation times.

In conclusion, the NRPKS gene *oesA* from *P. crustosum* was successfully expressed in *A. nidulans* LO8030 and proved its role as an OA synthase and a transferase. Domain deletion and recombination provided evidence that both ACPs contribute independently and complementarily to the 3-orsellinoxipropanoic acid (**4**) formation. Feeding experiments provided evidence that only the orsellinyl residue is derived from acetate.

For details on this work, please see the publication (section 4.2)

**Pan Xiang** and Shu-Ming Li (2022). Formation of 3-orsellinoxipropanoic acid in *Penicillium crustosum* is catalyzed by a bifunctional nonreducing polyketide synthase. *Organic Letters*, 24 (1), 462–466, DOI: 10.1021/acs.orglett.1c04189.



### 3.3 Biosynthesis of annullatin D in *Penicillium roqueforti* requires a BBE-like enzyme for the five-member lactone ring formation

Filamentous fungi are known as promising sources for bio-active NPs. For example, the cholesterol-lowering agent lovastatin from *Aspergillus terreus* is one important representative NP produced by HRPKS.<sup>112, 250</sup> The HRPKSs exhibit a higher degree of complexity in their programming and selectively catalyzing  $\beta$ -keto reductions and dehydrations during each extension cycle.<sup>251</sup> It was reported that, together with additional enzymes like SDRs, P450, and a PT, a *fog* cluster containing a HRPKS was discovered for the flavoglauclin biosynthesis in *Aspergillus ruber*.<sup>225</sup> Such kind of alkylated salicylaldehydes or derivatives usually have biological activities<sup>252-254</sup> that intrigued our interest to discover more SMs like this in *Penicillium roqueforti* FM164. *P. roqueforti* is widespread in silage and natural environments and also found in food waste.<sup>255</sup> It is used during the process for making blue-veined cheeses.<sup>75</sup> Similar to other filamentous fungi, *P. roqueforti* has the potential to produce bioactive SMs, such as the antitumor active andrastins and the antibiotic or immunosuppressant mycophenolic acid.<sup>74, 227, 256</sup>

Therefore, we carried out genome mining in *P. roqueforti* by using antiSMASH<sup>257</sup> and by comparison with the *fog* cluster, leading to the identification of a putative *anu* cluster containing eleven genes (*anuA*–*K*). Four genes in the *anu* cluster share more than 40% identity to those of the *fog* cluster on the amino acid level (**Figure 17**). The putative *anu* cluster contains genes coding for a HRPKS (AnuA), four SDRs (AnuB, AnuD, AnuF, and AnuI), an unknown protein (AnuC), a P450 (AnuE), a BBE-like enzyme (AnuG), a PT (AnuH), an aromatic ring hydroxylating dehydrogenase (ARHD, AnuJ), and a transcription factor (TF, AnuK). Bioinformatic analysis of the genes from the *anu* cluster indicated their putative functions as shown in **Table 2**. Accordingly, the product of the *anu* cluster was speculated to be a prenylated derivative of alkylated salicylaldehyde.

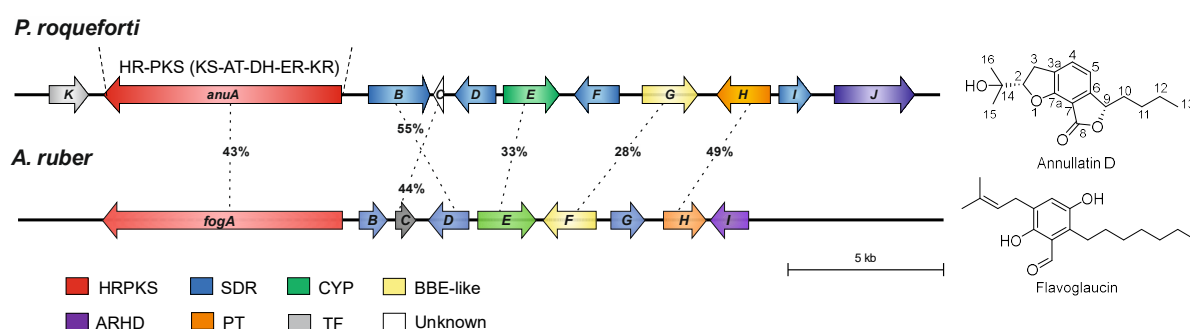


**Figure 17.** Comparison of the *anu* cluster in *P. roqueforti* with the *fog* cluster in *A. ruber*. The sequence identities on the amino acid level are given as percent.

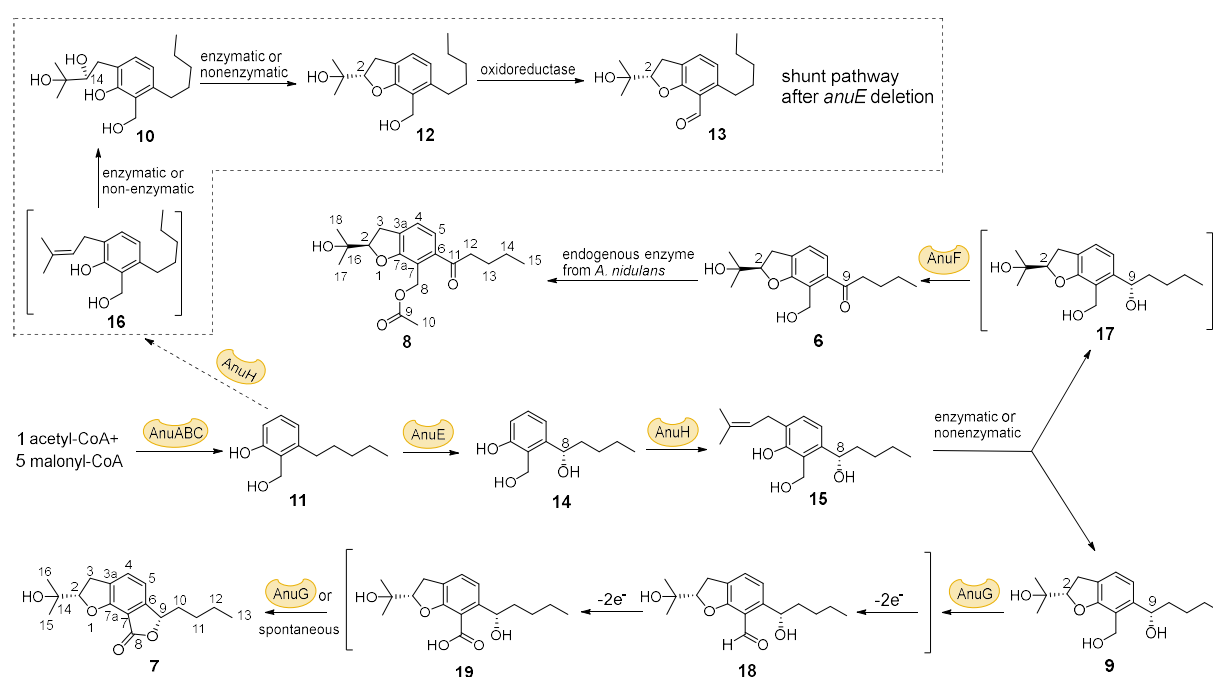
## RESULTS AND DISCUSSION

**Table 2.** Putative functions of the genes from *anu* gene cluster.

Protein (Acc. Nr.)	Size (AA)	Homologous protein, organism	Identity (%)	Putative function
AnuA (CDM34450.1)	2130	HRPKS (EYE95343) from <i>Aspergillus ruber</i>	43.1	HRPKS
AnuB (CDM34451.1)	283	SDR (EYE95338) from <i>Aspergillus ruber</i>	55.0	SDR
AnuC (CDM34452.1)	91	Hypothetical protein (EYE95337) from <i>Aspergillus ruber</i>	44.3	Hypothetical protein
AnuD (CDM34453.1)	381	SDR (KGO64723) from <i>Penicillium italicum</i>	87.7	SDR
AnuE (CDM34454.1)	490	P450 (EYE95339) from <i>Aspergillus ruber</i>	32.9	P450
AnuF (CDM34455.1)	276	SDR (RFU78523.1) from <i>Trichoderma arundinaceum</i>	70.1	SDR
AnuG (CDM34456.1)	509	Oxidoreductase (EYE95340) from <i>Aspergillus ruber</i>	28.1	BBE-like enzyme
AnuH (CDM34457.1)	451	PT (EYE95342) from <i>Aspergillus ruber</i>	49.2	PT
AnuI (CDM34458.1)	252	SDR (EYE95338) from <i>Aspergillus ruber</i>	22.6	SDR
AnuJ (CDM34459.1)	818	Monooxygenase (KGO64729) from <i>Penicillium italicum</i>	89.8	ARHD
AnuK (CDM34449.1)	261	TF (KGO64720) from <i>Penicillium italicum</i>	83.0	TF

To identify the pathway product, heterologous expression of the identified *anu* cluster in *Aspergillus nidulans* LO8030 was carried out. The cluster sequence was amplified from genomic DNA of *P. roqueforti* and cloned into the expression vector pJN017<sup>225</sup> by assembling in *S. cerevisiae*. The obtained construct was afterward integrated into the *A. nidulans* LO8030 genome. The resulting transformant *A. nidulans* BK08 was then cultivated in PDB liquid medium under static conditions. As expected, LCMS analysis of the extract from BK08 as well as isolation and structure elucidation proved the accumulation of **6** – **9**. This result also confirms that the *anu* cluster was indeed our target cluster. The MS, optical rotation, UV, and NMR data and spectra confirmed **7**, **8**, and **9** as annullatin derivatives by comparison with the reported data. The stereochemistry of **7** – **9** was determined by comparison of

its experimental ECD spectra with the calculated data, termed as (2S, 9S)-annullatin D, (2R)-annullatin G, and (2S, 9S)-annullatin H, respectively (**Figure 18**). However, attempts to obtain interpretable <sup>1</sup>H NMR spectrum for **6** failed, due to its instability during the routine isolation procedure. To overcome this, **6** in the BK08 extract was immediately acetylated for structural elucidation. MS and NMR analyses confirmed that the acetylated **6** should be **8**, which means **6** has a hydroxymethyl instead of an acetoxymethyl group at the aromatic ring in **8** and was termed as annullatin F (**Figure 18**). Since **8** appears only as a minor product in the culture of BK08 and there is no acetyltransferase in the *anu* cluster, we therefore speculate that acetylation of **6** to **8** was catalyzed by a host enzyme from *A. nidulans*.<sup>225, 258</sup> Further product conversion by host enzymes after gene expression was also observed in our previous works as described in section 3.1.



To investigate the biosynthetic pathway of annulatins and the function of each gene, deletion of single genes in BK08 and overexpression experiments in *A. nidulans* LO8030 were carried out. The HRPKS AnuA with a domain structure of KS-AT-DH-ER-KR was integrated into the host LO8030 genome under the control of the *gpdA* promoter to prove whether these annulatins are formed in a similar way as flavoglaucon. After cultivation in PDB media for 14 days, no additional product was detected by LCMS analysis in comparison to the control strain. This is in consistence with the results after expression of the PKS alone in the case of pyriculol,<sup>252</sup> sordarial,<sup>253</sup> and flavoglaucon.<sup>225</sup> Accumulation of aromatic polyketide products requires additional enzymes for modification, cyclization, and release of the PKS-assembled products. Accordingly, AnuBC would be these candidates.

## RESULTS AND DISCUSSION

In the deletion mutants of the SDRs AnuD, AnuI, and AnuJ, **6** – **9** were clearly detected, whereas no additional products accumulated, proving these genes are likely not involved in the annullatin formation.

Deletion of the P450 gene *anuE* resulted in the abolishment of **6** – **9**, but accumulation of **10** – **13** (**Figure 18**). Structure elucidation proved that **10** – **13** are annullatin derivatives without the oxygen function at the C<sub>5</sub> side chain. It can be deduced that AnuE catalyzes the hydroxylation of **11** at the side chain in the biosynthesis of **6** – **9**. The accumulated **11** in the  $\Delta$ *anuE* mutant was further metabolized to **10**, **12**, and **13** by other tailoring enzymes. To verify this hypothesis, we fed the precursor **11** to the *anuE* heterologous expression transformant. As expected, **11** was converted to **14** with a conversion yield of 92% after cultivation in PDB medium for 4 days (**Figure 19A**). The MS data and <sup>1</sup>H NMR spectrum of **14** revealed that there was an additional hydroxyl group at the C<sub>5</sub> side chain, proving AnuE as a hydroxylase.

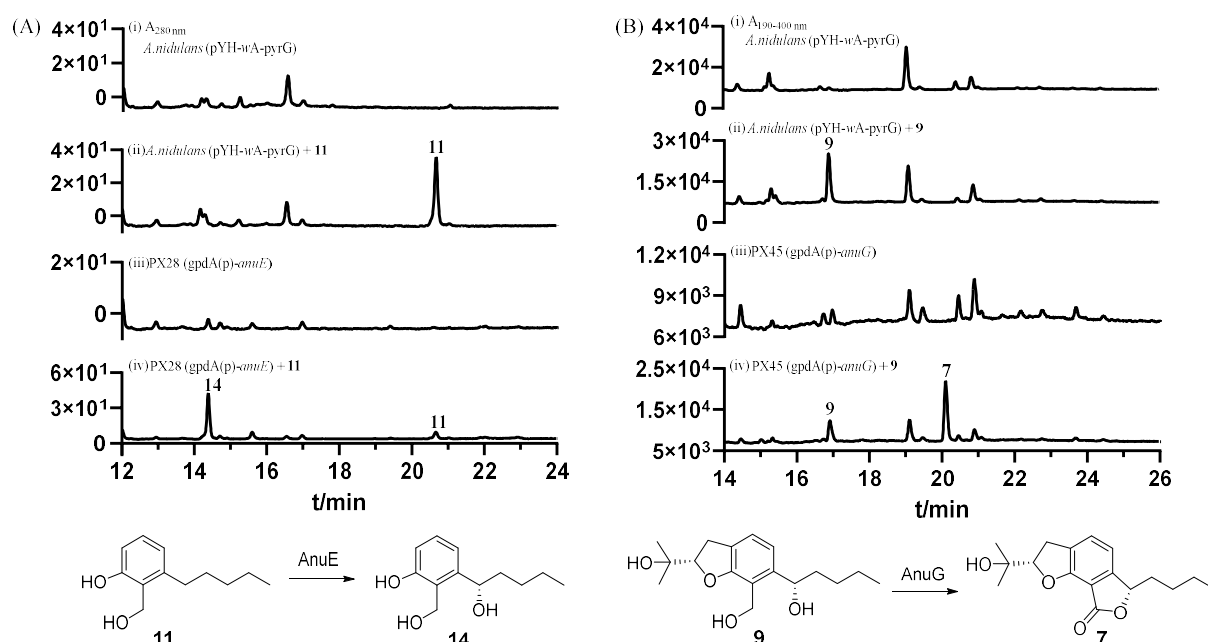


**Figure 19.** HPLC analysis of culture extracts. (A) With and without feeding of **11** to *anuE* expression strain PX28 and to the control strain. (B) With and without feeding of **9** to *anuG* expression strain PX45 and to the control strain.

Deletion of the PT gene *anuH* also completely abolished the production of **6** – **9**, but led to accumulation of **14** as the sole product, which indicated that the AnuE product **11** is a substrate of the PT AnuH. To confirm this hypothesis, the coding region of *anuH* without any introns was amplified from cDNA of *P. roqueforti* FM164. Subsequently, the *anuH* fragment was ligated into the expression vector pET-28a (+) with T4 DNA ligase. The obtained construct pPX52 was afterward expressed in *E. coli* BL21(DE3) and the recombinant AnuH was purified via Ni-NTA agarose and gel filtration. Incubation of AnuH and **14** with DMAPP as the prenyl donor at 37 °C for 30 min and 4 h resulted in

## RESULTS AND DISCUSSION

the formation of a prenylated product **15** with a conversion yield of 30% and 73%, respectively (**Figure 20A**). The results showed that AnuH exhibited clear activities toward **14** in the presence of DMAPP. Determination of the kinetic parameters for AnuH gave a  $K_M$  of 0.08 mM toward **14** and a  $K_M$  of 0.49 mM toward DMAPP. The average turnover number ( $k_{cat}$ ) was calculated to be  $0.13\text{ s}^{-1}$ . AnuH had no activity when GPP and FPP were used as prenyl donors (**Figure 20A**). Compound **11** without the hydroxyl group at the side chain was also accepted by AnuH, but only with low conversion yields, *i.e.* 4% after 30 min and 16% after 5 h incubation (**Figure 20B**). Due to the low conversion of **11**, it is difficult to determine the structures in this study. However, based on the results obtained from the  $\Delta anuE$  mutant and MS analysis, one of the prenylation products is expected to be **16**, the precursor of **10**, in the shunt pathway (**Figure 18**), which was subsequently metabolized to **10**, **12**, and **13**.

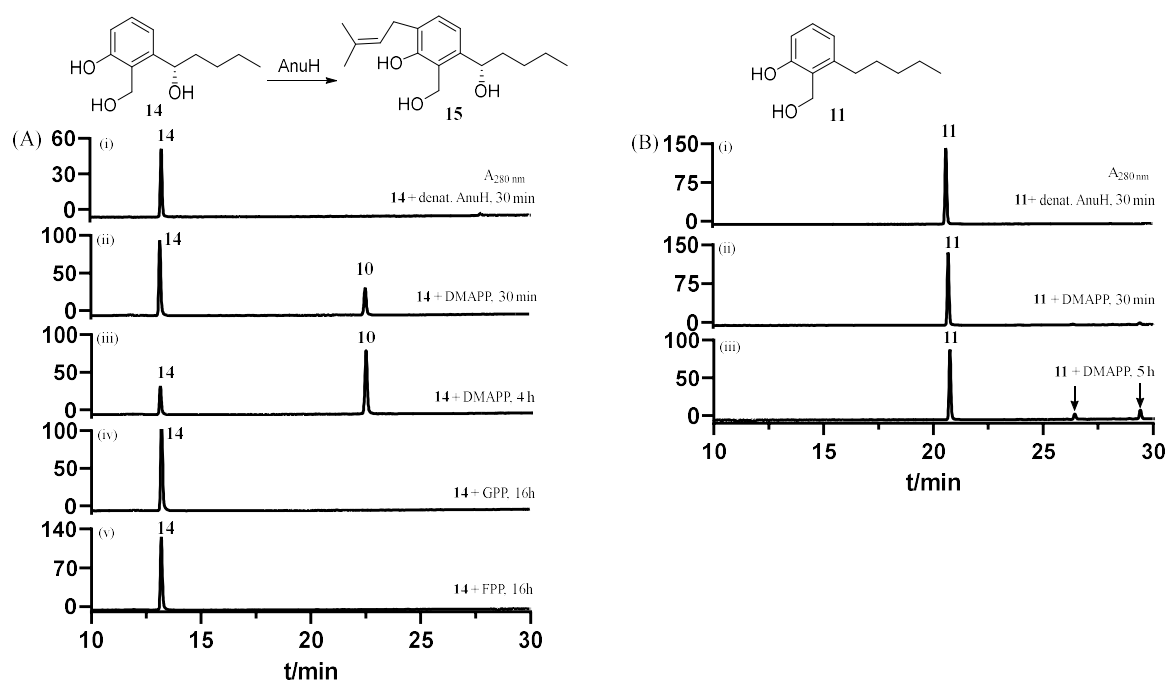


**Figure 20.** LCMS analysis of *in vitro* assays of AnuH. (A) With its natural substrate **14**. (B) With the precursor **11**.

Having identified the function of *anuE* and *anuH*, we intended to investigate the five-member lactone ring formation in annullatin D (**7**). LCMS analysis of the  $\Delta anuF$  mutant revealed the abolishment of **6** and **8**, whereas **7** and **9** were accumulated, implying the role of AnuF in the formation of **6**. Deletion of the BBE-like enzyme coding gene *anuG* indeed led to the accumulation of **6**, **8**, and **9**, but not that of **7**. Feeding **9** to the *anuG* overexpression *Aspergillus nidulans* strain led to the production of **7**, which clearly provided that AnuG catalyzed the five-member lactone ring formation in **7** *via* oxidative lactonization between the two hydroxyl groups (**Figure 19B**). BBE-like enzymes are a subfamily of flavin-containing proteins and usually catalyze diverse oxidations including dehydrogenation-mediated

C-C or C-N bond formation in the natural product biosynthesis.<sup>198, 201, 259, 260</sup>

Taken together, we identified a silent biosynthetic gene cluster for annullatins in *P. roqueforti* and postulated their biosynthetic pathway for (2*R*)-annullatin F (**6**) and (2*S*, 9*S*)-annullatin D (**7**) by heterologous expression, gene deletion, feeding experiments and biochemical investigations (**Figure 18**). As reported previously, the annullatin backbone is assembled by cooperation of AnuABC and hydroxylated at the C<sub>5</sub> alkyl chain by the cytochrome P450 AnuE. The prenyltransferase AnuH subsequently acts as a key enzyme to install one isoprenyl group at the benzene ring to form **15**. However, **15** was not identified in the deletion mutants obtained in this study. Enzymatic or non-enzymatic dihydrobenzofuran ring formation between the prenyl and the phenolic hydroxyl groups in **15** results in two diastereomers **9** and **17**. Similar reactions were also observed in many NPs biosynthesis.<sup>261</sup> Compound **9** is then converted to **7** by the BBE-like enzyme AnuG-catalyzed five-member lactone ring formation. Conversion of **9** to **7** requires extraction of four electrons from the substrate. It can be postulated that the hydroxymethyl group is first oxidized *via* aldehyde **18** to acid **19**, which then undergoes a spontaneous or AnuG-catalyzed lactonization with the hydroxyl group in the side chain. The SDR enzyme AnuF can accept the isomer **17** as a substrate and oxidize it to **6**, which is subsequently acetylated by an acetyltransferase from *A. nidulans*, leading to the formation of **8**. Consecutive and coordinated modifications enable (intramolecular) oxidation and condensation to form the final products **6** and **7**. Notably, we identified a new BBE-like enzyme for oxidative lactonization between two hydroxyl groups. To the best of our knowledge, no such functions have been reported for BBE-like enzymes prior to this study.

For details on this work, please see the publication (section 4.3)

**Pan Xiang\***, Bastian Kemmerich\*, Li Yang, and Shu-Ming Li (2022). Biosynthesis of annullatin D in *Penicillium roqueforti* implies oxidative lactonization between two hydroxyl groups catalyzed by a BBE-like enzyme. *Organic Letters*, 24 (32), 6072–6077, DOI: 10.1021/acs.orglett.2c02438. (\*equal contribution)

## **4 Publications**

### **4.1 Isocoumarin formation by heterologous gene expression and modification by host enzymes**







Cite this: *Org. Biomol. Chem.*, 2020, **18**, 4946

Received 13th May 2020,  
Accepted 22nd June 2020

DOI: 10.1039/d0ob00989j

rsc.li/obc

## Isocoumarin formation by heterologous gene expression and modification by host enzymes†

Pan Xiang,<sup>a</sup> Lena Ludwig-Radtke,<sup>a</sup> Wen-Bing Yin <sup>b</sup> and Shu-Ming Li \*<sup>a</sup>

**Heterologous expression has been proven to be a successful strategy for the identification of metabolites encoded by cryptic/silent genes. Expression of a nonreducing polyketide synthase (NR-PKS) gene from *Penicillium crustosum* in *Aspergillus nidulans* led to the accumulation of three isocoumarins 1–3. Feeding experiments revealed that the PKS product 1 can be converted by the host enzymes to its hydroxylated (2) and methylated (3) derivatives. These results provided one additional example that unexpected further modifications of an enzyme product can take place in a heterologous host.**

Natural products or derivatives contribute significantly to drug discovery and development.<sup>1</sup> Most of such so-called secondary metabolites are produced by actinobacteria<sup>2</sup> or ascomycetous fungi from the genera *Penicillium* and *Aspergillus*.<sup>3</sup> The majority of the known secondary metabolites belong to four important classes, *i.e.* polyketides, nonribosomal peptides, terpenoids and alkaloids.<sup>4</sup> Polyketides derived usually from acetyl-CoA and malonyl-CoA display a wide range of biological and pharmacological activities<sup>3</sup> and therefore have great commercial value. Polyketides are assembled in bacteria,<sup>5</sup> fungi<sup>6,7</sup> and plants<sup>8</sup> by multimodule polyketide synthases (PKSs) and then modified by diverse tailoring enzymes. In general, the genes for the biosynthesis of a given metabolite are organized into the so-called biosynthetic gene clusters. Bioinformatics analysis and prediction of putative gene clusters in the genome sequences and comparison with those of the accumulated metabolites in the native producer have shown that most of these genes are silent or their expression is very low under standard laboratory conditions.<sup>9</sup> For example, only four of the

56 putative gene clusters from *Penicillium crustosum* PRB-2<sup>10–12</sup> are expressed and their products could be detected by LC-MS analysis. To exploit the genetic potential hidden in microbial genomes, different strategies have been developed to reactivate silent clusters. These include optimisation of the cultivation conditions, media composition, and co-cultivation and the use of biotic and abiotic elicitors.<sup>13,14</sup> Significant success was also achieved by manipulation of global regulators and transcription factors.<sup>15–17</sup>

In addition, heterologous expression of secondary metabolite genes or whole gene clusters in an appropriate host is a very mature and promising method for the identification of new natural products of cryptic or silent genes hidden in the genome sequences.<sup>18,19</sup> Besides *Escherichia coli* and *Saccharomyces cerevisiae*, filamentous fungi, especially the genus *Aspergillus* are the most widely used heterologous expression hosts for functional proof of fungal genes and metabolite production. In recent years, the model organism *Aspergillus nidulans* has become an established and frequently used host for the expression of fungal genes.<sup>20–22</sup> Besides *A. nidulans*, other *Aspergillus* strains such as *A. oryzae* and *A. niger* were also proven to be suitable expression hosts.<sup>23</sup> However, heterologous expression may be hindered by host-dependent factors, such as insufficient or missing supply of biosynthetic precursors, different intron splicing behavior compared to the native host or host-dependent cross-chemistry. In a recent study, Geib *et al.*<sup>24</sup> detected host-dependent product formation in *A. niger* and *A. oryzae*. A similar phenomenon has also been observed in *Streptomyces* species.<sup>25,26</sup>

Using heterologous expression in *A. nidulans*, we provide in this study experimental evidence that the silent nonreducing polyketide synthase (NR-PKS) gene *pcr9304* from *P. crustosum* PRB-2 codes for an isocoumarin synthase. We observed furthermore modifications of the PKS product by the endogenous *A. nidulans* enzymes.

The deduced polypeptide Pcr9304 of the coding sequence of the candidate gene comprises 2147 amino acids and has a SAT-KS-AT-PT-ACP-ACP-TE domain structure (SAT: starter acyl

<sup>a</sup>Institut für Pharmazeutische Biologie und Biotechnologie, Philipps-Universität Marburg, Robert-Koch-Straße 4, 35037 Marburg, Germany.

E-mail: shuming.li@staff.uni-marburg.de

<sup>b</sup>State Key Laboratory of Mycology, Institute of Microbiology, Chinese Academy of Sciences, Beijing 100101, China

†Electronic supplementary information (ESI) available: Experimental procedures, NMR data and spectra. See DOI: 10.1039/d0ob00989j

transferase, KS: ketosynthase, AT: acyltransferase, PT: product template, ACP: acyl carrier protein, and TE: thioesterase). BLASTP search did not show significant sequence similarities with functionally characterised proteins and its function therefore cannot be predicted by sequence analysis and comparison. Gene deletion did not lead to detectable secondary metabolite changes in the  $\Delta pcr9304$  mutant, in comparison to the wildtype *P. crustosum* PRB-2. This indicates no expression of this gene under our cultivation conditions (Li and Kindinger, unpublished results).

To prove its function, we changed our strategy to heterologous expression in *Aspergillus nidulans*. For this purpose, a 6921 bp fragment containing the whole genomic sequence of *pcr9304* and a downstream region of 633 bp containing the native terminator was amplified *via* PCR and cloned into the expression vector pYH-wA-pyrG<sup>27</sup> by homologous recombination in *E. coli*.<sup>28</sup> The obtained construct pPX001 (Fig. S1†) was introduced into *A. nidulans* LO8030<sup>20</sup> by polyethylene glycol-mediated protoplast transformation. After selection by uridine and uracil autotrophy and subsequent confirmation by PCR amplification, ten resulting integration transformants includ-

ing PX001 were cultivated on solid rice medium. The 14 day-old cultures were extracted with ethyl acetate and analyzed by LC-MS for secondary metabolites. All ten extracts showed similar metabolite profiles. As shown in Fig. 1 for the representative transformant PX001, three additional peaks of 1–3 were detected in the extract in comparison to that of the control strain with the empty vector pYH-wA-pyrG. The three compounds share similar UV spectra with absorption maxima at 245 and 325 nm (Fig. S2†).  $[M + H]^+$  ions at  $m/z$  = 193.0493 for 1, 209.0451 for 2 and 207.0663 for 3 indicate the difference between them by hydroxylation and methylation. Isolation and structure elucidation by <sup>1</sup>H NMR analysis (Table S1, ESI†) proved 1, 2 and 3 to be 6,8-dihydroxy-3-methylisocoumarin, 6,8-dihydroxy-3-hydroxymethylisocoumarin and 6-methoxy-8-hydroxy-3-methylisocoumarin,<sup>29,30</sup> respectively. All the three compounds have been isolated from a number of fungal and bacterial strains including *Aspergillus terreus*.<sup>31,32</sup>

Compound 1 had been obtained, together with its acid form, from a *A. nidulans* transformant harboring NR-PKS ATEG\_00145.1 from *Aspergillus terreus*.<sup>20</sup> This transformant also produced 4-hydroxy-6-methyl-2-pyrone as the major and orsellinic acid as the minor product. Wu *et al.* proposed that the PKS IcmM from *Streptomyces* sp. MBT76 should be responsible for the formation of compound 1.<sup>32</sup> Interestingly, Pcr9304 shares sequence identities of only 19 and 41% at the amino acid level with IcmM and ATEG\_00145.1, respectively.

Unexpected accumulation of compounds 2 and 3 as hydroxylated and methylated derivatives of 1 raised the question on the origin of the hydroxylation and methylation activities, because no ketoreductase or methyl transferase domain was predicted in Pcr9304. In a previous work,<sup>33</sup> we observed the hydroxylation activity at the benzene ring from the heterologous host *A. nidulans*. Therefore, we proposed that endogenous enzymes from *A. nidulans* were also responsible for the conversion of 1 to 2 and 3. Intrigued by this hypothesis, we synthesized compound 1 as reported previously<sup>34</sup> and used it for feeding experiments in *A. nidulans* LO8030.

Already one day after feeding with compound 1, LC-MS analysis of the culture extract clearly revealed the presence of 2 and 3 (data not shown). The amounts of the converted products increased steadily in the following 7 days (Fig. 1). The integrity of the products was confirmed by comparison of their retention times, UV spectra, mass data including MS<sup>2</sup> fragmentation patterns. This proved that *A. nidulans* can modify the

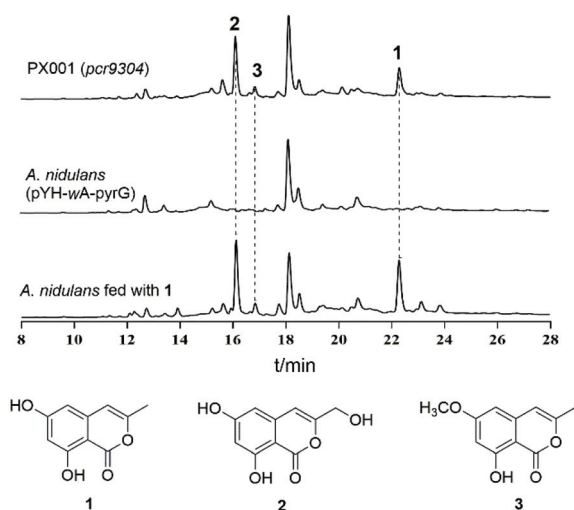


**Fig. 1** HPLC analysis of the secondary metabolites in *A. nidulans* strains with and without feeding. UV absorptions at 254 nm are illustrated. Extracted ion chromatograms (EICs) for the  $[M + H]^+$  ions detected at  $m/z$  193.049  $\pm$  0.005 (1),  $m/z$  209.045  $\pm$  0.005 (2) and 207.066  $\pm$  0.005 (3).

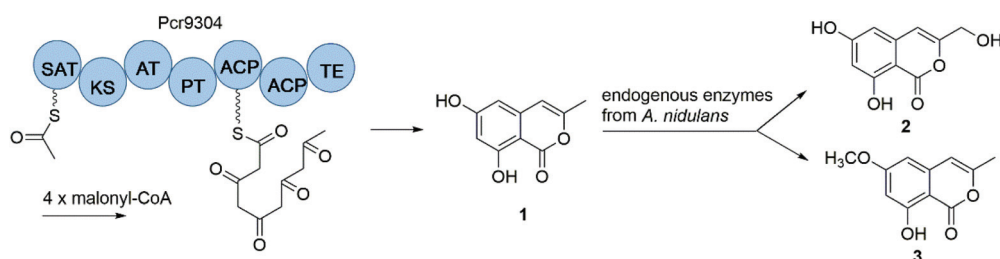


**Fig. 2** Formation of 1 and its conversion to 2 and 3 in *A. nidulans* LO8030.

initial polyketide product **1** by hydroxylation at the methyl and methylation of the 6-hydroxyl group. Unfortunately, no candidate enzymes from *A. nidulans* could be predicted for these two reactions.

In summary, we successfully expressed the NR-PKS gene *pcr9304* from *P. crustosum* in *A. nidulans* and proved its function as an isocoumarin synthase. Furthermore, we demonstrated by feeding experiment that **2** and **3** are modification products of **1** by uncharacterized endogenous host enzymes (Fig. 2). Our results, thus, provide one additional example that the products of a heterologous expressed gene can be further converted by host enzymes, which should always be taken into consideration for the interpretation of gene/cluster function.

## Conflicts of interest

The authors declare no competing financial interest.

## Acknowledgements

We thank S. Newel and R. Kraut from the Philipps-Universität Marburg for performing NMR and MS analyses, respectively. This project was funded in part by the Deutsche Forschungsgemeinschaft (DFG)-Li844/11-1 and INST 160/620-1 as well as the National Natural Science Foundation of China-31861133004. Pan Xiang (201708530222) is a recipient of a scholarship from the China Scholarship Council.

## Notes and references

- 1 D. J. Newman and G. M. Cragg, *J. Nat. Prod.*, 2020, **83**, 770–803.
- 2 E. A. Barka, P. Vatsa, L. Sanchez, N. Gaveau-Vaillant, C. Jacquard, H. P. Klenk, C. Clément, Y. Ouhdouch and G. P. Van Wezel, *Microbiol. Mol. Biol. Rev.*, 2016, **80**, 1–43.
- 3 G. F. Bills and J. B. Gloer, *Microbiol. Spectrum*, 2016, **4**, 1–32.
- 4 N. P. Keller, *Nat. Rev. Microbiol.*, 2019, **17**, 167–180.
- 5 H. Chen and L. Du, *Appl. Microbiol. Biotechnol.*, 2016, **100**, 541–557.
- 6 Y. M. Chiang, B. R. Oakley, N. P. Keller and C. C. Wang, *Appl. Microbiol. Biotechnol.*, 2010, **86**, 1719–1736.
- 7 R. J. Cox, *Org. Biomol. Chem.*, 2007, **5**, 2010–2026.
- 8 I. J. Flores-Sanchez and R. Verpoorte, *Plant Physiol. Biochem.*, 2009, **47**, 167–174.
- 9 A. A. Brakhage, P. Spröte, Q. Al-Abdallah, A. Gehrke, H. Plattner and A. Tuncher, *Adv. Biochem. Eng./Biotechnol.*, 2004, **88**, 45–90.
- 10 J. Fan, G. Liao, L. Ludwig-Radtke, W.-B. Yin and S.-M. Li, *Org. Lett.*, 2020, **22**, 88–92.
- 11 J. Fan, G. Liao, F. Kindinger, L. Ludwig-Radtke, W.-B. Yin and S.-M. Li, *J. Am. Chem. Soc.*, 2019, **141**, 4225–4229.
- 12 F. Kindinger, J. Nies, A. Becker, T. Zhu and S.-M. Li, *ACS Chem. Biol.*, 2019, **14**, 1227–1234.
- 13 H. B. Bode, B. Bethe, R. Hofs and A. Zeeck, *ChemBioChem*, 2002, **3**, 619–627.
- 14 N. P. Ariantari, G. Daletos, A. Mándi, T. Kurtán, W. E. G. Müller, W. Lin, E. Ancheeva and P. Proksch, *RSC Adv.*, 2019, **9**, 25119–25132.
- 15 R. H. Cichewicz, *Nat. Prod. Rep.*, 2010, **27**, 11–22.
- 16 A. Gacek and J. Strauss, *Appl. Microbiol. Biotechnol.*, 2012, **95**, 1389–1404.
- 17 H. Lin, H. Lyu, S. Zhou, J. Yu, N. P. Keller, L. Chen and W.-B. Yin, *Org. Biomol. Chem.*, 2018, **16**, 4973–4976.
- 18 T. Hautbergue, E. L. Jamin, L. Debrauwer, O. Puel and I. P. Oswald, *Nat. Prod. Rep.*, 2018, **35**, 147–173.
- 19 Y. He, B. Wang, W. Chen, R. J. Cox, J. He and F. Chen, *Biotechnol. Adv.*, 2018, **36**, 739–783.
- 20 Y. M. Chiang, C. E. Oakley, M. Ahuja, R. Entwistle, A. Schultz, S. L. Chang, C. T. Sung, C. C. Wang and B. R. Oakley, *J. Am. Chem. Soc.*, 2013, **135**, 7720–7731.
- 21 D. Lubertozzi and J. D. Keasling, *Biotechnol. Adv.*, 2009, **27**, 53–75.
- 22 J. Yaegashi, B. R. Oakley and C. C. Wang, *J. Ind. Microbiol. Biotechnol.*, 2014, **41**, 433–442.
- 23 D. C. Anyaogu and U. H. Mortensen, *Front. Microbiol.*, 2015, **6**, 77.
- 24 E. Geib, F. Baldeweg, M. Doerfer, M. Nett and M. Brock, *Cell Chem. Biol.*, 2019, **26**, 223–234.
- 25 C. Huang, C. Yang, W. Zhang, L. Zhang, B. C. De, Y. Zhu, X. Jiang, C. Fang, Q. Zhang, C. S. Yuan, H. W. Liu and C. Zhang, *Nat. Commun.*, 2018, **9**, 2088.
- 26 J. Liu, X. Xie and S.-M. Li, *Angew. Chem., Int. Ed.*, 2019, **58**, 11534–11540.
- 27 W. B. Yin, Y. H. Chooi, A. R. Smith, R. A. Cacho, Y. Hu, T. C. White and Y. Tang, *ACS Synth. Biol.*, 2013, **2**, 629–634.
- 28 A. P. Jacobus and J. Gross, *PLoS One*, 2015, **10**, e0119221.
- 29 H. Kumagai, M. Amemiya, H. Naganawa, T. Sawa, M. Ishizuka and T. Takeuchi, *J. Antibiot.*, 1994, **47**, 440–446.
- 30 W. A. Ayer, S. K. Attah-Poku, L. M. Browne and H. Orszanska, *Can. J. Chem.*, 1987, **65**, 765–769.
- 31 C. Zaehle, M. Gressler, E. Shelest, E. Geib, C. Hertweck and M. Brock, *Chem. Biol.*, 2014, **21**, 719–731.
- 32 C. Wu, H. Zhu, G. P. Van Wezel and Y. H. Choi, *Metabolomics*, 2016, **12**, 90.
- 33 J. Nies, H. Ran, V. Wohlgemuth, W. B. Yin and S.-M. Li, *Org. Lett.*, 2020, **22**, 2256–2260.
- 34 S. Nomoto and K. Mori, *Liebigs Ann.*, 1997, **1997**, 721–723.

## Supporting Information

### **Isocoumarin formation by heterologous gene expression and modification by host enzymes**

Pan Xiang,<sup>a</sup> Lena Ludwig-Radtke,<sup>a</sup> Wen-Bing Yin,<sup>b</sup> and Shu-Ming Li<sup>\*a</sup>

<sup>a</sup>Institut für Pharmazeutische Biologie und Biotechnologie, Philipps-Universität Marburg, Robert-Koch-Straße 4, Marburg 35037, Germany

<sup>b</sup>State Key Laboratory of Mycology, Institute of Microbiology, Chinese Academy of Sciences, Beijing 100101, China

Corresponding to Shu-Ming Li, E-mail: [shuming.li@staff.uni-marburg.de](mailto:shuming.li@staff.uni-marburg.de)

## Table of contents

Experimental procedures .....	3
1.1 General Experimental Procedures .....	3
1.2 Strains, Media, and Culture Conditions.....	3
1.3 Genetic Manipulations .....	4
1.4 Product Analysis, Large-Scale Fermentation, Extraction and Metabolite Isolation ....	5
1.5 Precursor Feeding in <i>A. nidulans</i> LO8030.....	6
Supplementary Tables .....	7
Table S1. <sup>1</sup> H NMR data of compounds 1, 2 and 3 (DMSO- <i>d</i> <sub>6</sub> ) .....	7
Supplementary Figures .....	8
Figure S1. Constructs used for heterologous expression in <i>A. nidulans</i> .....	8
Figure S2. UV spectra of compounds 1, 2 and 3.....	9
Figure S3. <sup>1</sup> H NMR spectrum of compound 1 in DMSO- <i>d</i> <sub>6</sub> (500MHz) .....	10
Figure S4. <sup>1</sup> H NMR spectrum of compound 2 in DMSO- <i>d</i> <sub>6</sub> (500MHz).....	10
Figure S5. <sup>1</sup> H NMR spectrum of compound 3 in DMSO- <i>d</i> <sub>6</sub> (500MHz).....	11
Supplementary References .....	11

## Experimental procedures

### 1.1 General Experimental Procedures

All chemicals were purchased from Sigma-Aldrich. High-resolution mass spectrometric data were generated by using a microTOF-Q III mass spectrometer with an ESI source (Bruker Daltonics, Bremen, Germany) connected to an Agilent HPLC series 1260 (Böblingen, Germany), which is equipped with a photodiode array detector. Separation was carried out on an Eclipse XDB-C18 column (4.6 × 150 mm, 5  $\mu$ m, Agilent, Germany). NMR spectra were recorded on a JEOL ECA-500 MHz spectrometer (JEOL, Tokyo, Japan). The spectra were processed by using the software MestReNova 6.1.0 (Metrelab). NMR data are given in Table S1 and spectra in Figures S3 – S5.

### 1.2 Strains, Media, and Culture Conditions

*Escherichia coli* DH5 $\alpha$  (Invitrogen) was used for cloning and plasmid propagation and grown in lysogeny broth (LB) at 37 °C. For cultivation on solid medium, 1.5% (w/v) agar was added. 50  $\mu$ g/mL carbenicillin were used for selection of the recombinant *E. coli* strains.

*P. crustosum* strain PRB-2 was cultivated under static conditions at 25 °C in potato dextrose broth (PDB, Sigma-Aldrich). *A. nidulans* LO8030 was cultivated at 37 °C in liquid minimal medium (LMM) supplemented with riboflavin, pyridoxine, uridine and uracil as reported previously.<sup>1</sup> For cultivation on solid medium, 1.5% (w/v) agar was added to the respective medium. Cultivation of *A. nidulans* strain PX001 (*gpdA::pcr9304::Afp<sub>pyrG</sub>* in *A. nidulans* LO8030) and negative control (*gpdA::Afp<sub>pyrG</sub>* in *A. nidulans* LO8030) were done on rice supplemented with riboflavin and pyridoxine at 25 °C.

### 1.3 Genetic Manipulations

For isolation of genomic DNA, *P. crustosum* and *A. nidulans* were cultivated in PDB or LMM for 2 days at 25 °C. Genomic DNA was isolated according to the method described previously.<sup>2</sup> Phusion high-fidelity DNA polymerase (New England Biolabs) was used for PCR amplifications on a T100 thermal cycler from Bio-Rad. Construction of the heterologous expression vector was done by homologous recombination in *E. coli*.<sup>3</sup> The construct pPX001 for heterologous expression in *A. nidulans* with afpyrG as a selection marker was based on the plasmid vector pYH-wA-pyrG.<sup>5</sup> Briefly, the vector backbone was linearized by cut with *NheI* followed by SAP treatment with subsequent purification *via* a HiYield PCR Clean-up and GelExtraction Kit (SLG Südlaborbedarf). For creation of pPX001, *pcr9304* with the accession number MT451935 (GenBank) including its downstream region of 633 bp was PCR amplified from genomic DNA of *P. crustosum* PRB-2 with the primer pairs

An-9304-For/Rev (An-9304-For: TATATTCATCTTCCCATCCAAGAACCTTTAATCATGCGTCGGCCAAATC; An-9304-Rev: CATATTTTCGTCAGACACAGAATAACTCTCGGTGACAATTCTCACCTTG). The underlined sequences in the primers are homologous regions with the vector for recombination. Subsequently, the PCR fragment and linearized vector were mixed and transformed into *E. coli* DH5 $\alpha$ . The assembled plasmid pPX001 was confirmed by enzyme restriction. 4  $\mu$ g of this construct were linearized with *SwaI* and transformed into *A. nidulans* LO8030 according to the protocol by Yin *et al.*<sup>5</sup> 65 Potential transformants were obtained after uracil and uridine autotrophy selection. The primers 9304-F (CCTTTTCGAGTAACAGTCGC) and 9304-R (ATGCTTGATTACTGCCTTTTG) target a 1718 bp partial fragment in *pcr9304* and

were used for transformant verification. All of the 10 selected transformants were confirmed by PCR amplification.

#### 1.4 Product Analysis, Large-Scale Fermentation, Extraction and Metabolite Isolation

*A. nidulans* strains were cultivated on rice medium at 25°C for 14 days for LC-MS analysis of the secondary metabolite production. For a small-scale analysis, 3 mL of the culture was extracted with equal volume of ethyl acetate. The organic phase was dried in vacuo using a Speedvac and the residue was dissolved in a mixture of MeOH and H<sub>2</sub>O (19 : 1) for LC-MS analysis.

To isolate the accumulated products, *A. nidulans* PX001 was cultivated in seven 1 L flasks containing 100 g rice each and 150 mL H<sub>2</sub>O with appropriate nutrition as supplement at 25°C for 21 days. After extraction with 3 L ethyl acetate for three times and concentration of the organic phases under reduced pressure, 3.4 g crude extract were obtained. Silica gel column chromatography of the crude extract by using dichloromethane / MeOH (100 : 1, 50 : 1, 10 : 1 and 0 : 1, v/v) as elution solvents, yielded 48 fractions. Further purification of fraction 8 on a semipreparative HPLC (Agilent series 1200 HPLC, Böblingen, Germany), with an Agilent Eclipse XDB-C18 column (9.4 × 250 mm, 5 μm) and CH<sub>3</sub>CN / H<sub>2</sub>O (55 : 45, flow rate of 2.5 mL/min) as solvents, resulted in compound **1** (9.0 mg) in high purity. Purification of the combined fractions 25 – 30 on the same HPLC equipment by using CH<sub>3</sub>CN / H<sub>2</sub>O (35 : 65, flow rate of 2.5 mL/min) as solvents led to 7.0 mg of **2** and 6.5 mg of **3**.

*6,8-Dihydroxy-3-methylisocoumarin (1)*: yellow powder; HRMS (m/z): (ESI/[M + H]<sup>+</sup>) calcd. for C<sub>10</sub>H<sub>9</sub>O<sub>4</sub>, 193.0495, found 193.0493.



*6,8-Dihydroxy-3-hydroxymethylisocoumarin (2)*: white needle powder; HRMS (m/z): (ESI/[M + H]<sup>+</sup>) calcd. for C<sub>10</sub>H<sub>9</sub>O<sub>5</sub>, 209.0444, found 209.0451.

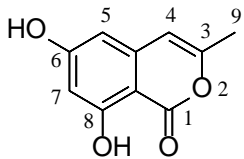
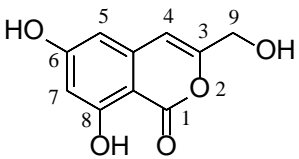
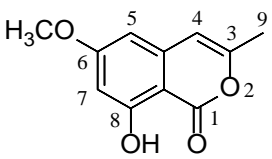
*6-Methoxy-8-hydroxy-3-methylisocoumarin (3)*: yellow oil; HRMS (m/z): (ESI/[M + H]<sup>+</sup>) calcd. for C<sub>11</sub>H<sub>11</sub>O<sub>4</sub>, 207.0652, found 207.0663.

### 1.5 Precursor Feeding in *A. nidulans* LO8030

*A. nidulans* LO8030 was cultured on solid rice medium (2 g rice, 3 mL H<sub>2</sub>O, containing the appropriate supplements) at room temperature at a static condition. After three days, 10  $\mu$ L of 6,8-dihydroxy-3-methylisocoumarin (**1**) as a 1 M stock solution in DMSO was added to the rice culture, resulting in a final concentration of 0.4 mM. After cultivation for 7 further days, the secondary metabolites were extracted with ethyl acetate, dissolved in a mixture of MeOH and H<sub>2</sub>O (19 : 1) and analyzed by LC-MS.

## Supplementary Tables

**Table S1.**  $^1\text{H}$  NMR data of compounds **1**, **2** and **3** ( $\text{DMSO}-d_6$ )

Compound			
	6,8-Dihydroxy-3-methylisocoumarin ( <b>1</b> ) <sup>4</sup>	6,8-Dihydroxy-3-hydroxymethylisocoumarin ( <b>2</b> ) <sup>4</sup>	6-Methoxy-8-hydroxy-3-methylisocoumarin ( <b>3</b> ) <sup>4</sup>
Position	$\delta_{\text{H}}$ , multi., $J$ in Hz	$\delta_{\text{H}}$ , multi., $J$ in Hz	$\delta_{\text{H}}$ , multi., $J$ in Hz
4	6.47, q, 1.0	6.61, s	6.27, q, 1.2
5	6.33, d, 2.5	6.43, d, 2.1	6.43, d, 2.2
7	6.30, d, 2.5	6.34, d, 2.1	6.33, d, 2.2
9	2.22, d, 1.0	4.25, d, 1.0	2.13, d, 1.2
6-OH	10.79, brs	-	-
8-OH	10.95, s	10.93, brs	10.66, brs
9-OH	-	5.57, brs	-
6-OCH <sub>3</sub>	-	-	3.81, s

The NMR data of the isolated compounds correspond very well to those reported in the literature.<sup>4</sup>

## Supplementary Figures

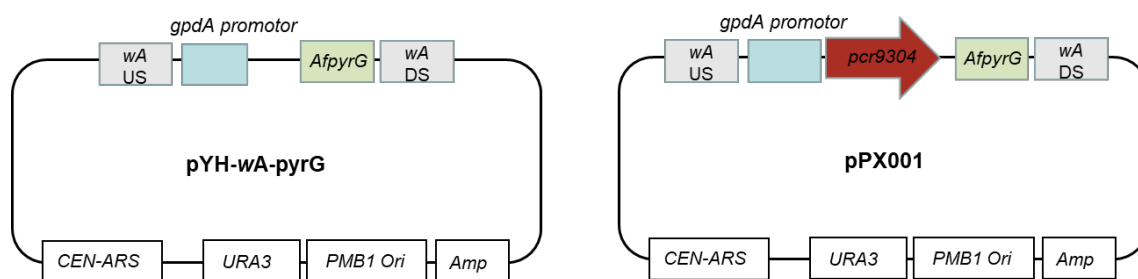


**Figure S1.** Constructs used for heterologous expression in *A. nidulans*

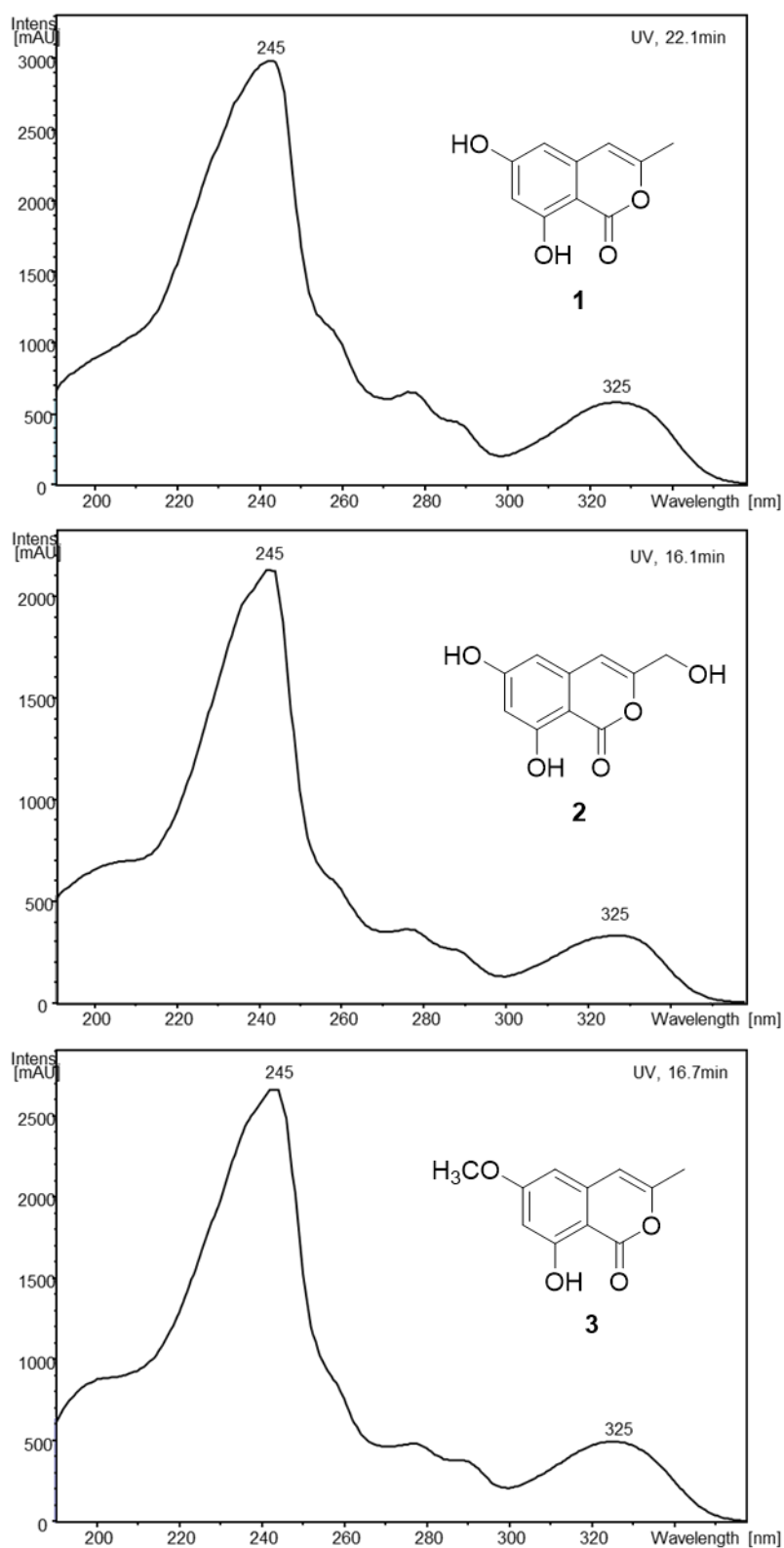


**Figure S2.** UV spectra of compounds **1**, **2** and **3**

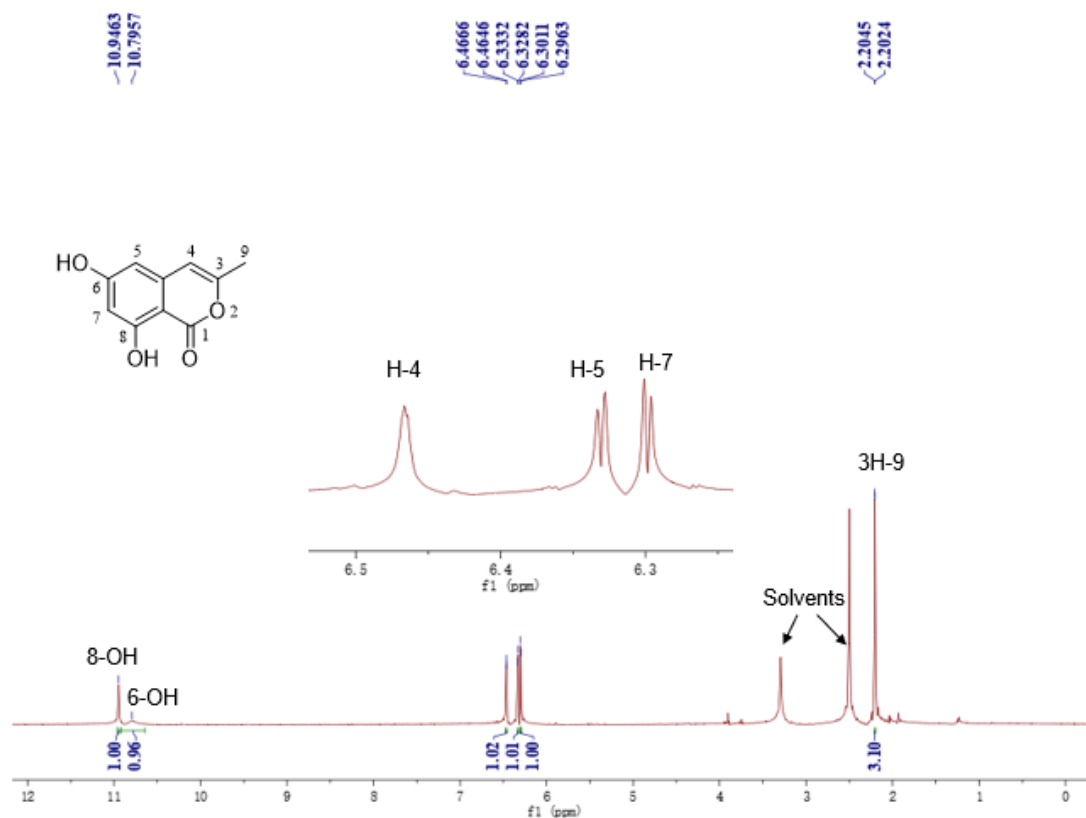


**Figure S3.** <sup>1</sup>H NMR spectrum of compound 1 in DMSO-*d*<sub>6</sub> (500MHz)

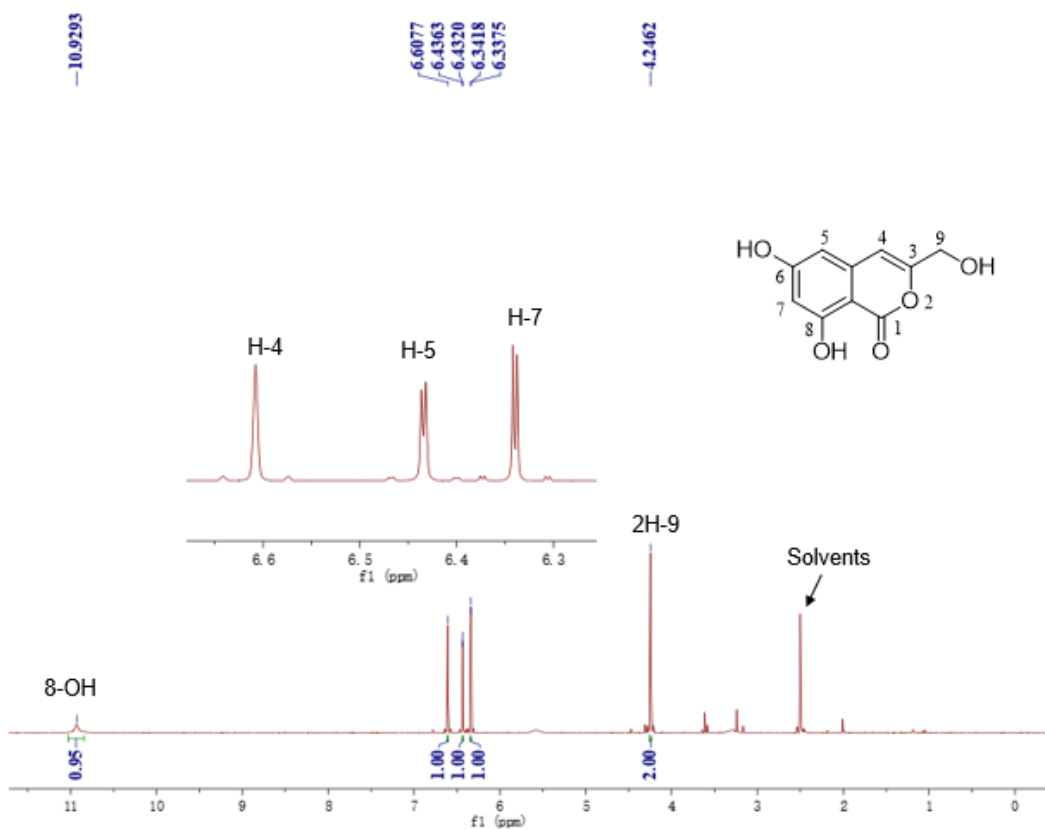


**Figure S4.** <sup>1</sup>H NMR spectrum of compound 2 in DMSO-*d*<sub>6</sub> (500MHz)

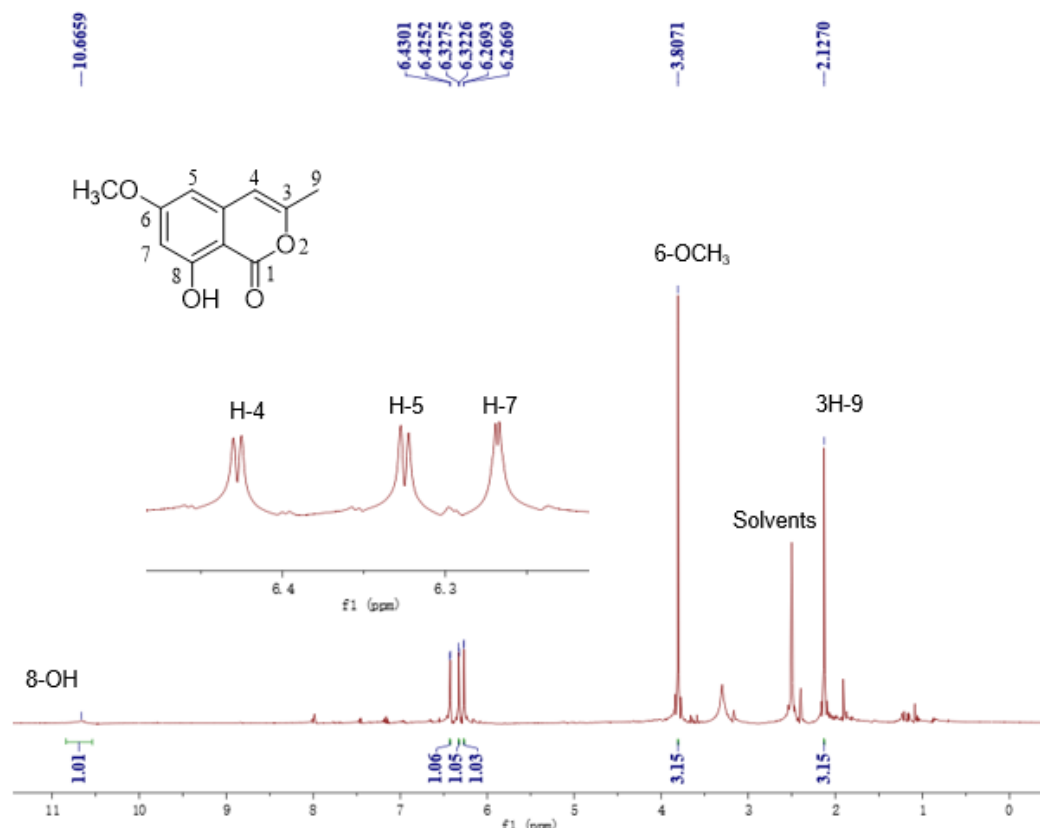


**Figure S5.** <sup>1</sup>H NMR spectrum of compound **3** in DMSO-*d*<sub>6</sub> (500MHz)

#### Supplementary References

- 1 Y. M. Chiang, M. Ahuja, C. E. Oakley, R. Entwistle, A. Asokan, C. Zutz, C. C. Wang, and B. R. Oakley, *Angew. Chem. Int. Ed. Engl.*, 2016, **55**, 1662-1665.
- 2 J. Fan, G. Liao, F. Kindinger, L. Ludwig-Radtke, W.-B. Yin, and S.-M. Li, *J. Am. Chem. Soc.*, 2019, **141**, 4225-4229.
- 3 A. P. Jacobus and J. Gross, *PLoS. One.*, 2015, **10**, e0119221.
- 4 H. Kumagai, M. Amemiya, H. Naganawa, T. Sawa, M. Ishizuka, and T. Takeuchi, *J. Antibiot.*, 1994, **47**, 440-446.
- 5 W. B. Yin, Y. H. Chooi, A. R. Smith, R. A. Cacho, Y. Hu, T. C. White, and Y. Tang, *ACS Synth. Biol.*, 2013, **2**, 629-634.

**4.2 Formation of 3-orsellinoxipropanoic acid in *Penicillium crustosum* is catalyzed by a bifunctional nonreducing polyketide synthase**





# Formation of 3-Orsellinoxipropanoic Acid in *Penicillium crustosum* is Catalyzed by a Bifunctional Nonreducing Polyketide Synthase

Pan Xiang and Shu-Ming Li\*



Cite This: *Org. Lett.* 2022, 24, 462–466



Read Online

ACCESS |



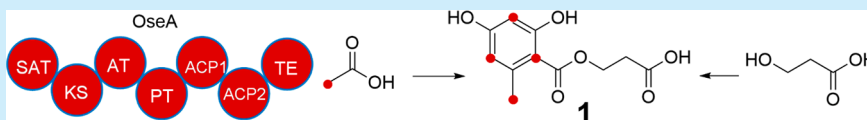
Metrics & More



Article Recommendations



Supporting Information



**ABSTRACT:** The heterologous expression of a nonreducing polyketide synthase gene *oesA* from *Penicillium crustosum* led to the identification of orsellinoylpropanoic acid (**1**). Domain deletion and recombination proved that OesA catalyzes not only the formation of orsellinic acid but also its transfer to 3-hydroxypropanoic acid. Both ACP domains contribute independently and complementarily to the product formation. Feeding experiments provided evidence that only the orsellinyl residue is derived from acetate.

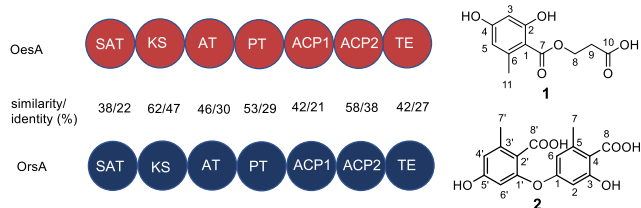
Polyketide natural products are structurally diverse and biologically active secondary metabolites produced by plants, bacteria, and fungi, including *Penicillium* and *Aspergillus* species.<sup>1–3</sup> Their backbones are biosynthesized by polyketide synthases (PKSs) and can be further modified by diverse tailoring enzymes.<sup>4</sup> PKSs are classified based on their architecture and mode of action. Fungal PKSs belong to iterative type I enzymes with catalytic domains as large programmed covalent complexes.<sup>5–7</sup> Nonreducing fungal PKSs comprise normally individual functional domains such as the starter acyl transferase (SAT),  $\beta$ -ketosynthase (KS), acyl transferase (AT), product template (PT), acyl carrier protein (ACP), and thioesterase (TE) domains.<sup>8</sup> These enzymes are usually responsible for the formation of aromatic acids like the archetypal phenolic polyketide orsellinic acid (OA).<sup>9</sup>

Orsellinic acid synthase (OSAS), as one of the first discovered fungal PKSs, was already isolated from *Penicillium madriti* in 1968.<sup>10</sup> Until now, a large number of OSASs have been identified in bacteria and fungi (Figure S1). Among them, OrsA (AN7909) from *Aspergillus nidulans* with two ACP domains catalyzes not only the formation of OA but also its dimerization (Figure 1).<sup>9,11</sup> Both ACPs are involved in the formation of the OA dimer diorcinolic acid (**2**). The domain structure and its

function for dimerization raised our interest in studying its homologues. We identified the gene *pcr7502* that codes for a putative nonreducing polyketide synthase, termed OesA hereafter, in the genome of *Penicillium crustosum* PRB-2.<sup>12</sup>

OesA is comprised of 2088 amino acids and has a similar domain architecture as OrsA, i.e., SAT-KS-AT-PT-ACP1-ACP2-TE (Figure 1). A sequence comparison revealed a 32.2% sequence identity between OrsA and OesA on the amino acid level. The identities among the corresponding domains of the both proteins were found to be 22% to 47% (Figure 1). It was reported that megasynthases with a low protein sequence identity can still produce the same or similar metabolites, which raised our interest in investigating the function of OesA.<sup>13</sup> Gene deletion in *Penicillium crustosum* PRB-2 did not lead to detectable secondary metabolite changes in the  $\Delta$ oesA mutant in comparison to the wildtype. This suggests that *oesA* is probably a silent gene not expressed under our cultivation conditions (Li and Kindinger, unpublished results).

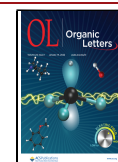
To prove its function, we changed our strategy to heterologous expression in *A. nidulans* LO8030.<sup>14</sup> For this purpose, a 6635 bp fragment consisting of the whole genomic sequence of *oesA* and a downstream region of 517 bp containing the native terminator was amplified via PCR and cloned into the expression vector pYH-wA-pyrG by homologous recombination in *Saccharomyces cerevisiae*, as described previously.<sup>15,16</sup> The obtained construct pPX15 (Figure S2) was introduced into *A. nidulans* LO8030 by a polyethylene glycol-mediated protoplast



**Figure 1.** Domain structures of OesA and OrsA with their main products.

**Received:** December 10, 2021

**Published:** December 28, 2021



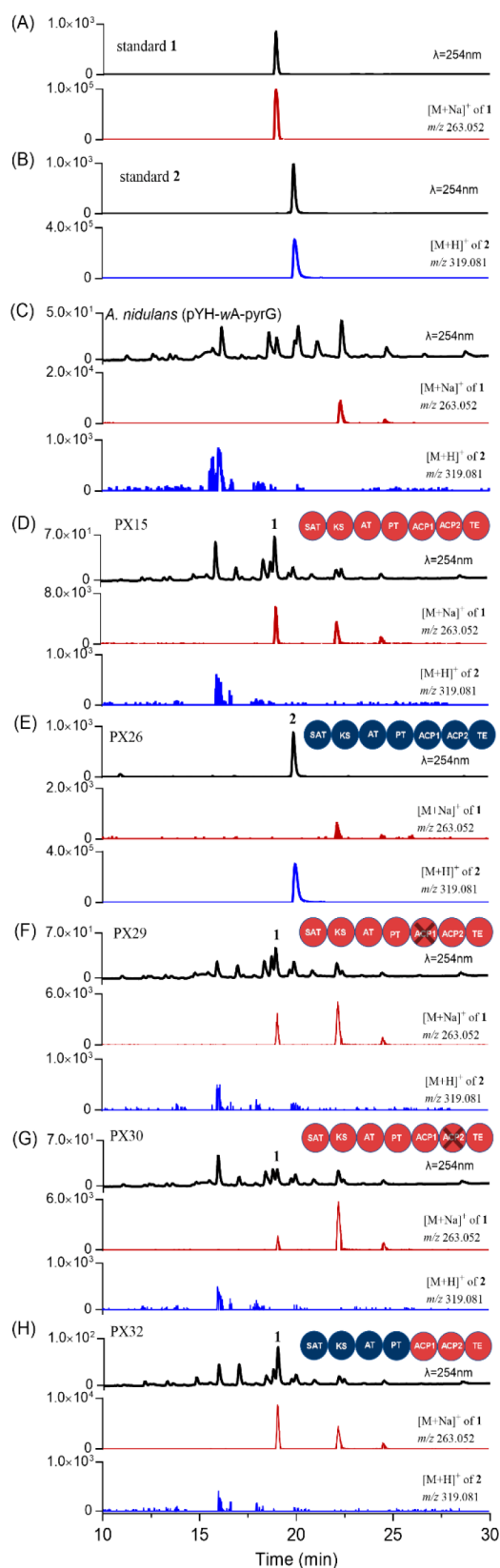


**Figure 2.** LC-MS analysis of *A. nidulans* extracts after 10 days of cultivation. UV absorptions at 254 nm are illustrated. A tolerance range of  $\pm 0.005$  was used for ion detection.

transformation. After selection with uridine and uracil autotrophy and subsequent confirmation by PCR amplification,

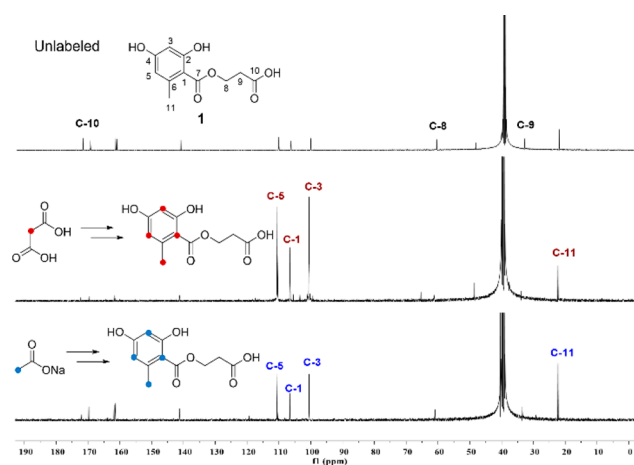


**Figure 3.**  $^{13}\text{C}$  NMR spectra of the unlabeled and labeled **1**. Solid blue and magenta circles represent the labeled carbons after feeding with  $[2-^{13}\text{C}]$  acetate and  $[2-^{13}\text{C}]$  malonic acid, respectively.

three integration transformants were cultivated on the PDB liquid medium under static condition. The 10 day-old cultures were extracted with ethyl acetate and analyzed by LC-MS for secondary metabolites. All three extracts showed similar metabolite profiles. As shown in Figure 2D for the transformant *Aspergillus nidulans* PX15, an additional peak **1** with a  $[\text{M} + \text{Na}]^+$  ion at  $m/z$  263.0522 for a deduced molecular formula of  $\text{C}_{11}\text{H}_{12}\text{O}_6$  was detected in the extract compared to that of the negative control strain carrying the empty vector pYH-wA-pyrG.

For structure elucidation, the analytically pure product **1** was isolated from the 3L PX15 culture and subjected to NMR and MS analyses. Detailed analysis of the 1D and 2D NMR spectra (Table S4 and Figures S6–S10) revealed **1** to be an OA derivative. In comparison to those of OA,<sup>11</sup> three additional  $^{13}\text{C}$  signals at  $\delta$  60.8 (C8), 33.3 (C9), and  $\delta$  172.0 (C10) were observed and could be assigned to those of a 3-hydroxypropionic acid (3-HP) residue (Table S4). This is also in consistent with its  $^1\text{H}$  NMR data. The connection of 3-HP to the OA moiety via an ester bond (C7–O–C8) was confirmed by the key correlation between H8 and C7 in the HMBC spectrum (Table S4 and Figure S10). Based on this evidence, **1** was unambiguously identified as orsellinoxipropanoic acid (Figure 1).

As mentioned above, OA has been identified in many species and is usually modified by hydroxylation, methoxylation, or halogenation.<sup>17,18</sup> The formation of OA dimers via an ester or ether bond was also reported.<sup>19,20</sup> The ester bond formation in **1** is likely an enzymatic or nonenzymatic transfer of the orsellinyl residue from OesA to the hydroxyl group of 3-HP, as was observed for the precursor of ustethylin A.<sup>21</sup> The enzymatic transesterification could be catalyzed by the TE domain of OesA, as reported for other PKSs,<sup>22</sup> or by an unknown host enzyme from *A. nidulans*. To understand the ester bond formation, we also heterologously expressed *orsA* from *A. nidulans* RSM011 in LO8030 without the endogenous *ors* cluster (Tables S1–S3 and Figure S2).<sup>14</sup> In analogy to the *oesA* transformant PX15, the expression strain *A. nidulans* PX26 harboring *orsA* was cultivated in liquid PD media, extracted with ethyl acetate, and analyzed by LC-MS. In comparison to the negative control, the sole product peak was detected with the expected  $[\text{M} + \text{H}]^+$  ion for diorcinolic acid (**2**) at  $m/z$  319.0814 (Figures 2C and E). The integrity of **2** was then proven by comparing its UV, MS, and  $^1\text{H}$  NMR data with those published

## Scheme 1. Proposed Formation Mechanism of 3-Orsellinoxypropanoic Acid

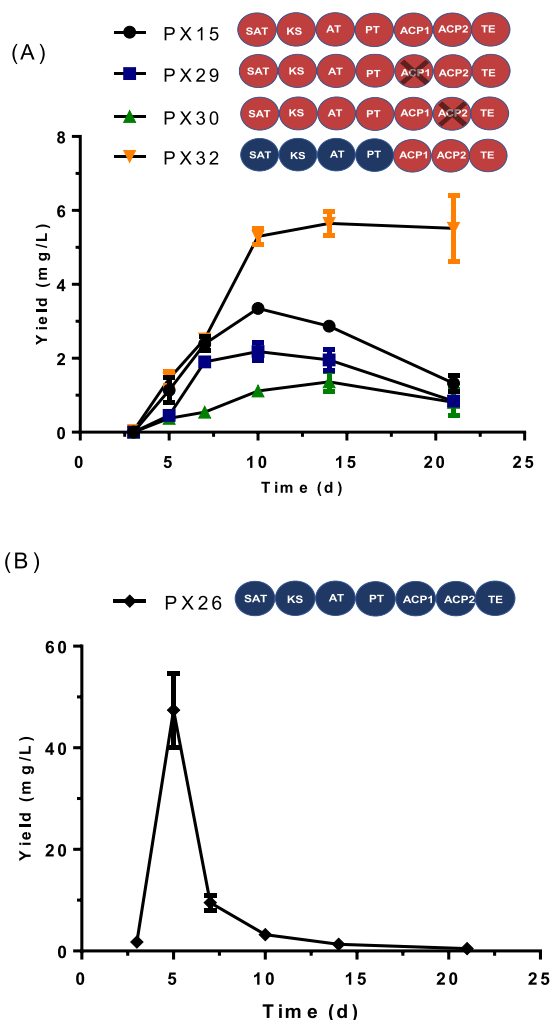
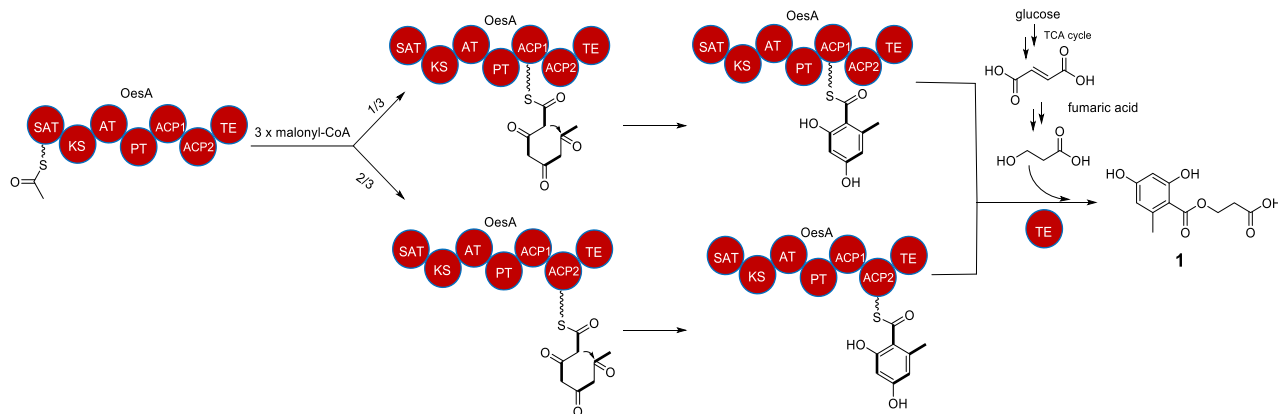


**Figure 4.** Dependence of (A) **1** and (B) **2** formation in *A. nidulans* on cultivation times.

previously (Table S5 and Figure S11).<sup>20</sup> These results are consistent with those of *orsA* expression in *Saccharomyces cerevisiae*<sup>20</sup> and rule out nonenzymatic events or the involvement of host enzymes in the formation of **1**. Taken together, both OesA and OrsA are OA synthases. Differing from OrsA with an activity for OA dimerization, OesA catalyzes the ester formation of OA with 3-HP.

It was reported that both ACP domains in OrsA are involved in the OA dimerization.<sup>20</sup> To probe the function of the ACP domains of OesA in the formation of **1**, we deleted both ACP domains in PX15 separately. The transformants were cultivated and treated as described above. As shown in Figures 2F and G, both deletion mutants, namely PX29 without ACP1 and PX30 without ACP2, can still produce **1**, which was identified by comparing its  $t_R$ , UV, and MS data. However, the product yields in PX29 and PX30 were lower compared to that of PX15. These results demonstrated that both ACP1 and ACP2 contribute independently to the OA formation, as reported for other PKSs.<sup>20,23,24</sup> The reason for ACP duplication or multiplication is still currently unknown.<sup>25</sup>

After the successful expression of *orsA* and *oesA* in *A. nidulans* and the identification of different products, we then constructed hybrid genes in pYH-wA-pyrG with the SAT-KS-AT-PT domains of one gene and the ACP1-ACP2-TE domains of another gene. The domains were defined according to the prediction results with BLASTP and 2ndFind. The plasmid pPX31 contains the SAT-KS-AT-PT domains of OesA and the ACP1-ACP2-TE domains of OrsA, while pPX32 contains the SAT-KS-AT-PT domains of OrsA and the ACP1-ACP2-TE domains of OesA (Table S2). Subsequently, pPX31 and pPX32 were transformed into *A. nidulans*, resulting in the transformants PX31 and PX32, respectively (Table S1). LC-MS analysis revealed that PX31 produced neither **1** nor **2** (Figure S4). In comparison, one additional peak with a  $[M + Na]^+$  ion at  $m/z$   $263.052 \pm 0.005$  accumulated in the PX32 culture (Figure 2H). The isolation and comparison of its <sup>1</sup>H NMR data confirmed this product to be **1**. The combination of the SAT-KS-AT-PT-ACP1 domains of OesA with the ACP2-TE domains of OrsA (PX34) or the SAT-KS-AT-PT-ACP1-ACP2 domains of OesA with the TE domain of OrsA (PX36) did not lead to any detected product. Similar negative results were obtained with constructs of the SAT-KS-AT-PT-ACP1 domains of OrsA with the ACP2-TE domains of OesA (PX35) as well as those of the SAT-KS-AT-PT-ACP1-ACP2 domains of OrsA with the TE domain of OesA (PX37) (Figure S4). These results proved that the ACP1-ACP2-TE domains of OesA can cooperate with SAT-KS-AT-PT domains of OrsA but not vice versa. They also provide evidence that the ACP1-ACP2-TE domains of OesA are responsible for the ester bond formation in **1**. Notably, no OA was accumulated in the transformants PX34–PX37 (Figure S5), indicating no gene expression, incorrect protein folding, or no product release from the PKS template.

To elucidate the origin of **1**, we performed feeding experiments with sodium [2-<sup>13</sup>C] acetate and [2-<sup>13</sup>C] malonic acid in *A. nidulans* PX15. After feeding with [2-<sup>13</sup>C] acetate (Figure 3), four signals at  $\delta_C$  106.6 (C-1), 100.4 (C-3), 110.5 (C-5), and 22.2 (C-11) ppm are enriched 3.0–4.3-fold in the <sup>13</sup>C NMR spectrum of **1** (Table S6), unequivocally proving incorporation of four intact acetate units in the OA moiety of **1**. Correspondingly, 5.9–21.3-fold enrichment was calculated for these four carbons after feeding with [2-<sup>13</sup>C] malonic acid (Table S6 and Figure 3). No enrichment was observed for the carbons in the 3-HP moiety, indicating that it did not originate from acetate or malonate. In view of the 3-HP metabolic pathways, this moiety could originate from fumaric acid.<sup>26,27</sup>

Based on the results obtained in this study, we postulated a formation mechanism for **1** in *Penicillium crustosum* as depicted in Scheme 1. One acetyl CoA moiety condenses with three malonyl CoA molecules on the OesA assembly line. The finished orsellinyl moiety is attached to ACP1 or ACP2. The TE domain catalyzes the transfer of the OA residue from both ACPs to 3-HP to form **1**. This transesterification mechanism occurs occasionally in natural product biosynthesis<sup>22</sup> and differs clearly from *trans*-acting enzymes with additional proteins for product release from the PKS.<sup>28</sup>

To monitor the productivity, the producing strains PX15, PX29, PX30, and PX32 of **1** as well as PX26 of **2** were cultivated up to three weeks. The accumulated **1** and **2** were quantified by LC-MS. As shown in Figure 4A, the product yields reached their maximal values after 10 days in the **1**-producing strains and 5 days in the PX26 strain producing **2**. Interestingly, the productivity of the strain PX32 with the SAT-KS-AT-PT of OrsA at  $5.3 \pm 0.16$  mg/L is approximately 1.6-fold that of PX15 with the intact OesA at  $3.3 \pm 0.1$  mg/L. This suggests a higher efficiency of the SAT-KS-AT-PT domains of OrsA for assembling the orsellinyl residue compared to those of OesA and corresponds to the high product yield of the strain PX26 with OrsA at  $47.4 \pm 5.4$  mg/L (Figure 4B). Meanwhile, these results indicate that the PKS-assembled orsellinyl moiety determined the yield of the final product. This could also be the reason for the almost unchanged product amount in PX15 after the addition of external 3-HP (data not shown). Interestingly, the productivity of **1** in the PX32 strain bearing a sequence for a hybrid enzyme remained constantly high, even after cultivation for 21 days. The reason for this phenomenon is unknown. Furthermore, the sum of the two strains with ACP deletion, i.e.,  $2.2 \pm 0.19$  mg/L in PX29 with ACP1 deletion and  $1.1 \pm 0.04$  mg/L in PX30 with ACP2 deletion, is almost the same as that of PX15 without deletion. This suggests the independent and complementary contribution of the both ACPs for ester formation with 3-HP.

In conclusion, the NR-PKS gene *oesA* from *P. crustosum* was successfully expressed in *A. nidulans* LO8030 and proved its role in the formation of 3-orsellinoxypropanoic acid (**1**) as an OA synthase and a transferase. Domain deletion and recombination provided evidence that both ACPs contribute independently and complementarily to the formation of the product **1**.

## ■ ASSOCIATED CONTENT

### SI Supporting Information

The Supporting Information is available free of charge at <https://pubs.acs.org/doi/10.1021/acs.orglett.1c04189>.

Experimental details, strains, primers, expression constructs, LC-MS analysis, and NMR data and spectra (PDF)

## ■ AUTHOR INFORMATION

### Corresponding Author

Shu-Ming Li – Institut für Pharmazeutische Biologie und Biotechnologie, Fachbereich Pharmazie, Philipps-Universität Marburg, 35037 Marburg, Germany; [orcid.org/0000-0003-4583-2655](https://orcid.org/0000-0003-4583-2655); Phone: + 49-6421-28-22461; Email: [shuming.li@staff.uni-marburg.de](mailto:shuming.li@staff.uni-marburg.de); Fax: + 49-6421-28-25365

### Author

Pan Xiang – Institut für Pharmazeutische Biologie und Biotechnologie, Fachbereich Pharmazie, Philipps-Universität Marburg, 35037 Marburg, Germany

Complete contact information is available at:

<https://pubs.acs.org/doi/10.1021/acs.orglett.1c04189>

### Notes

The authors declare no competing financial interest.

## ■ ACKNOWLEDGMENTS

We thank Lena Ludwig-Radtke and Stefan Newel (Philipps-Universität Marburg) for taking the MS and NMR spectra, respectively. This project was financially funded in part by the DFG (INST 160/620-1 and Li844/11-1 to S.M.L.). P.X. is a scholarship recipient of the China Scholarship Council (201708530222).

## ■ REFERENCES

- (1) Newman, D. J.; Cragg, G. M. Natural products as sources of new drugs over the nearly four decades from 01/1981 to 09/2019. *J. Nat. Prod.* **2020**, *83*, 770.
- (2) Flores-Sanchez, I. J.; Verpoorte, R. Plant polyketide synthases: a fascinating group of enzymes. *Plant Physiol. Biochem.* **2009**, *47*, 167.
- (3) Hoffmeister, D.; Keller, N. P. Natural products of filamentous fungi: enzymes, genes, and their regulation. *Nat. Prod. Rep.* **2007**, *24*, 393.
- (4) Hertweck, C. The biosynthetic logic of polyketide diversity. *Angew. Chem., Int. Ed.* **2009**, *48*, 4688.
- (5) Cox, R. J. Polyketides, proteins and genes in fungi: programmed nano-machines begin to reveal their secrets. *Org. Biomol. Chem.* **2007**, *5*, 2010.
- (6) Simpson, T. J. Fungal polyketide biosynthesis – a personal perspective. *Nat. Prod. Rep.* **2014**, *31*, 1247.
- (7) Kennedy, J.; Auclair, K.; Kendrew, S. G.; Park, C.; Vederas, J. C.; Hutchinson, C. R. Modulation of polyketide synthase activity by accessory proteins during lovastatin biosynthesis. *Science* **1999**, *284*, 1368.
- (8) Smith, S.; Tsai, S. C. The type I fatty acid and polyketide synthases: a tale of two megasynthases. *Nat. Prod. Rep.* **2007**, *24*, 1041.
- (9) Schroeckh, V.; Scherlach, K.; Nuttmann, H. W.; Shelest, E.; Schmidt-Heck, W.; Schuermann, J.; Martin, K.; Hertweck, C.; Brakhage, A. A. Intimate bacterial-fungal interaction triggers biosynthesis of archetypal polyketides in *Aspergillus nidulans*. *Proc. Natl. Acad. Sci. U. S. A.* **2009**, *106*, 14558.
- (10) Gaucher, G. M.; Shepherd, M. G. Isolation of orsellinic acid synthase. *Biochem. Biophys. Res. Commun.* **1968**, *32*, 664.
- (11) Sanchez, J. F.; Chiang, Y. M.; Szwedczyk, E.; Davidson, A. D.; Ahuja, M.; Oakley, C. E.; Bok, J. W.; Keller, N.; Oakley, B. R.; Wang, C. C. Molecular genetic analysis of the orsellinic acid/F9775 gene cluster of *Aspergillus nidulans*. *Mol. Biosyst.* **2010**, *6*, 587.



- (12) Wu, G.; Ma, H.; Zhu, T.; Li, J.; Gu, Q.; Li, D. Penilactones A and B, two novel polyketides from Antarctic deep-sea derived fungus *Penicillium crustosum* PRB-2. *Tetrahedron* **2012**, *68*, 9745.
- (13) Cochrane, R. V. K.; Gao, Z.; Lambkin, G. R.; Xu, W.; Winter, J. M.; Marcus, S. L.; Tang, Y.; Vederas, J. C. Comparison of 10,11-dehydrocurvularin polyketide synthases from *Alternaria cinerariae* and *Aspergillus terreus* highlights key structural motifs. *Chembiochem* **2015**, *16*, 2479.
- (14) Chiang, Y. M.; Oakley, C. E.; Ahuja, M.; Entwistle, R.; Schultz, A.; Chang, S. L.; Sung, C. T.; Wang, C. C.; Oakley, B. R. An efficient system for heterologous expression of secondary metabolite genes in *Aspergillus nidulans*. *J. Am. Chem. Soc.* **2013**, *135*, 7720.
- (15) Yin, W. B.; Chooi, Y. H.; Smith, A. R.; Cacho, R. A.; Hu, Y.; White, T. C.; Tang, Y. Discovery of cryptic polyketide metabolites from dermatophytes using heterologous expression in *Aspergillus nidulans*. *ACS Synth. Biol.* **2013**, *2*, 629.
- (16) Xiang, P.; Ludwig-Radtke, L.; Yin, W.-B.; Li, S.-M. Isocoumarin formation by heterologous gene expression and modification by host enzymes. *Org. Biomol. Chem.* **2020**, *18*, 4946.
- (17) Calcul, L.; Chow, R.; Oliver, A. G.; Tenney, K.; White, K. N.; Wood, A. W.; Fiorilla, C.; Crews, P. NMR strategy for unraveling structures of bioactive sponge-derived oxy-polyhalogenated diphenyl ethers. *J. Nat. Prod.* **2009**, *72*, 443.
- (18) Bashyal, B. P.; Wijeratne, E. M. K.; Faeth, S. H.; Gunatilaka, A. A. L. Globosumones A-C, cytotoxic orsellinic acid esters from the Sonoran desert endophytic fungus *Chaetomium globosum*. *J. Nat. Prod.* **2005**, *68*, 724.
- (19) Lünne, F.; Niehaus, E. M.; Lipinski, S.; Kunigkeit, J.; Kalinina, S. A.; Humpf, H. U. Identification of the polyketide synthase PKS7 responsible for the production of lecanoric acid and ethyl lecanorate in *Claviceps purpurea*. *Fungal Genet. Biol.* **2020**, *145*, 103481.
- (20) Feng, C.; Wei, Q.; Hu, C.; Zou, Y. Biosynthesis of diphenyl ethers in fungi. *Org. Lett.* **2019**, *21*, 3114.
- (21) Zheng, L.; Li, S.-M. Benzoyl ester formation in *Aspergillus ustus* by hijacking the polyketide acyl intermediates with alcohols. *Arch. Microbiol.* **2021**, *203*, 1795.
- (22) Little, R. F.; Hertweck, C. Chain release mechanisms in polyketide and non-ribosomal peptide biosynthesis. *Nat. Prod. Rep.* **2022**, DOI: 10.1039/D1NP00035G.
- (23) Fujii, I.; Watanabe, A.; Sankawa, U.; Ebizuka, Y. Identification of Claisen cyclase domain in fungal polyketide synthase WA, a naphthopyrone synthase of *Aspergillus nidulans*. *Chem. Biol.* **2001**, *8*, 189.
- (24) Kahlert, L.; Villanueva, M.; Cox, R. J.; Skellam, E. J. Biosynthesis of 6-hydroxymellein requires a collaborating polyketide synthase-like enzyme. *Angew. Chem., Int. Ed. Engl.* **2021**, *60*, 11423.
- (25) Braesel, J.; Fricke, J.; Schwenk, D.; Hoffmeister, D. Biochemical and genetic basis of orsellinic acid biosynthesis and prenylation in a stereaceous basidiomycete. *Fungal Genet. Biol.* **2017**, *98*, 12.
- (26) Kumar, V.; Ashok, S.; Park, S. Recent advances in biological production of 3-hydroxypropionic acid. *Biotechnol. Adv.* **2013**, *31*, 945.
- (27) Chen, Y.; Nielsen, J. Biobased organic acids production by metabolically engineered microorganisms. *Curr. Opin. Biotechnol.* **2016**, *37*, 165.
- (28) Skellam, E. Biosynthesis of fungal polyketides by collaborating and trans-acting enzymes. *Nat. Prod. Rep.* **2022**, DOI: 10.1039/D1NP00056J.

## Recommended by ACS

### Metabolic Blockade-Based Genome Mining Reveals Lipochain-Linked Dihydro- $\beta$ -alanine Synthetases Involved in Autucedine Biosynthesis

Huaran Zhang, Jianhua Ju, *et al.*

JULY 24, 2022  
ORGANIC LETTERS

READ 

### Deciphering Biosynthetic Enzymes Leading to 4-Chloro-6-Methyl-5,7-Dihydroxyphenylglycine, a Non-Proteinogenic Amino Acid in Totopotensamides

Bin Tan, Changsheng Zhang, *et al.*

MARCH 02, 2020  
ACS CHEMICAL BIOLOGY

READ 

### Targeted Discovery of the Polyene Macrolide Hexacosalactone A from *Streptomyces* by Reporter-Guided Selection of Fermentation Media

Peng Shi, Haoxin Wang, *et al.*

JUNE 25, 2021  
JOURNAL OF NATURAL PRODUCTS

READ 

### Elucidation of the Streptoazine Biosynthetic Pathway in *Streptomyces aurantiacus* Reveals the Presence of a Promiscuous Prenyltransferase/Cyclase

Jing Liu, Shu-Ming Li, *et al.*

NOVEMBER 30, 2021  
JOURNAL OF NATURAL PRODUCTS

READ 

Get More Suggestions >

## **Supporting Information**

### **Formation of 3-Orsellinoxypropanoic Acid in *Penicillium crustosum* is Catalyzed by a Bifunctional Nonreducing Polyketide Synthase**

**Pan Xiang and Shu-Ming Li\***

Institut für Pharmazeutische Biologie und Biotechnologie, Fachbereich Pharmazie, Philipps-Universität  
Marburg, Robert-Koch-Straße 4, Marburg 35037, Germany

## Table of content

Experiment Procedures .....	3
1. Computer-assisted sequence analysis .....	3
2. Strains, media and growth conditions .....	3
3. Genomic DNA isolation .....	3
4. PCR amplification, gene cloning and plasmid construction .....	3
5. Heterologous gene expression in <i>A. nidulans</i> LO8030 .....	4
6. Confirmation and cultivation of the <i>A. nidulans</i> transformants .....	4
7. Large-scale fermentation, extraction and isolation of secondary metabolites .....	5
8. Quantitative analysis the 1 and 2 formation .....	5
9. Feeding experiments in the <i>oesA</i> expression strain <i>A. nidulans</i> PX15 .....	5
10. HPLC and LC-MS analyses of secondary metabolites .....	5
11. NMR analysis .....	6
12. Physiochemical properties of the compounds described in this study .....	6
Supplementary Tables .....	7
Table S1. Strains used in this study .....	7
Table S2. Plasmids used and constructed in this study .....	8
Table S3. Primers used in this study .....	9
Table S4. NMR data of compound 1 .....	11
Table S5. <sup>1</sup> H NMR data of compound 2 .....	12
Table S6. Enrichments in 1 after feeding with <sup>13</sup> C labeled precursors .....	13
Supplementary Figures .....	14
Figure S1. Phylogenetic analysis of OesA with known OSASs .....	14
Figure S2. Constructs used for heterologous expression in <i>A. nidulans</i> LO8030 .....	14
Figure S3. Verification of domain exchange between OesA and OrsA in the transformants .....	15
Figure S4. LC-MS analysis of the metabolite profile of <i>A. nidulans</i> strains .....	16
Figure S5. LC-MS analysis of orsellinic acid (OA) in different <i>A. nidulans</i> transformants .....	17
Figure S6. <sup>1</sup> H NMR spectrum of compound 1 in DMSO- <i>d</i> <sub>6</sub> (500 MHz) .....	18
Figure S7. <sup>13</sup> C NMR spectrum of compound 1 in DMSO- <i>d</i> <sub>6</sub> (125 MHz) .....	19
Figure S8. <sup>1</sup> H- <sup>1</sup> H COSY spectrum of compound 1 in DMSO- <i>d</i> <sub>6</sub> .....	20
Figure S9. HSQC spectrum of compound 1 in DMSO- <i>d</i> <sub>6</sub> .....	21
Figure S10. HMBC spectrum of compound 1 in DMSO- <i>d</i> <sub>6</sub> .....	22
Figure S11. <sup>1</sup> H NMR spectrum of compound 2 in CD <sub>3</sub> OD (500 MHz) .....	23
Supplementary References .....	24

## Experiment Procedures

### 1. Computer-assisted sequence analysis

The genomic DNA sequence of OesA (Pcr7502) from *Penicillium crustosum* PRB-2 reported in this study is available at GenBank under the accession number OL773684. Sequence analysis of 3-orsellinoxypropanoic acid synthase was carried out by antiSMASH (<http://antismash.secondarymetabolites.org/>) and by comparison with known entries in NCBI database. The sequences of other proteins were obtained from NCBI databases (<http://www.ncbi.nlm.nih.gov>). Domain structure prediction was carried out by using online programmes BLAST (<http://blast.ncbi.nlm.nih.gov>) and 2ndFind (<https://biosyn.nih.go.jp/2ndfind/>). The phylogenetic tree of orsellinic acid synthases (OSAs, Figure S1) was created by MEGA version 7.0 (<http://www.megasoftware.net>).

### 2. Strains, media and growth conditions

The fungal strains used in this study are summarized in Table S1. *P. crustosum* PRB-2<sup>1</sup> was cultivated on PDA plates [potato dextrose broth (PDB), Sigma-Aldrich with 1.6% agar] at 25°C for sporulation and in PD surface culture at 25°C for detection of secondary metabolites (SMs).

*Aspergillus nidulans* strains were grown at 37°C on GMM medium [LMM medium (1.0% glucose, 50 mL/L salt solution, 1 mL/L trace element solution, and 0.5% yeast extract) with 1.6% agar] for sporulation and transformation supplemented with 0.5 g/L uridine, 0.5 g/L uracil, 2.5 mg/L riboflavin and/or 0.5 mg/L pyridoxine, depending on the selective marker genes. The created *A. nidulans* strains were cultivated at 25°C in PD medium under static conditions for SM detection.<sup>2-4</sup>

*Escherichia coli* DH5 $\alpha$  (Invitrogen) was used for cloning and plasmid propagation and was grown in liquid or on solid lysogeny broth (LB) at 37 °C. 50  $\mu$ g/mL carbenicillin was used for selection of the recombinant *E. coli* strains.

*Saccharomyces cerevisiae* HOD114-2B was used for cloning by homologous recombination.<sup>5</sup> Generally, yeast was grown at 30°C in YPD medium [1% yeast extract, 2% peptone and 2% glucose]. Selection was performed with synthetic complete (SC) medium without uracil (SC-Ura) [6.7 g/L yeast nitrogen base with ammonium sulfate, 650 mg/L CSM-His-Leu-Ura (MP Biomedicals), histidine and leucine].<sup>6</sup>

### 3. Genomic DNA isolation

For genomic DNA isolation, *P. crustosum* and *A. nidulans* strains were cultivated in PDB or LMM for 3 days at 25 °C and 37 °C, respectively. Genomic DNA was isolated according to the method described previously.<sup>7</sup>

### 4. PCR amplification, gene cloning and plasmid construction

Plasmids generated and used in this study are listed in Table S2. The oligonucleotide sequences for PCR amplification are given in Table S3. All primers were synthesized by SeqLab GmbH (Göttingen, Germany). Genetic manipulation in *E. coli* was carried out as described before.<sup>8</sup> PCR amplification was carried out by using Phusion® High-Fidelity DNA polymerase from New England Biolabs (NEB) on a T100TM Thermal cycler from Bio-Rad.

Plasmids for heterologous expression were constructed by homologous recombination in *Escherichia coli* or *Saccharomyces cerevisiae*. To construct the plasmids for heterologous



expression of *oesA* and *orsA* in *A. nidulans*, an assembly approach based on the homologous recombination in *S. cerevisiae* was used (Figure S2).<sup>5,9</sup> The full length of *oesA* including its terminator of 517 bp was amplified from genomic DNA of *P. crustosum* PRB-2 as the template by PCR with primer pairs pPX15-PKS281-1F/1R and pPX15-PKS281-2F/2R (Table S3) and subsequently inserted into the *NheI*-linearized vector pYH-*wA*-pyrG with homologous flanking sequences of the *wA* gene, the *gpdA* promoter, and the *afpyrG* selection marker.<sup>3</sup> The amplified genomic sequence of *oesA* was cloned between the *gpdA* promoter and the *afpyrG* marker by using 25-30 bps overlap to the *NheI* restriction site to create pPX15.

In analogy, for creation of pPX26, *orsA* (AN7909) including its downstream region of 590 bp was PCR amplified from genomic DNA of *A. nidulans* RSM011 and was cloned into the linearized pYH-*wA*-pyrG by homologous recombination. Herein, primers pPX26-1F/1R and pPX26-2F/2R (Table S3) were used for PCR amplification.

To construct the plasmids with domain deletion and domain exchange between *oesA* and *orsA*, the coding region of *oesA* and *orsA* were amplified by PCR from pPX15 and pPX26 with the corresponding primer pairs (Table S3) and were cloned together with the *NheI*-linearized pYH-*wA*-pyrG via homologous recombination in yeast to give pPX29–pPX32 and pPX34–pPX37.

For creation of the plasmid with an ACP1 domain deletion of *oesA*, the primers pPX15-PKS281-1F/pPX29-1R and pPX29-2F/pPX15-PKS281-2R were used to amplify the fragments of *oesA* containing SAT-KS-AT-PT and ACP2-TE domains including its terminator from pPX15, respectively. To construct pPX30 with the ACP2 domain deletion in *oesA*, pPX15-PKS281-1F/pPX30-1R and pPX30-2F/pPX15-PKS281-2R were used to amplify the fragments of *oesA* containing SAT-KS-AT-PT-ACP1 domains and TE domain including its terminator from pPX15, respectively.

For domain exchange experiments, the fragments of *oesA* were amplified from pPX15 and the fragments of *orsA* were amplified from pPX26 with primers listed in Table S3. The fragments were designed with a 20–28 bp overlap to each other, the fragments on the gene ends carried an overlap to the *NheI*-linearized pYH-*wA*-pyrG. The linearized plasmid and the DNA-fragments were cloned together via homologous recombination in yeast to give pPX31–pPX32 and pPX34–pPX37.

## 5. Heterologous gene expression in *A. nidulans* LO8030

*A. nidulans* LO8030 was used as the recipient host.<sup>4</sup> Fungal protoplast preparation and PEG-mediated protoplast transformation were performed according to the protocol described previously.<sup>7</sup>

## 6. Confirmation and cultivation of the *A. nidulans* transformants

Genomic DNA of the transformants was isolated and used for PCR amplification. After selection by uridine and uracil autotrophy, the correct integration into the *wA* PKS gene locus was first observed by a color change of the conidia from green to white, and subsequent confirmed by PCR amplification with primers flanking the inserted gene(s) (Table S2, Figure S3). PCR amplification for the domain exchanging transformants was performed using one primer binding in the *oesA* part and another binding in the *orsA* part.

For detection of secondary metabolites, transformants were cultivated in PDB medium with the

required supplements at 25°C. After 10 days, secondary metabolites were extracted with equivalent volumes of ethyl acetate for three times, dissolved in a mixture of methanol and distilled H<sub>2</sub>O (9:1) and analyzed *via* LC-MS.

### 7. Large-scale fermentation, extraction and isolation of secondary metabolites

To isolate **1** from *A. nidulans* carrying *oesA*, the transformant PX15.1 was cultivated in 10 x 1 L Erlenmeyer flasks each containing 300 mL PD liquid medium supplemented with 0.5 mg/L pyridoxine and 2.5 mg/L riboflavin at 25°C for 14 days. The supernatant and mycelia were separated, and extracted with ethyl acetate and acetone, separately. The acetone extract was concentrated under reduced pressure to afford an aqueous solution, and then extracted with ethyl acetate. The two ethyl acetate extracts were combined and evaporated under reduced pressure to give a crude extract (1.0 g). This crude extract was applied to silica gel column chromatography by using CH<sub>2</sub>Cl<sub>2</sub> / MeOH (100 : 1, 40 : 1, 10 : 1 and 0 : 1, v/v) as elution solvents, giving fractions 1 – 34. **1** (6.9 mg) was obtained from fraction 20 – 23 after purification on a semi-preparative HPLC (XDB-C18, H<sub>2</sub>O/CH<sub>3</sub>CN = 65/40, flow rate = 2.0 mL/min,  $\lambda$  = 254 nm,  $t_R$  = 12.3 min).

To isolate **2** from *A. nidulans* carrying *orsA*, the transformant PX26 was cultivated in 2 x 2.5 L Erlenmeyer flasks each containing 500 mL PD liquid medium supplemented with 0.5 mg/L pyridoxine and 2.5 mg/L riboflavin at 25°C for 7 days. After extracting with 6 L ethyl acetate and concentration under reduced pressure, the crude extract (0.3 g) was purified by using preparative HPLC (VDSpher PUR 100 C18-M-SE, H<sub>2</sub>O/CH<sub>3</sub>CN = 90/10 – 0/100, flow rate = 10.0 mL/min,  $\lambda$  = 254 nm) in 10 min, leading to the isolation of **2** (31.2 mg,  $t_R$  = 6.3 min).

### 8. Quantitative analysis the **1** and **2** formations

For quantitative experiments, 50 mL PDB medium supplemented with 2.5 mg/L riboflavin and 0.5 mg/L pyridoxine were inoculated with spores of *A. nidulans* PX15, PX26, PX29, PX30, and PX32 in 250 ml flasks. The cultures were kept at 25°C under static conditions as triplicates. 1 mL culture each was taken on day 3, 5, 7, 10, 14, and 21 and extracted with equivalent volumes of ethyl acetate for three times. The extracts were dissolved in 100  $\mu$ L mixture of MeOH and distilled H<sub>2</sub>O (9:1), and analyzed *via* LC-MS. The data were obtained by analysis with Compass DataAnalysis 4.2 software and GraphPad Prism 8.

### 9. Feeding experiments in the *oesA* expression strain *A. nidulans* PX15

To isolate the labeled products, the strain PX15 was cultivated in PDB liquid medium with appropriate supplements at 25°C. Aqueous stock solutions of the labeled compounds were fed to the cultures after 24 h cultivation. After cultivation for another 10 days, the fungal cultures were extracted with ethyl acetate for three times. The extracts were further purified on HPLC and subjected to NMR analysis. 5.0 mg of **1** were obtained from 2.5 L culture with 750 mg of sodium [2-<sup>13</sup>C] acetate and 2.2 mg from 1.0 L culture with 360 mg of [2-<sup>13</sup>C] malonic acid.

### 10. HPLC and LC-MS analyses of secondary metabolites

Analysis of SMs was performed on an Agilent series 1200 HPLC (Agilent Technologies, Böblingen, Germany) with an Agilent Eclipse XDB-C18 column (150 × 4.6 mm, 5  $\mu$ m). H<sub>2</sub>O (A) and CH<sub>3</sub>CN (B), both with 0.1% (v/v) HCOOH, were used as solvents at flow rate of 0.5 mL/min. The substances were eluted with a linear gradient from 5 – 100% B in 40 min, then washed with 100%

(v/v) solvent B for 5 min and equilibrated with 5% (v/v) solvent B for 10 min. UV absorptions at 254 nm were illustrated in this study. Semi-preparative HPLC was performed on the same equipment with an Agilent Eclipse XDB-C18 column (9.4 × 250 mm, 5 μm) column and a flow rate of 2 mL/min. Preparative HPLC was performed on an Agilent series 1260 Infinity II HPLC (Agilent Technologies, Böblingen, Germany) with an VDSpher PUR 100 C18-M-SE column (150 × 20 mm, 5 μm) and a flow rate of 10 mL/min.

LC-MS analysis was performed on an Agilent 1260 HPLC system equipped with a microTOF-Q III spectrometer (Bruker, Bremen, Germany) by using Multospher 120 RP18-5μ column (250 × 2 mm, 5 μm, CS-Chromatographie Service GmbH, Langerwehe, Germany). H<sub>2</sub>O (A) and CH<sub>3</sub>CN (B), both with 0.1% (v/v) formic acid, were used as solvents at flow rate of 0.25 mL/min. The substances were eluted using a linear gradient from 5–100% B within 40 min. For mass determination, positive ion mode electrospray ionization (ESI) in a microTOF-Q III mass spectrometer with ESI-source (Bruker Daltonics) was used with 5 mM sodium formate for mass calibration. The masses were scanned in the range of *m/z* 100 – 1500. Data were evaluated with the Compass DataAnalysis 4.2 software (Bruker Daltonik, Bremen, Germany).

## 11. NMR analysis

NMR spectra were recorded on a JEOL ECA-500 MHz spectrometer (JEOL, Tokyo, Japan). The spectra were processed with MestReNova 6.1.0 (Metrelab, Santiago de Compostela, Spain). Chemical shifts are referenced to those of the solvent signals. NMR data are given in Tables S4 – S6 and spectra in Figures S6 – S11.

## 12. Physiochemical properties of the compounds described in this study

3-Orsellinoxypropanoic acid (**1**): yellow oil; HRMS (ESI) *m/z*: [M + Na]<sup>+</sup> Calcd for C<sub>11</sub>H<sub>12</sub>O<sub>6</sub>Na 263.0526; Found 263.0522.

Diorcinolic acid (**2**): yellow oil; HRMS (ESI) *m/z*: [M + H]<sup>+</sup> Calcd for C<sub>16</sub>H<sub>15</sub>O<sub>7</sub> 319.0812; Found 319.0814.

## Supplementary Tables

**Table S1.** Strains used in this study

Strains	Genotype	Source/Ref.
<i>Penicillium crustosum</i>		
PRB-2	Wild type	1
<i>Aspergillus nidulans</i>		
LO8030	<i>pyroA4</i> , <i>riboB2</i> , <i>pyrG89</i> , <i>nkuA::argB</i> , sterigmatocystin cluster ( <i>AN7804-AN7825</i> ) $\Delta$ , emerellamide cluster ( <i>AN2545-AN2549</i> ) $\Delta$ , asperfuranone cluster ( <i>AN1039-AN1029</i> ) $\Delta$ , monodictyphenone cluster ( <i>AN10023-AN10021</i> ) $\Delta$ , terrequinone cluster ( <i>AN8512-AN8520</i> ) $\Delta$ , austinol cluster part 1 ( <i>AN8379-AN8384</i> ) $\Delta$ , austinol cluster part 2 ( <i>AN9246-AN9259</i> ) $\Delta$ , F9775 cluster ( <i>AN7906-AN7915</i> ) $\Delta$ , asperthecin cluster ( <i>AN6000-AN6002</i> ) $\Delta$	4
<i>Aspergillus nidulans</i> RSM011	Wild type	10
PX15	<i>gpdA::oesA::AfpYrG</i> in <i>A. nidulans</i> LO8030	This study
PX26	<i>gpdA::orsA::AfpYrG</i> in <i>A. nidulans</i> LO8030	This study
PX29	<i>gpdA::oesA(<math>\Delta</math>ACP1)::AfpYrG</i> in <i>A. nidulans</i> LO8030	This study
PX30	<i>gpdA::oesA(<math>\Delta</math>ACP2)::AfpYrG</i> in <i>A. nidulans</i> LO8030	This study
PX31	<i>gpdA::oesA(SAT-KS-AT-PT)+orsA(ACP1-ACP2-TE)::AfpYrG</i> in <i>A. nidulans</i> LO8030	This study
PX32	<i>gpdA::orsA(SAT-KS-AT-PT)+oesA(ACP1-ACP2-TE)::AfpYrG</i> in <i>A. nidulans</i> LO8030	This study
PX34	<i>gpdA::oesA(SAT-KS-AT-PT-ACP1)+orsA(ACP2-TE)::AfpYrG</i> in <i>A. nidulans</i> LO8030	This study
PX35	<i>gpdA::orsA(SAT-KS-AT-PT-ACP1)+oesA(ACP2-TE)::AfpYrG</i> in <i>A. nidulans</i> LO8030	This study
PX36	<i>gpdA::oesA(SAT-KS-AT-PT-ACP1-ACP2)+orsA(TE)::AfpYrG</i> in <i>A. nidulans</i> LO8030	This study
PX37	<i>gpdA::orsA(SAT-KS-AT-PT-ACP1-ACP2)+oesA(TE)::AfpYrG</i> in <i>A. nidulans</i> LO8030	This study

**Table S2.** Plasmids used and constructed in this study

Plasmids	Description	Source/Ref.
pYH-wA-pyrG	<i>URA3</i> , <i>wA</i> flanking, <i>Afp</i> pyrG, <i>Amp</i>	3
pESC-URA	<i>Saccharomyces cerevisiae</i> and <i>E. coli</i> shuttle vector	Agilent
pPX15	pYH-wA- <i>oesA</i> ; a 7205 bp fragment of <i>oesA</i> with its terminator from genomic DNA of <i>P. crustosum</i> PRB-2 were inserted in pYH-wA-pyrG	This study
pPX26	pYH-wA- <i>orsA</i> ; a 7092 bp fragment of <i>orsA</i> with its terminator from genomic DNA of <i>A. nidulans</i> RSM011 were inserted in pYH-wA-pyrG	This study
pPX29	$\Delta$ ACP1 of <i>oesA</i> ; a 5163 bp fragment and a 1908 bp fragment with its terminator of <i>oesA</i> from pPX15 were inserted in pYH-wA-pyrG	This study
pPX30	$\Delta$ ACP2 of <i>oesA</i> ; a 5548 bp fragment and a 1572 bp fragment with its terminator of <i>oesA</i> from pPX15 were inserted in pYH-wA-pyrG	This study
pPX31	a 5098 bp fragment of <i>oesA</i> from pPX15 and a 2207 bp fragment with its terminator of <i>orsA</i> from pPX26 were inserted in pYH-wA-pyrG	This study
pPX32	a 4850 bp fragment of <i>orsA</i> from pPX26 and a 2109 bp fragment with its terminator of <i>oesA</i> from pPX15 were inserted in pYH-wA-pyrG	This study
pPX34	a 5492 bp fragment of <i>oesA</i> from pPX15 and a 1774 bp fragment with its terminator of <i>orsA</i> from pPX26 were inserted in pYH-wA-pyrG	This study
pPX35	a 5291 bp fragment of <i>orsA</i> from pPX26 and a 1674 bp fragment with its terminator of <i>oesA</i> from pPX15 were inserted in pYH-wA-pyrG	This study
pPX36	a 5755 bp fragment of <i>oesA</i> from pPX15 and a 1449 bp fragment with its terminator of <i>orsA</i> from pPX26 were inserted in pYH-wA-pyrG	This study
pPX37	a 5630 bp fragment of <i>orsA</i> from pPX26 and a 1421 bp fragment with its terminator of <i>oesA</i> from pPX15 were inserted in pYH-wA-pyrG	This study

**Table S3.** Primers used in this study

Primer	Sequence	Targeted amplification
pPX15-PKS281-1F	<u>CATCTTCCCATCCAAGAACCTTTAATCATGGCGTCCAACAA</u> CTTCCTC	DNA of 1st <i>oesA</i> fragment 3698 bp from <i>P. crustosum</i> to construct pPX15
pPX15-PKS281-1R	GCATAAGATAGTCGGGCTCAATCAG	
pPX15-PKS281-2F	GCCTTTCATTCCGCTCAGATGG	DNA of 2nd <i>oesA</i> fragment 3661 bp from <i>P. crustosum</i> to construct pPX15
pPX15-PKS281-2R	<u>ATTTCGTCAGACACAGAATAACTCTCCTCAGACATGAACCA</u> GTCAGCG	
pPX15-test-1f	GAGCAACTATCATTGGTCGC	937 bp partial fragment of <i>oesA</i>
pPX15-test-1r	GAACACAAGTGCTTAGAGGC	
pPX26-1F	<u>CATCTTCCCATCCAAGAACCTTTAATCATGGCTCCAAATCA</u> CGTTCTT	DNA of 1st <i>orsA</i> fragment 3604 bp from <i>A. nidulans</i> RSM011 to construct pPX26
pPX26-1R	GCCATCAGACTGATGCAGATAG	
pPX26-2F	GTGCAGCATGCTTCCATACTC	DNA of 2nd <i>orsA</i> fragment 3834 bp from <i>A. nidulans</i> RSM011 to construct pPX26
pPX26-2R	<u>ATTTCGTCAGACACAGAATAACTCTCGTCAAGATGAGATGC</u> AGGAAGAG	
pPX26-test-1f	CGTCGTCGAGATGCATGGAAC	2070 bp partial fragment of <i>orsA</i>
pPX26-test-1r	CTGCTCAGCTCGTAGGTGTTT	
pPX29-1R	<u>GATTCCAACAGCATAAGATGCGCTCGGAGGAACATGTCAT</u> CAGAGGAAC	DNA of 1st <i>oesA</i> fragment 5163 bp from pPX15 to construct pPX29 (amplified with pPX15-PKS281-1F)
pPX29-1F	<u>CGAGTTCTCTGATGACATGTTCTCCGAGCGCATCTTAT</u> GCTGTTGG	DNA of 2nd <i>oesA</i> fragment 1908 bp from pPX15 to construct pPX29 (amplified with pPX15-PKS281-2R)
pPX30-1R	<u>CAGGGTGGGCTTAGGAGCCGAGCCGTTATGCTGCAAATC</u> GGACATTTTCG	DNA of 1st <i>oesA</i> fragment 5548 bp from pPX15 to construct pPX30 (amplified with pPX15-PKS281-1F)
pPX30-1F	<u>CTGGATGCCAAATGTCCGATTTGCAGCATAACGGCTCGGC</u> TCCTAAGC	DNA of 2nd <i>oesA</i> fragment 1572 bp from pPX15 to construct pPX30 (amplified with pPX15-PKS281-2R)
pPX31-1R	<u>CTTTGCCATAGACTTGGCCGGCGCAGCATCAGAGGAACT</u> CGTAGCTAAC	DNA of <i>oesA</i> fragment 5152 bp from pPX15 to construct pPX31 (amplified with pPX15-PKS281-1F, containing SAT-KS-AT-PT domains of <i>oesA</i> )
pPX31-2F	<u>CCAAAGTTAGCTACGAGTTCCTCTGATGCTGCGCCGGCCA</u> AGTCTATG	DNA of <i>orsA</i> fragment 2260 bp from pPX26 to construct pPX31 (containing ACP1-ACP2-TE domains and its terminator of <i>orsA</i> )
pPX31-2R	<u>ATTTCGTCAGACACAGAATAACTCTCGTTGGTCTCAGCTG</u> AAATGCCTG	
pPX31-test-1f	GTGCGATTCCCGGCAAAGTAC	1051 bp partial fragment of pPX31 for transformant verification
pPX31-test-1r	GGCGTGAGATCACTGGCTTCC	
pPX32-1R	<u>ATTATTTTGGCCACCCGGAGGAACATGTCAGCCACCGGCT</u> TGGTGGAGC	DNA of <i>orsA</i> fragment 4906 bp from pPX26 to construct pPX32 (amplified with pPX26-1F, containing SAT-KS-AT-PT domains of <i>orsA</i> )

Table S3 (continued)

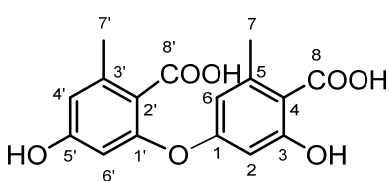
pPX32-2F	<u>CCCGCGGCCGCTCCACCAAGCCGGTGGCTGACATGTTCC</u> TCCGGGTGGC	DNA of <i>oesA</i> fragment 2109 bp from pPX15 to construct pPX32 (amplified with pPX15-PSK281-2R, containing ACP1-ACP2-TE domains and its terminator of <i>oesA</i> )
pPX32-test-1f	GACGATGCGTCTAGGCCAGC	1059 bp partial fragment of pPX32 for transformant verification
pPX32-test-1r	GCCAGGATACCCATGGACATC	
pPX34-1R	<u>CGAGAGAGAGCAGGTGCTGGCTTGGTGGCTGCAAATCGG</u> ACATTTCGC	DNA of <i>oesA</i> fragment 5546 bp from pPX15 to construct pPX34 (amplified with pPX15-PSK281-1F, containing SAT-KS-AT-PT-ACP1 domains of <i>oesA</i> )
pPX34-2F	<u>CTGGATGCGAAATGTCCGATTTGCAGCCACCAAGCCAGCA</u> CCTGCTCTC	DNA of <i>orsA</i> fragment 1827 bp from pPX26 to construct pPX34 (amplified with pPX31-2R, containing ACP2-TE domains and its terminator of <i>orsA</i> )
pPX34-test-1r	CGCTGGGTTCGTCGATGTCTG	1208 bp partial fragment of pPX34 for transformant verification (amplified with pPX31-test-1f)
pPX35-1R	<u>GAACTCAGTATCATGCTGCAAATCGGACGCTTGGTGCCGG</u> GCCTTGCTTC	DNA of <i>orsA</i> fragment 5346 bp from pPX26 to construct pPX35 (amplified with pPX26-1F, containing SAT-KS-AT-PT-ACP1 domains of <i>orsA</i> )
pPX35-2F	<u>GCCCGGAAGCAAGGCCCGGCACCAAGCGTCCGATTTGCA</u> GCATGATACTGAG	DNA of <i>oesA</i> fragment 1727 bp from pPX15 to construct pPX35 (amplified with pPX15-PSK281-2R, containing ACP2-TE domains and its terminator of <i>oesA</i> )
pPX35-test-1r	CGAGCCGTTCAACATTTTCG CAC	1214 bp partial fragment of pPX35 for transformant verification (amplified with pPX32-test-1f)
pPX36-1R	<u>GGAGCGGAGACTGACCCCTTTAGTAGAGGTAGACCAGAAG</u> TAGGATTGCC	DNA of <i>oesA</i> fragment 5807 bp from pPX15 to construct pPX36 (amplified with pPX15-PSK281-1F, containing SAT-KS-AT-PT-ACP1-ACP2 domains of <i>oesA</i> )
pPX36-2F	<u>CAAGGCAATCCTACTTCTGGTCTACCTCTACTAAAGGGGT</u> CAGTCTCGC	DNA of <i>orsA</i> fragment 1502 bp from pPX26 to construct pPX36 (amplified with pPX31-2R, containing TE domain and its terminator of <i>orsA</i> )
pPX36-test-1f	GCAGAGGAAGTTGGAATGGATACG	1069 bp partial fragment of pPX36 for transformant verification
pPX36-test-1r	GACTGAGAGGTCTTCAGGGAGG	
pPX37-1R	<u>GTGTAGGTAGACCAGAAGTAGGATTGCCGCGAGACTGAC</u> CCCTTTAGTAG	DNA of <i>orsA</i> fragment 5685 bp from pPX26 to construct pPX37 (amplified with pPX26-1F, containing SAT-KS-AT-PT-ACP1-ACP2 domains of <i>orsA</i> )
pPX37-2F	<u>CAGTCTACTAAAGGGGTCACTCTCGCGGCAATCCTACTTC</u> TGCTTACC	DNA of <i>oesA</i> fragment 1473 bp from pPX15 to construct pPX37 (amplified with pPX15-PSK281-2R, containing TE domain and its terminator of <i>oesA</i> )
pPX37-test-1f	CTAACTCCAGCGCACTACGG	1058 bp partial fragment of pPX37 for transformant verification
pPX37-test-1r	CCAGATCTGCATCACATAAGGCG	

The underlined sequences in the primers are homologous regions with the vector or the other fragment for recombination.



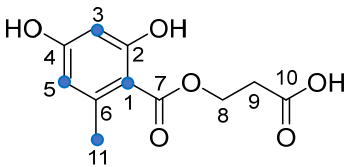
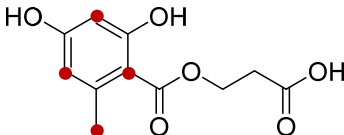


**Table S5.**  $^1\text{H}$  NMR data of compound **2**

<div>Compound</div> <div></div>	
Diorcinolic acid ( <b>2</b> , $\text{CD}_3\text{OD}$ )	
Position	$\delta_{\text{H}}$ , multi., $J$ in Hz
2	6.17, d, 2.8
6	6.29, d, 3.2
7	2.47, s
4'	6.51, d, 2.5
6'	6.24, d, 2.6
7'	2.31, s

The NMR data of the isolated compound correspond very well to those reported in the literature.<sup>11,12</sup>

**Table S6.** Enrichments in **1** after feeding with  $^{13}\text{C}$  labeled precursors

Position	$\delta_{\text{C}}$	sodium [2- $^{13}\text{C}$ ] acetate	[2- $^{13}\text{C}$ ] malonic acid
			
1	106.6 (C)	3.0	18.3
2	161.7 (C)	1.0	0.9
3	100.5 (CH)	4.3	15.7
4	161.4 (C)	1.1	0.8
5	110.5 (CH)	4.0	21.3
6	141.2 (C)	1.0	1.0
7	169.7 (C)	1.1	1.0
8	60.8 (CH <sub>2</sub> )	1.2	1.2
9	33.3 (CH <sub>2</sub> )	1.1	0.8
10	172.0 (C)	0.9	0.9
11	22.2 (CH <sub>3</sub> )	4.3	5.9

## Supplementary Figures

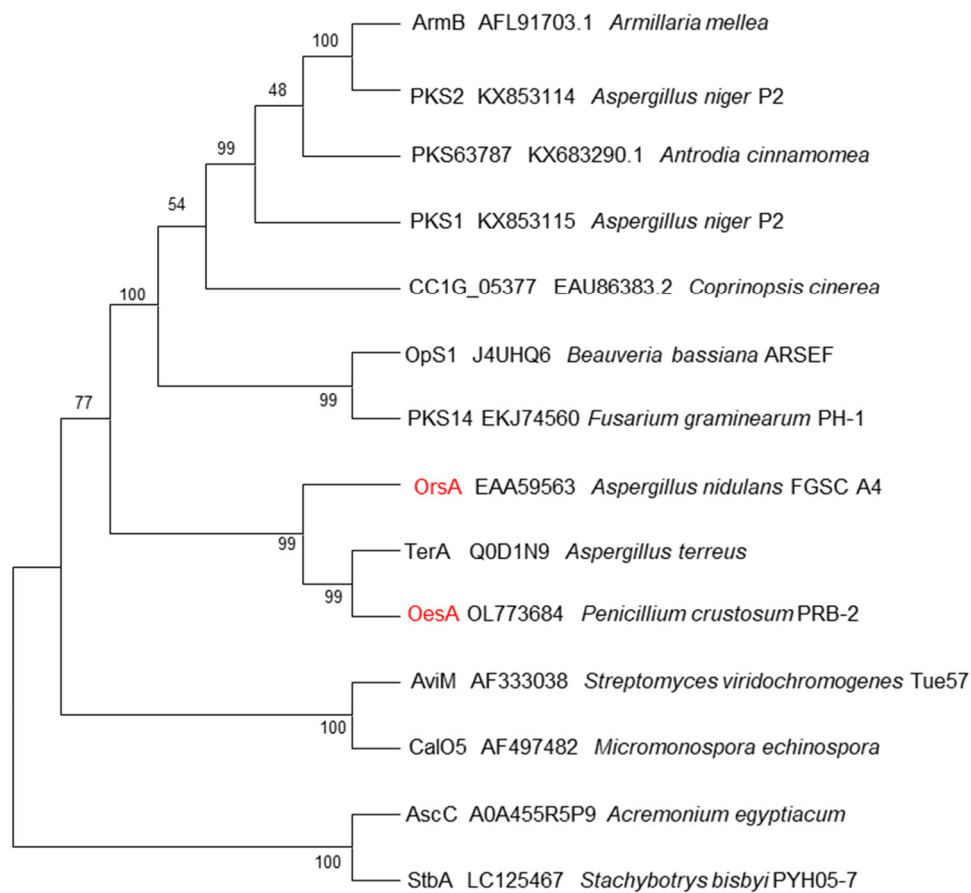


**Figure S1.** Phylogenetic analysis of OesA with known OSASs

The sequences of the known proteins were downloaded from NCBI database.

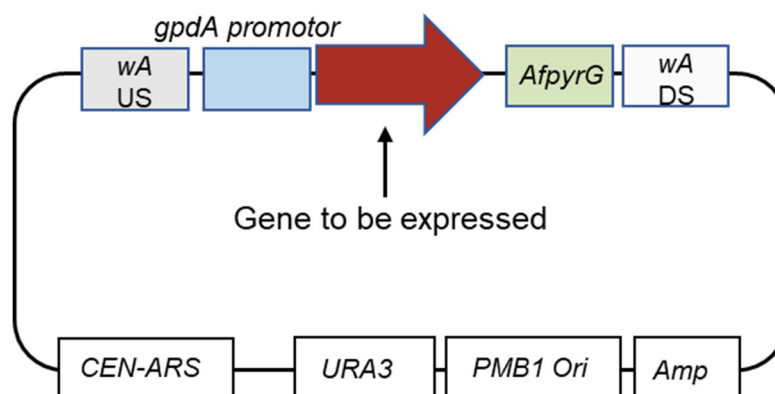


**Figure S2.** Constructs used for heterologous expression in *A. nidulans* LO8030

(A) Linearized integration vector

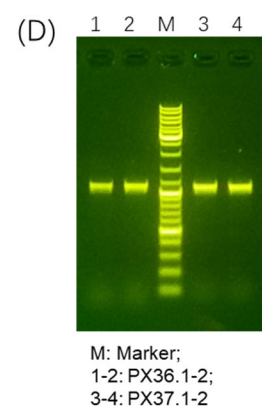
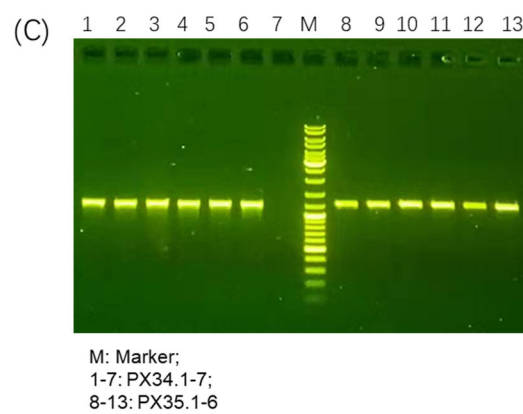
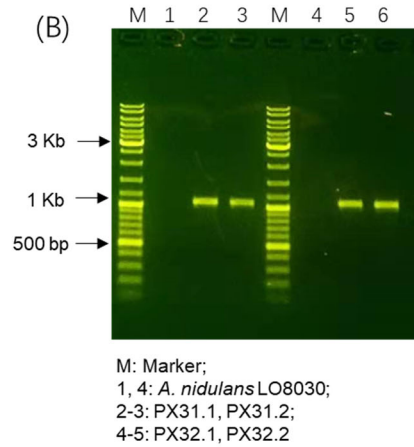
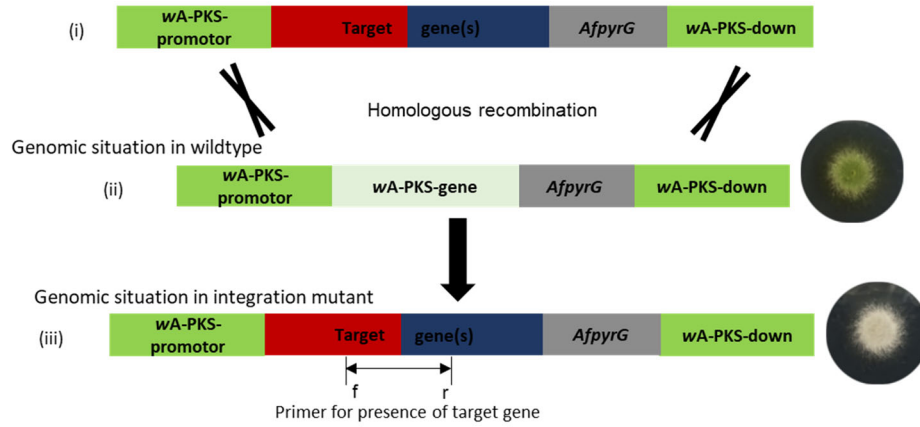


**Figure S3.** Verification of domain exchange between OesA and OrsA in the transformants

(A) Schematic representation of homologous recombination in *A. nidulans*. (iii) The genomic situation in the transformant shows the amplified fragment in the transformant which was used to prove the presence of the target gene. (B – D) PCR verifications were performed with genomic DNA of the *A. nidulans* transformants. The primers are given in Table S3.

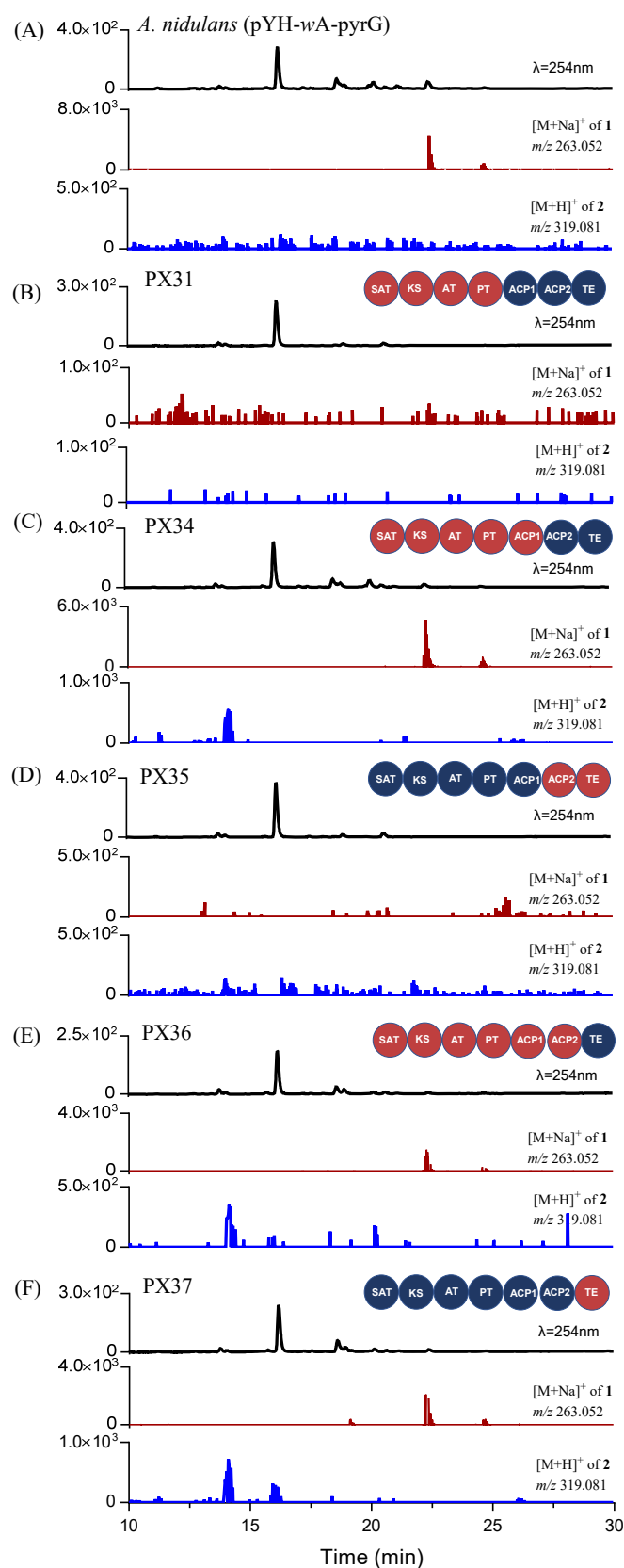


**Figure S4.** LC-MS analysis of the metabolite profile of *A. nidulans* strains PX31 carrying the expression construct for pPX31 and PX34 – 37 with plasmids pPX34 – 37 were cultivated in PD medium at 25 °C for 14 days. UV absorptions at 254 nm,  $[M+Na]^+$  of 1 at  $m/z$   $263.052 \pm 0.005$ , and  $[M+H]^+$  of 2 at  $m/z$   $319.081 \pm 0.005$  are illustrated.

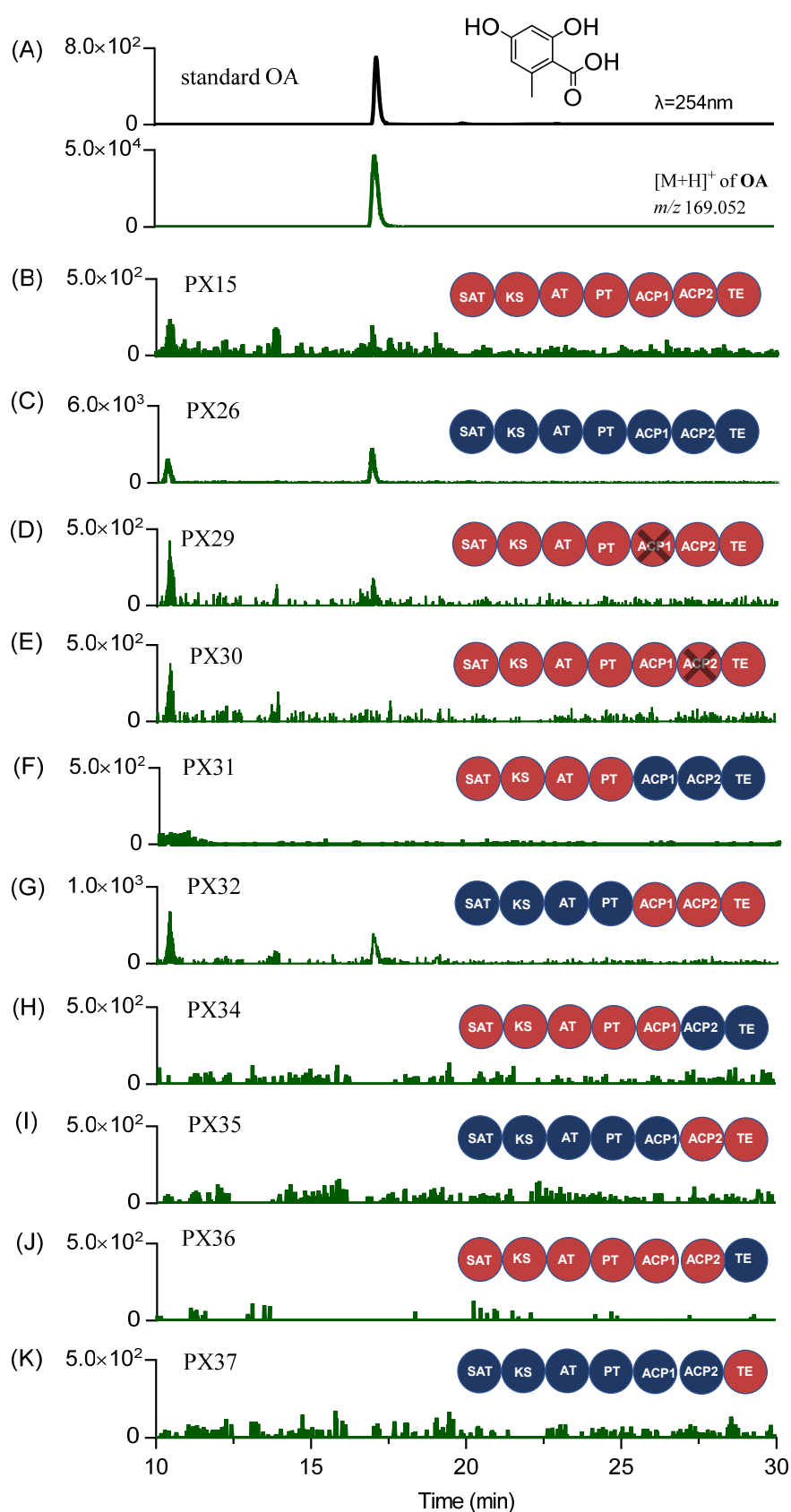


**Figure S5.** LC-MS analysis of orsellinic acid (OA) in different *A. nidulans* transformants. UV absorption of the OA standard at 254 nm is illustrated in (A). EICs in dark green refer total  $[M+H]^+$  ions of OA with a tolerance range of  $\pm 0.005$  (B – K).

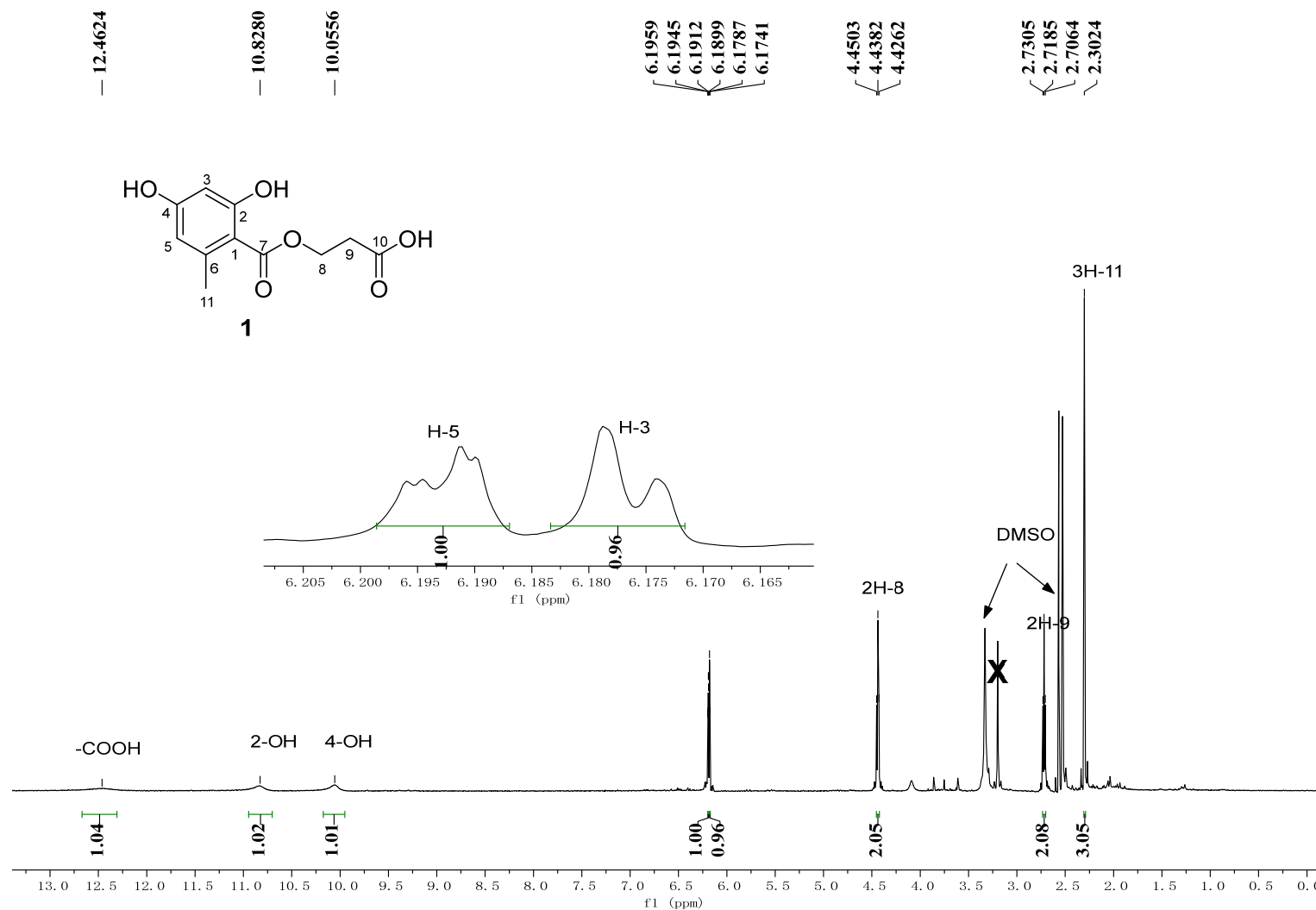


**Figure S6.** <sup>1</sup>H NMR spectrum of compound **1** in DMSO-*d*<sub>6</sub> (500 MHz)

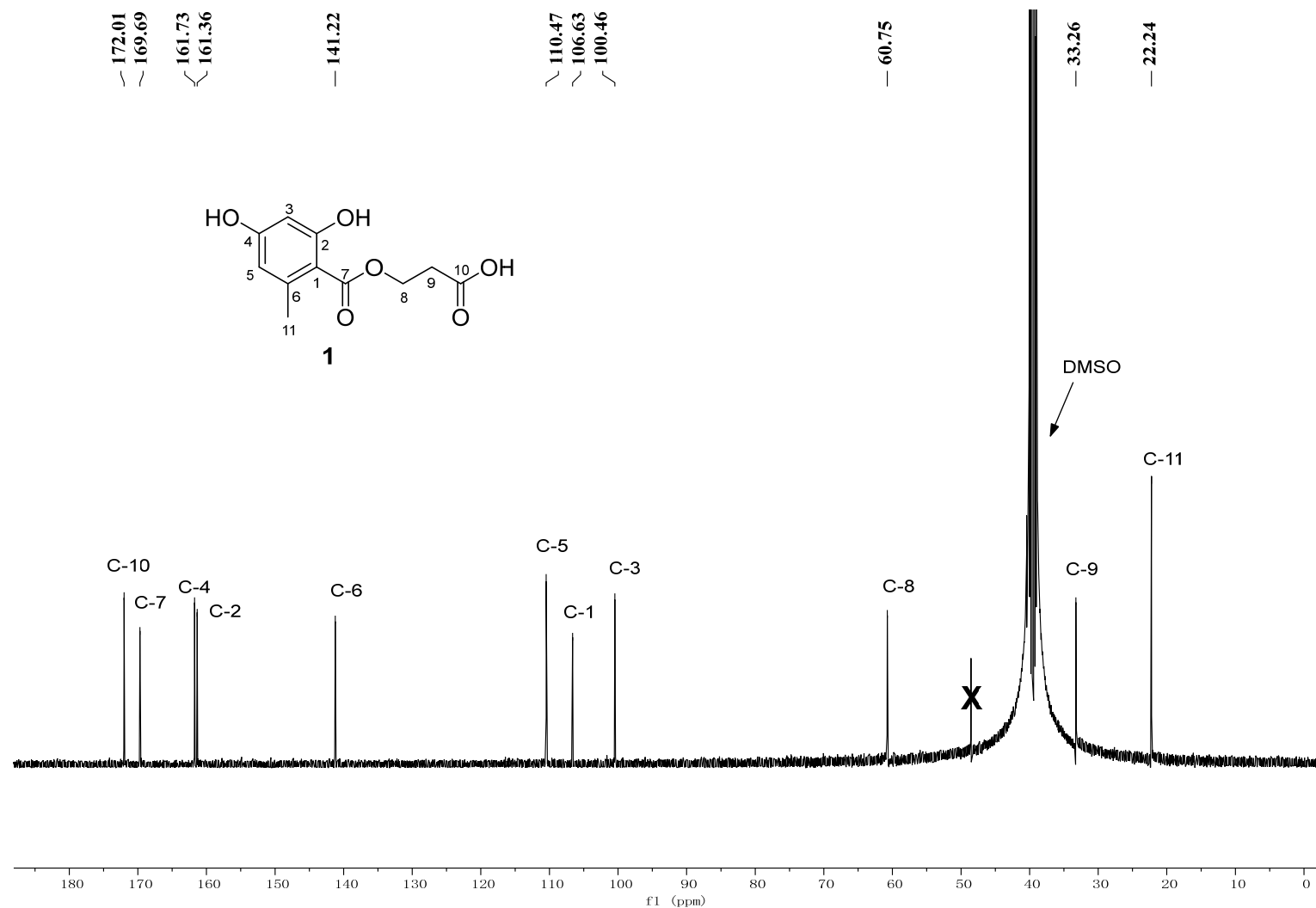


**Figure S7.**  $^{13}\text{C}$  NMR spectrum of compound **1** in  $\text{DMSO-}d_6$  (125 MHz)



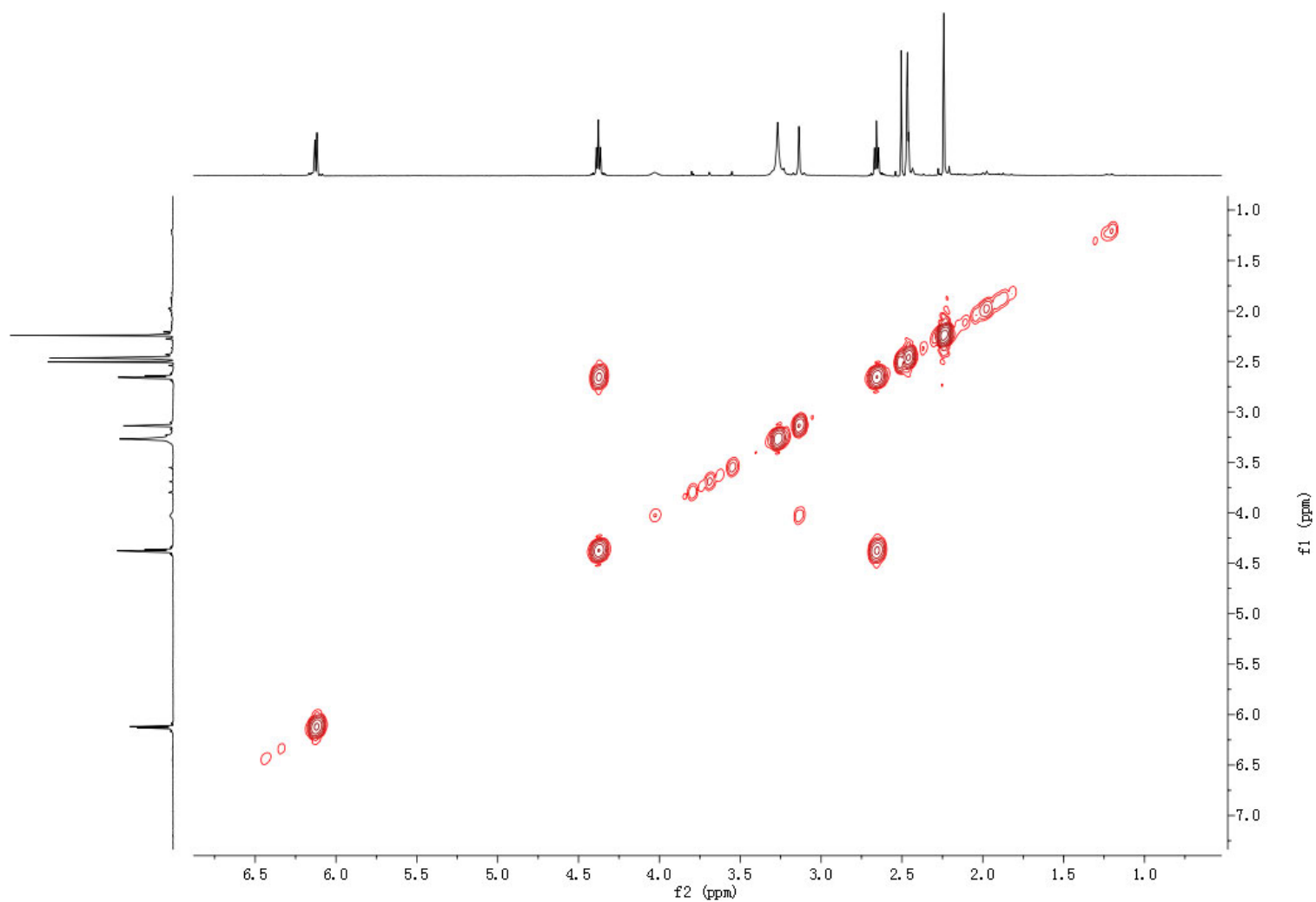


**Figure S8.**  $^1\text{H}$ - $^1\text{H}$  COSY spectrum of compound **1** in  $\text{DMSO}-d_6$

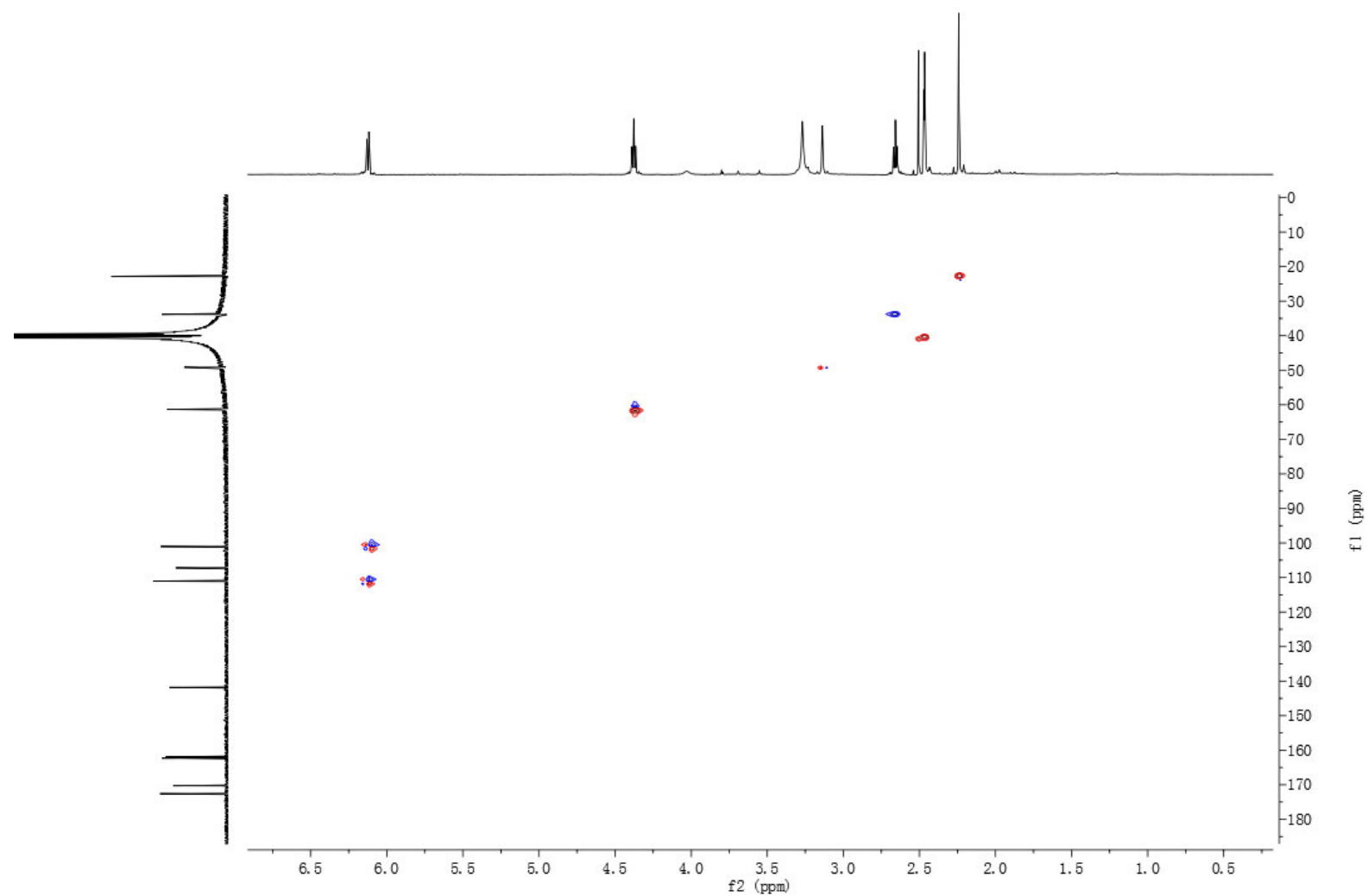


**Figure S9.** HSQC spectrum of compound **1** in DMSO- $d_6$

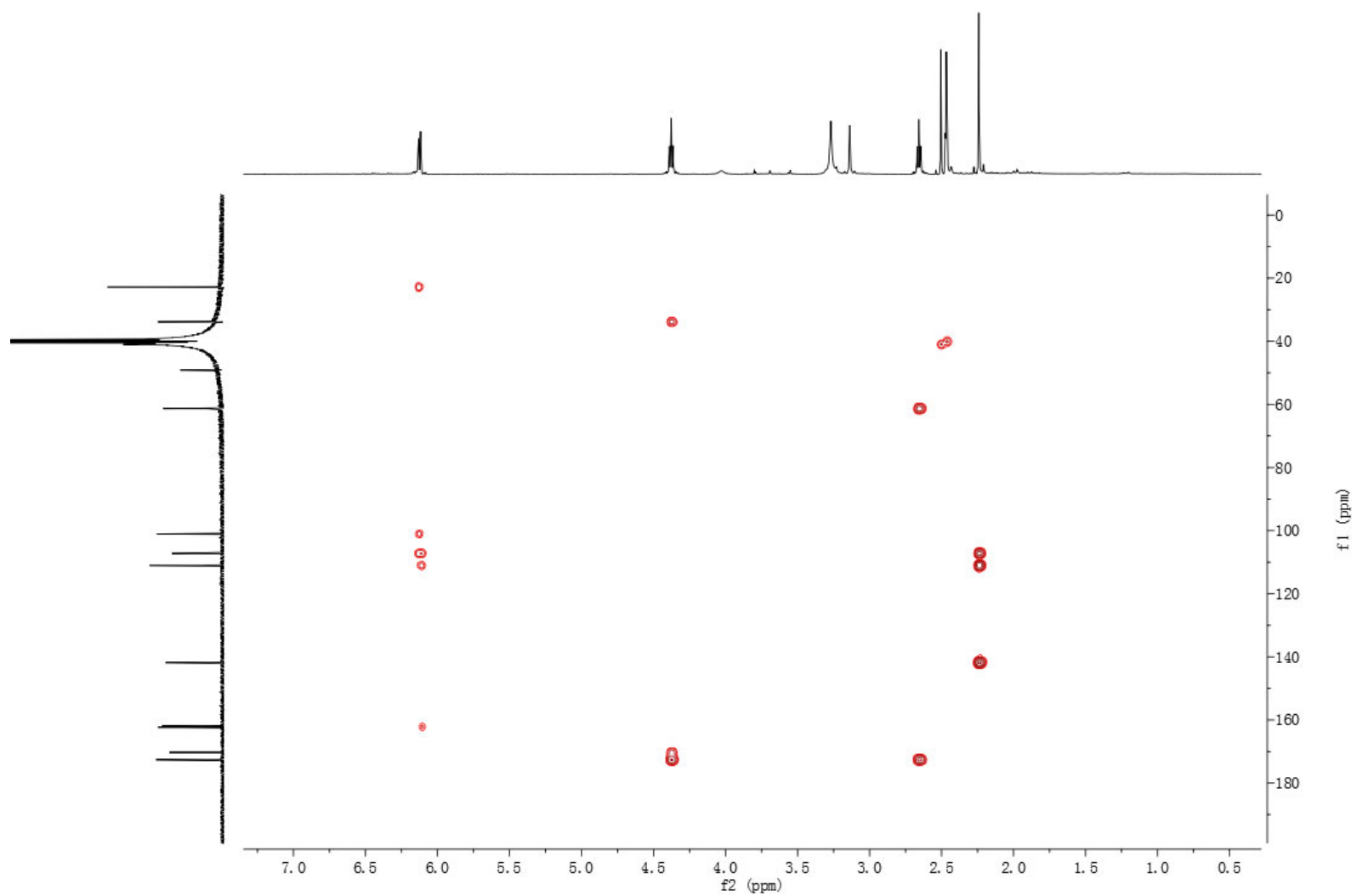


**Figure S10.** HMBC spectrum of compound **1** in DMSO- $d_6$

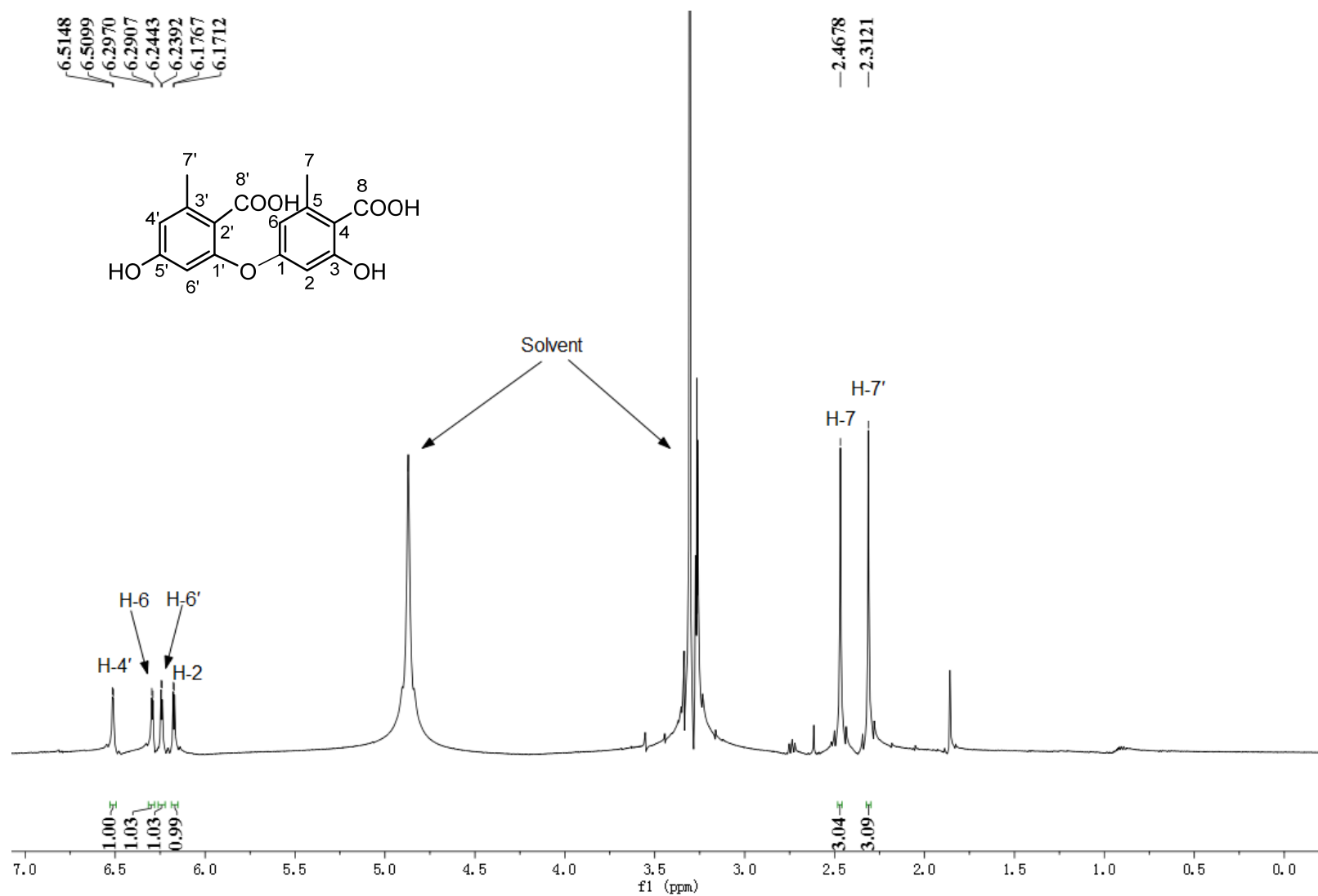


**Figure S11.**  $^1\text{H}$  NMR spectrum of compound **2** in  $\text{CD}_3\text{OD}$  (500 MHz)

## Supplementary References

- (1) Wu, G.; Ma, H.; Zhu, T.; Li, J.; Gu, Q.; Li, D. Penilactones A and B, two novel polyketides from Antarctic deep-sea derived fungus *Penicillium crustosum* PRB-2. *Tetrahedron* **2012**, *68*, 9745.
- (2) Li, W.; Fan, A.; Wang, L.; Zhang, P.; Liu, Z.; An, Z.; Yin, W.-B. Asperphenamate biosynthesis reveals a novel two-module NRPS system to synthesize amino acid esters in fungi. *Chem. Sci.* **2018**, *9*, 2589.
- (3) Yin, W. B.; Chooi, Y. H.; Smith, A. R.; Cacho, R. A.; Hu, Y.; White, T. C.; Tang, Y. Discovery of cryptic polyketide metabolites from dermatophytes using heterologous expression in *Aspergillus nidulans*. *ACS Synth. Biol.* **2013**, *2*, 629.
- (4) Chiang, Y. M.; Ahuja, M.; Oakley, C. E.; Entwistle, R.; Asokan, A.; Zutz, C.; Wang, C. C.; Oakley, B. R. Development of genetic dereplication strains in *Aspergillus nidulans* results in the discovery of aspercryptin. *Angew. Chem. Int. Ed. Engl.* **2016**, *55*, 1662.
- (5) Mojardín, L.; Vega, M.; Moreno, F.; Schmitz, H. P.; Heinisch, J. J.; Rodicio, R. Lack of the NAD<sup>+</sup>-dependent glycerol 3-phosphate dehydrogenase impairs the function of transcription factors Sip4 and Cat8 required for ethanol utilization in *Kluyveromyces lactis*. *Fungal. Genet. Biol.* **2018**, *111*, 16.
- (6) Nies, J.; Ran, H.; Wohlgemuth, V.; Yin, W. B.; Li, S.-M. Biosynthesis of the prenylated salicylaldehyde flavoglaucon requires temporary reduction to salicyl alcohol for decoration before reoxidation to the final product. *Org. Lett.* **2020**, *22*, 2256.
- (7) Fan, J.; Liao, G.; Kindinger, F.; Ludwig-Radtke, L.; Yin, W.-B.; Li, S.-M. Peniphenone and penilactone formation in *Penicillium crustosum* via 1,4-Michael additions of *ortho*-quinone methide from hydroxylavato to  $\gamma$ -butyrolactones from crustosic acid. *J. Am. Chem. Soc.* **2019**, *141*, 4225.
- (8) Xiang, P.; Ludwig-Radtke, L.; Yin, W.-B.; Li, S.-M. Isocoumarin formation by heterologous gene expression and modification by host enzymes. *Org. Biomol. Chem.* **2020**, *18*, 4946.
- (9) Jacobus, A. P. and Gross, J. Optimal cloning of PCR fragments by homologous recombination in *Escherichia coli*. *PLoS. One.* **2015**, *10*, e0119221.
- (10) Schroeckh, V.; Scherlach, K.; Nuttmann, H. W.; Shelest, E.; Schmidt-Heck, W.; Schuemann, J.; Martin, K.; Hertweck, C.; Brakhage, A. A. Intimate bacterial-fungal interaction triggers biosynthesis of archetypal polyketides in *Aspergillus nidulans*. *Proc. Natl. Acad. Sci. U. S. A* **2009**, *106*, 14558.
- (11) Feng, C.; Wei, Q.; Hu, C.; Zou, Y. Biosynthesis of diphenyl ethers in fungi. *Org. Lett.* **2019**, *21*, 3114.
- (12) Liu, S.; Wang, H.; Su, M.; Hwang, G. J.; Hong, J.; Jung, J. H. New metabolites from the sponge-derived fungus *Aspergillus sydowii* J05B-7F-4. *Nat. Prod. Res.* **2017**, *31*, 1682.



**4.3 Biosynthesis of annullatin D in *Penicillium roqueforti* implies oxidative lactonization between two hydroxyl groups catalyzed by a BBE-like enzyme**





# Biosynthesis of Annullatin D in *Penicillium roqueforti* Implies Oxidative Lactonization between Two Hydroxyl Groups Catalyzed by a BBE-like Enzyme

Pan Xiang,<sup>§</sup> Bastian Kemmerich,<sup>§</sup> Li Yang, and Shu-Ming Li\*



Cite This: *Org. Lett.* 2022, 24, 6072–6077



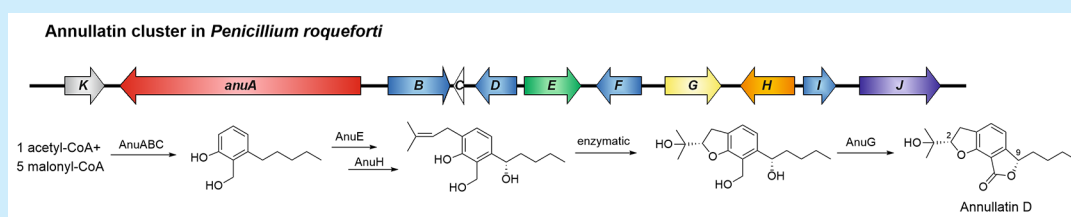
Read Online

ACCESS |

Metrics & More

Article Recommendations

Supporting Information



**ABSTRACT:** Annullatins from *Cordyceps annulata* are alkylated aromatic polyketides including annullatin D with a fused dihydrobenzofuran lactone ring system. Here, we report the identification of a silent biosynthetic gene cluster for annullatins from *Penicillium roqueforti* by heterologous expression in *Aspergillus nidulans*, gene deletion, and feeding experiments as well as by biochemical characterization. The polyketide core structure is consecutively modified by hydroxylation and prenylation. A berberine bridge enzyme-like protein catalyzes the final step, an oxidative lactonization between two hydroxyl groups, to form (2*S*, 9*S*)-annullatin D.

Natural products of highly reducing polyketide synthases (HRPKs) are of great importance by exhibiting a broad range of biological activities.<sup>1,2</sup> The cholesterol-lowering agent lovastatin from *Aspergillus terreus* is one important representative.<sup>3</sup> Iterative fungal HRPKSs are a large family of multi-domain enzymes being responsible for the formation of diverse structures with strongly reduced carbon chains by  $\beta$ -carbon reduction and dehydration.<sup>4–7</sup> Together with additional enzymes like short-chain dehydrogenases, HRPKSs were also reported to synthesize alkylated salicylaldehyde or derivatives thereof, such as pyriculol by MoPKS19,<sup>8</sup> sordarial by SrdA,<sup>9</sup> and 5-deoxyaurocitrin by VirA,<sup>6</sup> as well as flavoglaurin by FogA.<sup>10</sup>

*Penicillium roqueforti* is widespread in silage and natural environments and also found in food waste. It is used as a starter culture in the production of most blue-veined cheeses.<sup>11</sup> Similar to other filamentous fungi, *P. roqueforti* has the potential to produce biologically active secondary metabolites, such as the antitumor active andrastins and the antibiotic/immunosuppressant mycophenolic acid.<sup>12,13</sup> To strengthen our understanding on alkylated salicylaldehydes or derivatives, we used the *fog* gene cluster from *Aspergillus ruber*<sup>10</sup> as a probe for searching homologues in the genome of *P. roqueforti* FM164. This led to the identification of a putative 11-gene (*anu*) cluster in *P. roqueforti* with four genes of more than 40% identity to those of the *fog* cluster on the amino acid level (Figure 1). The putative *anu* cluster comprises genes for a HRPKS (AnuA), four short-chain dehydrogenases/reductases

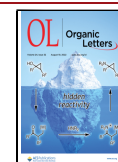
(SDRs, AnuB, AnuD, AnuF, and AnuI), an unknown protein (AnuC), a cytochrome P450 (CYP, AnuE), a berberine bridge enzyme-like protein (BBE-like enzyme, AnuG), a prenyltransferase (PT, AnuH), an aromatic ring hydroxylating dehydrogenase (ARHD, AnuJ), and a transcription factor (TF, AnuK) (Figure 1 and Table S1). Accordingly, the product of the *anu* cluster was speculated to be a prenylated derivative.

To identify the *anu* cluster product, genomic sequence of *anuA–K* was cloned into pJN017<sup>10</sup> by assembling in *Saccharomyces cerevisiae* and integrated into the *Aspergillus nidulans* LO8030 genome<sup>14</sup> under control of the *gpdA* promoter by protoplast transformation (Tables S2–S4 and Figure S1).<sup>15</sup> The resulting transformant *A. nidulans* BK08 was afterward cultivated in PDB liquid medium under static conditions.

LC–MS analysis of the EtOAc extract of the *A. nidulans* BK08 culture revealed the presence of four new products 1–4 (Figure 2C and Figure S5), which were absent in the isogenic control strain BK06 (Figure 2A). Large-scale fermentation and structural elucidation (see Tables S5–S7 and Figures S19, S28–S38, and S44–S49 for MS, optical rotation, UV, and

Received: July 19, 2022

Published: August 8, 2022



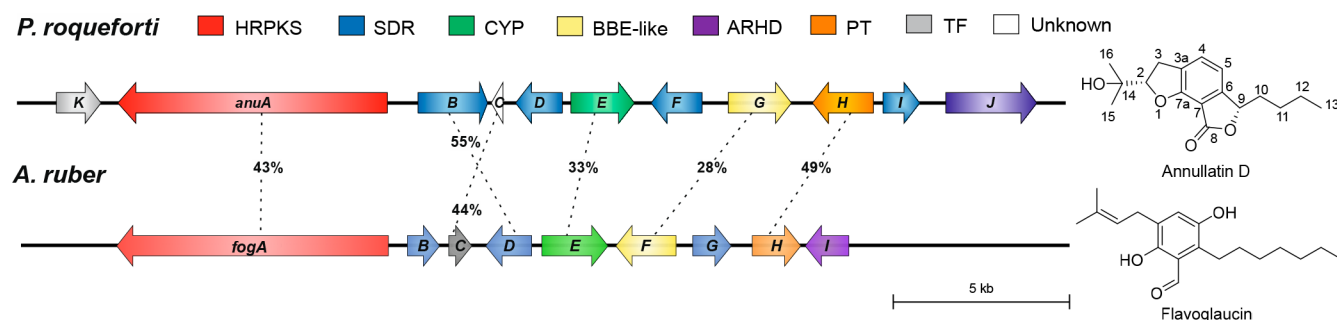


**Figure 1.** Comparison of the *anu* cluster in *P. roqueforti* with *fog* cluster in *A. ruber*. The sequence identities on the amino acid level are given as percentages.

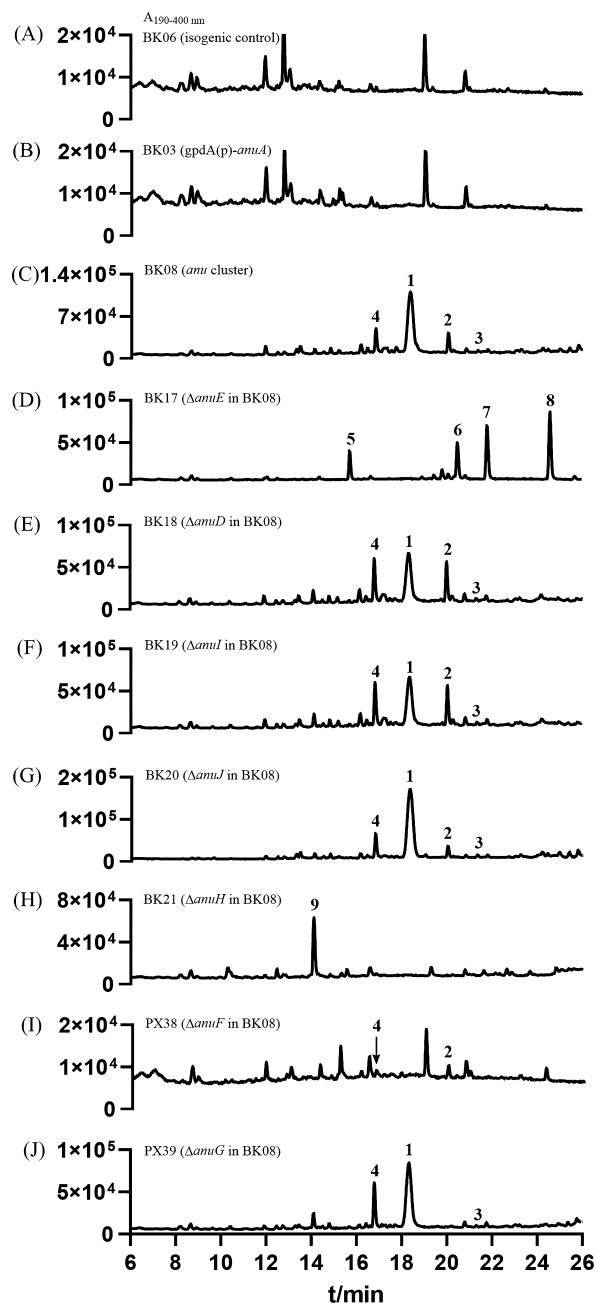


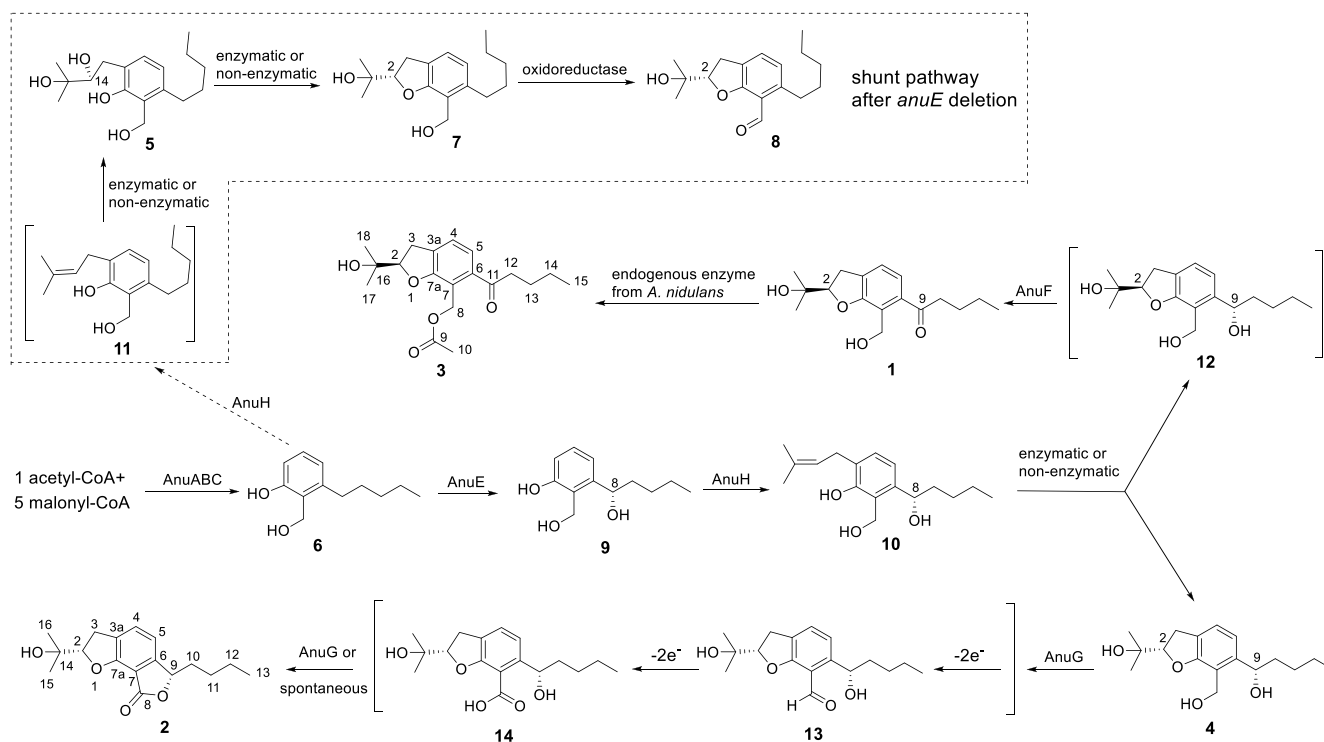
**Figure 2.** LC-MS analysis of *A. nidulans* transformant extracts after cultivation for 14 days. Only UV absorptions at are illustrated.

NMR data and spectra) confirmed 2, 3, and 4 as annullatin derivatives by comparison with the reported data.<sup>16</sup> Compound 2 has a planar structure of the reported (2*R*, 9*S*)-annullatin D,<sup>16</sup> but different ECD data (Figure S20). Compounds 3 and 4 have not been described before and termed as annullatins G and H, respectively. By comparison of the experimental ECD data with the calculated values, the configurations of 2, 3, and 4 were assigned to be (2*S*, 9*S*), (2*R*), and (2*S*, 9*S*), respectively (Scheme 1 and Figures S20–S22).

The predominant product peak 1 in the HPLC chromatogram has an  $[M + Na]^+$  ion at  $m/z$  315.1566 and a deduced molecular formula  $C_{17}H_{24}O_4$ . Unfortunately, attempts to obtain an interpretable  $^1H$  NMR spectrum for 1 failed, due to its low stability during a routine isolation procedure. To get a stable product, 1 in the BK08 extract was immediately acetylated.<sup>17</sup> MS and NMR analyses confirmed the acetylated product of 1 to be 3 (Table S6 and Figures S6 and S39–S43). Therefore, 1 has a hydroxymethyl instead of an acetoxymethyl group at the aromatic ring in 3 and was termed as annullatin F (Scheme 1). Since 3 appears only as a minor product in the culture of BK08 and there is no acetyltransferase in the *anu* cluster, we therefore speculate that acetylation of 1 to 3 was catalyzed by a host enzyme from *A. nidulans*. Further product conversion by host enzymes after gene expression was also observed in our previous works.<sup>10,18</sup>

Annulatins were isolated from the ascomycetous fungus *Cordyceps annullata* and exhibited potent agonistic activities toward the cannabinoid receptors.<sup>16</sup> However, such metabolites were neither reported for *P. roqueforti* nor detected in the cultures of *P. roqueforti* FM164 under different conditions (data not shown), proving the presence of a silent gene cluster.

To the best of our knowledge, despite the intriguing structural features and biological activities, biosynthetic studies on annulatins, especially on the formation of the lactone ring in annullatin D, have not been reported prior to this study. This encouraged us to elucidate their biosynthetic steps. Sequence analysis revealed that AnuA with a domain structure KS-AT-DH-ER-KR (abbreviations for PKS domains as given before<sup>4</sup>) shares a sequence identity of 43.1% with FogA from *A. ruber*.<sup>10</sup> LC-MS analysis of the *anuA* expression strain *A. nidulans* BK03 (Tables S2 and S3) did not lead to detection of any additional product compared with the control strain (Figure 2A,B and Figure S7). This is consistent with the results after expression of PKS alone in the case of pyriculol, sordarial, and flavoglucin. Accumulation of aromatic polyketide products requires additional enzymes for modification,

Scheme 1. Proposed Biosynthetic Pathway of Annullatins F (1) and D (2) in *P. roqueforti*

cyclization, and release of the PKS-assembled products.<sup>8–10</sup> AnuBC would be these candidates.

To identify modification enzymes, we deleted single genes in BK08. AnuD and AnuI are predicted to be SDRs and comprise 381 and 252 amino acids, respectively. LC–MS analysis of the deletion mutants *A. nidulans* BK18 ( $\Delta anuD$ ) and BK19 ( $\Delta anuI$ ) did not result in significant metabolite changes compared to BK08 (Figure 2E,F and Figures S9 and S10). A similar result was also observed in the  $\Delta anuJ$  strain BK20 (Figure 2G and Figure S11). This indicated that *anuD*, *anuI*, and *anuJ* are likely not involved in the annullatin biosynthesis.

AnuE shares its sequence homology with fungal cytochrome P450 enzymes, e.g., 32.9% identity with the hydroxylase FogE in the flavoglaucon biosynthesis.<sup>10</sup> Deletion of *anuE* in BK08 resulted in the abolishment of 1–4 and the appearance of four new metabolites 5–8 (Figure 2D and Figure S8). A detailed interpretation of the 1D and 2D NMR data (Tables S8–S11 and Figures S50–S65) proved 5–8 to be annullatin derivatives without the oxygen function at the C<sub>5</sub> side chain. Experimental ECD data of 5 coincided with the calculated ECD spectrum for (14*S*)-isomer (Figure S23). This new metabolite was termed as (14*S*)-annullatin I (Scheme 1). 6 with an  $[M - H]^-$  ion at  $m/z$  193.1215 was proven to be 2-hydroxymethyl-3-pentylphenol by comparing its UV, MS, and <sup>1</sup>H NMR data with those published previously (Table S9 and Figure S55).<sup>19</sup> With an exception for their optical rotation values, the planar structures of 7 and 8 were elucidated to be annullatin B and annullatin A, respectively, by comparing their UV, MS, and NMR data with those published previously.<sup>16</sup> 7 and 8 show opposite ECD spectra to the respective (*R*)-configured known compounds (Figures S24 and S25) and are therefore unambiguously identified as (2*S*)-annullatin B and (2*S*)-annullatin A, respectively (Scheme 1). It can be deduced that AnuE catalyzes the hydroxylation of 6 at the side chain in the biosynthesis of 1–4. The accumulated 6 in the  $\Delta anuE$

mutant was further metabolized to 5, 7, and 8 by other tailoring enzymes (Scheme 1).

To verify this hypothesis, *anuE* was cloned into pYH-wA-pyrG<sup>20</sup> and expressed in *A. nidulans*. Feeding 6 into the *anuE* overexpression strain *A. nidulans* PX28 (Tables S2) led to detection of a new peak 9 with a conversion yield of 92% after cultivation in PDB medium for 4 days (Figure 3A and Figure S15). The <sup>1</sup>H NMR spectrum and the optical rotation of 9 are consistent with those of (8*S*)-annullatin E with a hydroxyl group at the side chain (Table S9 and Figure S66),<sup>16</sup> proving AnuE as a hydroxylase.

Deletion of the prenyltransferase gene *anuH* also completely abolished the production of 1–4 but led to the accumulation of 9 as the sole product (Figure 2H and Figure S12). To explore the role of AnuH in the annullatin biosynthesis, *anuH* was amplified and cloned into pET-28a(+) for expression in *E. coli* (Table S3). The purified AnuH was incubated with 9 in the presence of dimethylallyl diphosphate (DMAPP) (Figure S17). As shown in Figure 4A, conversion of 9 to 10 was clearly detected, with a conversion yield of 30% after incubation with 2  $\mu$ g of AnuH at 37 °C for 30 min and 73% for 4 h. Structural elucidation confirmed 10 as the expected prenylated product, named annullatin J (Table S12 and Figures S67–S71). The stereochemistry of 10 was determined as (8*S*)-10 by comparison of its experiment ECD spectrum with the calculated one (Figure S27). Geranyl and farnesyl diphosphate were not consumed by AnuH for prenylation of 9 (Figure 4A). Determination of the kinetic parameters for AnuH gave a  $K_M$  of 0.08 mM toward 9 and a  $K_M$  of 0.49 mM toward DMAPP. The average turnover number ( $k_{cat}$ ) was calculated to be 0.13 s<sup>-1</sup> (Figure S18). Compound 6 without the hydroxyl group at the side chain was also accepted by AnuH, but only with low conversion yields, i.e., 4% after 30 min and 16% after 5 h incubation (Figure 4B). The two product peaks of 6 have the same  $[M - H]^-$  ion at  $m/z$  261.1859 for attachment of a

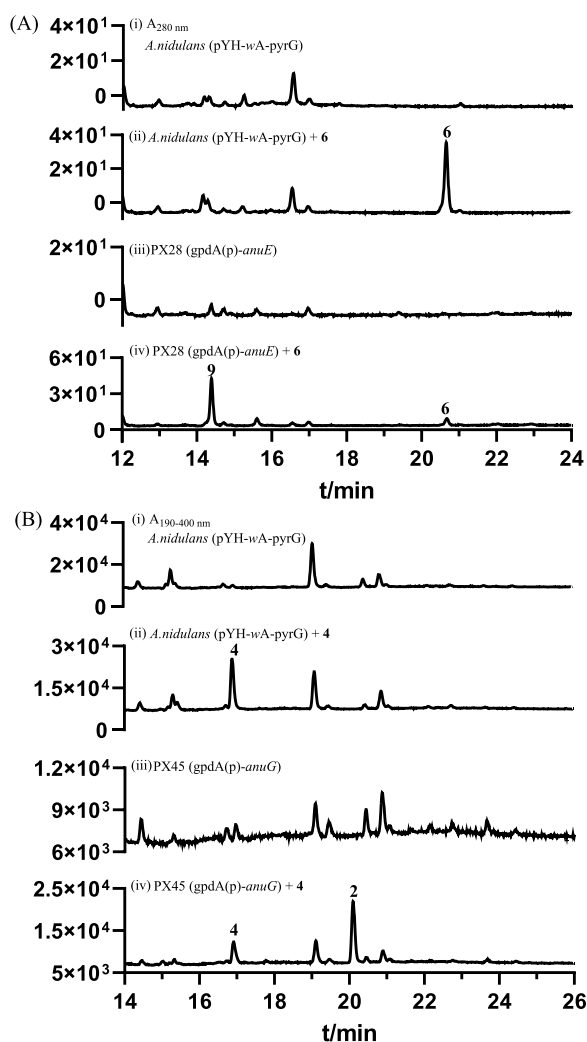


**Figure 3.** LC–MS analysis of culture extracts. (A) With and without feeding of **6** to *A. nidulans* PX28 harboring *anuE* and to the control strain. (B) With and without feeding of **4** to *A. nidulans* PX45 harboring *anuG* and to the control strain. Only UV absorptions are illustrated.

dimethylallyl group, indicating two unspecific prenylation reactions. Unfortunately, the low conversion of **6** made the product isolation difficult, so that their structures cannot be determined in this study. However, based on the results obtained from  $\Delta$ *anuE* mutant, one of the prenylation products is expected to be **11**, the precursor of **5**, in the shunt pathway (Scheme 1), which was subsequently metabolized to **5**, **7**, and **8**.

Deletion of the SDR gene *anuF* and the BBE-like gene *anuG* in BK08 resulted in the mutants *A. nidulans* PX38 and PX39, respectively (Table S2). LC–MS analysis revealed that PX38 ( $\Delta$ *anuF*) produced neither **1** nor **3**, but still **2** and **4** (Figure 2I and Figure S13), implying the role of AnuF in the formation of **1**. In comparison, deletion of *anuG* abolished the production of **2**, but not that of **1**, **3**, and **4** (Figure 2J and Figure S14), indicating that the BBE-like enzyme AnuG is responsible for the five-member lactone ring formation in **2** via oxidative lactonization between the two hydroxyl groups. BBE-like enzymes are a subfamily of flavin-containing proteins and have been identified in plants, fungi, and bacteria.<sup>21–25</sup> They usually catalyze diverse oxidations including dehydrogenation-medi-

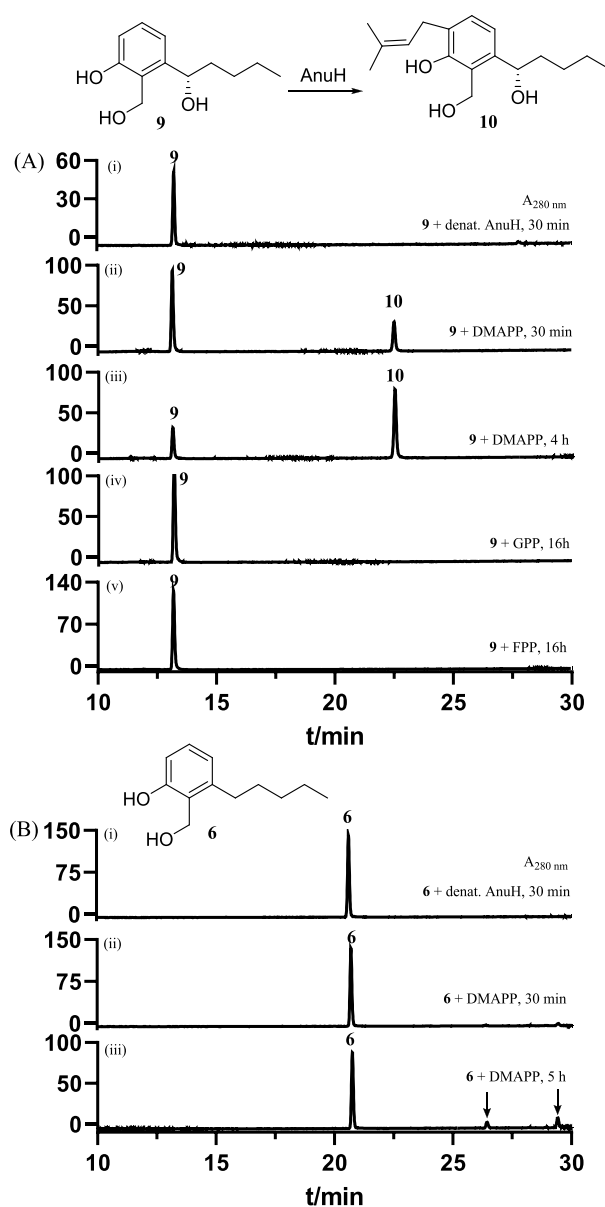


**Figure 4.** LC–MS analysis of *in vitro* assays of AnuH. (A) With its natural substrate **9**. (B) With the precursor **6**. Only UV absorptions at 280 nm are illustrated. DMAPP: dimethylallyl diphosphate. GPP: geranyl diphosphate. FPP: farnesyl diphosphate.

ated C–C or C–N bond formation in the natural product biosynthesis.<sup>23</sup>

Attempts to characterize AnuG biochemically failed, because no protein band with the expected size was detected after heterologous expression in *E. coli*, even after purification on Ni-NTA agarose resin (data not shown). We therefore verified its function by expressing *anuG* in *A. nidulans*. The overexpression strain PX45 was cultivated in PDB medium and fed with 10  $\mu$ M of **4**. After cultivation for 12 days, 74% of **4** was converted to **2** (Figure 3B and Figure S16), providing clear evidence for the oxidative lactonization between the two hydroxyl groups by AnuG.

Based on the results described above, we postulate a biosynthetic pathway for (2*R*)-annullatin F (**1**) and (2*S*, 9*S*)-annullatin D (**2**) in *P. roqueforti* as depicted in Scheme 1. As in the biosynthesis of flavoglucan,<sup>10</sup> the annullatin backbone is assembled by cooperation of AnuABC and hydroxylated at the



C<sub>5</sub> alkyl chain by the cytochrome P450 AnuE. The prenyltransferase AnuH subsequently installs one isoprenyl group at the benzene ring to form **10**, as demonstrated above. However, **10** was not identified in the deletion mutants obtained in this study. Enzymatic or nonenzymatic dihydrobenzofuran ring formation between the prenyl and the phenolic hydroxyl groups in **10**, as observed in many natural products,<sup>26</sup> results in two diastereomers **4** and **12**. Compound **4** is then converted to **2** by the BBE-like enzyme AnuG-catalyzed five-member lactone ring formation. Conversion of **4** to **2** needs to extract four electrons from the substrate. It can be postulated that the hydroxymethyl group is first oxidized via aldehyde **13** to acid **14**, which then undergoes a spontaneous or AnuG-catalyzed lactonization with the side chain hydroxyl group.

The isomer **12** acts as a substrate for the SDR enzyme AnuF and is oxidized to **1**, which is subsequently acetylated by an acetyltransferase from *A. nidulans*, leading to **3** formation. Compound **12** is likely very instable and was not detected in the obtained mutants including that of  $\Delta$ anuF. It can be speculated that this compound is immediately converted by AnuF to **1**. This is also the main reason that no anuF expression was carried out in *A. nidulans* or *E. coli*.

In conclusion, we identified a silent biosynthetic gene cluster for annullatins in *P. roqueforti* and elucidated their biosynthetic pathway by heterologous expression, gene deletion, and *in vitro* biochemical investigation, as well as feeding experiments. As reported previously, formation of the aromatic core structure requires not only PKS but also additional enzymes. Consecutive and coordinated modifications by at least four different types of enzymes enable (intramolecular) oxidation and condensation to form the final products **1** and **2**. Therefore, this study demonstrated a highly programmed biosynthetic pathway for annullatins. More importantly, we identified a new BBE-like enzyme for oxidative lactonization between two hydroxyl groups. To the best of our knowledge, no such functions have been reported for BBE-like enzymes prior to this study.

## ■ ASSOCIATED CONTENT

### Supporting Information

The Supporting Information is available free of charge at <https://pubs.acs.org/doi/10.1021/acs.orglett.2c02438>.

Experimental details, strains, plasmids, primers, LC–MS analysis, ECD spectra, NMR data, and spectra (PDF)

## ■ AUTHOR INFORMATION

### Corresponding Author

Shu-Ming Li – Institut für Pharmazeutische Biologie und Biotechnologie, Fachbereich Pharmazie, Philipps-Universität Marburg, 35037 Marburg, Germany; [orcid.org/0000-0003-4583-2655](https://orcid.org/0000-0003-4583-2655); Phone: + 49-6421-28-22461/25365; Email: [shuming.li@staff.uni-marburg.de](mailto:shuming.li@staff.uni-marburg.de)

### Authors

Pan Xiang – Institut für Pharmazeutische Biologie und Biotechnologie, Fachbereich Pharmazie, Philipps-Universität Marburg, 35037 Marburg, Germany  
Bastian Kemmerich – Institut für Pharmazeutische Biologie und Biotechnologie, Fachbereich Pharmazie, Philipps-Universität Marburg, 35037 Marburg, Germany

Li Yang – Haikou Key Laboratory for Research and Utilization of Tropical Natural Products, Institute of Tropical Bioscience and Biotechnology, CATAS, 571101 Haikou, China

Complete contact information is available at: <https://pubs.acs.org/10.1021/acs.orglett.2c02438>

## ■ Author Contributions

§P.X. and B.K. contributed equally.

## ■ Notes

The authors declare no competing financial interest.

## ■ ACKNOWLEDGMENTS

We thank Joelle Dupont from the National Museum of Natural History, Paris, for providing strain *P. roqueforti* FM164, and Lena Ludwig-Radtke and Stefan Newel (Philipps-Universität Marburg) for taking MS and NMR spectra, respectively. This project was financially funded in part by the Deutsche Forschungsgemeinschaft (DFG, INST 160/620-1 and Li844/11-1 to S.M.L.). P.X. is a scholarship recipient of the China Scholarship Council (201708530222).

## ■ REFERENCES

- (1) Atanasov, A. G.; Zotchev, S. B.; Dirsch, V. M.; Supuran, C. T. Natural products in drug discovery: advances and opportunities. *Nat. Rev. Drug Discov.* **2021**, *20*, 200.
- (2) Newman, D. J.; Cragg, G. M. Natural products as sources of new drugs over the nearly four decades from 01/1981 to 09/2019. *J. Nat. Prod.* **2020**, *83*, 770.
- (3) Cox, R. J.; Simpson, T. J. Fungal type I polyketide synthases. *Methods Enzymol.* **2009**, *459*, 49.
- (4) Cox, R. J. Polyketides, proteins and genes in fungi: programmed nano-machines begin to reveal their secrets. *Org. Biomol. Chem.* **2007**, *5*, 2010.
- (5) Chooi, Y. H.; Tang, Y. Navigating the fungal polyketide chemical space: from genes to molecules. *J. Org. Chem.* **2012**, *77*, 9933.
- (6) Liu, L.; Tang, M. C.; Tang, Y. Fungal highly reducing polyketide synthases biosynthesize salicylaldehydes that are precursors to epoxycyclohexenol natural products. *J. Am. Chem. Soc.* **2019**, *141*, 19538.
- (7) Herbst, D. A.; Townsend, C. A.; Maier, T. The architectures of iterative type I PKS and FAS. *Nat. Prod. Rep.* **2018**, *35*, 1046.
- (8) Jacob, S.; Grötsch, T.; Foster, A. J.; Schöffler, A.; Rieger, P. H.; Sandjo, L. P.; Liermann, J. C.; Opatz, T.; Thines, E. Unravelling the biosynthesis of pyriculol in the rice blast fungus *Magnaporthe oryzae*. *Microbiology* **2017**, *163*, 541.
- (9) Zhao, Z.; Ying, Y.; Hung, Y. S.; Tang, Y. Genome mining reveals *Neurospora crassa* can produce the salicylaldehyde sordarial. *J. Nat. Prod.* **2019**, *82*, 1029.
- (10) Nies, J.; Ran, H.; Wohlgemuth, V.; Yin, W. B.; Li, S.-M. Biosynthesis of the prenylated salicylaldehyde flavoglaucin requires temporary reduction to salicyl alcohol for decoration before reoxidation to the final product. *Org. Lett.* **2020**, *22*, 2256.
- (11) Cheeseman, K.; Ropars, J.; Renault, P.; Dupont, J.; Gouzy, J.; Branca, A.; Abraham, A. L.; Ceppi, M.; Conseiller, E.; Debuchy, R.; Malagnac, F.; Goarin, A.; Silar, P.; Lacoste, S.; Sallet, E.; Bensimon, A.; Giraud, T.; Brygoo, Y. Multiple recent horizontal transfers of a large genomic region in cheese making fungi. *Nat. Commun.* **2014**, *5*, 2876.
- (12) García-Estrada, C.; Martin, J. F. Biosynthetic gene clusters for relevant secondary metabolites produced by *Penicillium roqueforti* in blue cheeses. *Appl. Microbiol. Biotechnol.* **2016**, *100*, 8303.
- (13) Fernández-Bodega, A.; Álvarez-Álvarez, R.; Liras, P.; Martin, J. F. Silencing of a second dimethylallyltryptophan synthase of

*Penicillium roqueforti* reveals a novel clavine alkaloid gene cluster. *Appl. Microbiol. Biotechnol.* **2017**, *101*, 6111.

(14) Chiang, Y. M.; Ahuja, M.; Oakley, C. E.; Entwistle, R.; Asokan, A.; Zutz, C.; Wang, C. C.; Oakley, B. R. Development of genetic dereplication strains in *Aspergillus nidulans* results in the discovery of aspercryptin. *Angew. Chem., Int. Ed. Engl.* **2016**, *55*, 1662.

(15) Fan, J.; Liao, G.; Kindinger, F.; Ludwig-Radtke, L.; Yin, W.-B.; Li, S.-M. Peniphenone and penilactone formation in *Penicillium crustosum* via 1,4-Michael additions of *ortho*-quinone methide from hydroxylclavatul to  $\gamma$ -butyrolactones from crustosic acid. *J. Am. Chem. Soc.* **2019**, *141*, 4225.

(16) Asai, T.; Luo, D.; Obara, Y.; Taniguchi, T.; Monde, K.; Yamashita, K.; Oshima, Y. Dihydrobenzofurans as cannabinoid receptor ligands from *Cordyceps annulata*, an entomopathogenic fungus cultivated in the presence of an HDAC inhibitor. *Tetrahedron Lett.* **2012**, *53*, 2239.

(17) Zheng, L.; Yang, Y.; Wang, H.; Fan, A.; Zhang, L.; Li, S.-M. Ustethylin biosynthesis implies phenethyl derivative formation in *Aspergillus ustus*. *Org. Lett.* **2020**, *22*, 7837.

(18) Xiang, P.; Ludwig-Radtke, L.; Yin, W.-B.; Li, S.-M. Isocoumarin formation by heterologous gene expression and modification by host enzymes. *Org. Biomol. Chem.* **2020**, *18*, 4946.

(19) Chang, J. C.; Hsiao, G.; Lin, R. K.; Kuo, Y. H.; Ju, Y. M.; Lee, T. H. Bioactive constituents from the termite nest-derived medicinal fungus *Xylaria nigripes*. *J. Nat. Prod.* **2017**, *80*, 38.

(20) Yin, W. B.; Chooi, Y. H.; Smith, A. R.; Cacho, R. A.; Hu, Y.; White, T. C.; Tang, Y. Discovery of cryptic polyketide metabolites from dermatophytes using heterologous expression in *Aspergillus nidulans*. *ACS Synth. Biol.* **2013**, *2*, 629.

(21) Wallner, S.; Dully, C.; Daniel, B.; Macheroux, P. *Berberine Bridge Enzyme and the Family of Bicovalent Flavoenzymes*; Hille, R., Miller, S., Palfey, B., Eds.; De Gruyter, 2013; pp 1–30.

(22) Winkler, A.; Motz, K.; Riedl, S.; Puhl, M.; Macheroux, P.; Gruber, K. Structural and mechanistic studies reveal the functional role of bicovalent flavinylation in berberine bridge enzyme. *J. Biol. Chem.* **2009**, *284*, 19993.

(23) Daniel, B.; Konrad, B.; Toplak, M.; Lahham, M.; Messenlehner, J.; Winkler, A.; Macheroux, P. The family of berberine bridge enzyme-like enzymes: A treasure-trove of oxidative reactions. *Arch. Biochem. Biophys.* **2017**, *632*, 88.

(24) Toplak, M.; Wiedemann, G.; Ulicevic, J.; Daniel, B.; Hoernstein, S. N. W.; Kothe, J.; Niederhauser, J.; Reski, R.; Winkler, A.; Macheroux, P. The single berberine bridge enzyme homolog of *Physcomitrellapatens* is a cellobiose oxidase. *FEBS J.* **2018**, *285*, 1923.

(25) Zou, Y.; Zhan, Z.; Li, D.; Tang, M.; Cacho, R. A.; Watanabe, K.; Tang, Y. Tandem prenyltransferases catalyze isoprenoid elongation and complexity generation in biosynthesis of quinolone alkaloids. *J. Am. Chem. Soc.* **2015**, *137*, 4980.

(26) Ran, H.; Li, S.-M. Fungal benzene carbaldehydes: occurrence, structural diversity, activities and biosynthesis. *Nat. Prod. Rep.* **2021**, *38*, 240.

## Recommended by ACS

### Fungal Highly Reducing Polyketide Synthases Biosynthesize Salicylaldehydes That Are Precursors to Epoxycyclohexenol Natural Products

Ling Liu, Yi Tang, *et al.*

DECEMBER 02, 2019

JOURNAL OF THE AMERICAN CHEMICAL SOCIETY

READ 

### Elucidation of the Complete Biosynthetic Pathway of Phomoxanthone A and Identification of a Para-Para Selective Phenol Coupling Dimerase

Si-Wen Yuan, Zhi-Zeng Gao, *et al.*

APRIL 20, 2022

ORGANIC LETTERS

READ 

### Discovery and Activation of the Cryptic Cluster from *Aspergillus* sp. CPCC 400735 for Asperphenalenone Biosynthesis

Tao Zhang, Liyan Yu, *et al.*

MAY 26, 2022

ACS CHEMICAL BIOLOGY

READ 

### Oxidative Carbon Backbone Rearrangement in Rishirilide Biosynthesis

Olga Tsypik, Andreas Bechthold, *et al.*

MARCH 17, 2020

JOURNAL OF THE AMERICAN CHEMICAL SOCIETY

READ 

Get More Suggestions >

## Supporting Information

### **Biosynthesis of Annullatin D in *Penicillium roqueforti* Implies Oxidative Lactonization between Two Hydroxyl Groups Catalyzed by a BBE-like Enzyme**

**Pan Xiang,<sup>1,§</sup> Bastian Kemmerich,<sup>1,§</sup> Li Yang,<sup>2</sup> and Shu-Ming Li<sup>1,\*</sup>**

<sup>1</sup>Institut für Pharmazeutische Biologie und Biotechnologie, Fachbereich Pharmazie, Philipps-Universität Marburg, Robert-Koch-Straße 4, Marburg 35037, Germany

<sup>2</sup>Haikou Key Laboratory for Research and Utilization of Tropical Natural Products, Institute of Tropical Bioscience and Biotechnology, CATAS, 571101 Haikou, China

§ These authors contributed equally to this work.

\* Email: [shuming.li@staff.uni-marburg.de](mailto:shuming.li@staff.uni-marburg.de)

## Table of content

<b>Experiment Procedures</b> .....	5
1. Computer-assisted sequence analysis .....	5
2. Strains, media, and growth conditions .....	5
3. Genomic DNA isolation.....	5
4. RNA isolation and cDNA synthesis .....	5
5. PCR amplification, gene cloning, and plasmid construction .....	5
6. Heterologous gene expression in <i>A. nidulans</i> LO8030 .....	6
7. Confirmation and cultivation of the <i>A. nidulans</i> transformants .....	6
8. Large-scale fermentation, extraction, and isolation of secondary metabolites .....	7
9. Cloning of the heterologous expression construct for <i>anuH</i> in <i>E. coli</i> .....	7
10. Overproduction and purification of AnuH .....	8
11. <i>In vitro</i> assays of AnuH.....	8
12. Enzyme assays for determination of the kinetic parameters .....	8
13. Heterologous expression of <i>anuE</i> and <i>anuG</i> in <i>A. nidulans</i> LO8030.....	8
14. Precursor feeding in <i>A. nidulans</i> PX28 and PX45 .....	9
15. HPLC and LC–MS analyses of secondary metabolites .....	9
16. NMR analysis .....	9
17. Measurement of optical rotations.....	9
18. The experimental and calculated electronic circular dichroism (ECD) spectroscopic analysis .....	10
19. Physiochemical properties of the compounds described in this study .....	10
20. Gene and protein sequences of AnuH .....	11
<b>Supplementary Tables</b> .....	13
Table S1. Putative functions of the genes from annullatin ( <i>anu</i> ) gene cluster.....	13
Table S2. Strains used in this study.....	14
Table S3. Plasmids used and constructed in this study .....	15
Table S4. Primers used in this study .....	16
Table S5. NMR data of (2 <i>S</i> , 9 <i>S</i> )-annullatin D ( <b>2</b> ) in DMSO- <i>d</i> <sub>6</sub> .....	19
Table S6. NMR data of (2 <i>R</i> )-annullatin G ( <b>3</b> ) in DMSO- <i>d</i> <sub>6</sub> .....	20
Table S7. NMR data of (2 <i>S</i> , 9 <i>S</i> )-annullatin H ( <b>4</b> ) in DMSO- <i>d</i> <sub>6</sub> .....	21
Table S8. NMR data of (14 <i>S</i> )-annullatin I ( <b>5</b> ) in CD <sub>3</sub> OD .....	22
Table S9. <sup>1</sup> H NMR data of 2-hydroxymethyl-3-pentylphenol ( <b>6</b> ) and (8 <i>S</i> )-annullatin E ( <b>9</b> ) in CD <sub>3</sub> OD ...	23
Table S10. NMR data of (2 <i>S</i> )-annullatin B ( <b>7</b> ) in CD <sub>3</sub> OD .....	24
Table S11. NMR data of (2 <i>S</i> )-annullatin A ( <b>8</b> ) in CD <sub>3</sub> OD .....	25
Table S12. NMR data of (8 <i>S</i> )-annullatin J ( <b>10</b> ) in CDCl <sub>3</sub> .....	26
<b>Supplementary Figures</b> .....	27
Figure S1. Schematic representation of gene integration into the <i>wA</i> -PKS locus of <i>A. nidulans</i> LO803027	
Figure S2. Schematic representation of gene deletion from <i>anu</i> cluster in <i>A. nidulans</i> strains .....	28
Figure S3. PCR verification of the heterologous expression transformants and the deletion mutants .....	29
Figure S4. LC–MS analysis of the negative control strain <i>A. nidulans</i> BK06 .....	30
Figure S5. LC–MS analysis of the <i>anu</i> cluster expression strain <i>A. nidulans</i> BK08.....	31
Figure S6. LC–MS analysis of the acetylated EtOAc extract from <i>A. nidulans</i> BK08 .....	32
Figure S7. LC–MS analysis of <i>anuA</i> heterologous expression in <i>A. nidulans</i> LO8030 .....	33
Figure S8. LC–MS analysis of the <i>anuE</i> deletion strain <i>A. nidulans</i> BK17 .....	34
Figure S9. LC–MS analysis of the <i>anuD</i> deletion strain <i>A. nidulans</i> BK18.....	35



Figure S10. LC–MS analysis of the <i>anuI</i> deletion strain <i>A. nidulans</i> BK19 .....	36
Figure S11. LC–MS analysis of the <i>anuJ</i> deletion strain <i>A. nidulans</i> BK20.....	37
Figure S12. LC–MS analysis of the <i>anuH</i> deletion strain <i>A. nidulans</i> BK21.....	38
Figure S13. LC–MS analysis of the <i>anuF</i> deletion strain <i>A. nidulans</i> PX38 .....	39
Figure S14. LC–MS analysis of the <i>anuG</i> deletion strain <i>A. nidulans</i> PX39 .....	40
Figure S15. LC–MS analysis of <i>anuE</i> expression strain <i>A. nidulans</i> PX28 after feeding with <b>6</b> .....	41
Figure S16. LC–MS analysis of <i>anuG</i> expression strain <i>A. nidulans</i> PX45 after feeding with <b>4</b> .....	42
Figure S17. Analysis of the purified AnuH on SDS-PAGE .....	43
Figure S18. Determination of the kinetic parameters of AnuH .....	44
Figure S19. UV spectra of compounds <b>1</b> – <b>10</b> .....	45
Figure S20. The experimental and calculated ECD spectra of compound <b>2</b> and its isomers .....	46
Figure S21. The experimental and calculated ECD spectra of compound <b>3</b> and its isomer .....	46
Figure S22. The experimental and calculated ECD spectra of compound <b>4</b> and its isomers .....	47
Figure S23. The experimental and calculated ECD spectra of compound <b>5</b> and its isomer .....	47
Figure S24. The experimental and calculated ECD spectra of compound <b>7</b> and its isomer .....	48
Figure S25. The experimental and calculated ECD spectra of compound <b>8</b> and its isomer .....	48
Figure S26. The experimental ECD spectrum of compound <b>9</b> .....	49
Figure S27. The experimental and calculated ECD spectra of compound <b>10</b> and its isomer .....	49
Figure S28. <sup>1</sup> H NMR spectrum of (2 <i>S</i> , 9 <i>S</i> )-annullatin D ( <b>2</b> ) in CDCl <sub>3</sub> (500 MHz).....	50
Figure S29. <sup>1</sup> H NMR spectrum of (2 <i>S</i> , 9 <i>S</i> )-annullatin D ( <b>2</b> ) in DMSO- <i>d</i> <sub>6</sub> (500 MHz) .....	50
Figure S30. <sup>13</sup> C NMR spectrum of (2 <i>S</i> , 9 <i>S</i> )-annullatin D ( <b>2</b> ) in DMSO- <i>d</i> <sub>6</sub> (125 MHz) .....	51
Figure S31. <sup>1</sup> H- <sup>1</sup> H COSY spectrum of (2 <i>S</i> , 9 <i>S</i> )-annullatin D ( <b>2</b> ) in DMSO- <i>d</i> <sub>6</sub> .....	51
Figure S32. HSQC spectrum of (2 <i>S</i> , 9 <i>S</i> )-annullatin D ( <b>2</b> ) in DMSO- <i>d</i> <sub>6</sub> .....	52
Figure S33. HMBC spectrum of (2 <i>S</i> , 9 <i>S</i> )-annullatin D ( <b>2</b> ) in DMSO- <i>d</i> <sub>6</sub> .....	52
Figure S34. <sup>1</sup> H NMR spectrum of (2 <i>R</i> )-annullatin G ( <b>3</b> ) in DMSO- <i>d</i> <sub>6</sub> (500 MHz), isolated from fungal culture .....	53
Figure S35. <sup>13</sup> C NMR spectrum of (2 <i>R</i> )-annullatin G ( <b>3</b> ) in DMSO- <i>d</i> <sub>6</sub> (125 MHz), isolated from fungal culture .....	53
Figure S36. <sup>1</sup> H- <sup>1</sup> H COSY spectrum of (2 <i>R</i> )-annullatin G ( <b>3</b> ) in DMSO- <i>d</i> <sub>6</sub> , isolated from fungal culture .....	54
Figure S37. HSQC spectrum of (2 <i>R</i> )-annullatin G ( <b>3</b> ) in DMSO- <i>d</i> <sub>6</sub> , isolated from fungal culture .....	54
Figure S38. HMBC spectrum of (2 <i>R</i> )-annullatin G ( <b>3</b> ) in DMSO- <i>d</i> <sub>6</sub> , isolated from fungal culture .....	55
Figure S39. <sup>1</sup> H NMR spectrum of (2 <i>R</i> )-annullatin G ( <b>3</b> ) in DMSO- <i>d</i> <sub>6</sub> (500 MHz), obtained after acetylation of annullatin F .....	55
Figure S40. <sup>13</sup> C NMR spectrum of (2 <i>R</i> )-annullatin G ( <b>3</b> ) in DMSO- <i>d</i> <sub>6</sub> (125 MHz), obtained after acetylation of annullatin F .....	56
Figure S41. <sup>1</sup> H- <sup>1</sup> H COSY spectrum of (2 <i>R</i> )-annullatin G ( <b>3</b> ) in DMSO- <i>d</i> <sub>6</sub> , obtained after acetylation of annullatin F .....	56
Figure S42. HSQC spectrum of (2 <i>R</i> )-annullatin G ( <b>3</b> ) in DMSO- <i>d</i> <sub>6</sub> , obtained after acetylation of annullatin F .....	57
Figure S43. HMBC spectrum of (2 <i>R</i> )-annullatin G ( <b>3</b> ) in DMSO- <i>d</i> <sub>6</sub> , obtained after acetylation of annullatin F .....	57
Figure S44. <sup>1</sup> H NMR spectrum of (2 <i>S</i> , 9 <i>S</i> )-annullatin H ( <b>4</b> ) in CDCl <sub>3</sub> (500 MHz).....	58
Figure S45. <sup>1</sup> H NMR spectrum of (2 <i>S</i> , 9 <i>S</i> )-annullatin H ( <b>4</b> ) in DMSO- <i>d</i> <sub>6</sub> (500 MHz) .....	58
Figure S46. <sup>13</sup> C NMR spectrum of (2 <i>S</i> , 9 <i>S</i> )-annullatin H ( <b>4</b> ) in DMSO- <i>d</i> <sub>6</sub> (125 MHz) .....	59
Figure S47. <sup>1</sup> H- <sup>1</sup> H COSY spectrum of (2 <i>S</i> , 9 <i>S</i> )-annullatin H ( <b>4</b> ) in DMSO- <i>d</i> <sub>6</sub> .....	59

Figure S48. HSQC spectrum of (2 <i>S</i> , 9 <i>S</i> )-annullatin H ( <b>4</b> ) in DMSO- <i>d</i> <sub>6</sub> .....	60
Figure S49. HMBC spectrum of (2 <i>S</i> , 9 <i>S</i> )-annullatin H ( <b>4</b> ) in DMSO- <i>d</i> <sub>6</sub> .....	60
Figure S50. <sup>1</sup> H NMR spectrum of (14 <i>S</i> )-annullatin I ( <b>5</b> ) in CD <sub>3</sub> OD (500 MHz) .....	61
Figure S51. <sup>13</sup> C NMR spectrum of (14 <i>S</i> )-annullatin I ( <b>5</b> ) in CD <sub>3</sub> OD (125 MHz) .....	61
Figure S52. <sup>1</sup> H- <sup>1</sup> H COSY spectrum of (14 <i>S</i> )-annullatin I ( <b>5</b> ) in CD <sub>3</sub> OD .....	62
Figure S53. HSQC spectrum of (14 <i>S</i> )-annullatin I ( <b>5</b> ) in CD <sub>3</sub> OD.....	62
Figure S54. HMBC spectrum of (14 <i>S</i> )-annullatin I ( <b>5</b> ) in CD <sub>3</sub> OD.....	63
Figure S55. <sup>1</sup> H NMR spectrum of 2-hydroxymethyl-3-pentylphenol ( <b>6</b> ) in CD <sub>3</sub> OD (500 MHz) .....	63
Figure S56. <sup>1</sup> H NMR spectrum of (2 <i>S</i> )-annullatin B ( <b>7</b> ) in CD <sub>3</sub> OD (500 MHz) .....	64
Figure S57. <sup>13</sup> C NMR spectrum of (2 <i>S</i> )-annullatin B ( <b>7</b> ) in CD <sub>3</sub> OD (125 MHz) .....	64
Figure S58. <sup>1</sup> H- <sup>1</sup> H COSY spectrum of (2 <i>S</i> )-annullatin B ( <b>7</b> ) in CD <sub>3</sub> OD .....	65
Figure S59. HSQC spectrum of (2 <i>S</i> )-annullatin B ( <b>7</b> ) in CD <sub>3</sub> OD .....	65
Figure S60. HMBC spectrum of (2 <i>S</i> )-annullatin B ( <b>7</b> ) in CD <sub>3</sub> OD .....	66
Figure S61. <sup>1</sup> H NMR spectrum of (2 <i>S</i> )-annullatin A ( <b>8</b> ) in CD <sub>3</sub> OD (500 MHz) .....	66
Figure S62. <sup>13</sup> C NMR spectrum of (2 <i>S</i> )-annullatin A ( <b>8</b> ) in CD <sub>3</sub> OD (125 MHz) .....	67
Figure S63. <sup>1</sup> H- <sup>1</sup> H COSY spectrum of (2 <i>S</i> )-annullatin A ( <b>8</b> ) in CD <sub>3</sub> OD .....	67
Figure S64. HSQC spectrum of (2 <i>S</i> )-annullatin A ( <b>8</b> ) in CD <sub>3</sub> OD.....	68
Figure S65. HMBC spectrum of (2 <i>S</i> )-annullatin A ( <b>8</b> ) in CD <sub>3</sub> OD.....	68
Figure S66. <sup>1</sup> H NMR spectrum of (8 <i>S</i> )-annullatin E ( <b>9</b> ) in CD <sub>3</sub> OD (500 MHz) .....	69
Figure S67. <sup>1</sup> H NMR spectrum of (8 <i>S</i> )-annullatin J ( <b>10</b> ) in CDCl <sub>3</sub> (500 MHz) .....	69
Figure S68. <sup>13</sup> C NMR spectrum of (8 <i>S</i> )-annullatin J ( <b>10</b> ) in CDCl <sub>3</sub> (125 MHz) .....	70
Figure S69. <sup>1</sup> H- <sup>1</sup> H COSY spectrum of (8 <i>S</i> )-annullatin J ( <b>10</b> ) in CDCl <sub>3</sub> .....	70
Figure S70. HSQC spectrum of (8 <i>S</i> )-annullatin J ( <b>10</b> ) in CDCl <sub>3</sub> .....	71
Figure S71. HMBC spectrum of (8 <i>S</i> )-annullatin J ( <b>10</b> ) in CDCl <sub>3</sub> .....	71
<b>Supplementary References</b> .....	72

## Experiment Procedures

### 1. Computer-assisted sequence analysis

The genomic DNA sequence of annullatin cluster from *Penicillium roqueforti* FM164 on scaffold ProqFM164S03 (GenBank: HG792017.1) reported in this study was obtained from NCBI databases (<http://www.ncbi.nlm.nih.gov>). Sequence analysis was carried out by antiSMASH (<http://antismash.secondarymetabolites.org/>) and by comparison with known entries in NCBI database. Domain structures were predicted by using online programs BLAST (<http://blast.ncbi.nlm.nih.gov>) and 2ndFind (<https://biosyn.nih.go.jp/2ndfind/>).

### 2. Strains, media, and growth conditions

Fungal strains used in this study are summarized in Table S2. *P. roqueforti* FM164 was cultivated on PDA plates [potato dextrose broth (PDB), Sigma-Aldrich with 1.6% agar] at 25°C for sporulation and in PD surface culture without agar at 25°C for detection of secondary metabolites (SMs).

*Aspergillus nidulans* strains were grown at 37°C on GMM medium [LMM medium (1.0% glucose, 50 mL/L salt solution, 1 mL/L trace element solution, and 0.5% yeast extract) with 1.6% agar] for sporulation and transformation supplemented with 0.5 g/L uridine, 0.5 g/L uracil, 2.5 mg/L riboflavin, and/or 0.5 mg/L pyridoxine, depending on the selective marker genes. The salt solution comprises (w/v) 12% NaNO<sub>3</sub>, 1.04% KCl, 1.04% MgSO<sub>4</sub>·7H<sub>2</sub>O, and 3.04% KH<sub>2</sub>PO<sub>4</sub>. The trace element solution contains (w/v) 2.2% ZnSO<sub>4</sub>·7H<sub>2</sub>O, 1.1% H<sub>3</sub>BO<sub>3</sub>, 0.5% MnCl<sub>2</sub>·4H<sub>2</sub>O, 0.16% FeSO<sub>4</sub>·7H<sub>2</sub>O, 0.16% CoCl<sub>2</sub>·5H<sub>2</sub>O, 0.16% CuSO<sub>4</sub>·5H<sub>2</sub>O, 0.11% (NH<sub>4</sub>)<sub>6</sub>Mo<sub>7</sub>O<sub>24</sub>·4H<sub>2</sub>O, and 5% Na<sub>4</sub>EDTA. The created *A. nidulans* strains were cultivated at 25°C in PD medium under static conditions for SM detection.<sup>1-3</sup>

*Escherichia coli* DH5α (Invitrogen) was used for cloning and plasmid propagation, and grown in liquid or on solid lysogeny broth (LB) at 37 °C. 50 µg/mL carbenicillin were used for selection of the recombinant *E. coli* strains.

*Saccharomyces cerevisiae* HOD114-2B was used for cloning by homologous recombination.<sup>4</sup> Generally, yeast was grown at 30°C in YPD medium (1% yeast extract, 2% peptone, and 2% glucose). Selection was performed with synthetic complete (SC) medium without uracil or leucine (SC-Ura or SC-Leu) [6.7 g/L yeast nitrogen base with ammonium sulfate, 650 mg/L CSM-His-Leu-Ura (MP Biomedicals), histidine, and leucine].<sup>5</sup>

### 3. Genomic DNA isolation

For genomic DNA isolation, *P. roqueforti* and *A. nidulans* strains were cultivated in PDB or LMM for 3 days at 25 °C and 37 °C, respectively. Genomic DNA was isolated according to the method described previously.<sup>6</sup>

### 4. RNA isolation and cDNA synthesis

For isolation of RNA from *P. roqueforti* FM164, the fungus was grown as a shaking culture in liquid PD medium for 7 days at 25°C and the cells were collected by centrifugation. RNA extraction was performed by using Fungal RNA Mini kit (VWR OMEGA bio-tek E.Z.N.A®) according to the manufacturer's instruction. The ProtoScript® II First Strand cDNA Synthesis kit (New England BioLabs) was used for cDNA synthesis with Oligo-dT primers.

### 5. PCR amplification, gene cloning, and plasmid construction

Plasmids generated and used in this study are listed in Table S3. The oligonucleotide sequences for PCR

amplification are given in Table S4. All primers were synthesized by SeqLab GmbH (Göttingen, Germany). Genetic manipulation in *E. coli* or *S. cerevisiae* was carried out as described before.<sup>7,8</sup> PCR amplification was carried out by using Phusion® High-Fidelity DNA polymerase from New England Biolabs (NEB) on a T100™ Thermal cycler from Bio-Rad. Plasmids for heterologous expression were constructed by homologous recombination in *Escherichia coli* or *Saccharomyces cerevisiae*.

The annullatin cluster (PROQFM164\_S03g001173 – PROQFM164\_S03g001183 + 502 bp downstream of the last gene, bp 2700147 – 2728545 of HG792017.1) was amplified from genomic DNA of *P. roqueforti* FM164 in six fragments with primers listed in Table S4. The fragments were designed with a 103 – 118 bp overlap to each other, the outside fragments carried a 30 bp overlap to the linearized pJN017 which in turn had an overlap to the outside fragments of 20 bp (Table S4). The reconstruction of the cluster was carried out by yeast homologous recombination, leading to pBK21 (Table S3). In analogy, other heterologous expression constructs for gene overexpression in *A. nidulans* were created. The cluster fragments ended before the first or started after the last base of the genes to be deleted and shared 25 bp overlap to each other.

For deletion of the single genes of the annullatin gene cluster, 1.2 kb upstream and downstream of the gene of interest were amplified with primers listed in Table S2 introducing complementary overhangs of 30 – 35 bp to the backbone of pESC-Leu / pESC-Ura and the *AfpYrG*-gene cassette of pYH-wA-pyrG, which served as a selection marker. Clone of *AfpYrG* between the 5'- and 3'-regions into pESC-Leu / pESC-Ura to form the deletion vector was performed via yeast homologous recombination.

To construct the plasmid for heterologous expression of *anuE* and *anuG* in *A. nidulans*, an assembly approach based on the homologous recombination in *E. coli* was used (Figure S1). The full length of *anuE* including its terminator of 603 bp or *anuG* including its terminator of 613 bp was amplified from genomic DNA of *P. roqueforti* FM164 as template by PCR with primer pairs pPX28-1F/1R or pPX45-1F/1R (Table S4) and subsequently inserted into the *NheI*-linearized vector pYH-wA-pyrG with homologous flanking sequences of the *wA* gene, the *gpdA* promoter, and the *AfpYrG* selection marker.<sup>2</sup> The amplified genomic sequences of *anuE* and *anuG* were cloned between the *gpdA* promoter and the *AfpYrG* marker by using 25 – 30 bp overlap to the *NheI* restriction site to create pPX28 and pPX45, respectively.

## 6. Heterologous gene expression in *A. nidulans* LO8030

*A. nidulans* LO8030 was used as the recipient host.<sup>3</sup> Fungal protoplast preparation and PEG-mediated protoplast transformation were performed according to the protocol described previously.<sup>6</sup>

## 7. Confirmation and cultivation of the *A. nidulans* transformants

Genomic DNA of the transformants was isolated and used for PCR amplification. After selection by uridine and uracil or riboflavin autotrophy, the correct integration into the *wA* PKS gene locus was first observed by a color change of the conidia from green to white, and subsequent confirmed by PCR amplification with primers flanking the inserted gene(s) (Table S4 and Figure S1). Primers for the control of gene deletion mutants were targeted the upstream or downstream of the homologous parts used for integration with counterparts binding in the marker gene. Additionally, a PCR with primers for the deleted gene was performed to ensure its absence (Figure S2).

For detection of secondary metabolites, transformants were cultivated in PDB medium with the required supplements at 25°C. After 14 days, secondary metabolites were extracted with equal volumes of EtOAc for three times, evaporated and dissolved in a mixture of MeOH and distilled H<sub>2</sub>O (9:1), and analyzed via LC-MS.

## 8. Large-scale fermentation, extraction, and isolation of secondary metabolites

For metabolite extraction after large-scale fermentation, the supernatant was separated from mycelia by filtration and extracted with equal volume of EtOAc for three times. The mycelia were extracted with acetone and concentrated under reduced pressure to afford an aqueous solution and then extracted with EtOAc for three times. Both EtOAc extracts were combined and evaporated under reduced pressure to afford the crude extracts for further purification.

To identify the structure of compound **1**, we used the previously published acetylation method.<sup>9</sup> *A. nidulans* BK08 (*anu* cluster) spores were cultivated in 4 x 1 L flasks containing 250 mL PDB liquid medium each, and supplemented with 0.5 mg/L pyridoxine, 500 mg/L uracil and 500 mg/L uridine at 25°C for 13 days. The cultures were harvested and extracted as mentioned above to give 270 mg crude extract. The obtained crude extract was immediately acetylated with acetic anhydride (21.24 mmol) and NaOAc·3H<sub>2</sub>O (0.3 mmol) at room temperature for 16 h. The mixture was extracted with 15 mL EtOAc and washed with 15 mL saturated solution of NaHCO<sub>3</sub> for three times. After evaporation of the solvent, 5 mg of acetylated product was isolated by using semi-preparative HPLC [XDB-C18 (details see below), H<sub>2</sub>O/CH<sub>3</sub>CN = 45/55, flow rate = 2.0 mL/min,  $\lambda$  = 310 nm,  $t_R$  = 17.9 min,  $\lambda$  = 310 nm] for MS and NMR analyses.

To isolate compounds **2** – **4**, spores of *A. nidulans* BK08 bearing the *anu* cluster were inoculated in 10 x 1 L Erlenmeyer flasks each containing 300 mL PD liquid medium supplemented with 0.5 mg/L pyridoxine and 2.5 mg/L riboflavin at 25°C for 14 days. After extraction, 1.6 g crude extract was obtained. This crude extract was applied to silica gel column chromatography by using petroleum ether : EtOAc (30 : 1, 10 : 1, 5 : 1, 1 : 1 and 0 : 1, v/v) as elution solvents, giving fractions 1 – 40. **2** (8 mg,  $t_R$  = 16.3 min) was obtained from fraction 34 after purification on a semi-preparative HPLC [VDSpher PUR 100 C18-M-SE (details see below), H<sub>2</sub>O/CH<sub>3</sub>CN = 35/65, flow rate = 2.0 mL/min,  $\lambda$  = 310 nm]. Fractions 30 – 33 were further purified on a semi-preparative HPLC (VDSpher PUR 100 C18-M-SE, H<sub>2</sub>O/CH<sub>3</sub>CN = 40/60, flow rate = 2.0 mL/min,  $\lambda$  = 310 nm) to yield **3** (6 mg,  $t_R$  = 34.2 min). **4** (6 mg) was obtained from fraction 23 after purification on semi-preparative HPLC (VDSpher PUR 100 C18-M-SE, H<sub>2</sub>O/CH<sub>3</sub>CN = 54/46, flow rate = 2.0 mL/min,  $\lambda$  = 290 nm,  $t_R$  = 19.2 min).

To isolate **5** – **8**, *A. nidulans* BK17 ( $\Delta anuE$ ) was cultivated in 4 x 2.5 L Erlenmeyer flasks each containing 500 mL PD liquid medium supplemented with 0.5 mg/L pyridoxine at 25°C for 14 days. After extracting with 6 L EtOAc and concentration under reduced pressure, the crude extract (0.3 g) was purified by using semi-preparative HPLC (XDB-C18, H<sub>2</sub>O/CH<sub>3</sub>CN = 60/40 – 0/100, flow rate = 2.0 mL/min,  $\lambda$  = 280 nm and 290 nm) in 40 min, to yield **5** (5 mg,  $t_R$  = 9.7 min), **6** (6 mg,  $t_R$  = 17.6 min), **7** (10 mg,  $t_R$  = 20.0 min) and **8** (3 mg,  $t_R$  = 25.1 min).

To isolate **9**, *A. nidulans* BK21 ( $\Delta anuH$ ) was cultivated in 4 x 2.5 L Erlenmeyer flasks each containing 500 mL PD liquid medium supplemented with 0.5 mg/L pyridoxine at 25°C for 14 days. After extraction, the crude extract (0.6 g) was subjected to silica gel column chromatography by using stepwise gradient elution with the mixtures of petroleum ether : EtOAc (10 : 1, 5 : 1 to 1 : 1, v/v) to give eighteen fractions (1 – 18). Fraction 11 was purified by using semi-preparative HPLC (XDB-C18, H<sub>2</sub>O/CH<sub>3</sub>CN = 60/40, flow rate = 2.0 mL/min,  $\lambda$  = 280 nm), leading to the isolation of **9** (9 mg,  $t_R$  = 10.9 min).

## 9. Cloning of the heterologous expression construct for *anuH* in *E. coli*

The coding region of *anuH* without any introns was amplified from *P. roqueforti* FM164 cDNA with primers

pPX-PTN-F and pPX-PTN-R with recognition sites for BamHI (5') and HindIII (3'). The commercially available vector pET-28a (+) (Qiagen, Venlo, Netherlands) and the *anuH* fragment were digested with HindIII and BamHI and purified via EtOH precipitation. The *anuH* fragment was ligated into pET-28a (+) with T4 DNA ligase (Jena Bioscience, Jena, Germany).

## 10. Overproduction and purification of AnuH

The *anuH* expression plasmid pPX52 was used to express in *E. coli* BL21(DE3). An overnight preculture was used to inoculate 4 x 500 mL Terrific Broth medium (TB medium, with 2.4% yeast extract, 2.0% tryptone, 0.4% glycerol, and 0.1 M phosphate buffer, pH 7.4) to an OD<sub>600</sub> of 0.6 and then the cultures were induced with 0.1 mM IPTG at 16°C for 20 h. The recombinant 6xHis-tagged protein was purified via Ni-NTA agarose column (Qiagen, Hilden, Germany) and further subjected to preparative gel filtration chromatography using a Superdex 200 16/60 pg column connected to a ÄKTAprius plus (GE Healthcare, Chalfont St Giles, Great Britain) with storage buffer [50 mM Tris-HCl, 150 mM NaCl, and 20 % (w/v) glycerol, pH 7.5] at a flow rate of 0.5 mL/min. The purified protein was analyzed on SDS-PAGE (12%, Figure S17).

## 11. In vitro assays of AnuH

To determine the enzyme activity of AnuH toward **9** or **6**, the reaction mixtures (50 µL) contained Tris-HCl buffer (50 mM, pH 7.5), CaCl<sub>2</sub> (5 mM), dimethylallyl phosphate (DMAPP) (1 mM), **9** (0.5 mM) or **6** (0.5 mM), glycerol (0.5 – 5%), DMSO (up to 5%), and the purified recombinant AnuH (2 µg). Geranyl diphosphate (GPP) and farnesyl diphosphate (FPP) were also incubated with **9**.

The enzyme assays were incubated at 37°C for 30 min or 4 h and terminated with one volume of CH<sub>3</sub>CN. The reaction mixtures were centrifuged at 13,000 rpm for 30 min before further analysis on HPLC.

To isolate the enzyme product **10**, 4 mg of **9** was incubated in 10 mL reaction mixtures, containing Tris-HCl buffer (50 mM, pH 7.5), CaCl<sub>2</sub> (5 mM), DMAPP (1 mM) and AnuH (400 µg) at 37°C for 16 h. The reaction mixture was extracted subsequently with double volume of EtOAc for three times and then subjected on semi-preparative HPLC (VDSpher PUR 100 C18-M-SE, ACN/H<sub>2</sub>O = 60/40, flow rate = 2.0 mL/min, λ = 290 nm) to give **10** (2 mg, *t<sub>R</sub>* = 16.9 min).

## 12. Enzyme assays for determination of the kinetic parameters

For determination of the kinetic parameters of AnuH toward **9** (Figure S18), the enzyme assays were performed in 50 µL reaction mixtures containing Tris-HCl buffer (50 mM, pH 7.5), CaCl<sub>2</sub> (5 mM), DMAPP (1 mM), and the purified AnuH (2 µg). The concentrations of substrate **9** were 0.01, 0.02, 0.05, 0.1, 0.2, 0.5, 1, 2, 3, and 5 mM. The reactions were carried out at 37 °C for 30 min. For kinetic parameters toward DMAPP, reaction mixtures with 2 µg AnuH, **9** (0.5 mM), CaCl<sub>2</sub> (5 mM), and DMAPP at final concentrations of 0.01, 0.02, 0.05, 0.1, 0.2, 0.5, 1, 2, 3, and 5 mM were incubated at 37 °C for 30 min. The assays were performed as duplicates and subsequently terminated with one volume of CH<sub>3</sub>CN, and centrifuged at 13,000 rpm for 30 min before further analysis on LC–MS. The kinetic parameters *K<sub>M</sub>* and *k<sub>cat</sub>* were determined using non-linear regression analysis of Michaelis-Menten equation by GraphPad Prism 6.

## 13. Heterologous expression of *anuE* and *anuG* in *A. nidulans* LO8030

Fungal protoplast preparation and transformation were performed according to the method described previously.<sup>6</sup> pPX28 containing *anuE* and pPX45 containing *anuG* were transformed into *A. nidulans* LO8030

to create the expression strain PX28 for *anuE* and PX45 for *anuG*, respectively. Potential transformants were verified by PCR using the primers pPX28-test-1f/1r and pPX39-*anuG*-tf/tr (Table S4). PDB liquid medium was used to cultivate the transformants (25°C, 4 – 12d) for LC–MS analysis of the SM production.

#### 14. Precursor feeding in *A. nidulans* PX28 and PX45

For feeding experiments in *A. nidulans* PX28, the precursor **6** was dissolved in DMSO to give a 20 mM stock solution. 15 µL of **6** were then added to 15 mL of PDB liquid medium with appropriate supplements of the transformant strain PX28, the control strain pYH-*wA*-pyrG, as well as to media for nonenzymatic reaction, resulting in a final concentration of 20 µM. After cultivation for another 3 and 7 days, the fungal cultures were extracted with EtOAc for three times and analyzed on LC–MS.

For feeding experiments in *A. nidulans* PX45, the precursor **4** was dissolved in DMSO to give a 10 mM stock solution. 15 µL of **4** were then added to 15 mL of PDB liquid medium with appropriate supplements of the transformant strain PX45, the control strain pYH-*wA*-pyrG, as well as to media for nonenzymatic experiment, resulting in a final concentration of 10 µM, respectively. After cultivation for another 3, 5, 7 and 12 days, the fungal cultures were extracted with EtOAc for three times and analyzed on LC–MS.

#### 15. HPLC and LC–MS analyses of secondary metabolites

Analysis of SMs was performed on an Agilent series 1200 HPLC (Agilent Technologies, Böblingen, Germany) with an Agilent Eclipse XDB-C18 column (150 × 4.6 mm, 5 µm, Agilent Technologies, Böblingen, Germany). H<sub>2</sub>O (A) and CH<sub>3</sub>CN (B), both with 0.1% (v/v) HCOOH, were used as solvents at flow rate of 0.5 mL/min. The substances were eluted with a linear gradient from 5 – 100% B in 40 min, then washed with 100% (v/v) solvent B for 5 min and equilibrated with 5% (v/v) solvent B for 10 min. UV absorptions at 190 – 400 nm were illustrated in this study. Semi-preparative HPLC was performed on the same equipment with an Agilent Eclipse XDB-C18 column (9.4 × 250 mm, 5 µm, Agilent Technologies, Böblingen, Germany) or VDSpher PUR 100 C18-M-SE column (250 × 10 mm, 5 µm, VDS optilab Chromatographie Technik GmbH, Berlin, Germany) and a flow rate of 2 mL/min.

LC–MS analysis was performed on an Agilent 1260 HPLC system equipped with a microTOF-Q III spectrometer (Bruker, Bremen, Germany) by using VDSpher PUR100 C18-M-SE column (150 × 2.0 mm, 3 µm, VDS optilab Chromatographie Technik GmbH, Berlin, Germany). H<sub>2</sub>O (A) and CH<sub>3</sub>CN (B), both with 0.1% (v/v) formic acid, were used as solvents at flow rate of 0.3 mL/min. The substances were eluted using a linear gradient from 5 – 100% B within 30 min. For mass determination, positive ion mode electrospray ionization (ESI) in a microTOF-Q III mass spectrometer (Bruker Daltonics) was used with 5 mM sodium formate for mass calibration. The masses were scanned in the range of *m/z* 100 – 1500. Data were evaluated with the Compass DataAnalysis 4.2 software (Bruker Daltonik, Bremen, Germany).

#### 16. NMR analysis

NMR spectra were recorded on a JEOL ECA-500 MHz spectrometer (JEOL, Tokyo, Japan). The spectra were processed with MestReNova 6.1.0 (Metrelab, Santiago de Compostela, Spain). Chemical shifts are referenced to those of the solvent signals. NMR data are given in Tables S5–S12 and spectra in Figures S28–S71.

#### 17. Measurement of optical rotations

The optical rotation was measured with the polarimeter Jasco DIP-370 at 20°C using the D-line of the sodium lamp at  $\lambda = 589.3$  nm. Prior to the measurement, the polarimeter was calibrated with MeOH as solvent.

## 18. The experimental and calculated electronic circular dichroism (ECD) spectroscopic analysis

The experimental ECD spectra were taken on a J-1500 CD spectrometer (Jasco Deutschland GmbH, Pfungstadt, Germany). The samples were dissolved in EtOH or MeOH and measured in the range of 200 – 400 nm by using a 1 mm path length quartz cuvette (Hellma Analytics, Müllheim, Germany).

For ECD calculation, conformers of a given compound were generated by the Confab<sup>10</sup> program embedded in the Openbabel 3.1.1 software. The conformers were further optimized with xtb at GFN2 level<sup>11</sup> and the conformers with population over 1% were subjected to geometry optimization using the Gaussian 16 package (<https://gaussian.com/gaussian16/>) at B3LYP/6-31G(d) level and frequency analysis, then proceeded to calculation of excitation energies, oscillator strength, and rotatory strength at B3LYP/TZVP level in the polarizable continuum model (PCM, methanol). The calculated ECD spectra were Boltzmann-weighted and generated using SpecDis 1.71 software.<sup>12</sup> The experimental and calculated ECD spectra are given in Figures S20–S27.

## 19. Physiochemical properties of the compounds described in this study

(2*R*)-annullatin F (**1**): HRMS (ESI) *m/z*: [M + Na]<sup>+</sup> Calcd for C<sub>17</sub>H<sub>24</sub>O<sub>4</sub>Na 315.1567; Found 315.1566.

(2*S*, 9*S*)-annullatin D (**2**): yellow oil; [ $\alpha$ ]<sub>D</sub><sup>20</sup> = -9.5 (*c* 0.15, CHCl<sub>3</sub>); ECD (2.27 mM, EtOH)  $\lambda_{\text{max}}$  ( $\Delta\epsilon$ ) 315 (-0.18), 278 (+0.13), 252 (-0.21), 242 (+0.94), 224 (+0.13), 205 (+1.2) nm; HRMS (ESI) *m/z*: [M + Na]<sup>+</sup> Calcd for C<sub>17</sub>H<sub>22</sub>O<sub>4</sub>Na 313.1410; Found 313.1414.

(2*R*)-annullatin G (**3**): tawny oil; [ $\alpha$ ]<sub>D</sub><sup>20</sup> = +158.6 (*c* 0.29, CHCl<sub>3</sub>); ECD (1.29 mM, EtOH)  $\lambda_{\text{max}}$  ( $\Delta\epsilon$ ) 302 (-0.29), 224 (+1.18), 202 (-0.78) nm; HRMS (ESI) *m/z*: [M + Na]<sup>+</sup> Calcd for C<sub>19</sub>H<sub>26</sub>O<sub>5</sub>Na 357.1672; Found 357.1675.

(2*S*, 9*S*)-annullatin H (**4**): yellow oil; [ $\alpha$ ]<sub>D</sub><sup>20</sup> = -42.5 (*c* 0.4, CHCl<sub>3</sub>); ECD (2.92 mM, EtOH)  $\lambda_{\text{max}}$  ( $\Delta\epsilon$ ) 286 (-0.08), 236 (+0.70), 216 (-0.26) nm; HRMS (ESI) *m/z*: [M + Na]<sup>+</sup> Calcd for C<sub>17</sub>H<sub>26</sub>O<sub>4</sub>Na 317.1723; Found 317.1721.

(14*S*)-annullatin I (**5**): light yellow oil; [ $\alpha$ ]<sub>D</sub><sup>20</sup> = +14.2 (*c* 0.64, CHCl<sub>3</sub>); ECD (0.97 mM, EtOH)  $\lambda_{\text{max}}$  ( $\Delta\epsilon$ ) 288 (+0.53), 252 (+0.12), 232 (+1.25), 218 (+0.94), 202 (+3.09) nm; HRMS (ESI) *m/z*: [M - H]<sup>-</sup> Calcd for C<sub>17</sub>H<sub>27</sub>O<sub>4</sub> 295.1915; Found 295.1909.

2-Hydroxymethyl-3-pentylphenol (**6**): white solid; HRMS (ESI) *m/z*: [M - H]<sup>-</sup> Calcd for C<sub>12</sub>H<sub>17</sub>O<sub>2</sub> 193.1234; Found 193.1215.

(2*S*)-annullatin B (**7**): pale yellow oil; [ $\alpha$ ]<sub>D</sub><sup>20</sup> = +13.4 (*c* 0.12, CHCl<sub>3</sub>); ECD (0.96 mM, EtOH)  $\lambda_{\text{max}}$  ( $\Delta\epsilon$ ) 287 (-0.15), 236 (+1.14), 211 (-1.59), 205 (+0.72) nm; HRMS (ESI) *m/z*: [M + Na]<sup>+</sup> Calcd for C<sub>17</sub>H<sub>26</sub>O<sub>3</sub>Na 301.1774; Found 301.1778.

(2*S*)-annullatin A (**8**): yellow oil; [ $\alpha$ ]<sub>D</sub><sup>20</sup> = -104.0 (*c* 0.17, CHCl<sub>3</sub>); ECD (0.74 mM, EtOH)  $\lambda_{\text{max}}$  ( $\Delta\epsilon$ ) 360 (-1.36), 314 (+0.66), 258 (-0.99), 220 (+2.89) nm; HRMS (ESI) *m/z*: [M + H]<sup>+</sup> Calcd for C<sub>17</sub>H<sub>25</sub>O<sub>3</sub> 277.1798; Found 277.1815.

(8*S*)-annullatin E (**9**): light yellow oil; [ $\alpha$ ]<sub>D</sub><sup>20</sup> = -15.6 (*c* 0.9, CHCl<sub>3</sub>); ECD (3.43 mM, MeOH)  $\lambda_{\text{max}}$  ( $\Delta\epsilon$ ) 288



(+0.08), 210 (-0.80), 202 (+0.01) nm; HRMS (ESI)  $m/z$ :  $[M - H]^-$  Calcd for  $C_{12}H_{17}O_3$  209.1183; Found 209.1199.

(8*S*)-annullatin J (**10**): light yellow oil;  $[\alpha]_D^{20} = -43.5$  ( $c$  0.23,  $CHCl_3$ ); ECD (1.44 mM, MeOH)  $\lambda_{max}$  ( $\Delta\epsilon$ ) 257 (+0.28), 219 (-0.50), 210 (+0.89), 202 (-0.46) nm; HRMS (ESI)  $m/z$ :  $[M - H]^-$  Calcd for  $C_{17}H_{25}O_3$  277.1809; Found 277.1824.

## 20. Gene and protein sequences of AnuH

### Genomic sequence of *anuH*

ATGGTTGAAGTGACAAGACCACCCACCAAGGCATGGGCAACTCTATCACCATGGCTGCCCTCACGAGGGCCTG  
ATGCAGATTATTGGTGGAGACTGACAGGCCAGCATCTGTCTAACATGGTCGAGGCTGCTGGATACTCAACAGAC  
CAGCAATATGTGGCACTTCTCTTCCACTATCATTGGATCGTGCATCCCTGTTCCCTTTTCCCCACTCTTCTCT  
CCATGTTTCACTAGAAACGCAGCAACACTAACGGAGTGGCTAGCATAGGTTCCCTACATGGGCCCCGCACCTGG  
ACCAGACGGCAACCTCAAATGGAAATCTTTGCTGGGAGTTGAAGGGTCTCCGATTGAATATTCTTGGAATGGA  
ATACTGCGGCAGGCAAGCCCGATGTCCGCTACACCACAGAGGCAATTGGCTCCTTCACAGGAACCCTTTTGGAT  
CCTCTGAACCAGCAAGCCACACTTGAGATGCTGCATCGCATAGCAGATTTCTGTGCGCAACTGTGGACCTTACCTG  
GACCAACCATTTCTTCGCCACCCTCTACGATCATGACCGCTCCAAATATGCCAAGGAAGCGGCGGCAGGTGCGC  
ACTTCACCACTACGGTGGTAGTCGCCGCGGAGTGGCTCAAGAATGGTCTGAATCTCAAAACGTATTTTGTTCCT  
CGTCGTCTGGGTCAATCGGATGGGAAGTTGCCCATCGCTCTGTGGGAAGAATCACTCAAGCAGCTTGATCCGAA  
CAGTGAATCTCGAGCCGCAATGCACGAATTTCTCAACAATGACCCGGAAGGAAAATTGCTGAGCCCCCTGTAAAG  
CCTTTATCTTTGCATCTCAATAATAGATGCTTCCTCGTTTGGAAATATTGCTAACGAGAATCTTAGCATGCTGGCTG  
TTGATAATGTCGTCCCTGAAAAATCGAGGCTCAAGTTCTACTTCCAATCTCCCCATACCAGCTTTGCCTCTGTGC  
GGCAGGTGATGACAATGGGAGGGCGCATCCCCGTCCCTGAATCGCAGCTCCAGGAGCTCCGCAGTCTCATTGCA  
GCTGTTACAGGCCTAGACTCGGACTTCCCTGAGGATTCTGAGGTCCCTTGATATCAGAGTACAACCCAGCCGC  
TAAAGATAACTTCGTTGAGATTGATCTTTTGCTTTCTGGGTATTTATACTATTTGATATTGCTCCTGGAGCAACAG  
TGCCGGATATCAATTTTATACTCCTGTTGCTGCTATGGACCGGACGATGGTGGCCTTGCAAAAGGCATCGCTG  
ACTGGATGACATCTCGCGGAAGGGGTGAATATAGCCAGAGATACCTGGACATGCTTGCAGATCTACCGAGCAT  
CGAAACTAGAAAGATGGAAAGGGCATGCAGACATACGTTAGTTGTCTGTTCAAGAAGAGCCACTTGACGTTA  
CGTCCTATATTGGCCCGGAGGCATTTGATCCCGCCCGCTTTCTGAAGCATAAAGCACACACCACCCGGTCCACCC  
GAAGACGGAGCGATAGTCATTGA

### Coding region of *anuH*

ATGGTTGAAGTGACAAGACCACCCACCAAGGCATGGGCAACTCTATCACCATGGCTGCCCTCACGAGGGCCTG  
ATGCAGATTATTGGTGGAGACTGACAGGCCAGCATCTGTCTAACATGGTCGAGGCTGCTGGATACTCAACAGAC  
CAGCAATATGTGGCACTTCTCTTCCACTATCATTGGATCGTTCCTTACATGGGCCCCGCACCTGGACCAGACGGC  
AACCTCAAATGGAAATCTTTGCTGGGAGTTGAAGGGTCTCCGATTGAATATTCTTGGAATGGAATACTGCGGC  
AGGCAAGCCCGATGTCCGCTACACCACAGAGGCAATTGGCTCCTTCACAGGAACCCTTTTGGATCCTCTGAACC  
AGCAAGCCACACTTGAGATGCTGCATCGCATAGCAGATTTCTGTGCGCAACTGTGGACCTTACCTGGACCAACCAT  
TTCTTCGCCACCCTCTACGATCATGACCGCTCCAAATATGCCAAGGAAGCGGCGGCAGGTGCGCACTTACCCAC  
TACGGTGGTAGTCGCCGCGGAGTGGCTCAAGAATGGTCTGAATCTCAAAACGTATTTTGTTCCTCGTCTGG  
GTCAATCGGATGGGAAGTTGCCCATCGCTCTGTGGGAAGAATCACTCAAGCAGCTTGATCCGAACAGTGAATCT  
CGAGCCGCAATGCACGAATTTCTCAACAATGACCCGGAAGGAAAATTGCTGAGCCCCCTCATGCTGGCTGTTGA  
TAATGTCGTCCCTGAAAAATCGAGGCTCAAGTTCTACTTCCAATCTCCCCATACCAGCTTTGCCTCTGTGCGGCA  
GGTCATGACAATGGGAGGGCGCATCCCCGTCCCTGAATCGCAGCTCCAGGAGCTCCGCAGTCTCATTGCAGCTG  
TTACAGGCCTAGACTCGGACTTCCCTGAGGATTCTGAGGTCCCTTGATATCAGAGTACAACCCAGCCGCTAAA  
GATAACTTCGTTGAGATTGATCTTTTGCTTTCTGGGTATTTATACTATTTGATATTGCTCCTGGAGCAACAGTGCC

GGATATCAAATTTTATACTCCTGTTCTGTCGCTATGGACCGGACGATGGTGCCCTTGCAAAAGGCATCGCTGACTG  
GATGACATCTCGCGGAAGGGGTGAATATAGCCAGAGATACCTGGACATGCTTGCAGATCTCACCGAGCATCGCA  
AACTAGAAGATGGAAAGGGCATGCAGACATACGTTAGTTGTCTGTTCAAGAAGAGCCACTTGGACGTTACGTCC  
TATATTGGCCCGGAGGCATTTGATCCCGCCCGCTTTCTGAAGCATAAAGCACACACCACCCGGTCCACCCGAAG  
ACGGAGCGATAGTCATTGA

Protein sequence of *anuH*

MVEVTRPPTKAWATLSPWLPSRGPADYWWRLTGQHLSNMVEAAGYSTDQQYVALLFHYHWIVPYMGPA PGPDG  
NLKWKSLLGVEGSPIEYSWKWNTAAGKPDVRYTTEAIGSFTGTLLDPLNQQATLEMLHRIADFVPTVDLTWTNHFF  
ATLYDHDRSKYAKEAAAGAHFTTTVVVAAEWLKNGLNLKTYFVPRRLGQSDGKLPIALWEESLKQLDPNSESRAA  
MHEFLNNDPEGKLLSPFMLAVDNVVPESRLKFYFQSPHTSFASVRQVMTMGG RIPVPESQLQELRSLIAAVTGLDS  
DFPEDSEVPCISEYNPAAKDNFVEIDL LLSGYLYYFDIAPGATVPDIKFYTPVRRYGPDDGALAKGIADWMTSRGRG  
EYSQRYLDMLADLTEHRKLEDGKGMQTYVSCLFKKSHLDVTSYIGPEAFD PARFLKHKHAHTTRSTRRRSDSH

## Supplementary Tables

**Table S1.** Putative functions of the genes from annullatin (*anu*) gene cluster

Protein (Acc. Nr.)	Size (aa)	Identity (%)	Homologous protein, organism	Putative function
AnuA (CDM34450.1)	2130	43.1	Highly reducing polyketide synthase, FogA (EYE95343) from <i>Aspergillus</i> <i>ruber</i>	Reducing polyketide synthase (KS-AT-DH-ER-KR)
AnuB (CDM34451.1)	283	55.0	Short-chain dehydrogenase / reductase, FogD (EYE95338) from <i>Aspergillus</i> <i>ruber</i>	Short-chain dehydrogenase / reductase
AnuC (CDM34452.1)	91	44.3	Short-chain dehydrogenase / reductase, FogBC (EYE95337) from <i>Aspergillus</i> <i>ruber</i>	Protein of unknown function
AnuD (CDM34453.1)	381	87.7	Short-chain dehydrogenase / reductase (KGO64723) from <i>Penicillium italicum</i>	Short-chain dehydrogenase / reductase
AnuE (CDM34454.1)	490	32.9	Cytochrome P450, FogE (EYE95339) from <i>Aspergillus ruber</i>	Cytochrome P450
AnuF (CDM34455.1)	276	70.1	Short-chain dehydrogenase / reductase (RFU78523.1) from <i>Trichoderma</i> <i>arundinaceum</i>	Short-chain dehydrogenase / reductase
AnuG (CDM34456.1)	509	28.1	FAD-binding oxidoreductase, FogF (EYE95340) from <i>Aspergillus ruber</i>	BBE-like enzyme: Berberine bridge enzyme-like enzyme
AnuH (CDM34457.1)	451	49.2	Prenyltransferase, FogH (EYE95342) from <i>Aspergillus ruber</i>	Prenyltransferase
AnuI (CDM34458.1)	252	22.6	Short-chain dehydrogenase / reductase, FogD (EYE95338) from <i>Aspergillus</i> <i>ruber</i>	Short-chain dehydrogenase / reductase
AnuJ (CDM34459.1)	818	89.8	Monooxygenase, FAD-binding (KGO64729) from <i>Penicillium italicum</i>	Aromatic ring hydroxylating dehydrogenase
AnuK (CDM34449.1)	261	83.0	Transcription factor (KGO64720) from <i>Penicillium italicum</i>	Fungal specific transcription factor

**Table S2.** Strains used in this study

Strains	Genotype	Source/Ref.
<i>Penicillium roqueforti</i>		
FM164	Wild type	13
<i>Aspergillus nidulans</i>		
LO8030	<i>pyroA4</i> , <i>riboB2</i> , <i>pyrG89</i> , <i>nkuA::argB</i> , sterigmatocystin cluster ( <i>AN7804</i> – <i>AN7825</i> ) $\Delta$ , emericellamide cluster ( <i>AN2545</i> – <i>AN2549</i> ) $\Delta$ , asperfuranone cluster ( <i>AN1039</i> – <i>AN1029</i> ) $\Delta$ , monodictyphenone cluster ( <i>AN10023</i> – <i>AN10021</i> ) $\Delta$ , terrequinone cluster ( <i>AN8512</i> – <i>AN8520</i> ) $\Delta$ , austinol cluster part 1 ( <i>AN8379</i> – <i>AN8384</i> ) $\Delta$ , austinol cluster part 2 ( <i>AN9246</i> – <i>AN9259</i> ) $\Delta$ , F9775 cluster ( <i>AN7906</i> – <i>AN7915</i> ) $\Delta$ , asperthecin cluster ( <i>AN6000</i> – <i>AN6002</i> ) $\Delta$	3
BK03	<i>wA-PKS::gpdA(p)-anuA::Afribo</i> in <i>A. nidulans</i> LO8030	This study
BK06	<i>wA-PKS::Afribo</i> in <i>A. nidulans</i> LO8030 (isogenic control strain)	This study
BK08	<i>wA-PKS::gpdA(p)-annullatin</i> cluster (PROQFM164_S03g001173 – PROQFM164_S03g001183 + 502 bp 3'UTR):: <i>Afribo</i> in <i>A. nidulans</i> LO8030	This study
BK17	$\Delta$ <i>anuE::AfpYrG</i> in BK08	This study
BK18	$\Delta$ <i>anuD::AfpYrG</i> in BK08	This study
BK19	$\Delta$ <i>anuI::AfpYrG</i> in BK08	This study
BK20	$\Delta$ <i>anuJ::AfpYrG</i> in BK08	This study
BK21	$\Delta$ <i>anuH::AfpYrG</i> in BK08	This study
PX38	$\Delta$ <i>anuF::AfpYrG</i> in BK08	This study
PX39	$\Delta$ <i>anuG::AfpYrG</i> in BK08	This study
PX28	<i>wA-PKS::gpdA(p)-anuE::AfpYrG</i> in <i>A. nidulans</i> LO8030	This study
PX45	<i>wA-PKS::gpdA(p)-anuG::AfpYrG</i> in <i>A. nidulans</i> LO8030	This study

**Table S3.** Plasmids used and constructed in this study

Plasmids	Description	Source/Ref.
pYH-wA-pyrG	<i>URA3</i> , <i>wA</i> flanking, <i>AfpYrG</i> , <i>Amp</i> , <i>gpdA(p)</i>	2
pJN017	<i>URA3</i> , <i>wA</i> flanking, <i>AfRiboB</i> , <i>Amp</i> , <i>gpdA(p)</i>	5
pESC-Ura	<i>Saccharomyces cerevisiae</i> and <i>E. coli</i> shuttle vector	Agilent
pESC-Leu	<i>Saccharomyces cerevisiae</i> and <i>E. coli</i> shuttle vector	Agilent
pBK18	Heterologous expression of <i>anuA</i> _FL in <i>A. nidulans</i> LO8030 (pJN017 backbone)	This study
pBK21	Heterologous expression of <i>anu</i> cluster without natural promoter of <i>anuK</i> (pJN017 backbone)	This study
pBK45	Deletion of <i>anuE</i> via <i>AfpYrG</i> selection in <i>A. nidulans</i> BK08 (pESC-Leu backbone)	This study
pBK46	Deletion of <i>anuD</i> via <i>AfpYrG</i> selection in <i>A. nidulans</i> BK08 (pESC-Leu backbone)	This study
pBK47	Deletion of <i>anuI</i> via <i>AfpYrG</i> selection in <i>A. nidulans</i> BK08 (pESC-Leu backbone)	This study
pBK48	Deletion of <i>anuJ</i> via <i>AfpYrG</i> selection in <i>A. nidulans</i> BK08 (pESC-Leu backbone)	This study
pBK49	Deletion of <i>anuH</i> via <i>AfpYrG</i> selection in <i>A. nidulans</i> BK08 (pESC-Leu backbone)	This study
pPX28	Heterologous expression of <i>anuE</i> (cytochrome P450) in <i>A. nidulans</i> LO8030 (pYH-wA-pyrG backbone)	This study
pPX38	Deletion of <i>anuF</i> via <i>AfpYrG</i> selection in <i>A. nidulans</i> BK08 (pESC-URA backbone)	This study
pPX39	Deletion of <i>anuG</i> via <i>AfpYrG</i> selection in <i>A. nidulans</i> BK08 (pESC-URA backbone)	This study
pPX45	Heterologous expression of <i>anuG</i> (BBE) in <i>A. nidulans</i> LO8030 (pYH-wA-pyrG backbone)	This study
pPX52	<i>anuH</i> (without introns) in pET-28a (+)	This study

**Table S4.** Primers used in this study

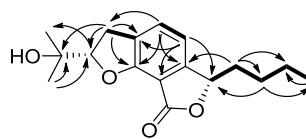
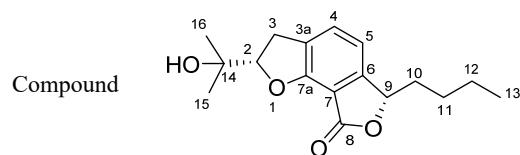
Primer	Sequence	Targeted amplification
prBK77	<u>CAACACCATA</u> TTTTAATCCCATGTGGGCCCAGTTCAATACATATATCG	For cloning of pBK18
prBK78	CTACCCCGCTTGAGCAGACATCACCGGCATGTCGCCTATTTACTAGATTC	
prBK50	GAGTACCCGGCGCGTAAG	2015 bp partial fragment of <i>anuA</i>
prBK51	GAGACGAGTGGTTTGGCC	
prBK102	<u>CTAACAGCTACCCCGCTTGAGCAGACATCACCATGAAAGCCAGTAAACTCA</u> C	For cloning of pBK21: fragment 1
prBK84	CAACGCAACATTATTGGTGTG	For cloning of pBK21: fragment 2
prBK85	CTTAAGCGAGGGTTGTTCTAGC	
prBK86	CAGATATGGCGGGTCTTAGCC	For cloning of pBK21: fragment 3
prBK87	GTTTCGAAAAAGAAGTAATAG	
prBK88	CAAGTTTCCCTTCTCTCTTG	For cloning of pBK21: fragment 4
prBK89	GTAATCCAGTGGCATAAAC	
prBK90	GGATTTGAGGGTCCGGAAG	For cloning of pBK21: fragment 5
prBK91	GAGATATCAACAGTATGCCG	
prBK92	CAATACGTCGGTCATGGTAC	For cloning of pBK21: fragment 6
prBK93	GAGCTACCGAGCTGTGTTTG	
prBK96	<u>CTCAACACCATA</u> TTTTAATCCCATGTGGGCCGGATCGTACAACAGGACGCC	Verification of BK08: fragment 1
prBK101	ATGTCCCAGATGATGGCTC	
prBK103	TCGCCCGATAAGAATGCTG	Verification of BK08: fragment 2
prBK100	ACGAGGCTCTTAAACGCAAG	
prBK104	ATTCGACTCGAGTGACAG	Verification of BK08: fragment 3
prBK33	GAATCCCAGGCCCTGGTTTG	
prBK34	CAAGTATGATCCTGAGGGCCG	For cloning of pBK45: <i>anuE</i> 5'-region
prBK151	<u>GGATCCGTAATACGACTCACTATAGGGCCC</u> ACCACATGGTGCAGTAGAATC	
prBK175	<u>CAACATAT</u> TCGTCAGACACAGAATAACTCTCCATAGGATGGTCACCAGC	For cloning of pBK45: <i>anuE</i> 3'-region
prBK154	<u>GAAATCAACTTCTGTTCCATGTCGACGCCC</u> TATACAACGAAGGTGCATC	
prBK176	<u>CACGCATCAGTGCCTCCTCTCAGACAGAATGTGACATCAAGCCCCGACTG</u>	For cloning of pBK46: <i>anuD</i> 5'-region
prBK155	<u>GGATCCGTAATACGACTCACTATAGGGCCC</u> TCCGAGTCATCATTAGCAGG	
prBK177	<u>CATAT</u> TCGTCAGACACAGAATAACTCTCACATTGGTCGCAGCTATTGC	For cloning of pBK46: <i>anuD</i> 3'-region
prBK158	<u>GAAATCAACTTCTGTTCCATGTCGACGCCC</u> AGATTCTACTGCACCATGTG	
prBK178	<u>CACGCATCAGTGCCTCCTCTCAGACAGAATGATCCAGTTCCTCGACTTGG</u>	For cloning of pBK47: <i>anuI</i> 5'-region
prBK159	<u>GGATCCGTAATACGACTCACTATAGGGCCC</u> ACGACTTCGGGCACTAACTTG	
prBK179	<u>CATAT</u> TCGTCAGACACAGAATAACTCTCACTTGGCTGCCGCAGTGATAG	For cloning of pBK47: <i>anuI</i> 3'-region
prBK162	<u>GAAATCAACTTCTGTTCCATGTCGACGCCC</u> TGTGGAGTGCTTGGATTG	
prBK180	<u>ACGCATCAGTGCCTCCTCTCAGACAGAATGAGAACACGCTGGTCGAGTTC</u>	For cloning of pBK48: <i>anuJ</i> 5'-region
prBK163	<u>GGATCCGTAATACGACTCACTATAGGGCCC</u> CAGATGAGCAGTTTATGTTCGG	
prBK181	<u>CATAT</u> TCGTCAGACACAGAATAACTCTCAGGAGGAGAGTGCAACATGG	For cloning of pBK48: <i>anuJ</i> 3'-region
prBK166	<u>GAAATCAACTTCTGTTCCATGTCGACGCCC</u> GGATCGTACAACAGGACGCC	

prBK182	<u>CACGCATCAGTGCCTCCTCTCAGACAGAATGACGAGATCGAGGTGCTGTTG</u>	
prBK24	<u>CCGTAATACGACTCACTATAGGGCCCGTATTGAAGGGATGAAAGATG</u>	For cloning of pBK49: <i>anuH</i> 5'-region
prBK183	<u>CATATTCGTCAGACACAGAATAACTCTCGATTTCGATTCAAACAAATGCC</u>	
prBK27	<u>CAACTTCTGTTCCATGTCGACGCCCCACGCGCACAGTGCAAATTTGTC</u>	For cloning of pBK49: <i>anuH</i> 3'-region
prBK184	<u>GCATCAGTGCCTCCTCTCAGACAGAATGTAGGCAGAGCAGACGAAGAATC</u>	
prBK75	TAGAATGGGGTAGACAGG	Verification of BK17: 5'-region
prBK178	CACGCATCAGTGCCTCCTCTCAGACAGAATGATCCAGTTCCTCGACTTGG	
prBK144	TGCTCATAGACTACGTCTG	Verification of BK17: 3'-region
prBK185	GAGAGTTATTCTGTGTCTGAC	Verification of BK18: 3'-region, prBK185 used with prBK175 together Verification of BK19: <i>anuJ</i> , prBK185 used with prBK181 together
prBK186	CATTCTGTCTGAGAGGAGGC	Verification of BK17: <i>anuE</i> , used with prBK178 together For cloning of pBK45 – 49: <i>Afp<sub>yrG</sub></i> - marker, used with prBK185 together
prBK120	CTTCCGTTTGAGACATGAATG	Verification of BK18: 5'-region, used with prBK75 together Verification of BK18: <i>anuD</i> , used with prBK186 together
prBK34	CAAGTATGATCCTGAGGGCCG	Verification of BK19: 5'-region, used with prBK75 together Verification of BK21: 5'-region, used with prBK185 together
prBK38	GTGTCGACATGACTATCGCTCCGTCTTC	Verification of BK19: 3'-region, used with prBK75 together
prBK93	GAGCTACCGAGCTGTGTTTG	Verification of BK20: 5'-region, used with prBK75 together Verification of BK20: 3'-region, used with prBK186 together
JN105	TGTTGATATCGAAGCGC	Verification of BK20: <i>anuJ</i> , used with prBK185 together
prBK33	GAATCCCAGGCCCTGGTTTG	Verification of BK21: <i>anuH</i> , used with prBK34 together Verification of BK21: 3'-region, used with prBK186 together
pPX-PTN-F	<u>GGTGGACAGCAAATGGGTCGCGGATCCATGGTTGAAGTGACAAGACCAC</u>	For cloning of pPX52 (Amplification of <i>AnuH</i> without introns from cDNA)
pPX-PTN-R	<u>GGTGCTCGAGTGC GGCCGCAAGCTTTCAATGACTATCGCTCCGTCTTC</u>	
pPX28-1F	<u>CATCTTCCCATCCAAGAACCCTTTAATCATGGCTATCGAGCTGGGTC</u>	For cloning of pPX28
pPX28-1R	<u>TATTTCGTCAGACACAGAATAACTCTCTGAGCCGGGTACATTACTAGC</u>	
pPX28-test-1f	GGTCTTTGCTGGTGACCATCC	1026 bp partial fragment of <i>anuE</i>
pPX28-test-1r	CGAGACGGTTCGAAAGTCTCG	
pPX38-1F	<u>CGTAATACGACTCACTATAGGGCCCATATCGGAGAGTGAGAATGGGAC</u>	For cloning of pPX38: <i>anuF</i> 5'-region

pPX38-1R	<u>ATTTCGTCAGACACAGAATAACTCTCGTTTATTTCGCTGCGATCAAAC</u>	
pPX38-3F	<u>CATCAGTGCCTCCTCTCAGACAGAATAATGATCATGTATCTCTCTGAGCCG</u>	For cloning of pPX38: <i>anuF</i> 3'-region
pPX38-3R	<u>TCAACTTCTGTTCCATGTCGACGCCCCGACAGTTCACCCACCCTACATG</u>	
pPX38-2F	<u>CAAAGTTTGATCGCAGCGAAATAAACGAGAGTTATTCTGTGTCTGACG</u>	For cloning of pPX38: <i>Afp<sub>pyr</sub>G</i> -marker
pPX38-2R	<u>CGGCTCAGAGAGATACATGATCATTATTCTGTCTGAGAGGAGGCACTG</u>	
pPX38- <i>anuF</i> -tf	GTTTGCACTTGCAGCGTTGTTC	906 bp partial fragment of <i>anuF</i>
pPX38- <i>anuF</i> -tr	GCAGTGGTGAAGTGGTGCTG	
pPX38-test-1f	CATATCGGAGAGTGAGAATGGGAC	Verification of <i>anuF</i> : 5'-region
pPX3839-test-1r	GCTTCGGCAATCTCAAAAAGTC	Binding in <i>Afp<sub>pyr</sub>G</i> facing outwards as complementary primer for 5'- and 3'-region verification for PX38 and PX39
pPX3839-test-2f	CGGAGGATGAAGATTCGTGGTC	
pPX38-test-2r	GACAGTTCACCCACCCTACATGC	Verification of <i>anuF</i> : 3'-region
pPX39-1F	<u>CCGTAATACGACTCACTATAGGGCCCCAGAACCTTGATGTGTGCCTTG</u>	For cloning of pPX39: <i>anuG</i> 5'-region
pPX39-1R	<u>TTCGTCAGACACAGAATAACTCTCCCTGTTGAGTATACAGTGAGATGG</u>	
pPX39-3F	<u>CATCAGTGCCTCCTCTCAGACAGAATCGTCTGATAAACCAACTGTTCTGTG</u>	For cloning of pPX39: <i>anuG</i> 3'-region
pPX39-3R	<u>CAACTTCTGTTCCATGTCGACGCCCCGATATACGTGGAGAGTGACAGAAG</u>	
pPX39-2F	<u>CACCCATCTCACTGTATACTCAACAGGGAGAGTTATTCTGTGTCTGACG</u>	For cloning of pPX39: <i>Afp<sub>pyr</sub>G</i> -marker
pPX39-2R	<u>CCACGAACAGTTGGTTTATCAGACGATTCTGTCTGAGAGGAGGCAC</u>	
pPX39-test-1f	CAGAACCTTGATGTGTGCCTTG	Verification of <i>anuG</i> : 5'-region
pPX39-test-2r	CGATATACGTGGAGAGTGACAGAAG	Verification of <i>anuG</i> : 3'-region
pPX39- <i>anuG</i> -tf	GCTCGCAATCTGACGTTTC	1192 bp partial fragment of <i>anuG</i>
pPX39- <i>anuG</i> -tr	CTCGCATAGGATAGGCGGATG	
pPX45-1F	<u>CATCTTCCCATCCAAGAACCTTTAATCATGGTGCAAATATCGAATGTTTGG</u>	For cloning of pPX45
pPX45-1R	<u>ATTTCGTCAGACACAGAATAACTCTCCGATATACGTGGAGAGTGACAGAAG</u>	

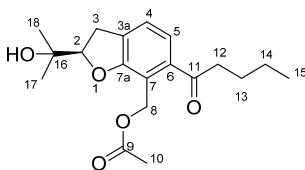
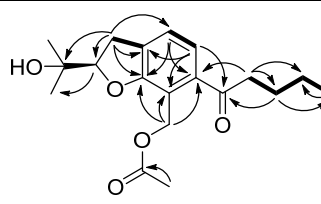
The underlined sequences in the primers are homologous regions with the vector or the other fragment for recombination.



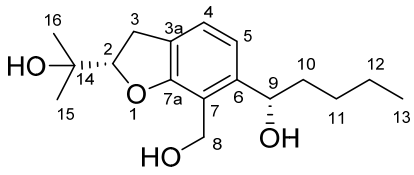
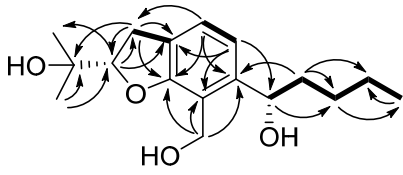
**Table S5.** NMR data of (2*S*, 9*S*)-annullatin D (**2**) in DMSO-*d*<sub>6</sub>

Position	$\delta_{\text{H}}$ , multi., $J$ in Hz	$\delta_{\text{C}}$	Key HMBC correlations	$\delta_{\text{H}}$ , multi., $J$ in Hz (CDCl <sub>3</sub> )
2	4.79, dd, 9.6, 8.2	91.5	C-15, C-16	4.85, dd, 9.5, 8.6
3	3.24, br dd, 16.0, 8.2 3.18, br dd, 16.0, 9.6	28.6	C-2, C-3a, C-7a, C-14	3.24, br dd, 15.8, 8.6 3.18, br dd, 15.8, 9.5
3a		129.3		
4	7.55, d, 7.5	130.7	C-3, C-6, C-7a	7.40, dt, 7.5, 1.0
5	6.99, dd, 7.5, 0.8	112.9	C-3a, C-6, C-7, C-7a, C-9	6.82, dd, 7.5, 0.8
6		150.0		
7		107.2		
7a		157.3		
8		167.4		
9	5.53, dd, 7.2, 3.9	80.6		5.40, dd, 7.9, 4.0
10	2.01, m 1.68, m	33.9	C-11, C-12	1.98, m 1.72, m
11	1.38, m	26.3	C-9, C-12, C-13	1.47, m
12	1.30, m	21.8	C-11, C-13	1.35, m
13	0.89, t, 7.1	13.7	C-11, C-12	0.90, t, 7.3
14		69.9		
15	1.22, s	26.0	C-2, C-14, C-16	1.42, s
16	1.18, s	25.1	C-2, C-14, C-15	1.24, s


**Table S6.** NMR data of (2*R*)-annullatin G (**3**) in DMSO-*d*<sub>6</sub>

Compound					
	Isolated from fungal culture		Annullatin F ( <b>1</b> ) acetate		
Position	$\delta_{\text{H}}$ , multi., $J$ in Hz	$\delta_{\text{C}}$	$\delta_{\text{H}}$ , multi., $J$ in Hz	$\delta_{\text{C}}$	Key HMBC correlations
2	4.61, t, 8.5	89.1	4.61, t, 8.5	89.1	C-17, C-18
3	3.21, dd, 8.5, 0.7	29.9	3.21, dd, 8.5, 0.7	29.9	C-2, C-3a, C-4, C-7a, C-16
3a		131.5		131.5	
4	7.26, d, 7.6	124.5	7.26, d, 7.6	124.5	C-6, C-7a
5	7.23, d, 7.6	120.5	7.23, d, 7.6	120.5	C-3a, C-6, C-7, C-11
6		138.7		138.7	
7		114.2		114.2	
7a		159.4		159.4	
8	5.16, d, 11.5 5.09, d, 11.5	57.6	5.16, d, 11.5 5.09, d, 11.5	57.6	C-6, C-7, C-7a, C-9
9		170.0		170.0	
10	1.94, s	20.4	1.94, s	20.4	C-9
11		203.8		203.8	
12	2.87, td, 7.2, 1.8	40.7	2.87, td, 7.2, 1.8	40.7	C-11, C-13, C-14
13	1.54, m	26.0	1.55, m	26.0	C-11, C-12, C-14, C-15
14	1.32, m	21.6	1.31, m	21.6	C-12, C-13, C-15
15	0.88, t, 7.4	13.7	0.88, t, 7.4	13.7	C-13, C-14
16		70.2		70.2	
17	1.12	25.8	1.13	25.8	C-2, C-16, C-18
18	1.10	24.4	1.10	24.4	C-2, C-16, C-17

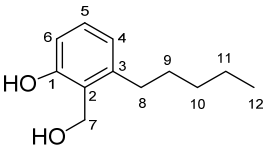
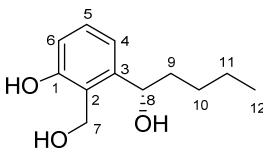
**Table S7.** NMR data of (2*S*, 9*S*)-annullatin H (**4**) in DMSO-*d*<sub>6</sub>

Compound						
						
Position	$\delta_{\text{H}}$ , multi., <i>J</i> in Hz	$\delta_{\text{C}}$	Key HMBC correlations	$\delta_{\text{H}}$ , multi., <i>J</i> in Hz (CDCl <sub>3</sub> )		
2	4.52, dd, 9.4, 8.0	88.3	C-3, C-3a, C-15, C-16	4.58, dd, 9.4, 8.6		
3	3.11, m	30.0	C-2, C-3a, C-7a, C-14	3.20, dd, 15.7, 8.6		
				3.09, dd, 15.7, 9.4		
3a		124.8				
4	7.05, d, 7.7	123.2	C-3, C-5, C-6, C-7a	7.05, d, 7.7		
5	6.89, d, 7.7	117.6	C-3a, C-7, C-9, C-7a	6.89, d, 7.7		
6		145.1				
7		119.3				
7a		158.0				
8	4.54, d, 11.5	54.0	C-6, C-7, C-7a	4.77, d, 12.0		
	4.49, d, 11.5			4.66, d, 12.0		
9	4.84, dd, 7.9, 4.7	68.5	C-5, C-6, C-7, C-10, C-11	4.83, dd, 7.8, 6.0		
10	1.60, m	38.5	C-6, C-9, C-11, C-12	1.86, m		
				1.76, m		
11	1.39, m	28.0	C-12, C-13	1.42, m		
	1.29, m			1.26, m		
12	1.29, m	22.1	C-10, C-11, C-13	1.33, m		
13	0.87, t, 7.1	14.0	C-10, C-11, C-12	0.89, t, 7.2		
14		70.2				
15	1.15, s	25.8	C-2, C-14, C-16	1.36, s		
16	1.13, s	24.6	C-2, C-14, C-15	1.15, s		

**Table S8.** NMR data of (14*S*)-annullatin I (**5**) in CD<sub>3</sub>OD


<div>Compound</div> <div></div>			
Position	$\delta_{\text{H}}$ , multi., $J$ in Hz	$\delta_{\text{C}}$	Key HMBC correlations
1		155.9	
2		125.7	
3		142.6	
4	6.57, d, 8.3	113.7	C-1, C-2, C-6
5	7.0, d, 8.3	132.3	C-1, C-3, C-13
6		130.2	
7	4.71, d, 11.5 4.68, d, 11.5	57.5	C-1, C-2, C-3
8	2.76, m 2.64, m	29.9	C-2, C-3, C-9
9	1.45, m	32.5	C-3, C-10, C-11
10	1.39, m	33.6	C-8, C-11, C-12
11	1.39, m	23.6	C-10, C-12
12	0.90, t, 7.6	14.5	C-10, C-11
13	2.93, dd, 14.2, 1.6 2.38, dd, 14.2, 10.5	35.2	C-5, C-6, C-14
14	3.40, dd, 10.5, 1.6	80.7	C-6, C-15, C-17
15		73.9	
16	1.22, s	26.1	C-14, C-15, C-17
17	1.20, s	24.7	C-14, C-15, C-16

**Table S9.** <sup>1</sup>H NMR data of 2-hydroxymethyl-3-pentylphenol (**6**) and (8*S*)-annullatin E (**9**) in CD<sub>3</sub>OD


Compounds			
		2-Hydroxymethyl-3-pentylphenol ( <b>6</b> , CD <sub>3</sub> OD)	(8 <i>S</i> )-Annullatin E ( <b>9</b> , CD <sub>3</sub> OD)
Position	$\delta_{\text{H}}$ , multi., $J$ in Hz	$\delta_{\text{H}}$ , multi., $J$ in Hz	
4	6.62, d, 8.0	6.92, dd, 7.9, 0.8	
5	6.97, t, 8.0	7.08, t, 7.9	
6	6.60, d, 8.0	6.68, dd, 7.9, 1.0	
7	4.69, s	4.77, d, 11.7	
		4.73, d, 11.7	
8	2.62, t, 8.0	4.92, dd, 8.1, 6.3	
9	1.53, m	1.70, m	
10	1.33, m	1.44, m	
		1.27, m	
11	1.33, m	1.37, m	
12	0.88, t, 7.0	0.88, t, 7.1	

The NMR data of the isolated compounds correspond very well to those reported in the literature.<sup>14,15</sup>


**Table S10.** NMR data of (2*S*)-annullatin B (**7**) in CD<sub>3</sub>OD

<div>Compound</div> <div></div>			
Position	$\delta_H$ , multi., $J$ in Hz	$\delta_C$	Key HMBC correlations
2	4.57, t, 8.5	90.4	C-3, C-16
3	3.13, dd, 15.7, 8.5 3.08, dd, 15.7, 8.5	31.5	C-2, C-3a, C-7a, C-14
3a		125.8	
4	6.96, d, 7.7	125.1	C-3, C-6, C-7a
5	6.61, d, 7.7	122.4	C-3a, C-6, C-7, C-9
6		142.8	
7		120.9	
7a		160.4	
8	4.62, d, 11.4 4.59, d, 11.4	56.4	C-6, C-7, C-7a
9	2.62, m	33.3	C-5, C-6, C-7, C-11
10	1.54, m	33.0	C-11, C-12
11	1.32, m	33.0	C-9, C-12, C-13
12	1.32, m	23.6	C-10, C-11, C-13
13	0.88, t 7.2	14.4	C-11, C-12
14		72.7	
15	1.27, s	25.8	C-2, C-14, C-16
16	1.16, s	24.6	C-2, C-14, C-15

**Table S11.** NMR data of (2*S*)-annullatin A (**8**) in CD<sub>3</sub>OD

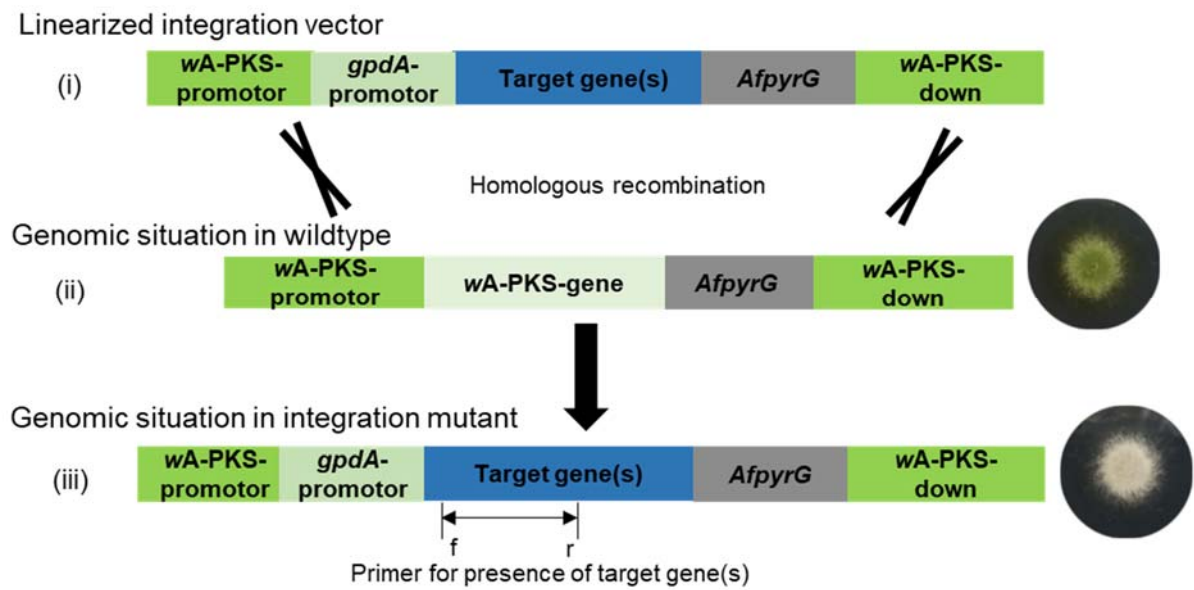
<div>Compound</div> <div></div>			
Position	$\delta_{\text{H}}$ , multi., $J$ in Hz	$\delta_{\text{C}}$	Key HMBC correlations
2	4.71, t, 8.9	92.3	C-3, C-15, C-16
3	3.14, d, 8.9	30.2	C-2, C-3a, C-4, C-7a, C-14
3a		128.5	
4	7.26, d, 7.5	131.6	C-3, C-6, C-7a
5	6.65, d, 7.5	123.8	C-3a, C-4, C-6, C-7, C-9
6		145.4	
7		118.3	
7a		166.0	
8	10.36, s	191.6	C-6, C-7, C-7a
9	2.88, m	34.5	C-5, C-6, C-7, C-10
10	1.47, m	32.6	C-6, C-9, C-12
11	1.31, m	33.0	C-12, C-13
12	1.31, m	23.6	C-10, C-11, C-13
13	0.88, t, 7.0	14.4	C-11, C-12
14		72.4	
15	1.27, s	25.5	C-2, C-14, C-16
16	1.20, s	25.1	C-2, C-14, C-15

**Table S12.** NMR data of (8*S*)-annullatin J (**10**) in CDCl<sub>3</sub>

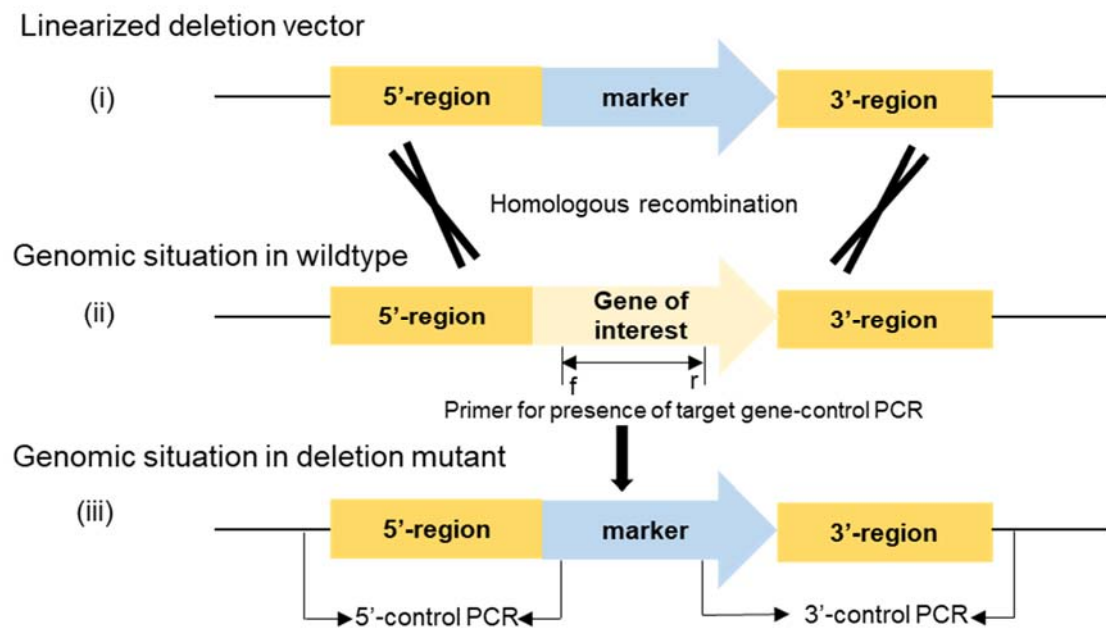
<div>Compound</div> <div></div>			
Position	$\delta_H$ , multi., $J$ in Hz	$\delta_C$	Key HMBC correlations
1		154.7	
2		123.3	
3		140.8	
4	6.86, d, 7.8	117.9	C-2, C-6, C-8
5	7.05, d, 7.8	129.3	C-1, C-3, C-4, C-13
6		127.7	
7	4.91, m 4.84, m	58.6	C-1, C-2, C-3
8	4.74, m	71.9	C-2, C-3, C-4, C-9, C-10,
9	1.73, m 1.66, m	37.9	C-3, C-10, C-11
10	1.40, m 1.24, m	28.5	C-8, C-9, C-11, C-12
11	1.32, m	22.8	C-9, C-10, C-12
12	0.89, t, 7.2	14.2	C-10, C-11
13	3.34, d, 7.4	29.2	C-1, C-5, C-6, C-14, C-15
14	5.31, m	122.1	C-13, C-16, C-17
15		134.2	
16	1.76, s	26.0	C-14, C-15, C-17
17	1.75, s	18.0	C-14, C-15, C-16



## Supplementary Figures

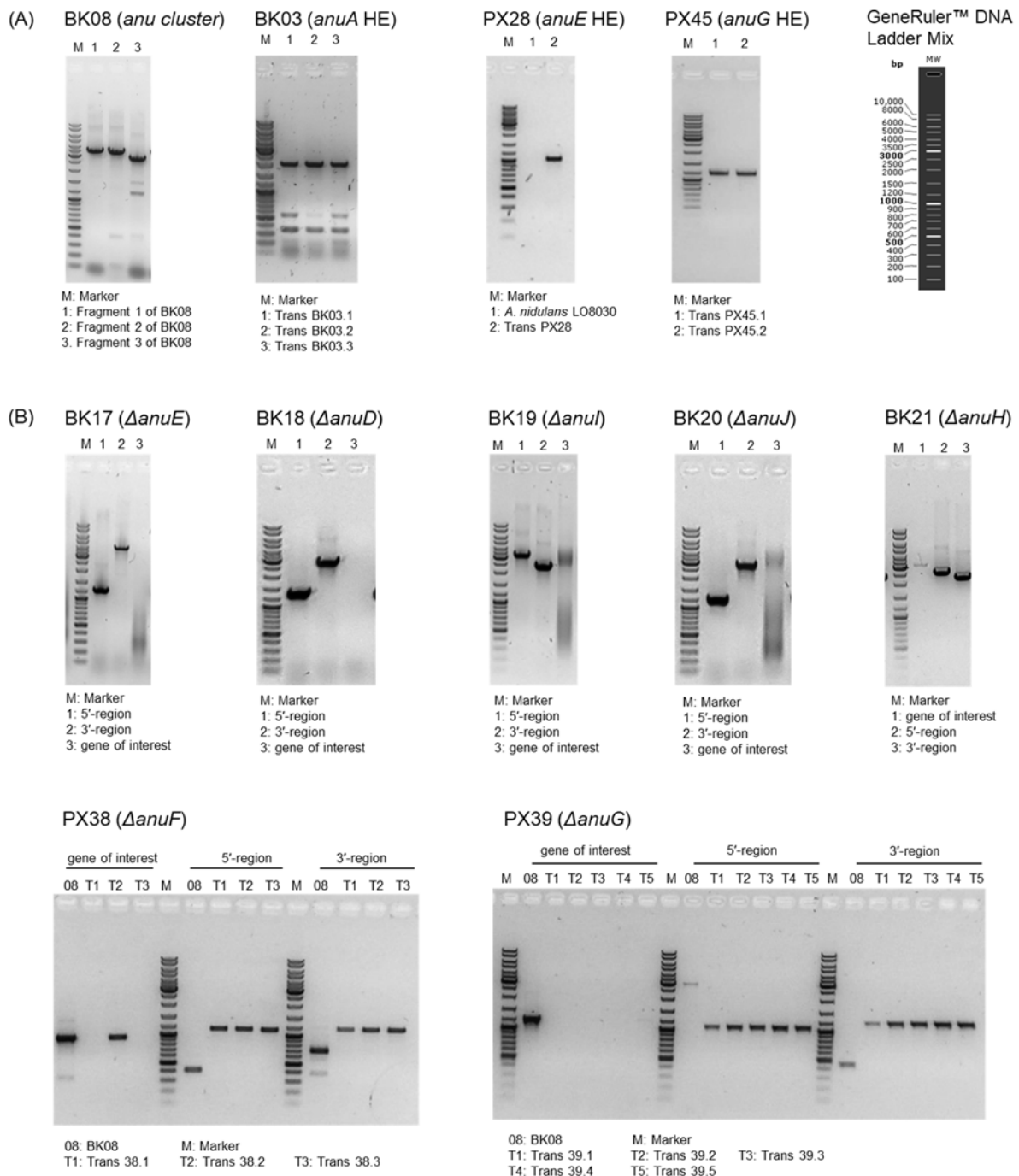


**Figure S1.** Schematic representation of gene integration into the *wA*-PKS locus of *A. nidulans* LO8030. Verification of the integration mutants was performed via detection of the white phenotype indicating the integration into the *wA*-PKS-locus and a PCR with primers binding in the integrated gene(s) proving their presence.

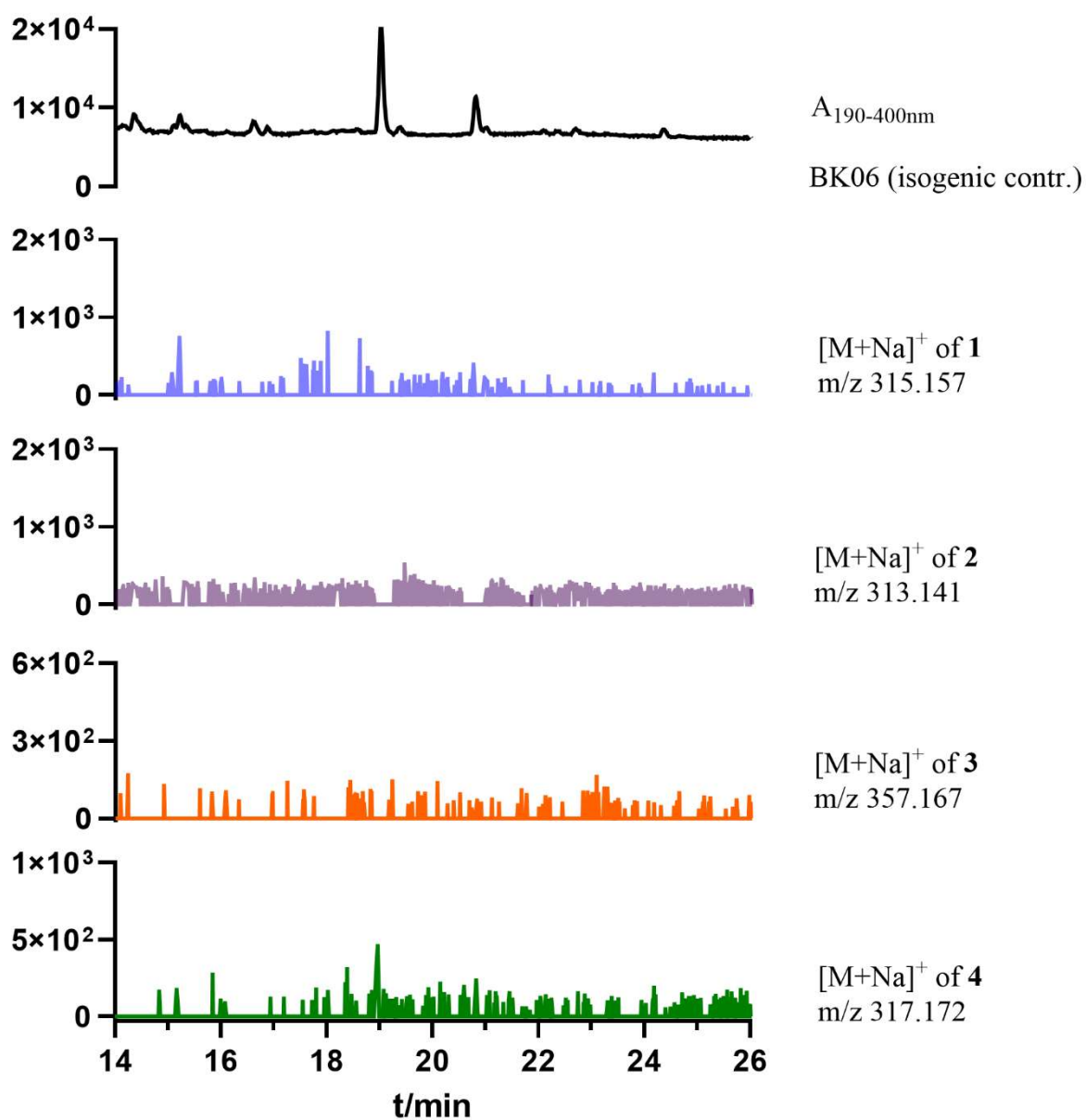


**Figure S2.** Schematic representation of gene deletion from *anu* cluster in *A. nidulans* strains

Verification of deletion mutants was carried out by proving the absence of the gene(s) of interest with primers binding in the region which should be deleted. Additionally, the correct integration of the 5'- and 3'-regions were checked by PCR with primers binding in the marker and the unmodified DNA 5'- or 3'- of the up- or downstream region. Control PCRs were performed with genomic DNA of *A. nidulans* LO8030 and that of the deletion mutant.

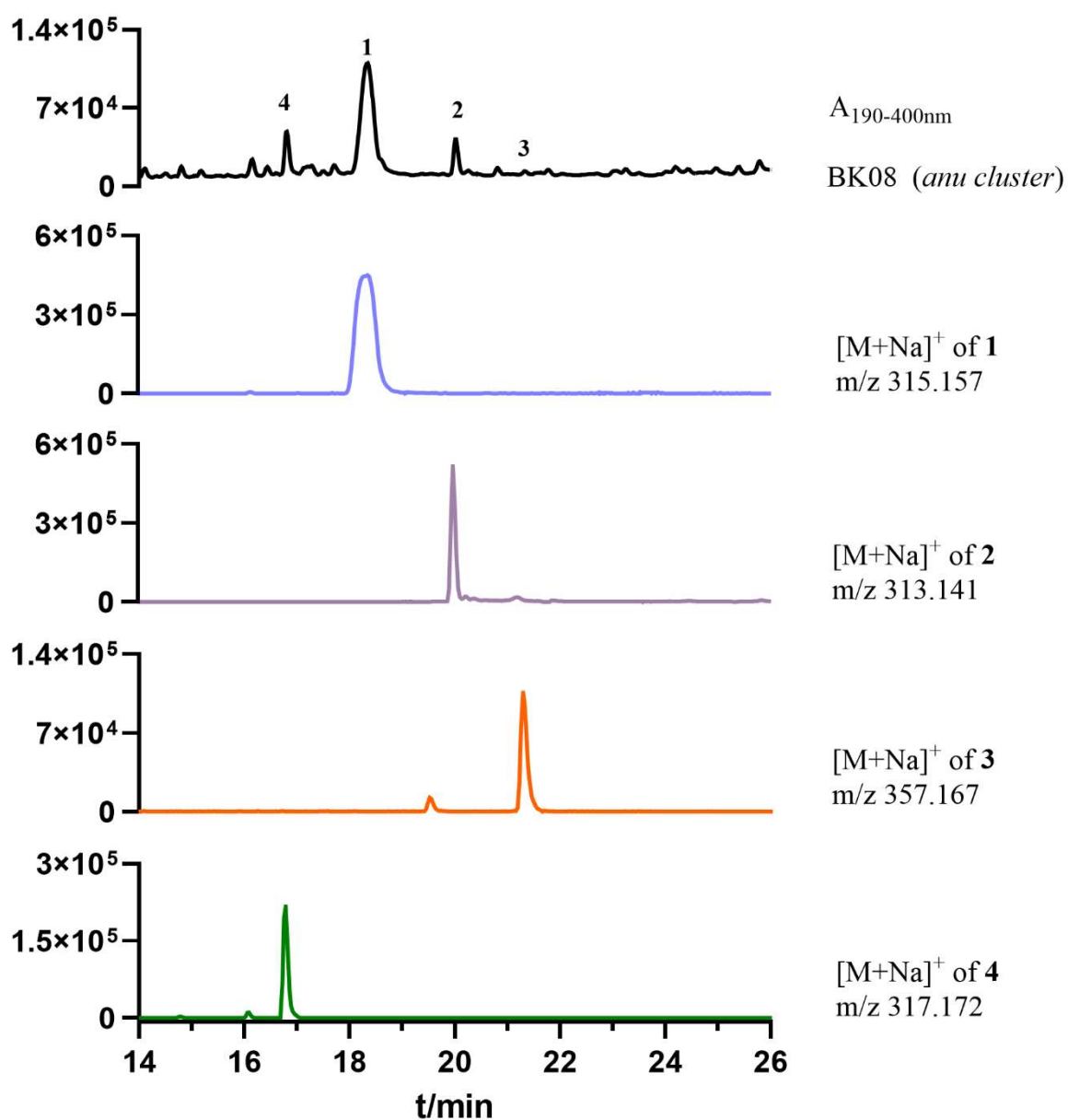


**Figure S3.** PCR verification of the heterologous expression transformants and the deletion mutants (A) PCR verifications were performed with genomic DNA of the heterologous expression (HE) *A. nidulans* transformants, which was used to prove the presence of the target gene/cluster. (B) PCR amplification of single gene deletions from the *anu* cluster in *A. nidulans* BK08. Three different fragments amplified from genomic DNA of deletion mutants were used to prove the presence/absence of the gene of interest and the correct site-specific integration of the corresponding 5'- and 3'-regions. The primers are given in Table S3.



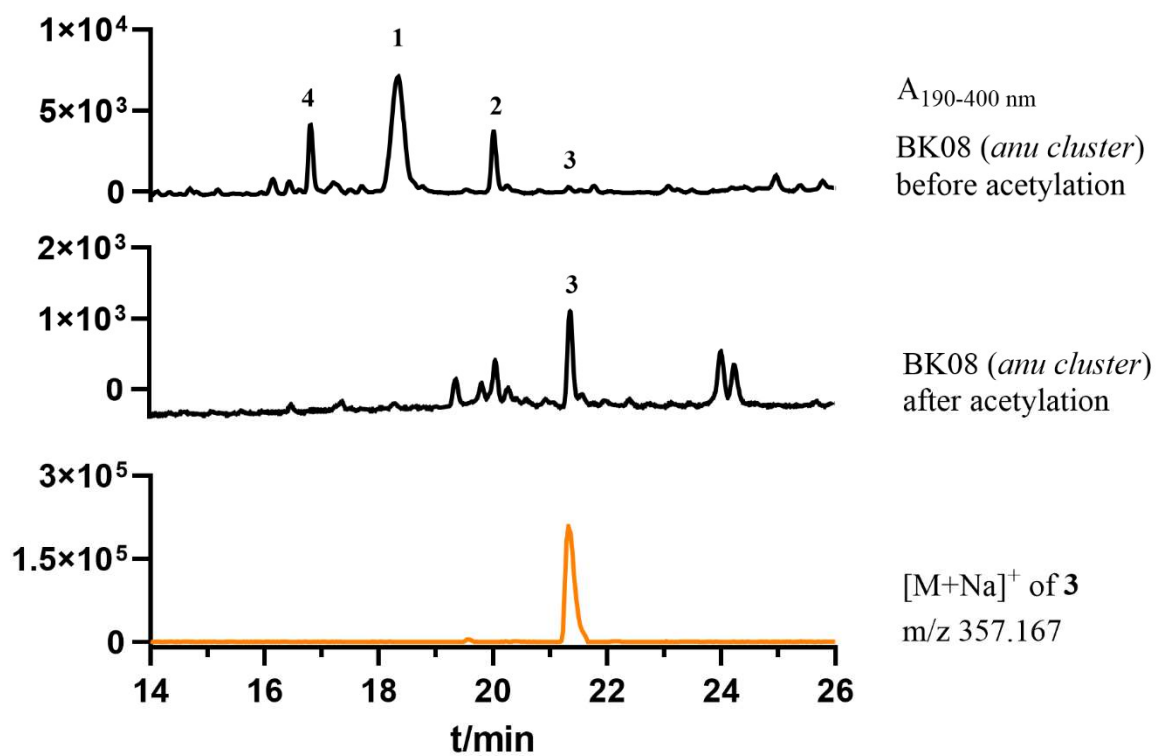
**Figure S4.** LC-MS analysis of the negative control strain *A. nidulans* BK06

The chromatograms depicted in color are EICs for the accumulated products **1** – **4**. A tolerance range of  $\pm 0.005$  was used for ion detection.

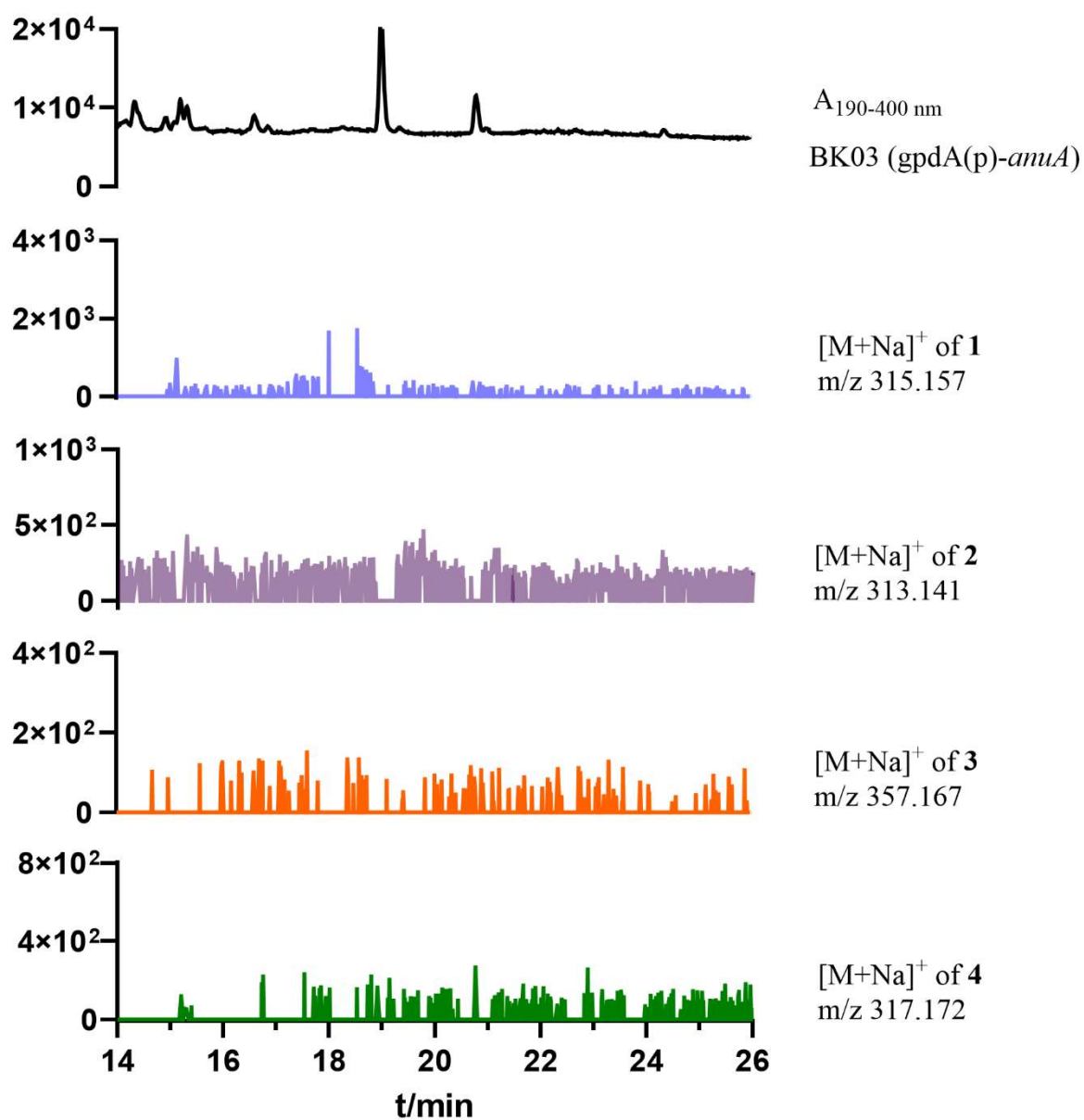


**Figure S5.** LC–MS analysis of the *anu* cluster expression strain *A. nidulans* BK08

The chromatograms depicted in color are EICs for the accumulated products **1** – **4**. A tolerance range of  $\pm 0.005$  was used for ion detection.

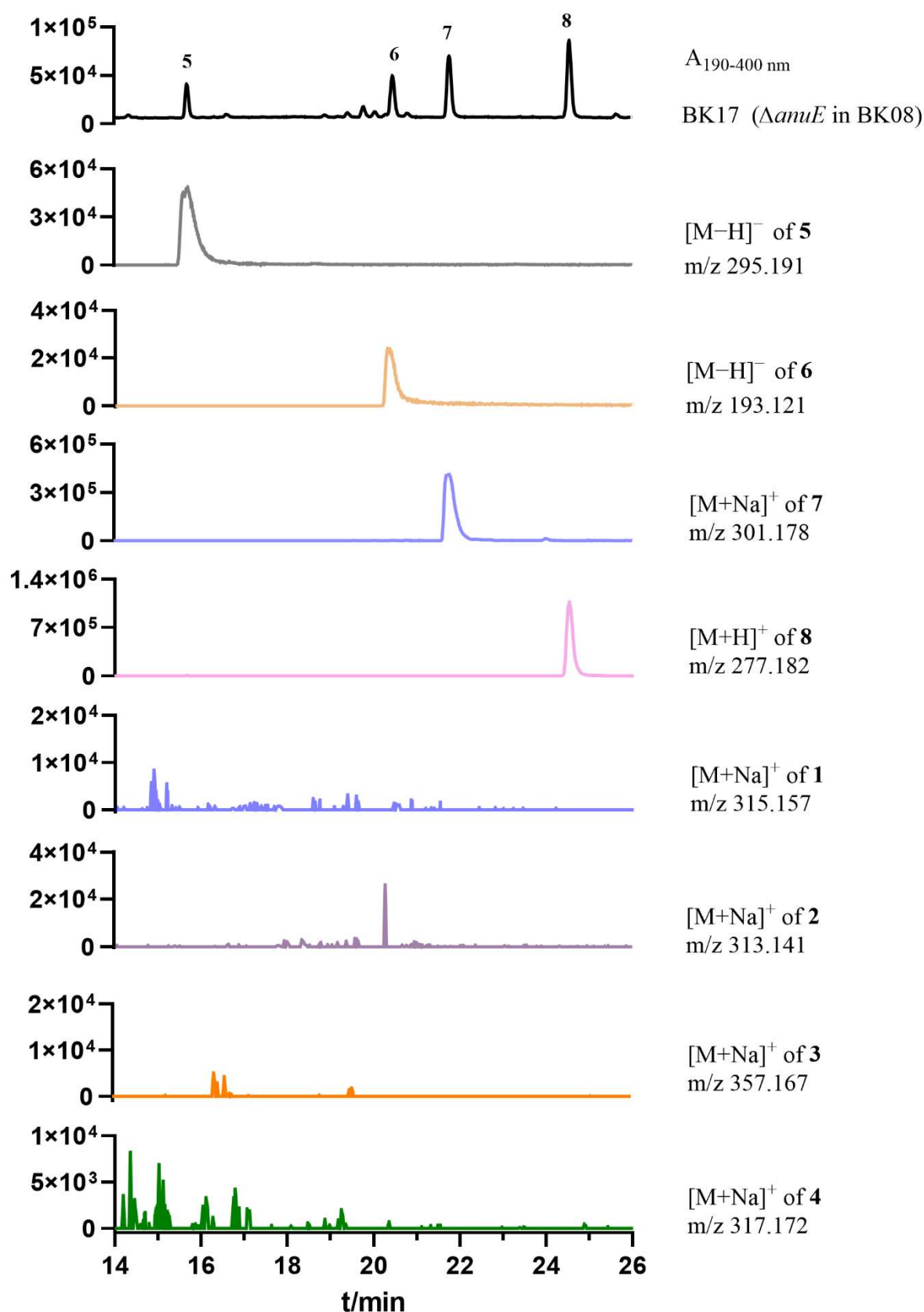


**Figure S6.** LC–MS analysis of the acetylated EtOAc extract from *A. nidulans* BK08  
EIC of **3** was selected with a tolerance range of  $\pm 0.005$ .



**Figure S7.** LC–MS analysis of *anuA* heterologous expression in *A. nidulans* LO8030

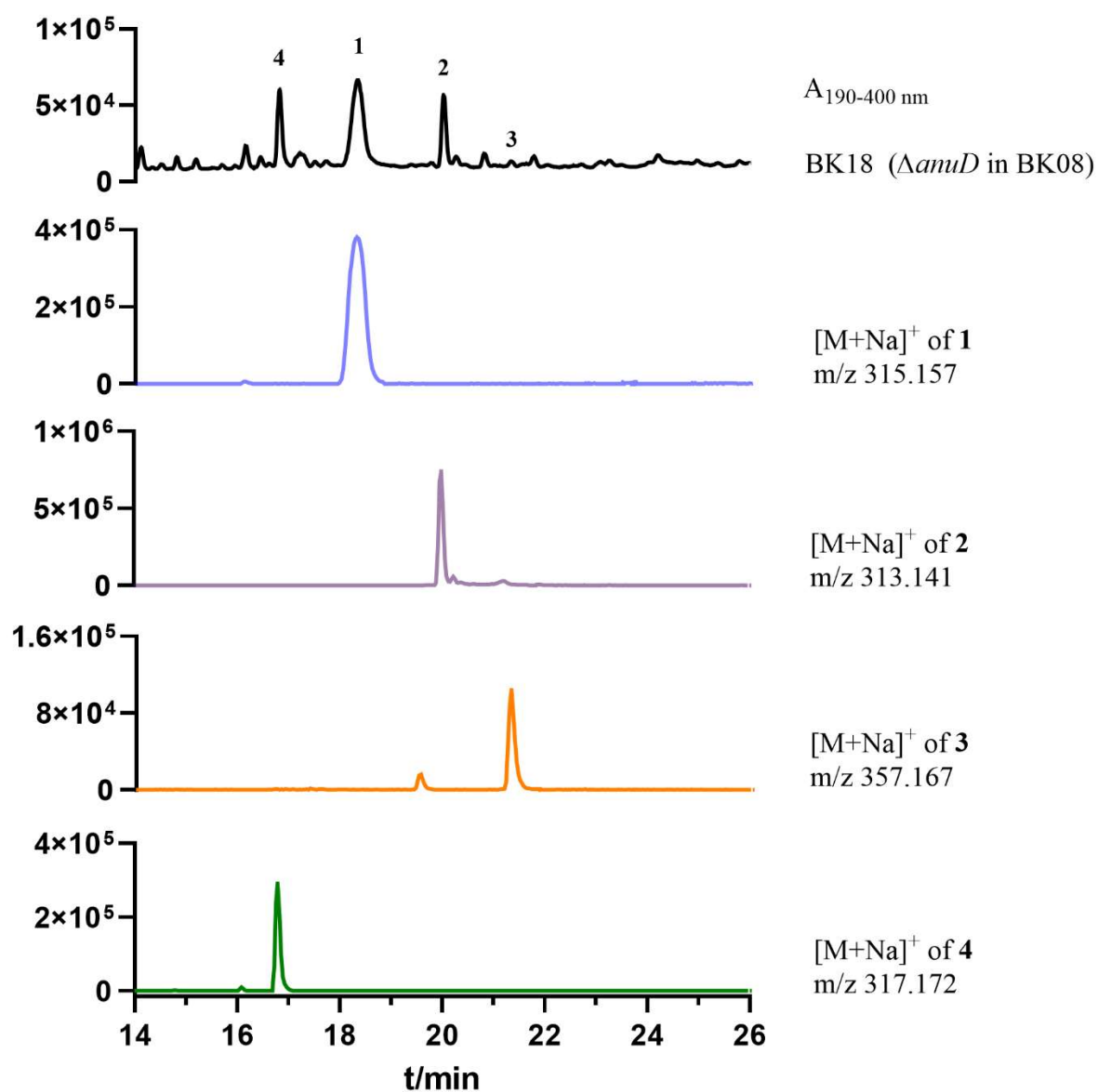
The chromatograms depicted in color are EICs for the accumulated end products **1** – **4**. A tolerance range of  $\pm 0.005$  was used for ion detection.



**Figure S8.** LC–MS analysis of the *anuE* deletion strain *A. nidulans* BK17

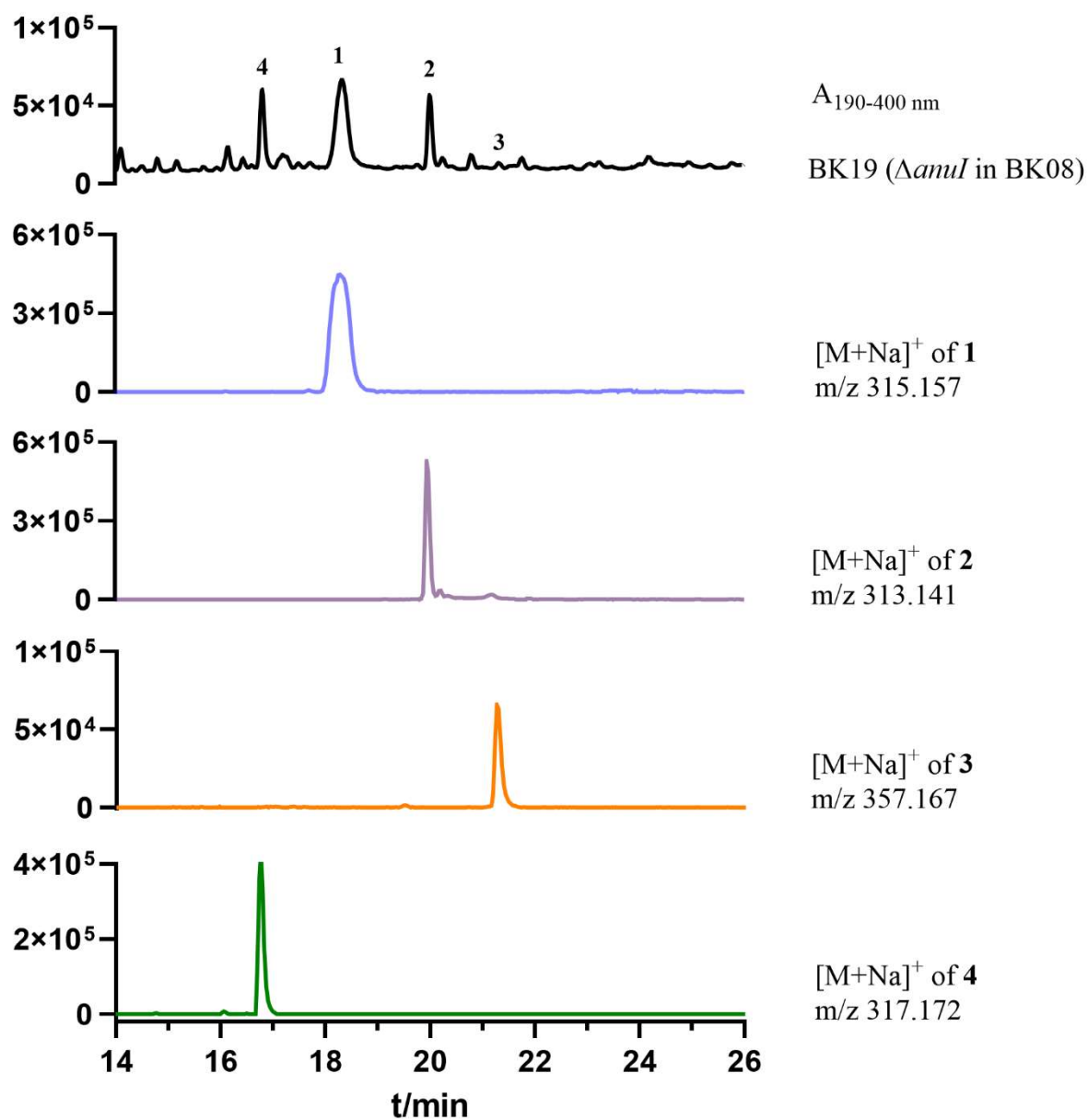
The chromatograms depicted in color are EICs for the accumulated products **1** – **8**. A tolerance range of  $\pm 0.005$  was used for ion detection.





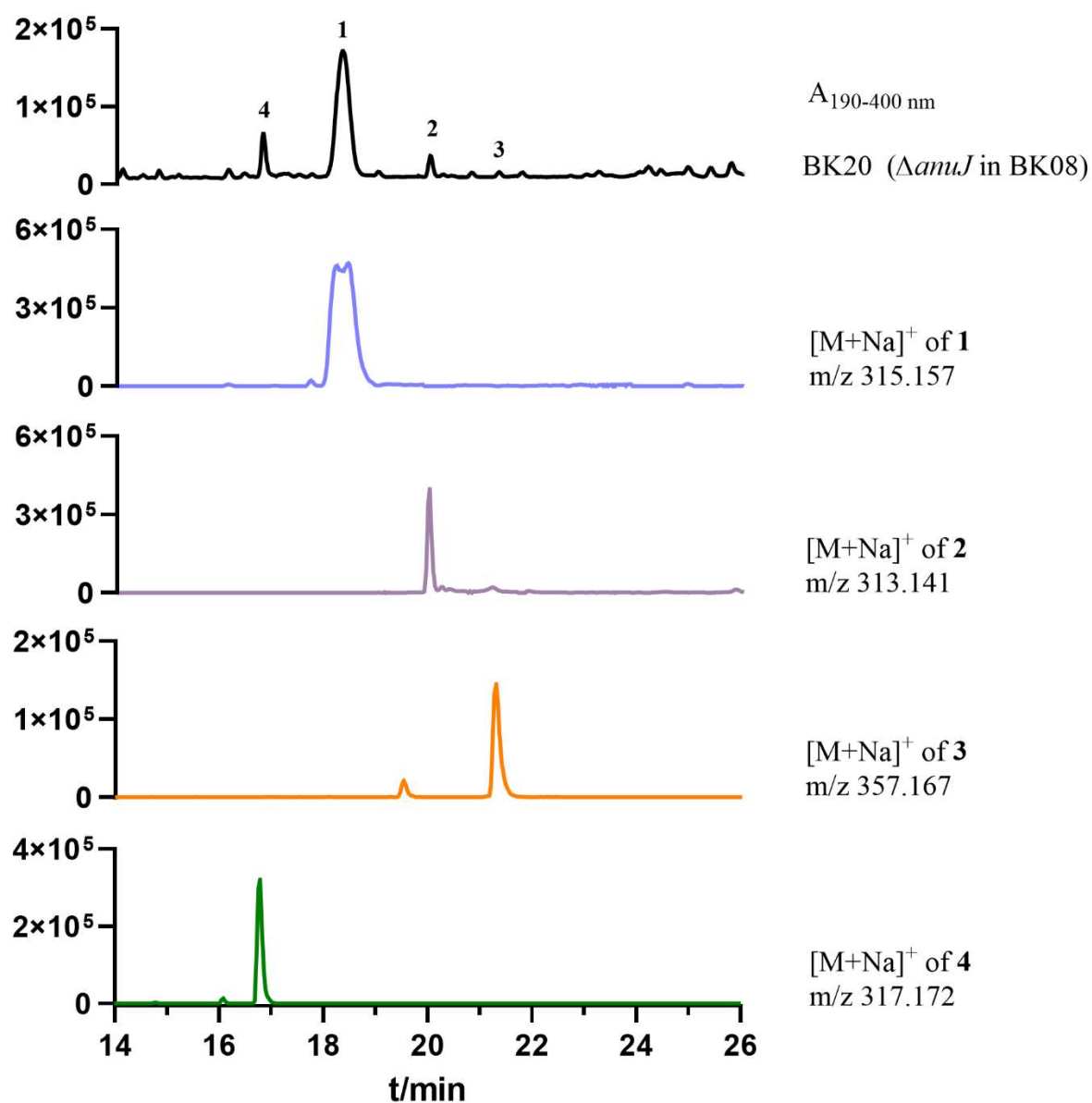
**Figure S9.** LC–MS analysis of the *anuD* deletion strain *A. nidulans* BK18

The chromatograms depicted in color are EICs for the accumulated products **1** – **4**. A tolerance range of  $\pm 0.005$  was used for ion detection.



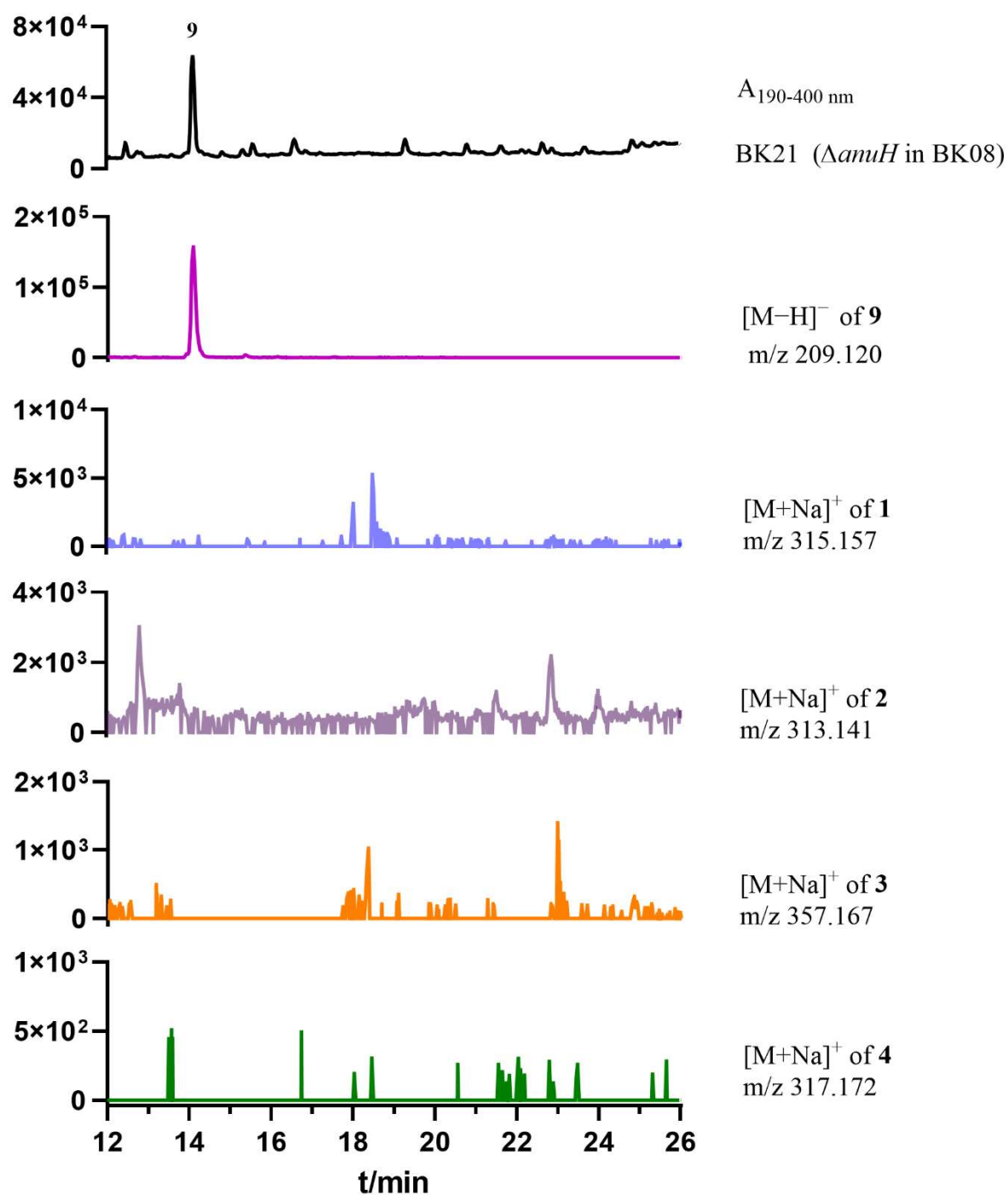
**Figure S10.** LC-MS analysis of the *anuI* deletion strain *A. nidulans* BK19

The chromatograms depicted in color are EICs for the accumulated products **1** – **4**. A tolerance range of  $\pm 0.005$  was used for ion detection.



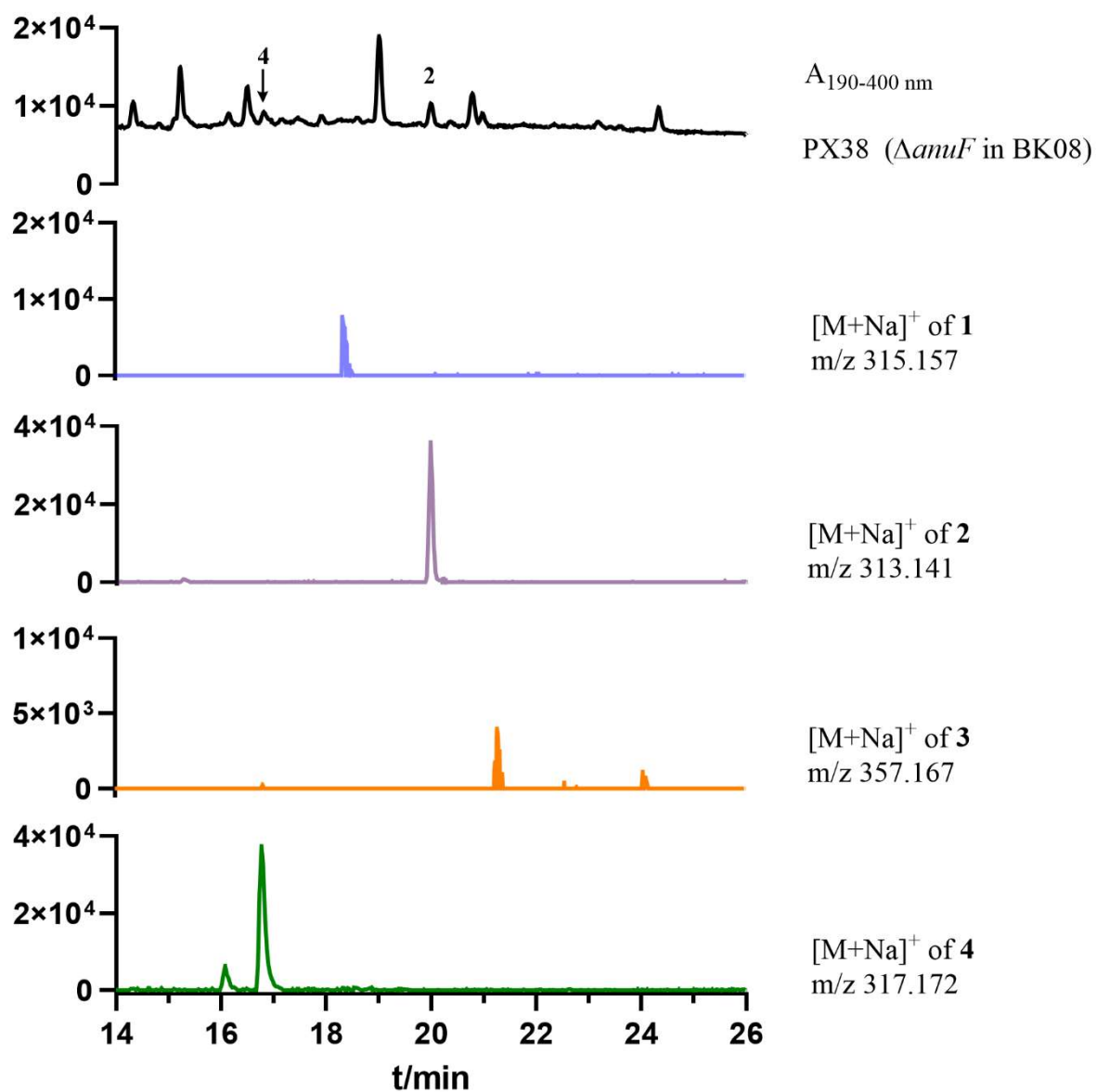
**Figure S11.** LC–MS analysis of the *anuJ* deletion strain *A. nidulans* BK20

The chromatograms depicted in color are EICs for the accumulated products **1** – **4**. A tolerance range of  $\pm 0.005$  was used for ion detection.



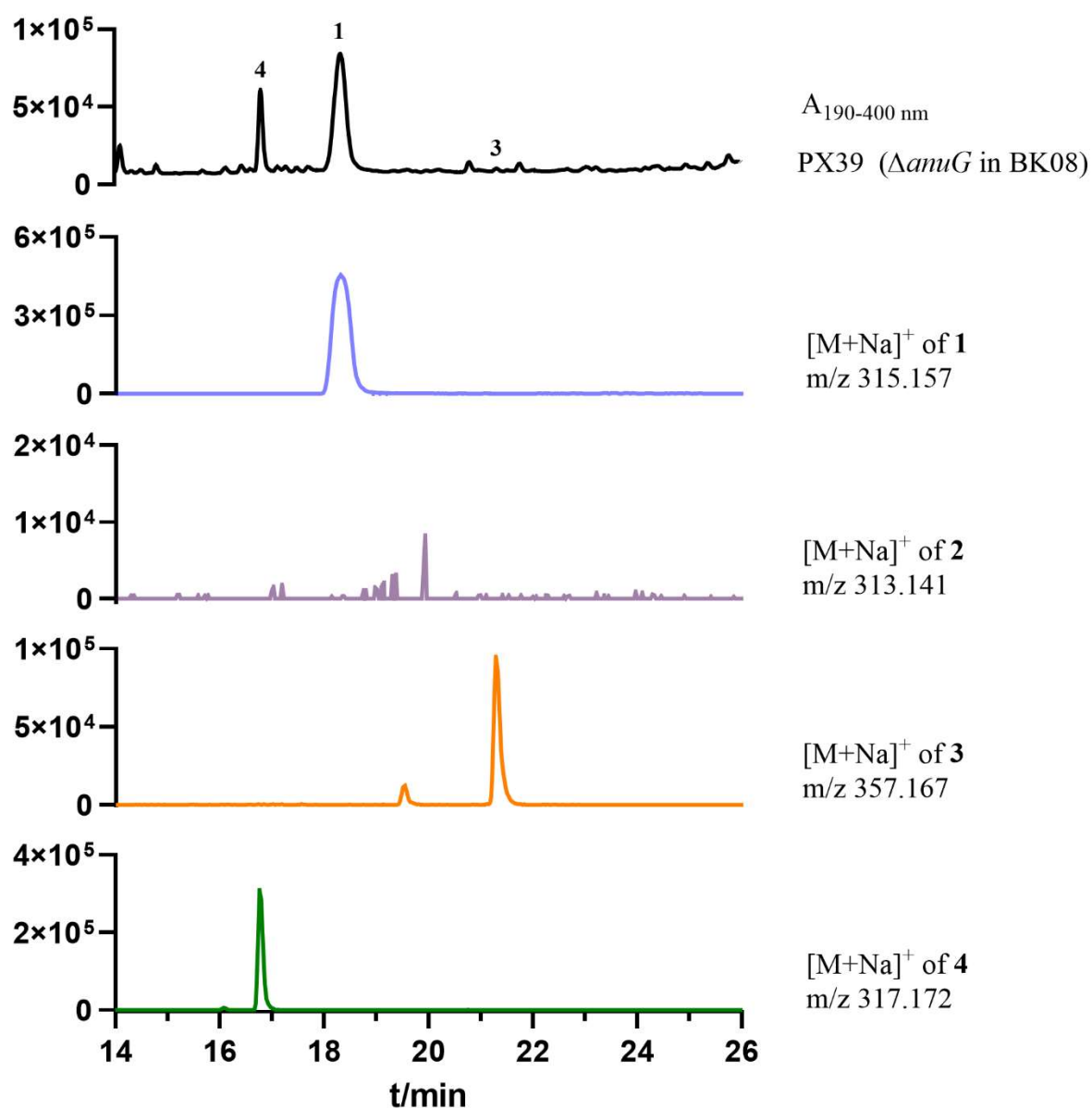
**Figure S12.** LC-MS analysis of the *anuH* deletion strain *A. nidulans* BK21

The chromatograms depicted in color are EICs for the accumulated products **1** – **4** and **9**. A tolerance range of  $\pm 0.005$  was used for ion detection.



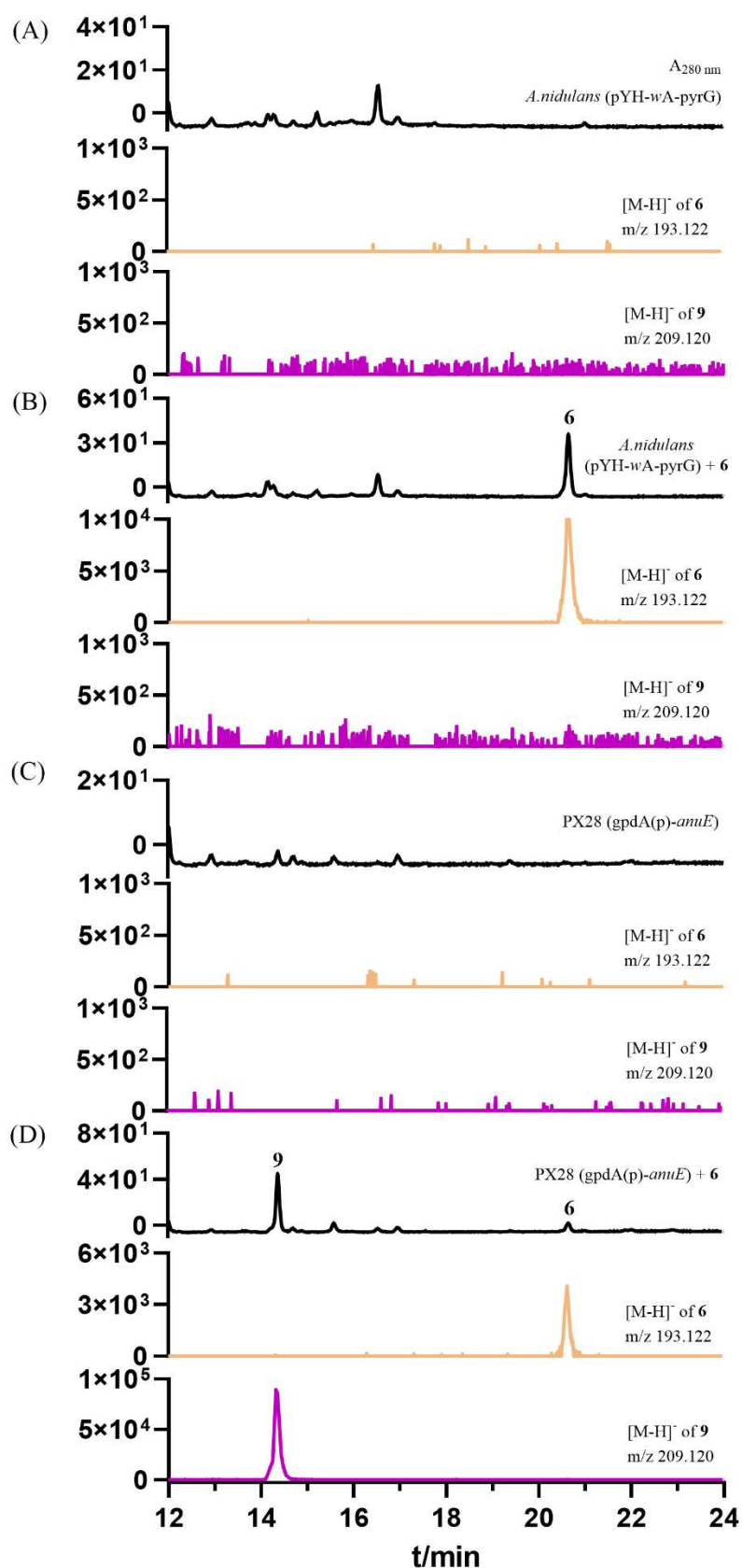
**Figure S13.** LC-MS analysis of the *anuF* deletion strain *A. nidulans* PX38

The chromatograms depicted in color are EICs for the accumulated products **1** – **4**. A tolerance range of  $\pm 0.005$  was used for ion detection.



**Figure S14.** LC–MS analysis of the *anuG* deletion strain *A. nidulans* PX39

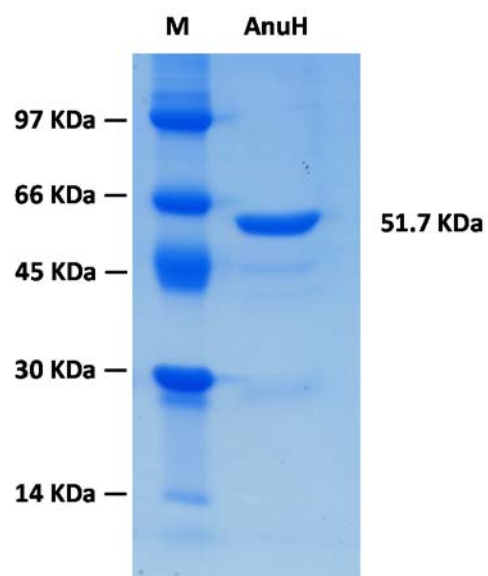
The chromatograms depicted in color are EICs for the accumulated products **1** – **4**. A tolerance range of  $\pm 0.005$  was used for ion detection.



**Figure S15.** LC–MS analysis of *anuE* expression strain *A. nidulans* PX28 after feeding with 6  
The chromatograms depicted in color are EICs for 6 and 9. A tolerance range of  $\pm 0.005$  was used for ion detection.

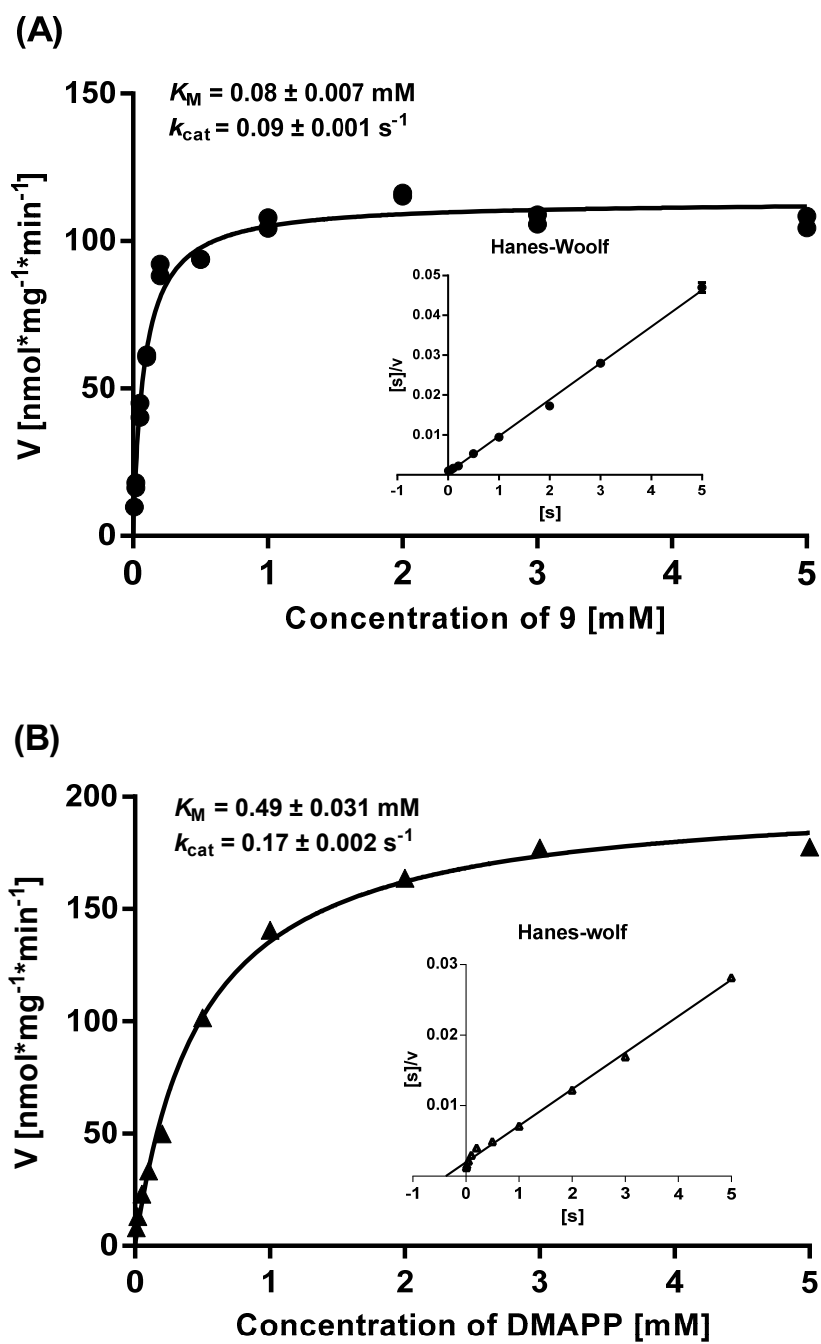




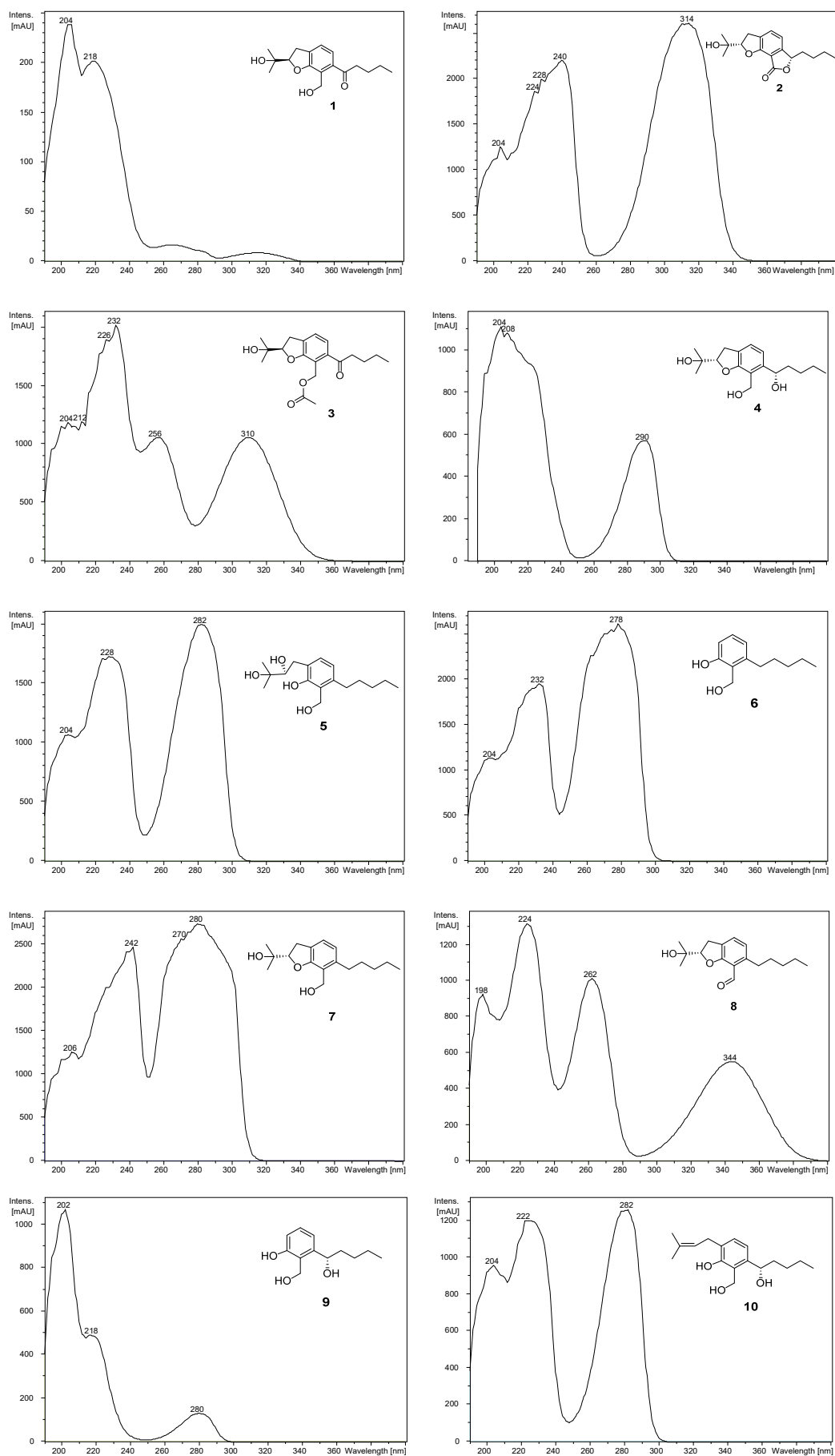


**Figure S17.** Analysis of the purified AnuH on SDS-PAGE (12%)

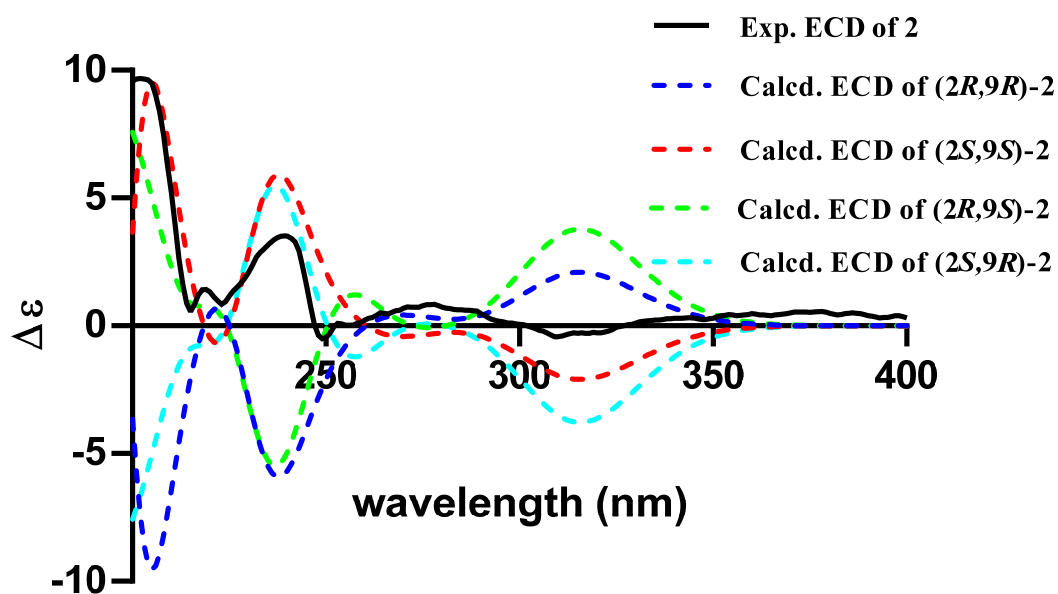
AnuH with a C-terminal 6xHis-tag (~51.7 kDa) was purified from *E. coli* BL21(DE3) cultures via Ni-NTAagarose with subsequent preparative gel filtration.



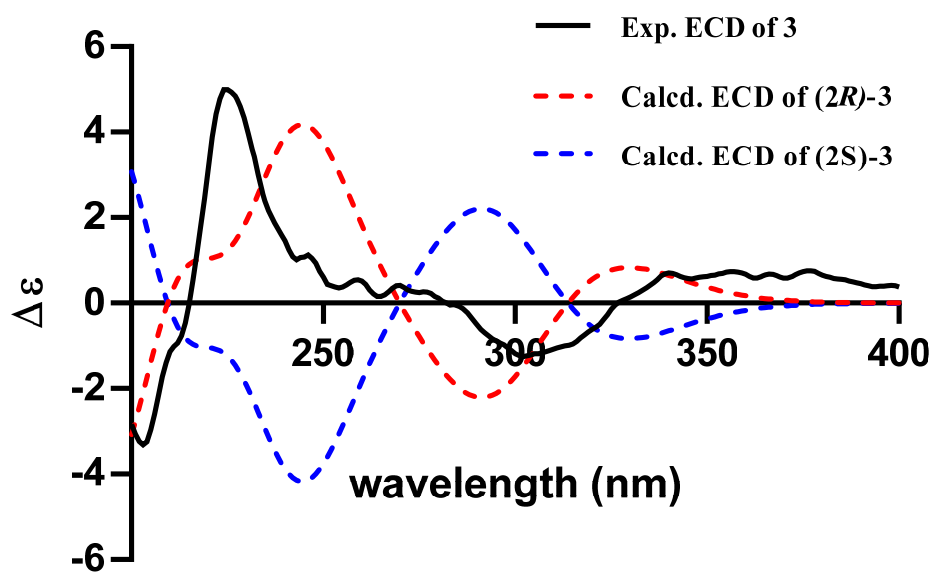
**Figure S18.** Determination of the kinetic parameters of AnuH with the substrates **9** (A) and DMAPP (B)



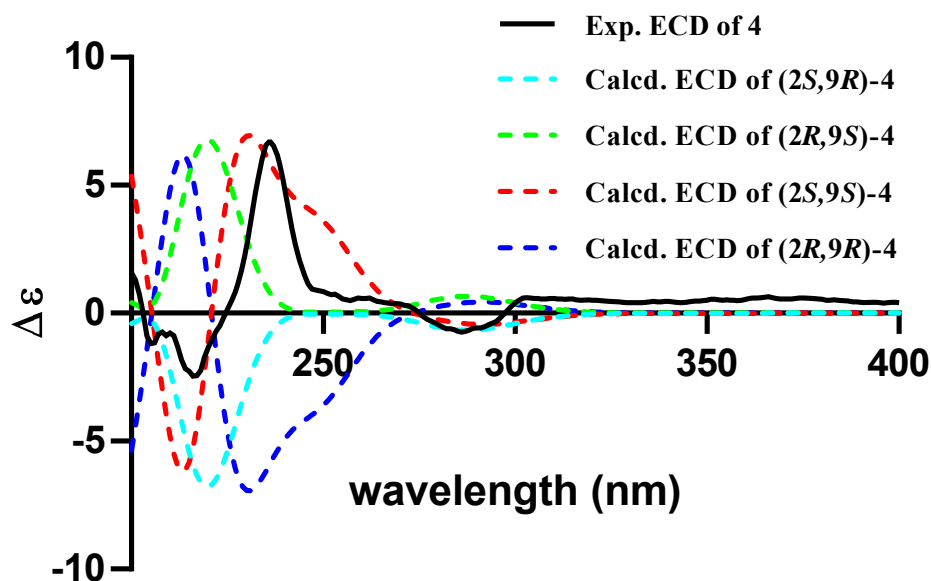
**Figure S19.** UV spectra of compounds 1 – 10



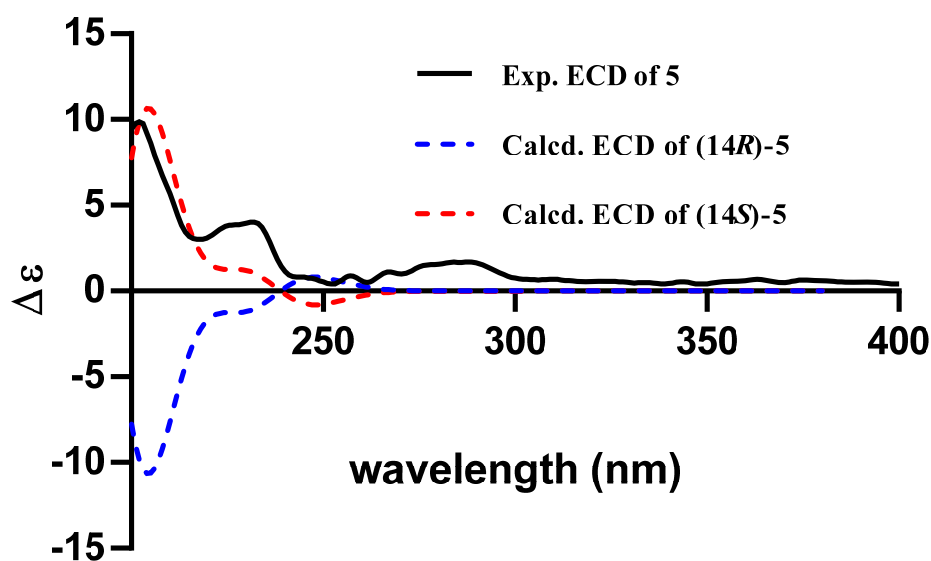
**Figure S20.** The experimental and calculated ECD spectra of compound **2** and its isomers ( $\sigma = 0.30$  eV, UV shift = +15.0 nm)



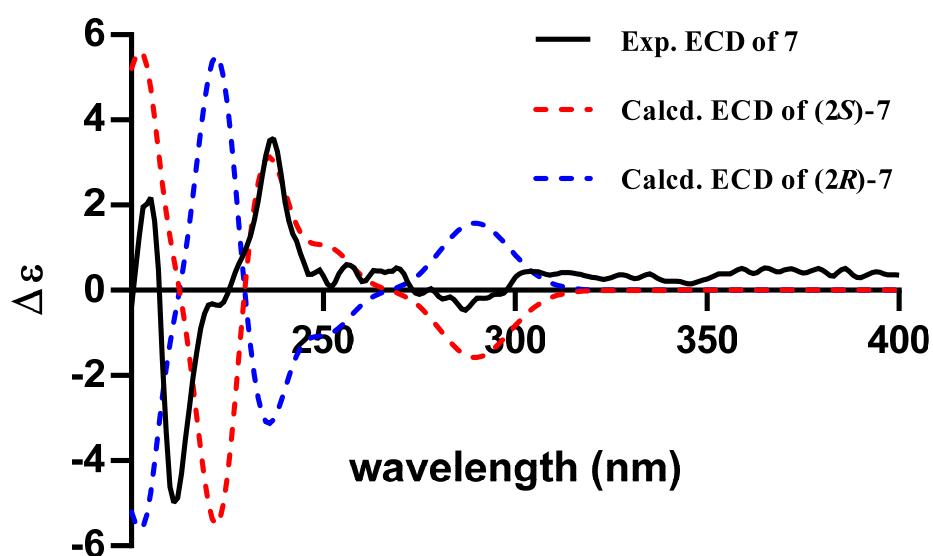
**Figure S21.** The experimental and calculated ECD spectra of compound **3** and its isomer ( $\sigma = 0.30$  eV, UV shift = 0 nm)



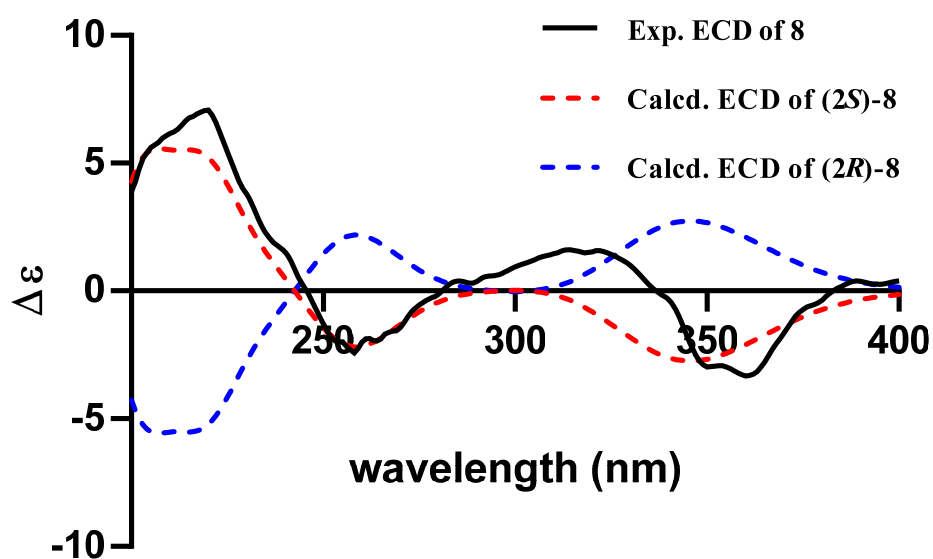
**Figure S22.** The experimental and calculated ECD spectra of compound **4** and its isomers ( $\sigma = 0.30$  eV, UV shift = +20 nm)



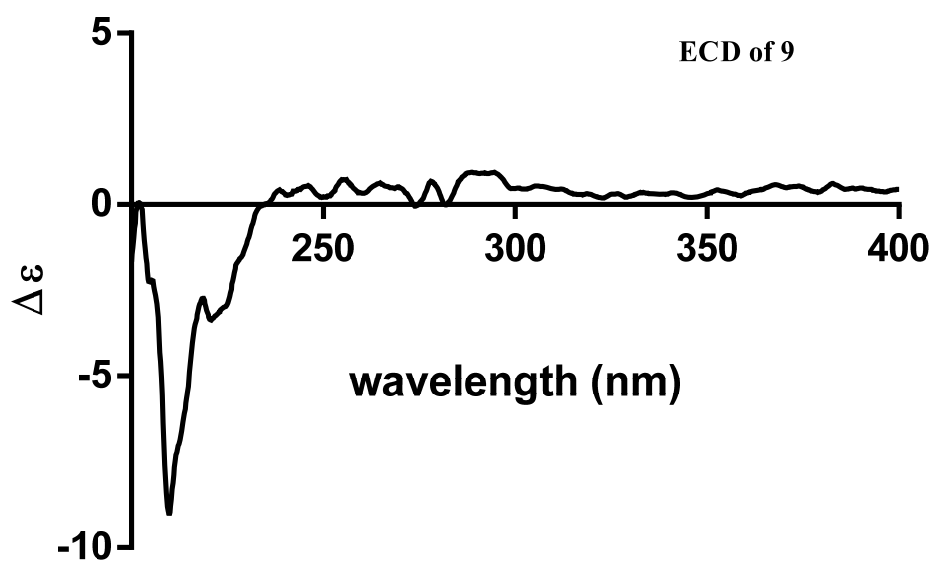
**Figure S23.** The experimental and calculated ECD spectra of compound **5** and its isomer ( $\sigma = 0.30$  eV, UV shift = +20 nm)



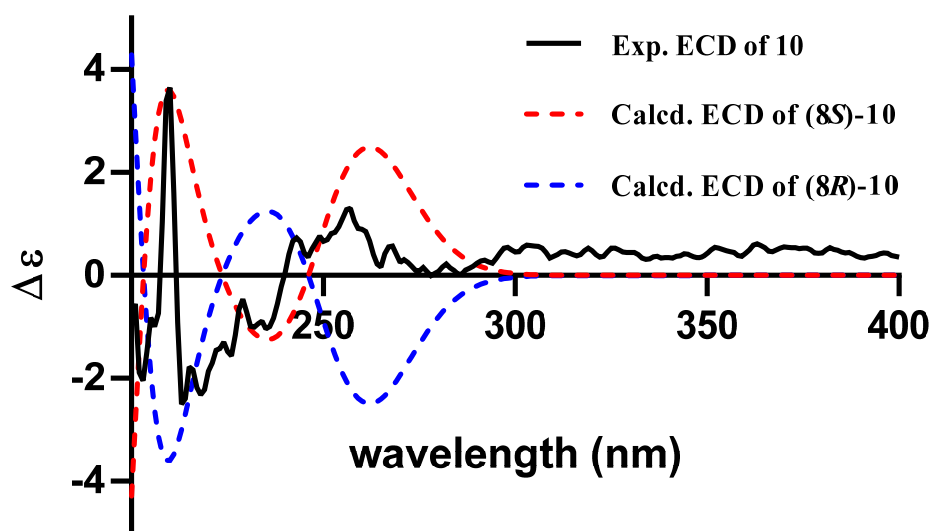
**Figure S24.** The experimental and calculated ECD spectra of compound **7** and its isomer ( $\sigma = 0.30$  eV, UV shift = +25.0 nm)



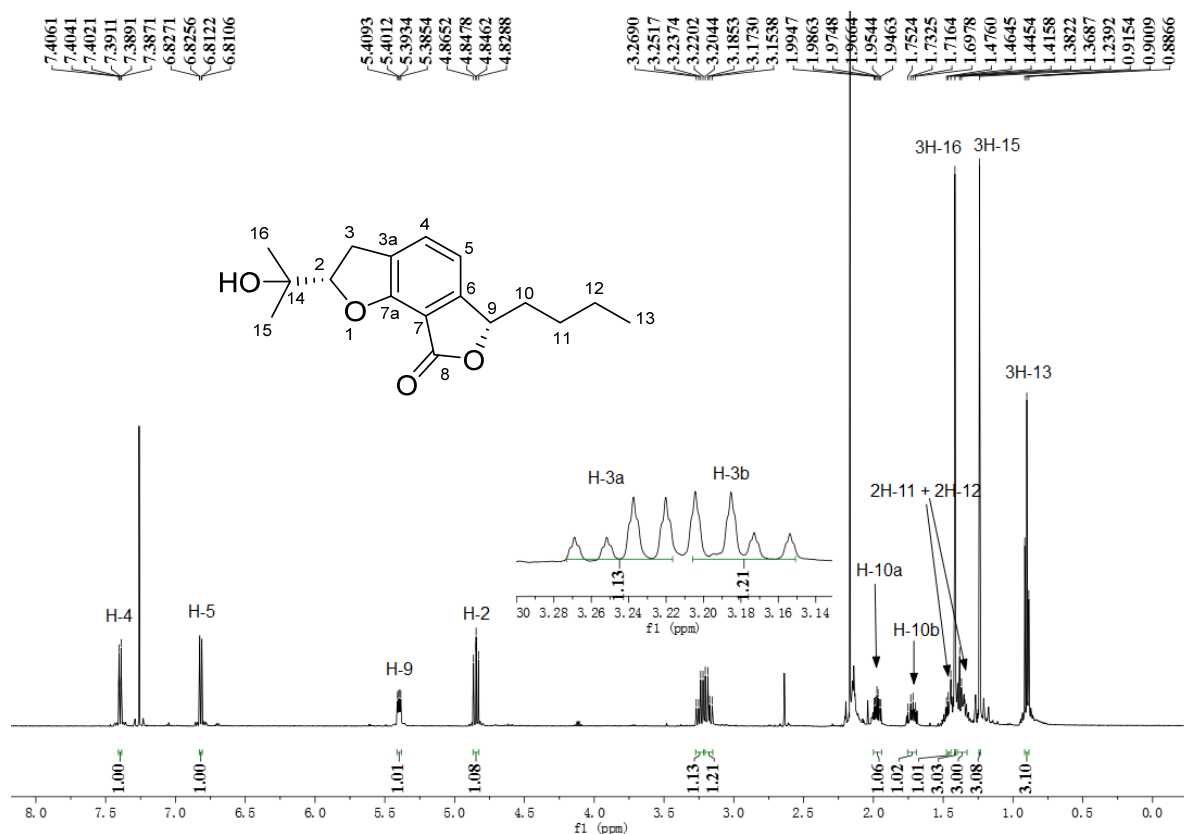
**Figure S25.** The experimental and calculated ECD spectra of compound **8** and its isomer ( $\sigma = 0.30$  eV, UV shift = 0 nm)



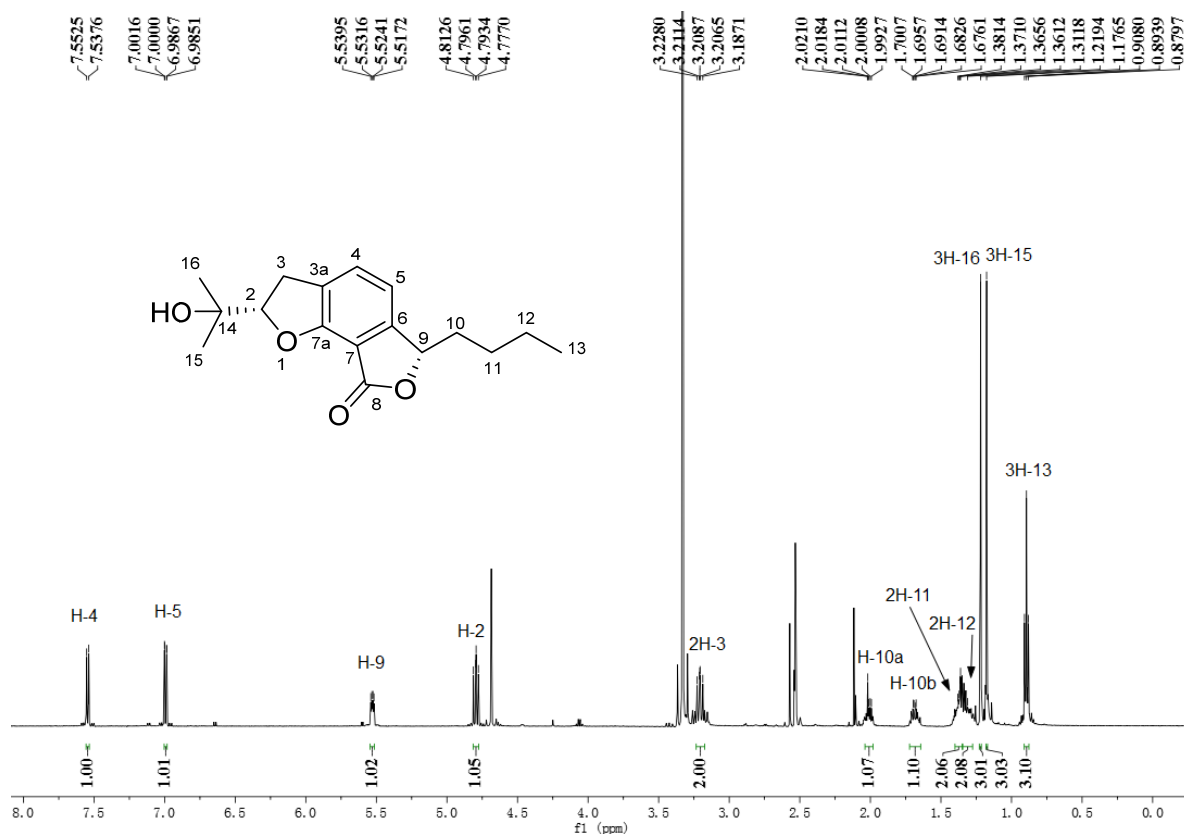
**Figure S26.** The experimental ECD spectrum of compound **9**



**Figure S27.** The experimental and calculated ECD spectra of compound **10** and its isomer ( $\sigma = 0.30$  eV, UV shift = 0 nm)

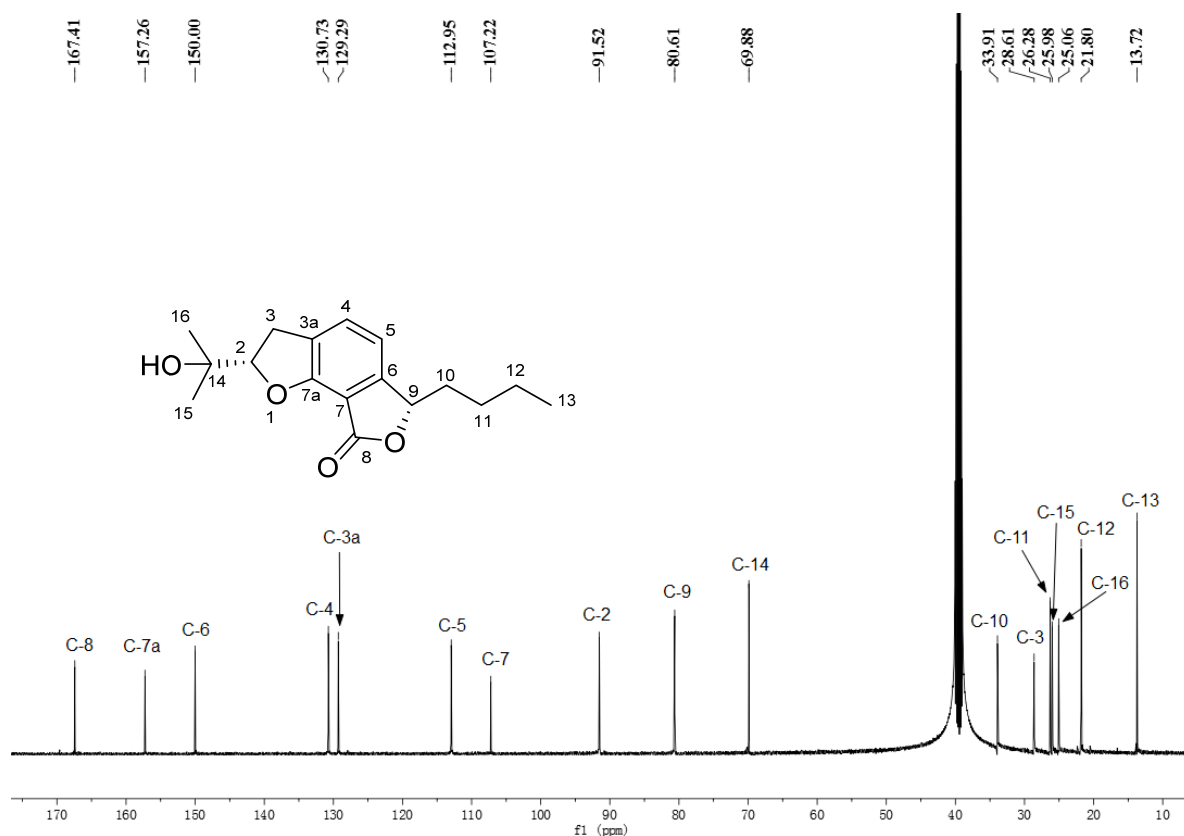


**Figure S28.** <sup>1</sup>H NMR spectrum of (2S, 9S)-annullatin D (**2**) in CDCl<sub>3</sub> (500 MHz)

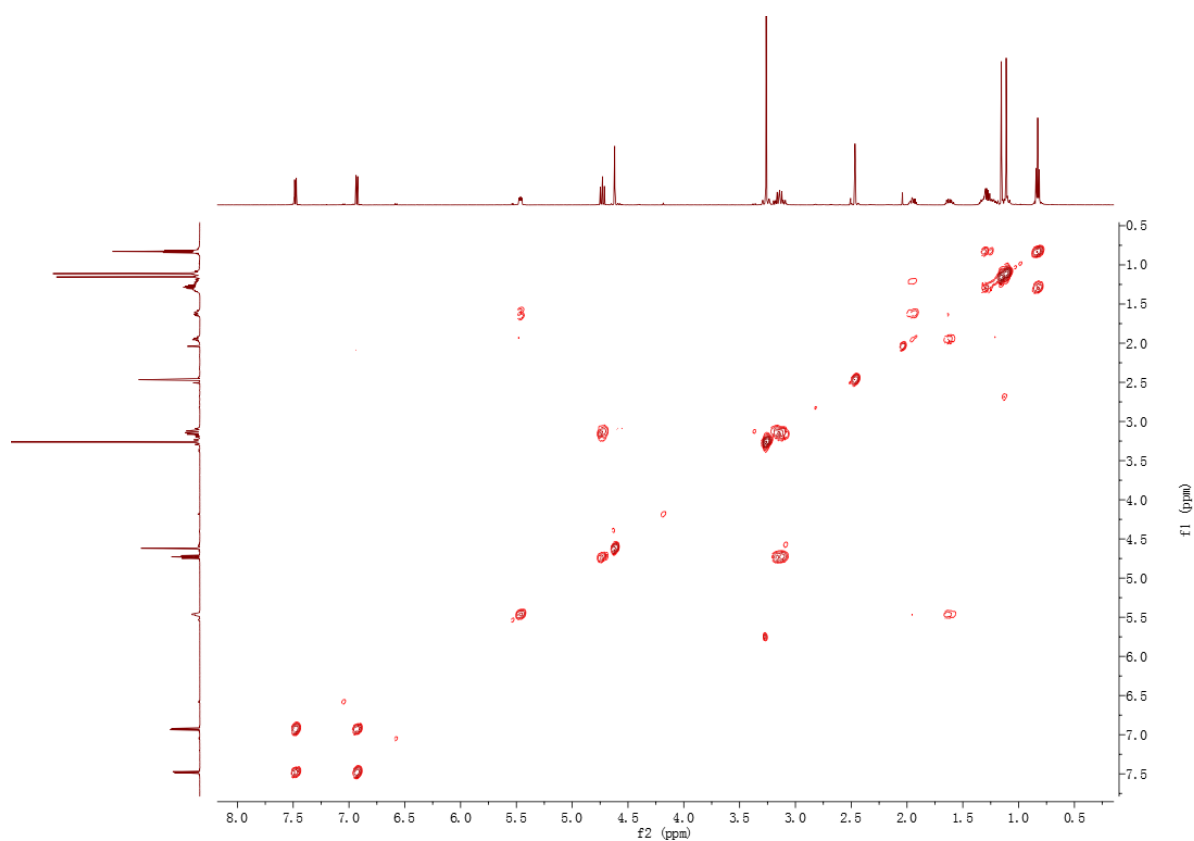


**Figure S29.** <sup>1</sup>H NMR spectrum of (2S, 9S)-annullatin D (**2**) in DMSO-*d*<sub>6</sub> (500 MHz)

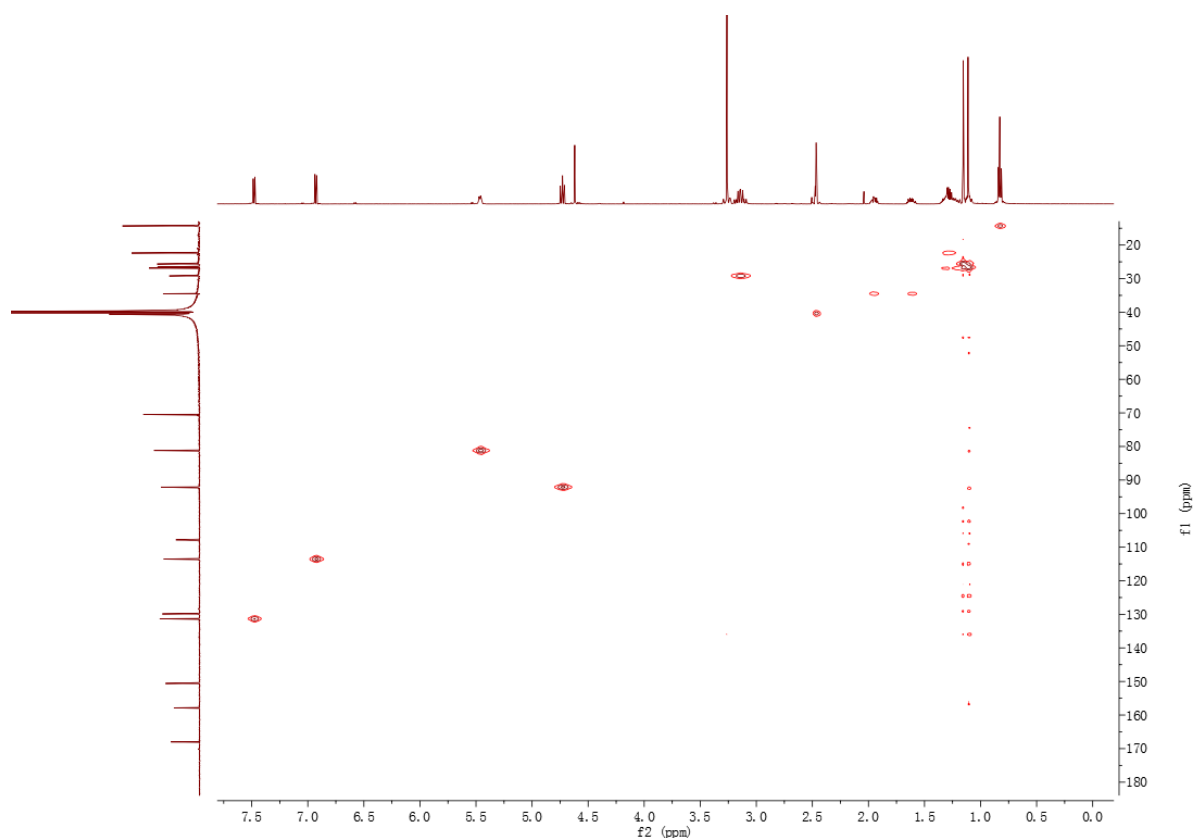




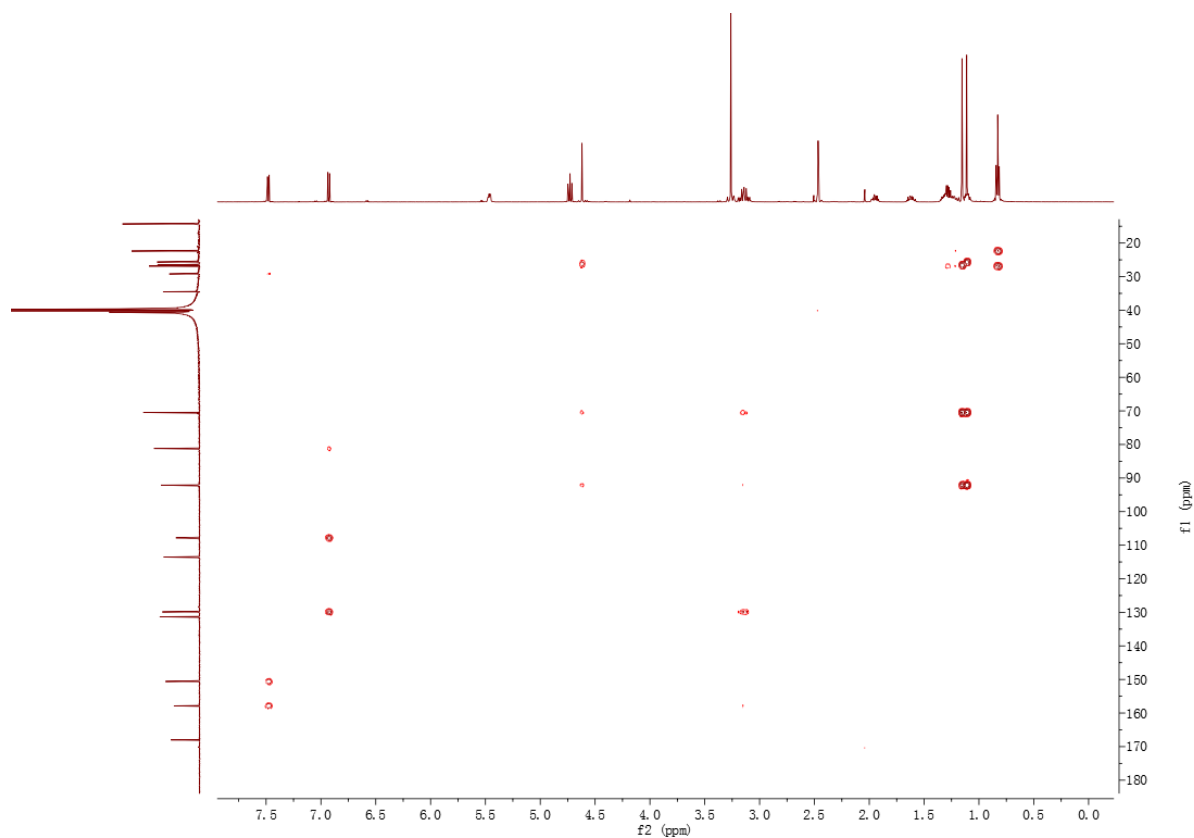
**Figure S30.** <sup>13</sup>C NMR spectrum of (2S, 9S)-annullatin D (2) in DMSO-*d*<sub>6</sub> (125 MHz)



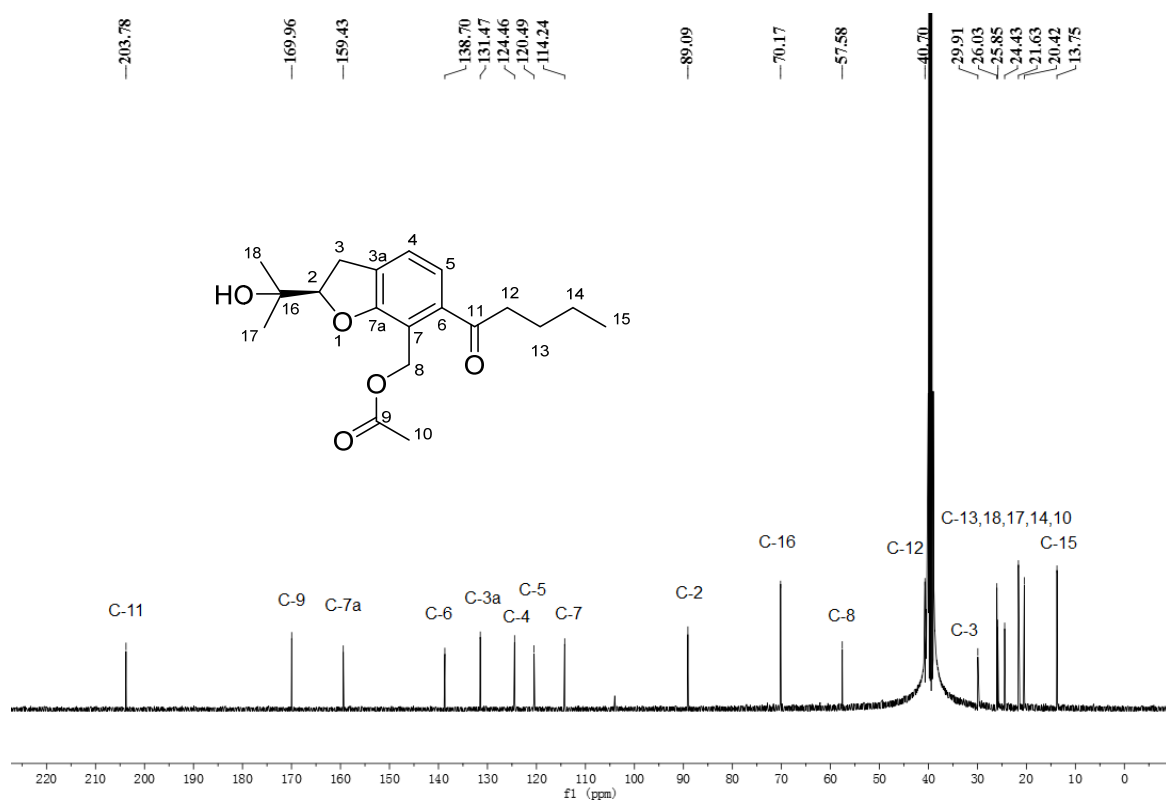
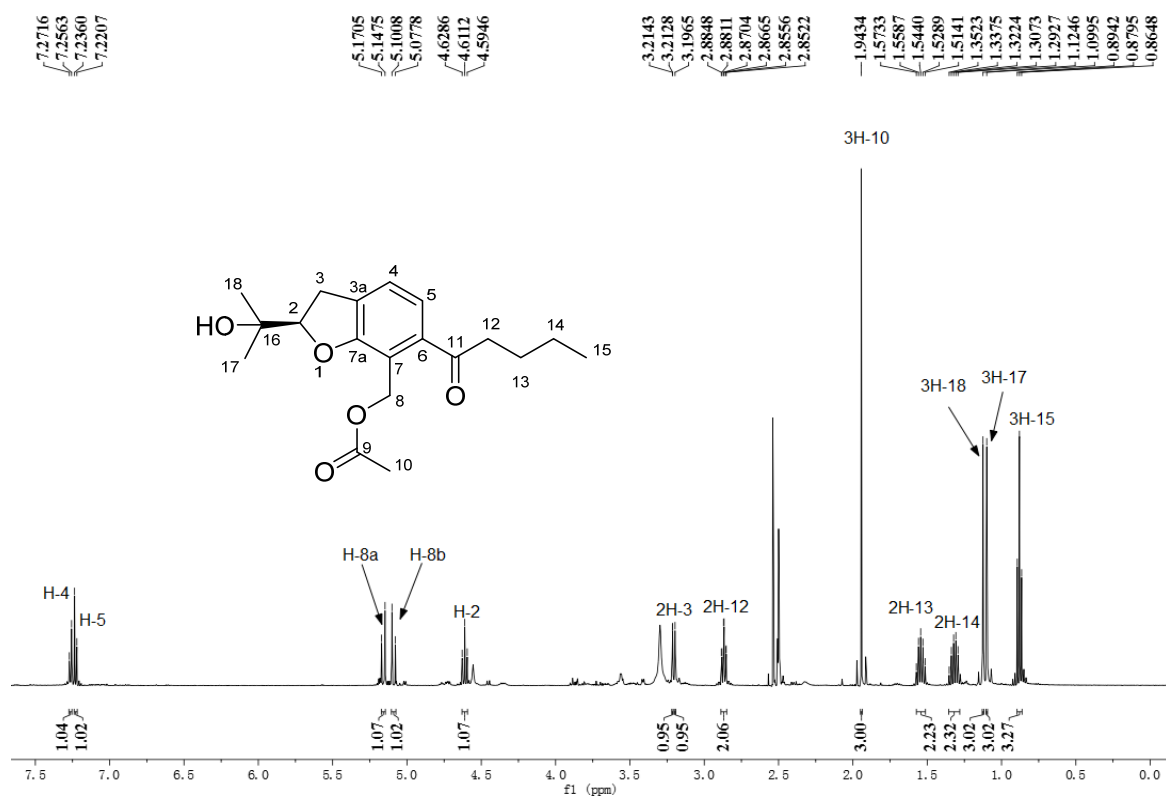
**Figure S31.** <sup>1</sup>H-<sup>1</sup>H COSY spectrum of (2S, 9S)-annullatin D (2) in DMSO-*d*<sub>6</sub>

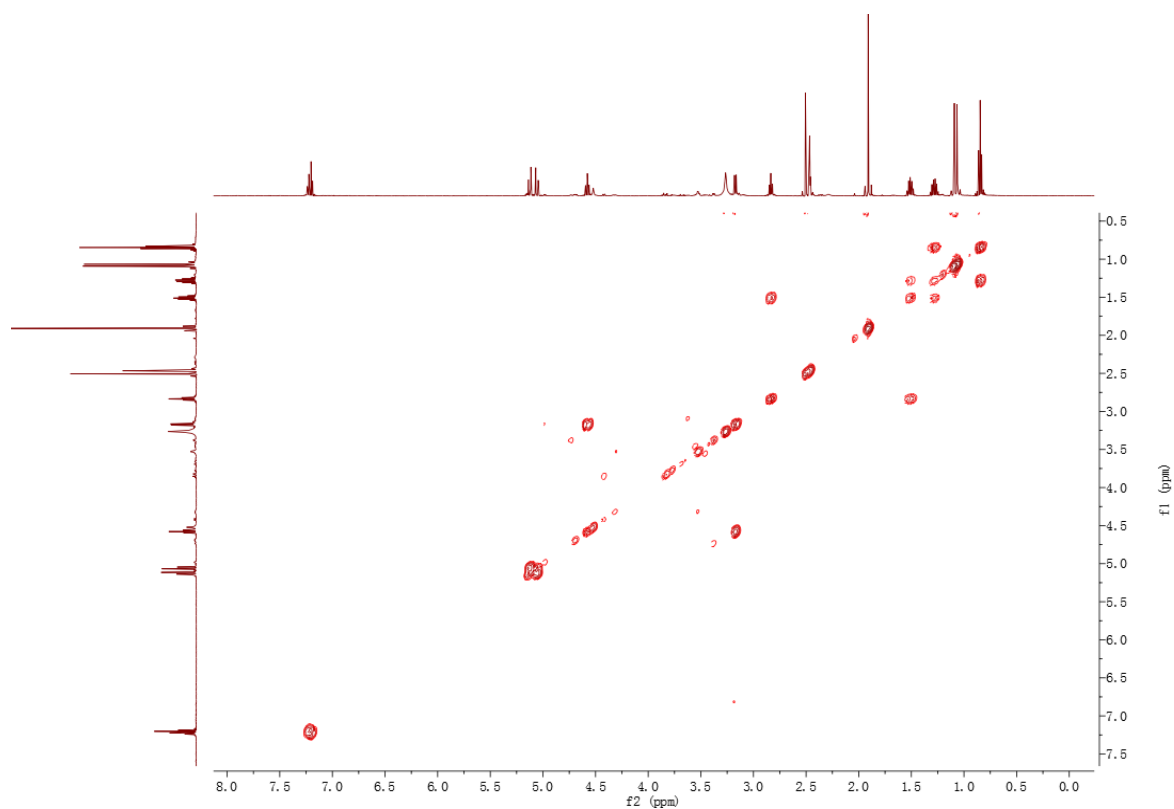


**Figure S32.** HSQC spectrum of (2S, 9S)-annullatin D (**2**) in DMSO- $d_6$

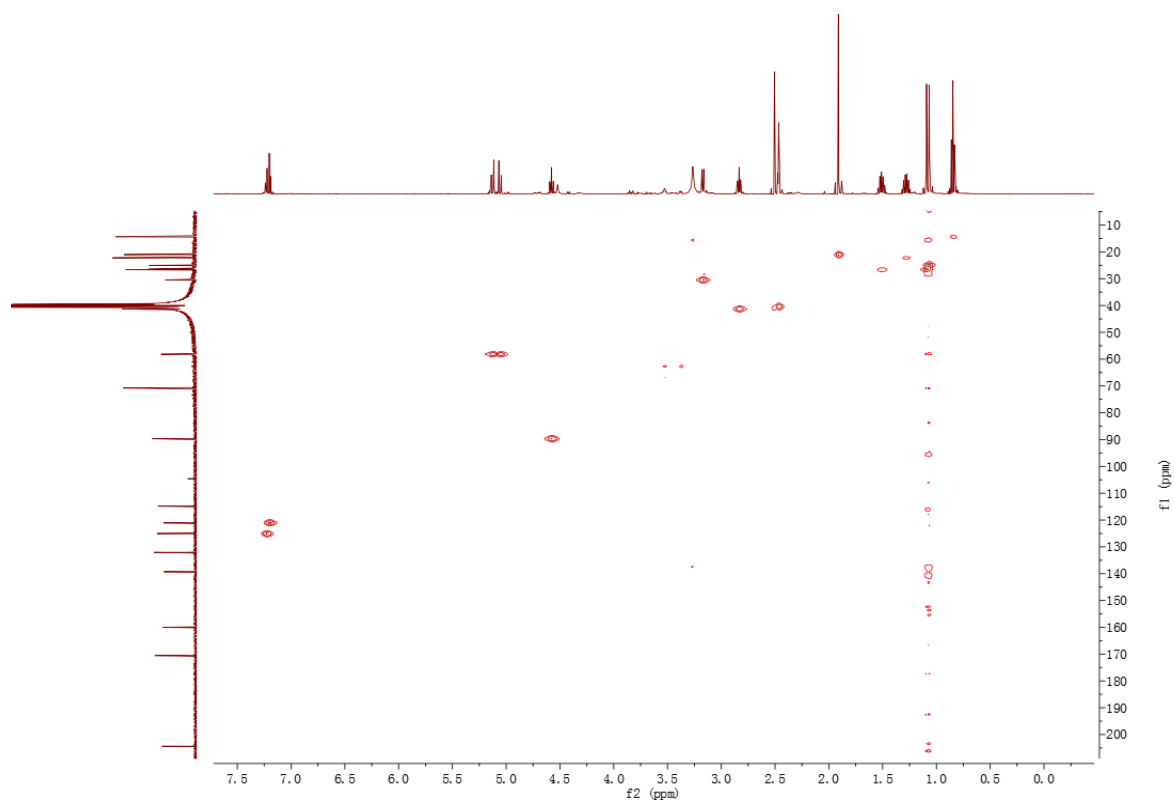


**Figure S33.** HMBC spectrum of (2S, 9S)-annullatin D (**2**) in DMSO- $d_6$

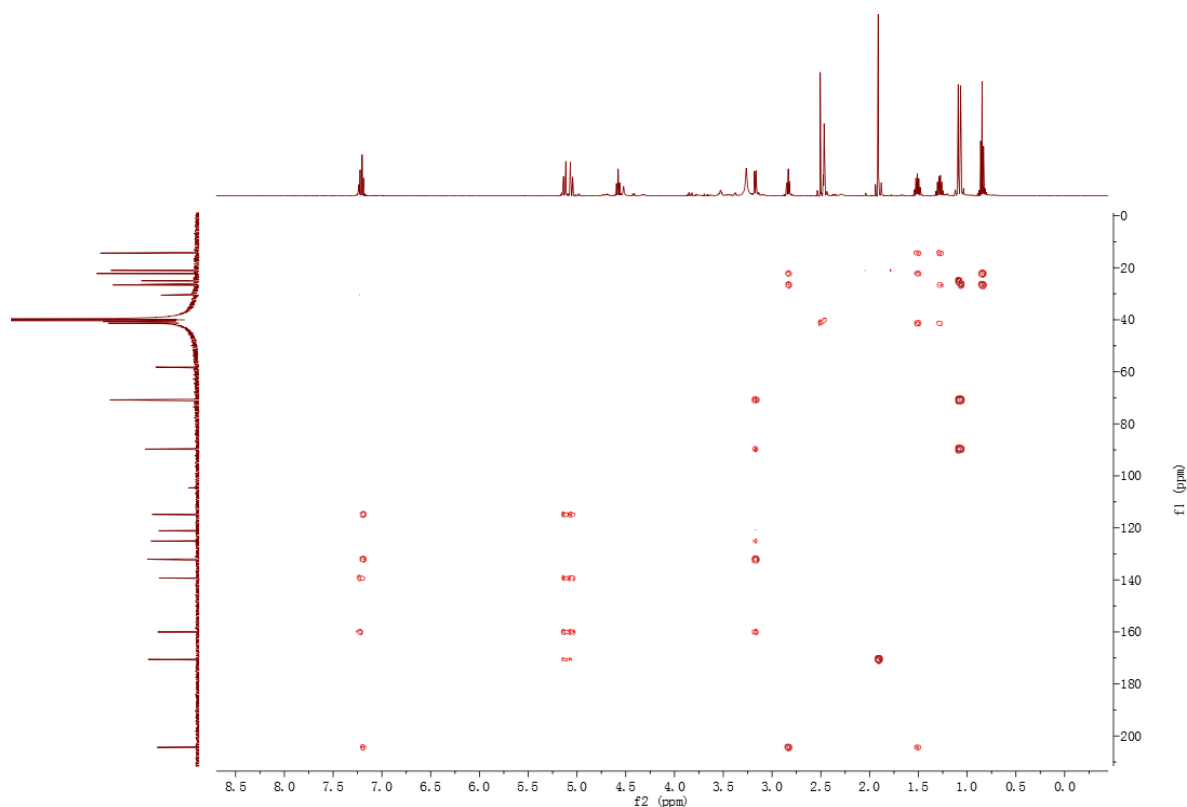




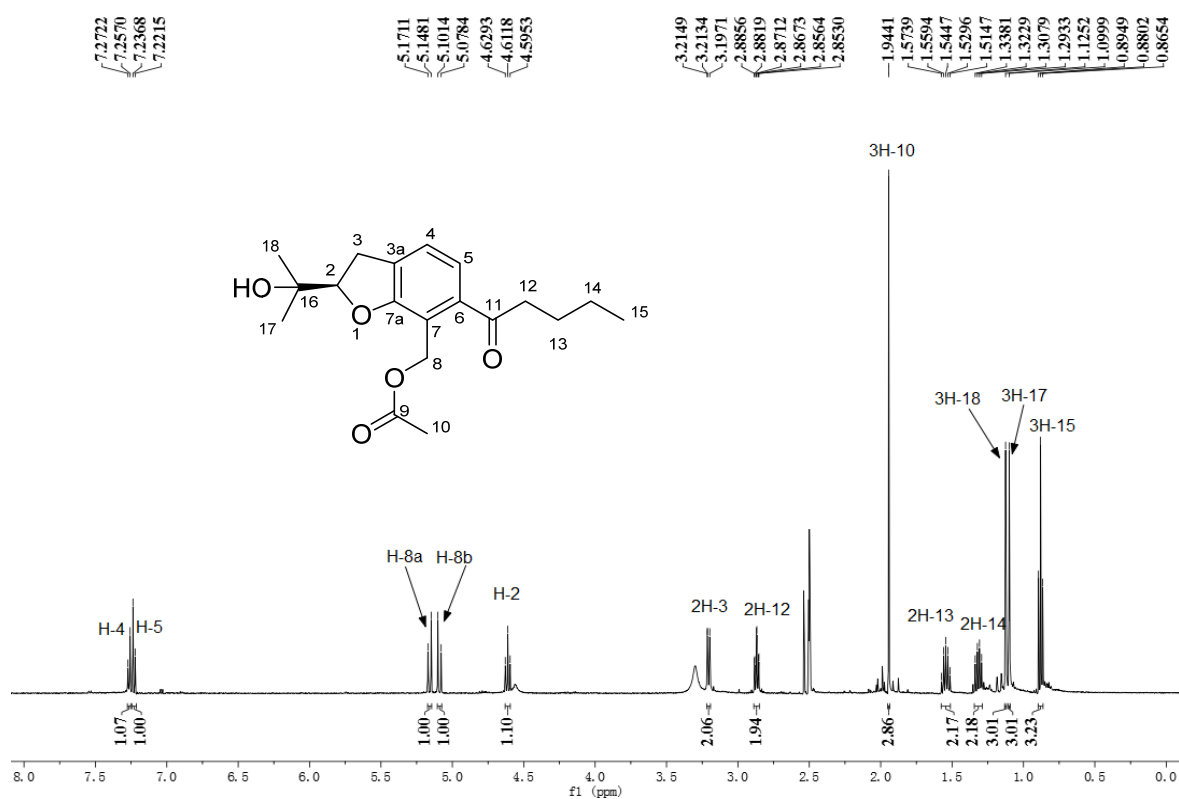
**Figure S36.**  $^1\text{H}$ - $^1\text{H}$  COSY spectrum of (2*R*)-annullatin G (**3**) in  $\text{DMSO-}d_6$ , isolated from fungal culture



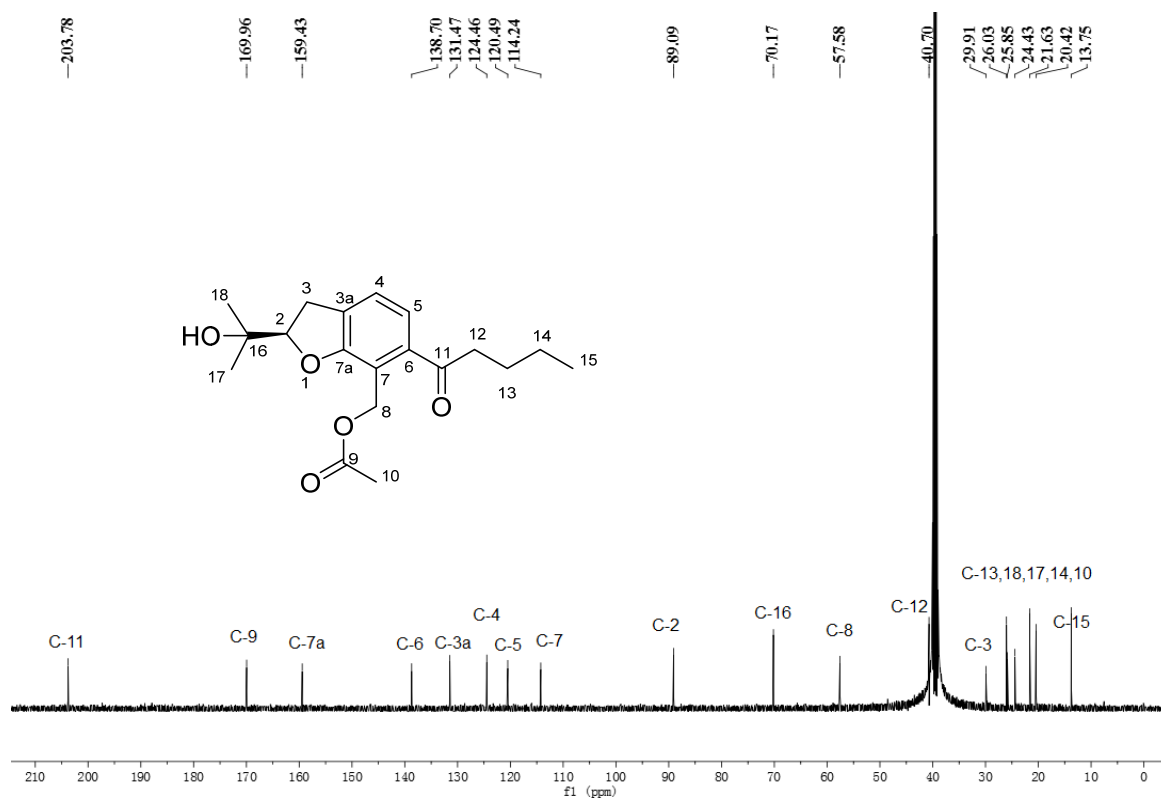
**Figure S37.** HSQC spectrum of (2*R*)-annullatin G (**3**) in  $\text{DMSO-}d_6$ , isolated from fungal culture



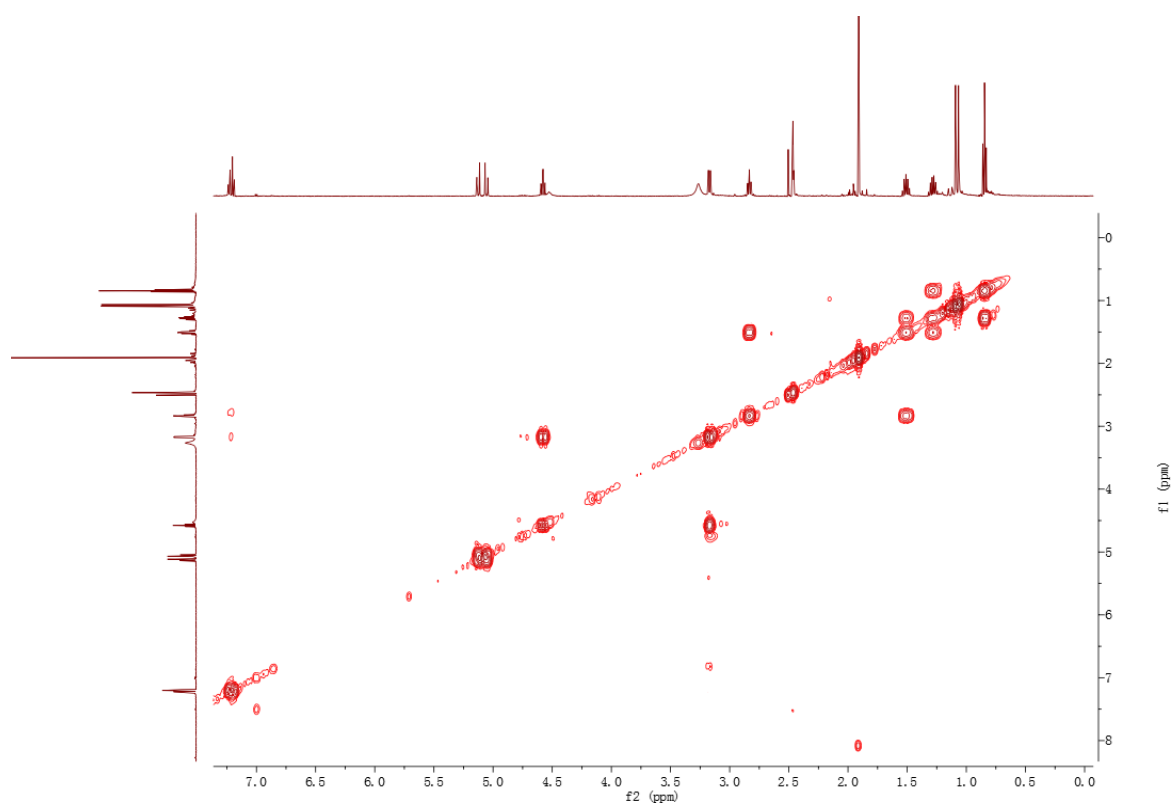
**Figure S38.** HMBC spectrum of (2*R*)-annullatin G (**3**) in DMSO-*d*<sub>6</sub>, isolated from fungal culture



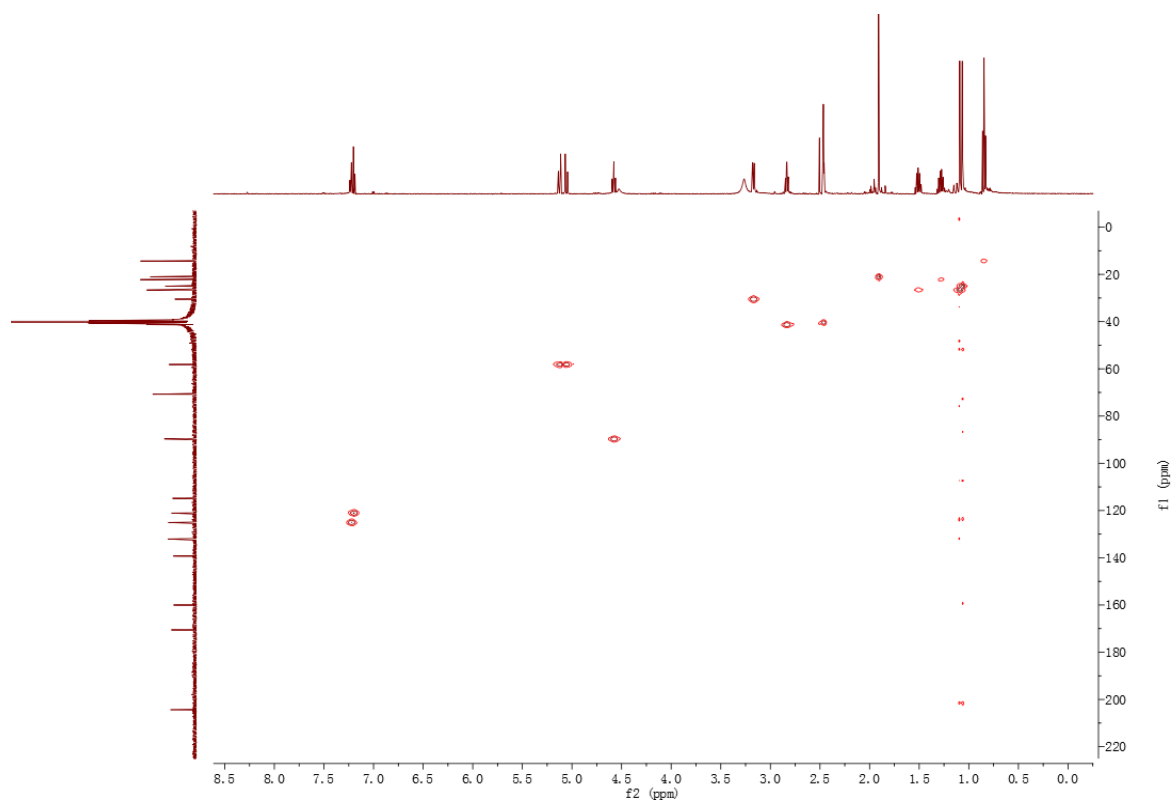
**Figure S39.** <sup>1</sup>H NMR spectrum of (2*R*)-annullatin G (**3**) in DMSO-*d*<sub>6</sub> (500 MHz), obtained after acetylation of annullatin F



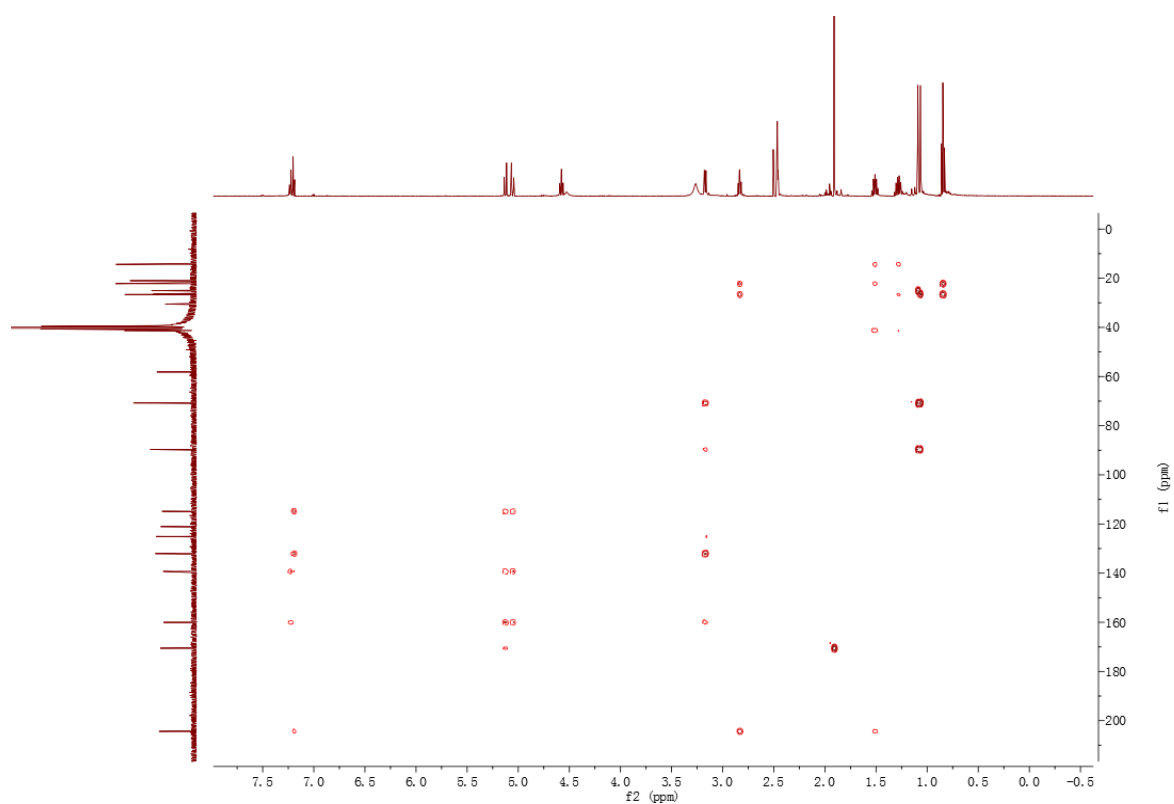
**Figure S40.**  $^{13}\text{C}$  NMR spectrum of (2R)-annullatin G (**3**) in  $\text{DMSO-}d_6$  (125 MHz), obtained after acetylation of annullatin F



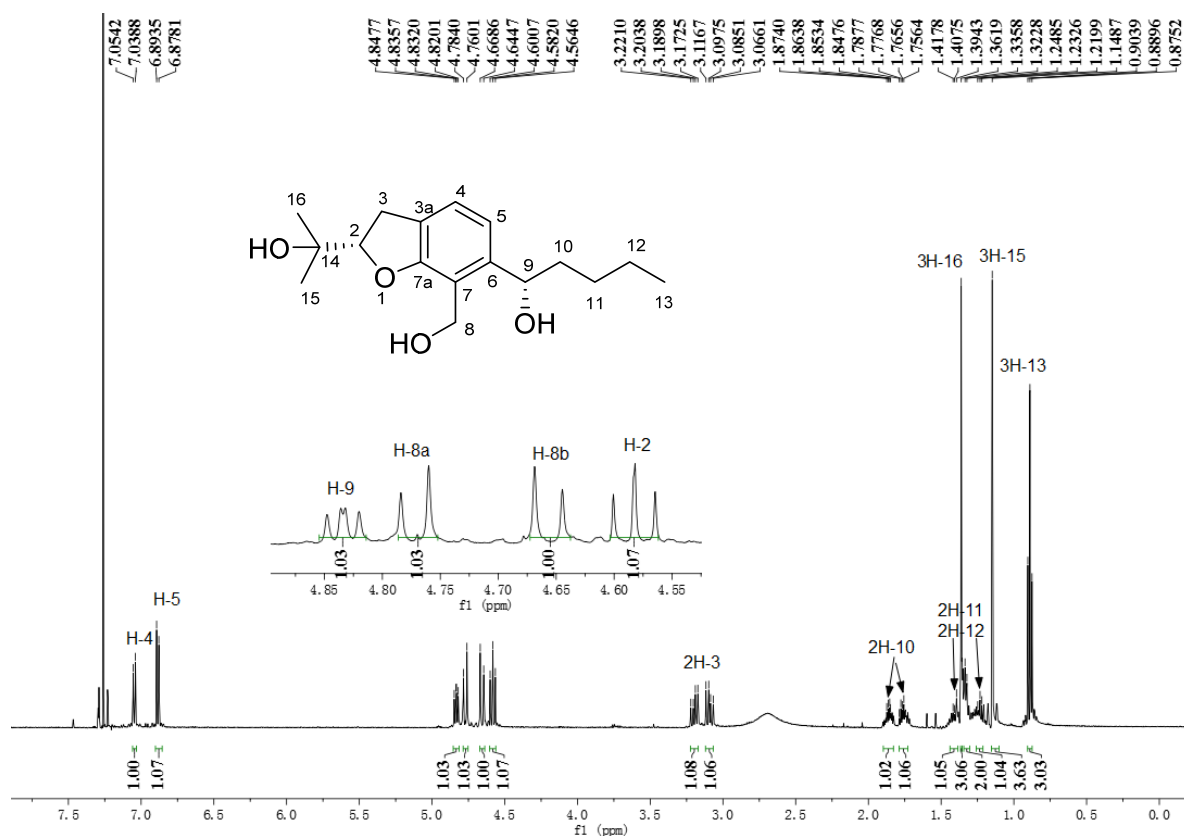
**Figure S41.**  $^1\text{H}$ - $^1\text{H}$  COSY spectrum of (2R)-annullatin G (**3**) in  $\text{DMSO-}d_6$ , obtained after acetylation of annullatin F



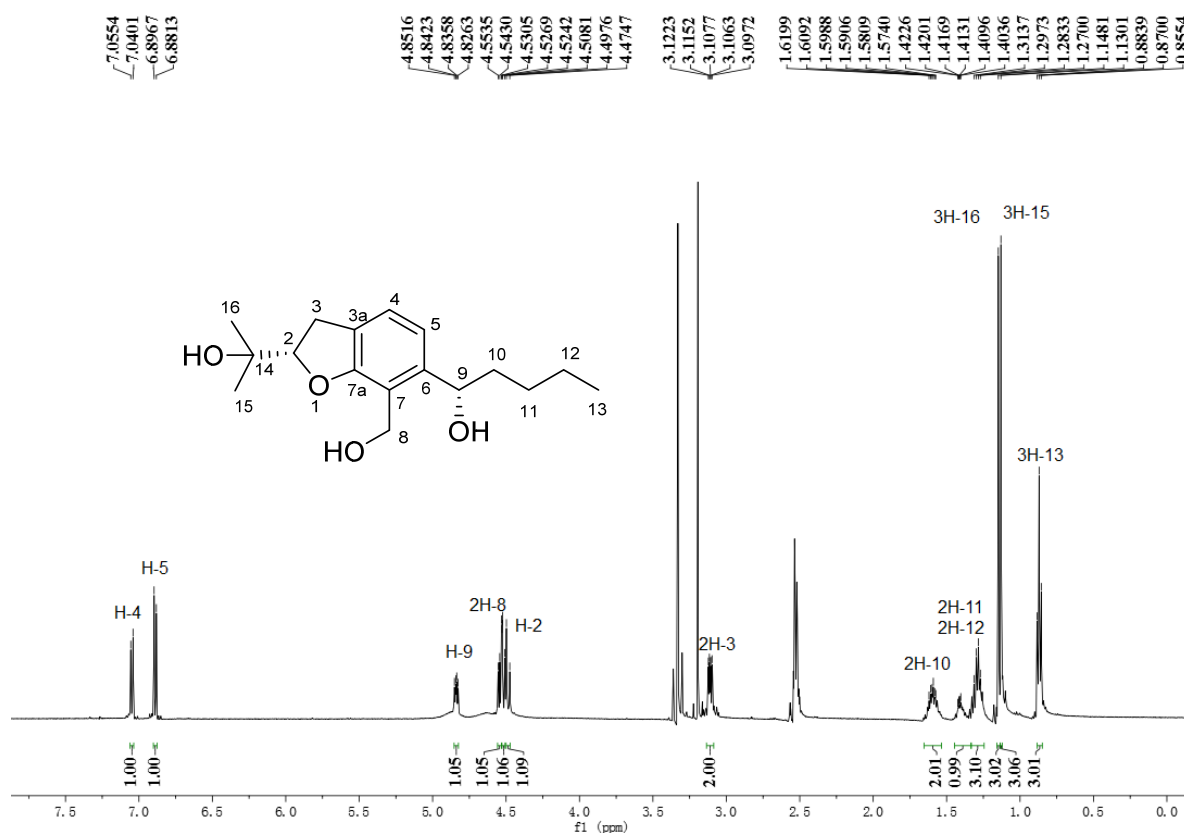
**Figure S42.** HSQC spectrum of (2*R*)-annullatin G (**3**) in DMSO-*d*<sub>6</sub>, obtained after acetylation of annullatin F



**Figure S43.** HMBC spectrum of (2*R*)-annullatin G (**3**) in DMSO-*d*<sub>6</sub>, obtained after acetylation of annullatin F

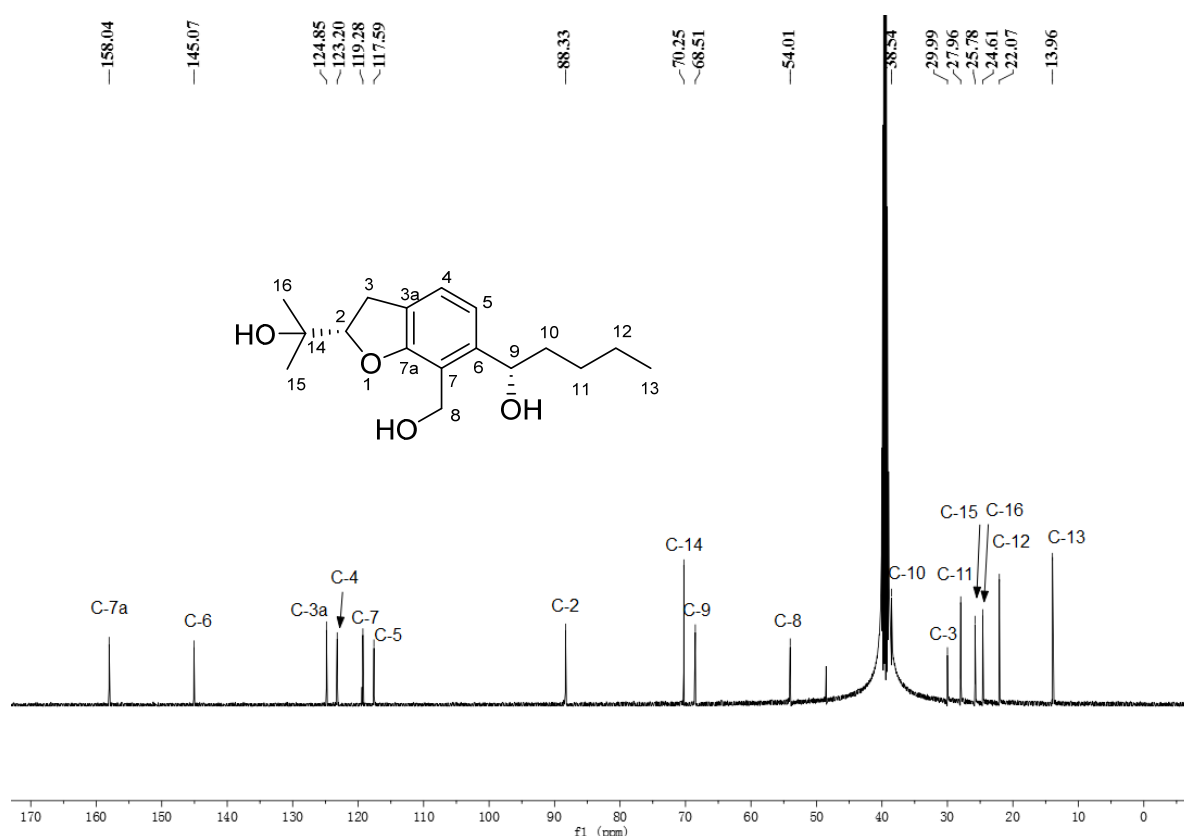


**Figure S44.**  $^1\text{H}$  NMR spectrum of (2S, 9S)-annullatin H (4) in  $\text{CDCl}_3$  (500 MHz)

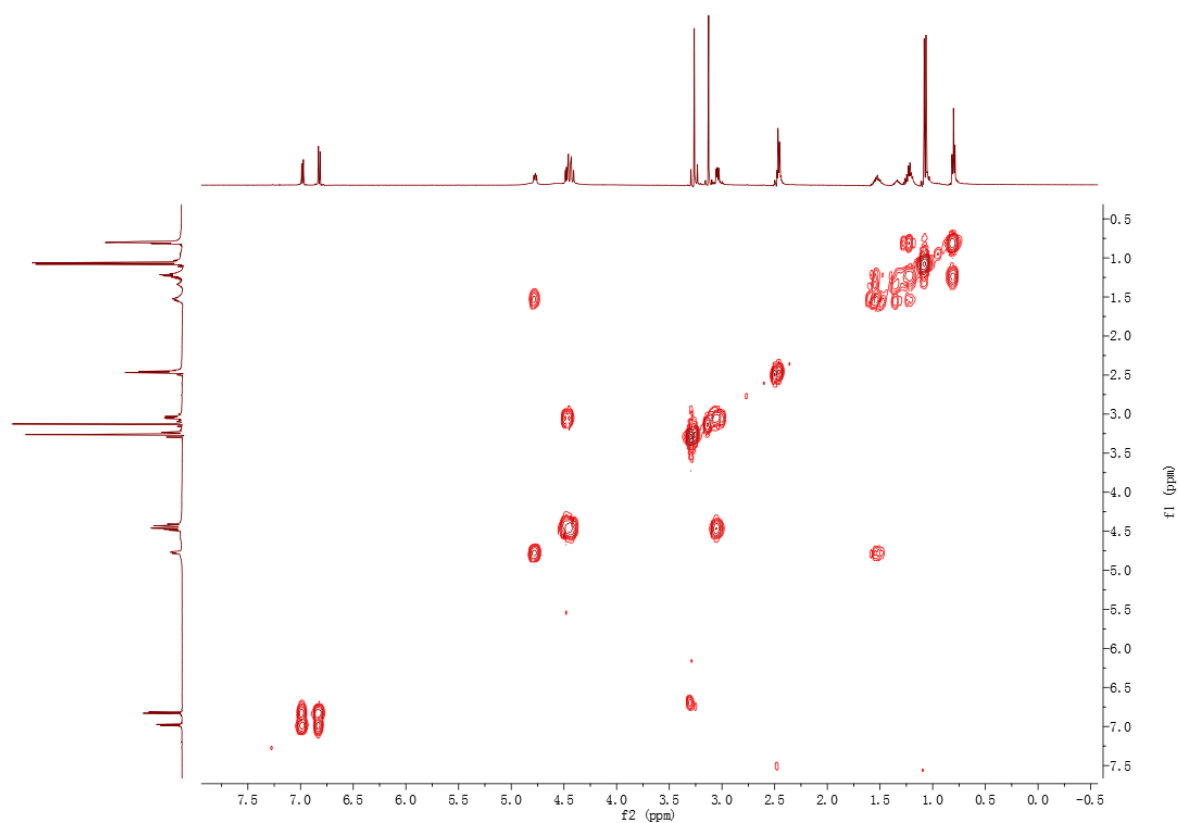


**Figure S45.**  $^1\text{H}$  NMR spectrum of (2S, 9S)-annullatin H (4) in  $\text{DMSO}-d_6$  (500 MHz)

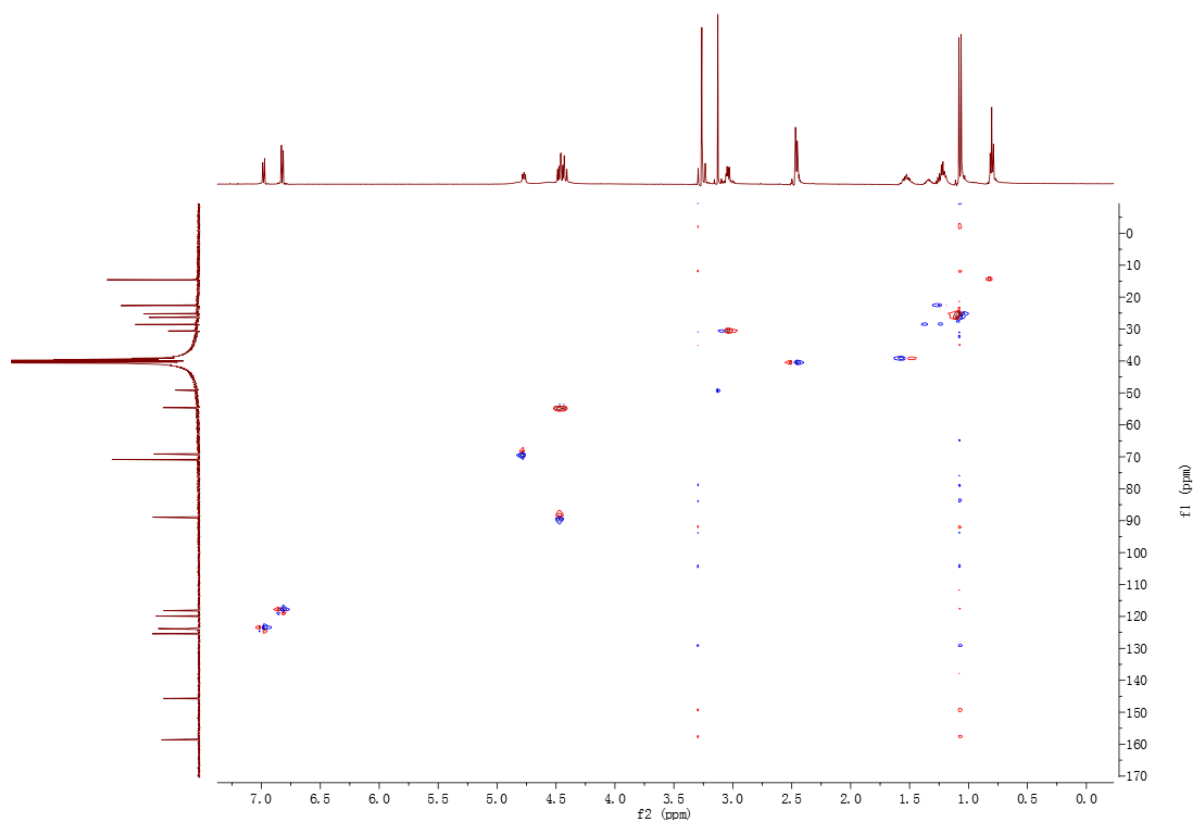




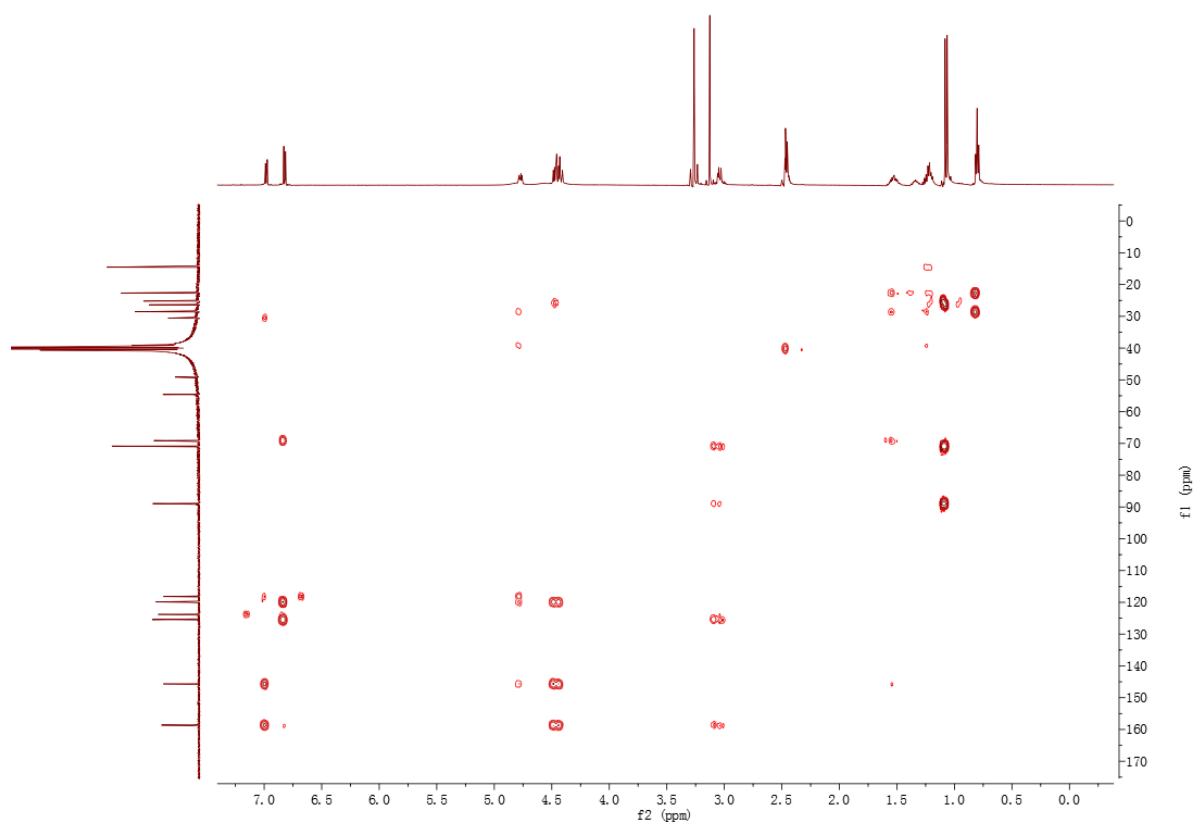
**Figure S46.** <sup>13</sup>C NMR spectrum of (2*S*, 9*S*)-annullatin H (**4**) in DMSO-*d*<sub>6</sub> (125 MHz)



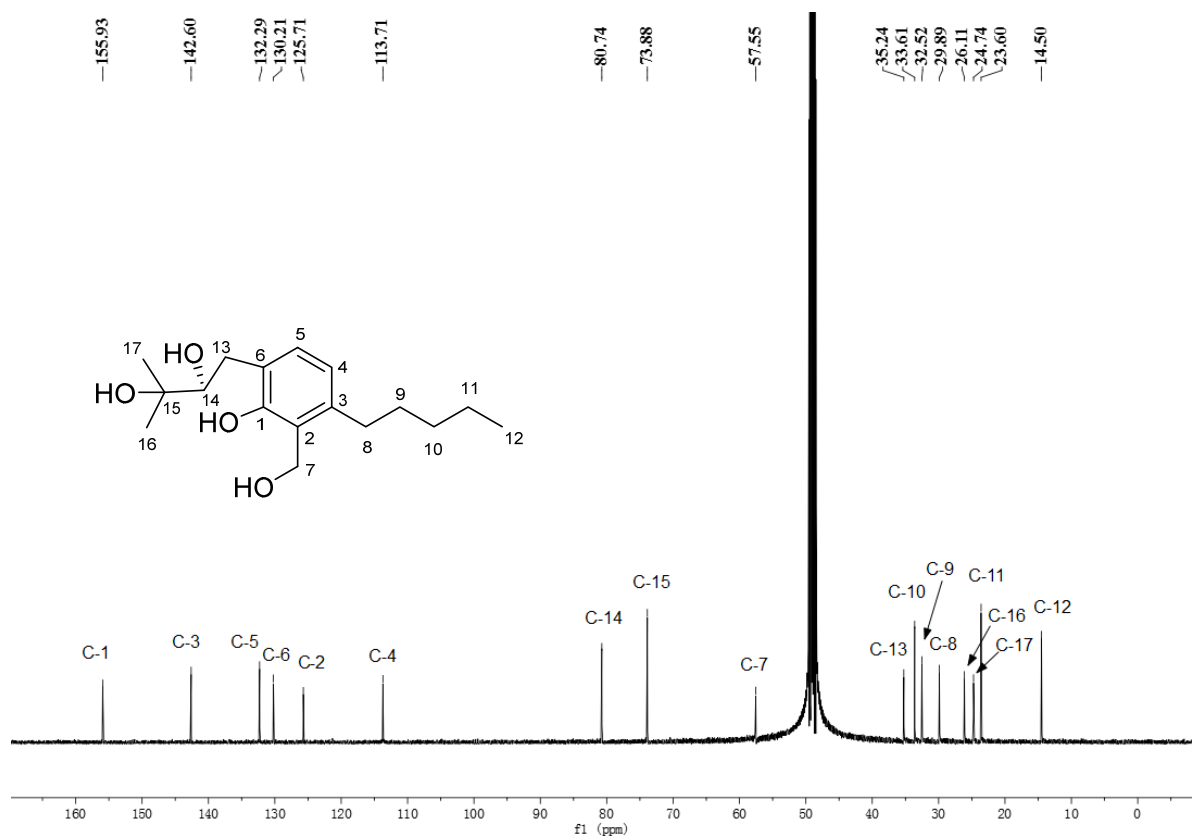
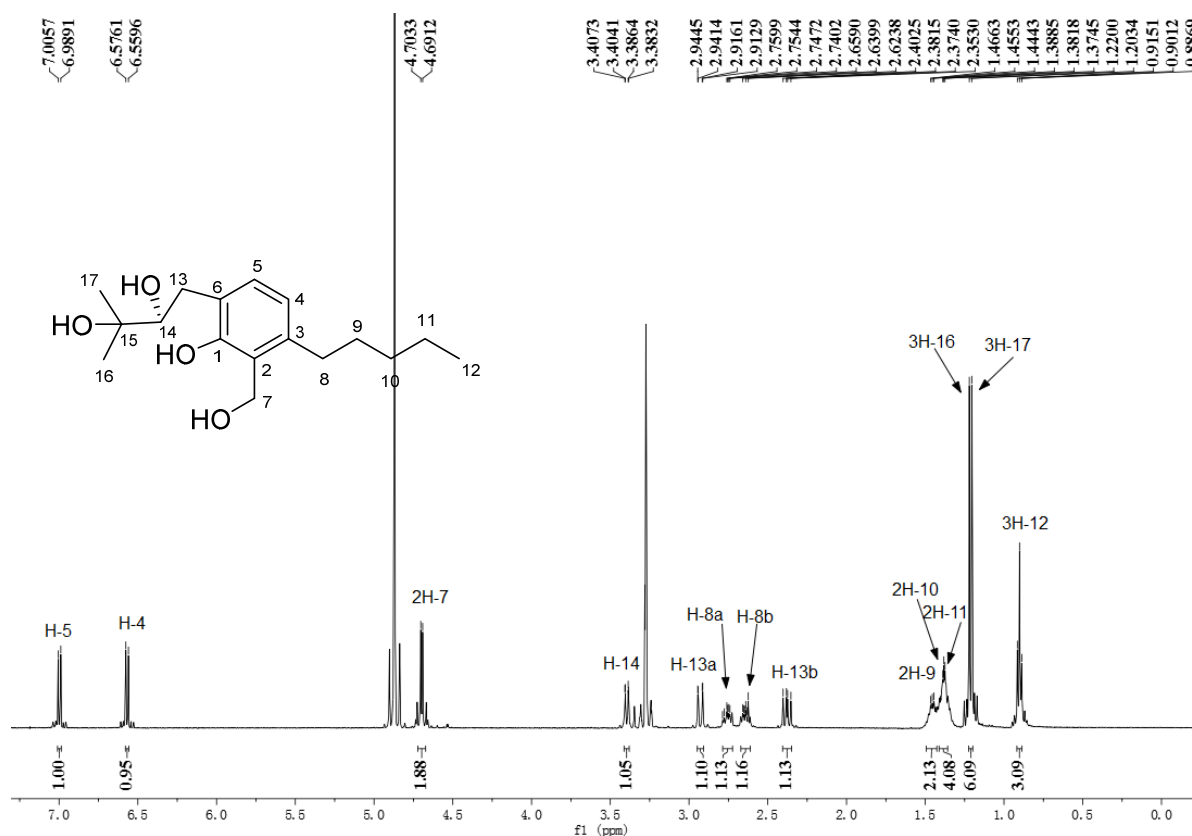
**Figure S47.** <sup>1</sup>H-<sup>1</sup>H COSY spectrum of (2*S*, 9*S*)-annullatin H (**4**) in DMSO-*d*<sub>6</sub>

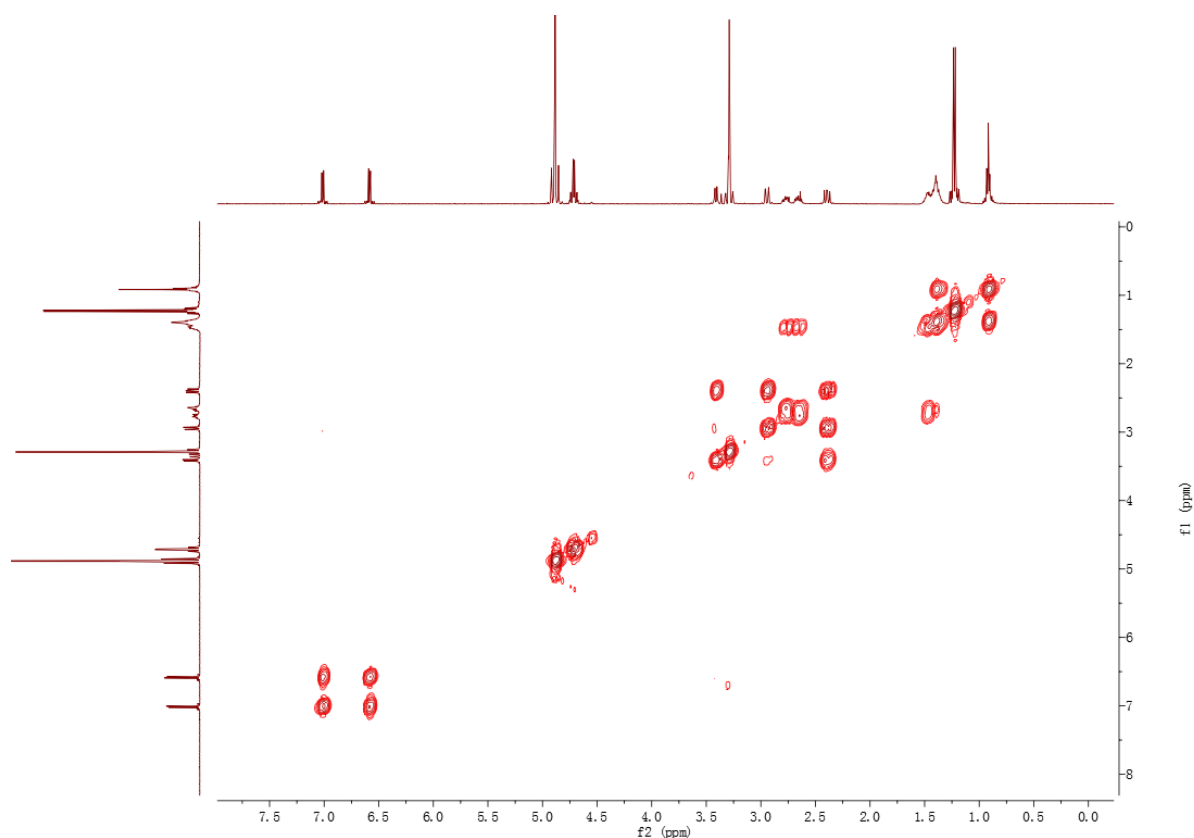


**Figure S48.** HSQC spectrum of (2*S*, 9*S*)-annullatin H (**4**) in DMSO-*d*<sub>6</sub>

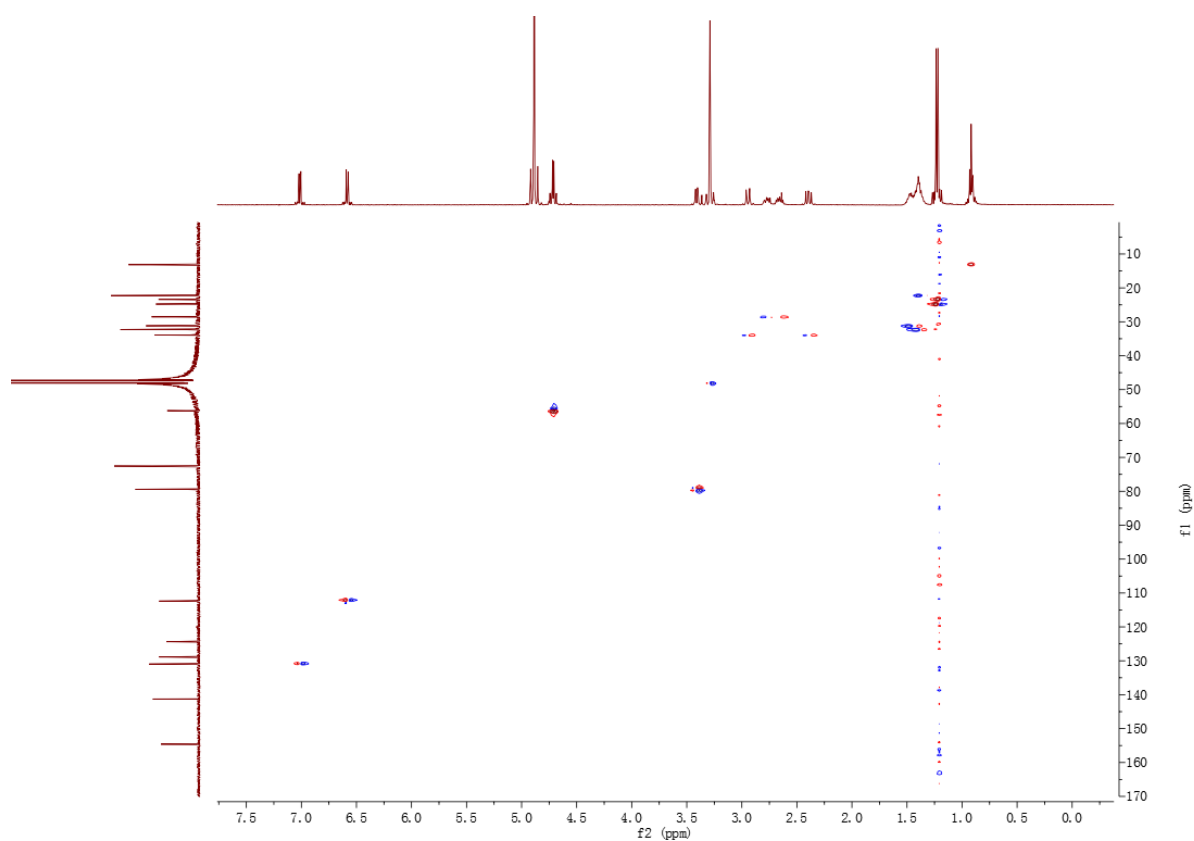


**Figure S49.** HMBC spectrum of (2*S*, 9*S*)-annullatin H (**4**) in DMSO-*d*<sub>6</sub>

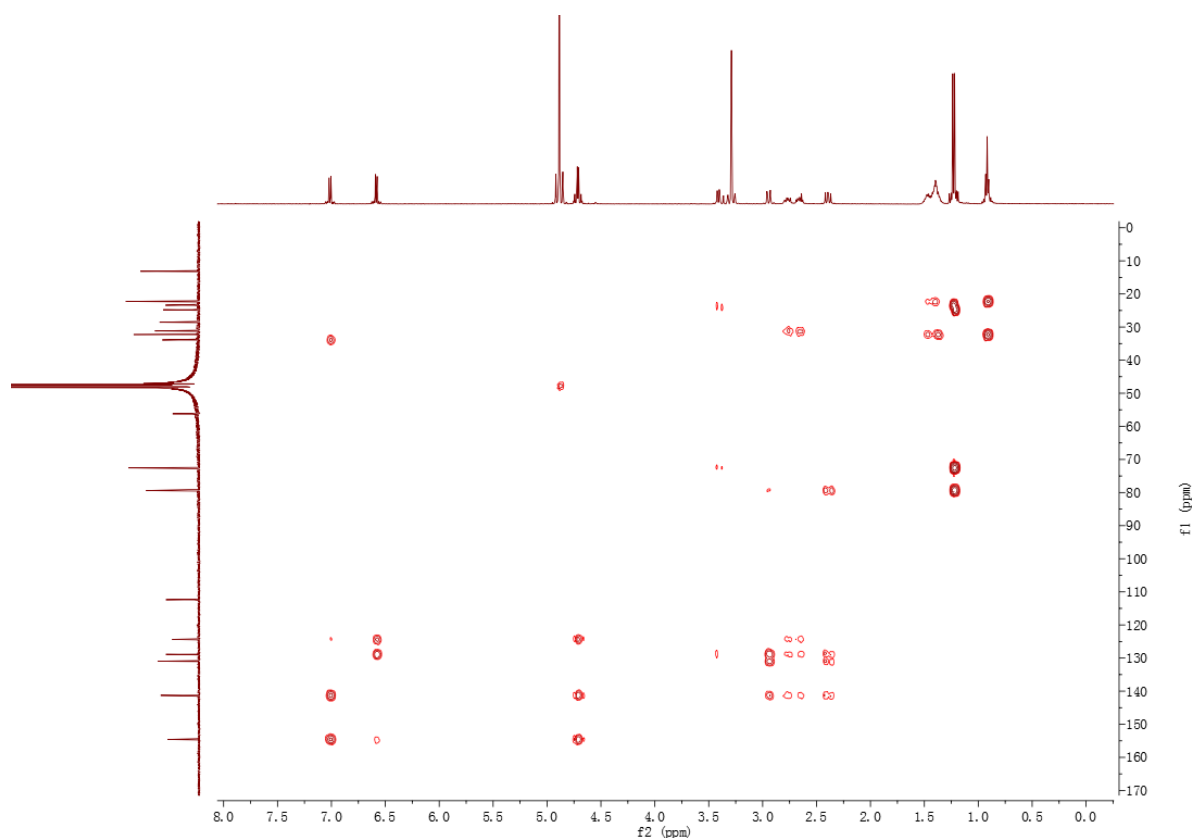




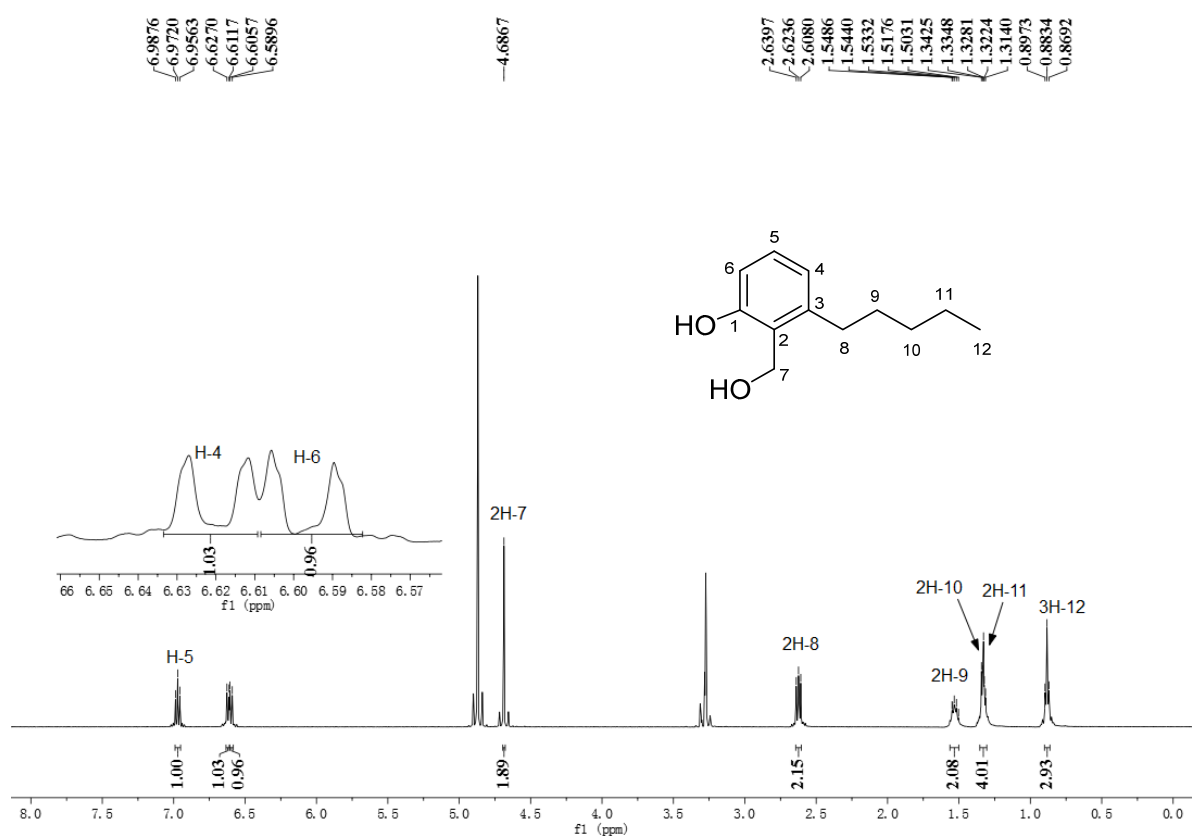
**Figure S52.**  $^1\text{H}$ - $^1\text{H}$  COSY spectrum of (14*S*)-annullatin I (**5**) in  $\text{CD}_3\text{OD}$



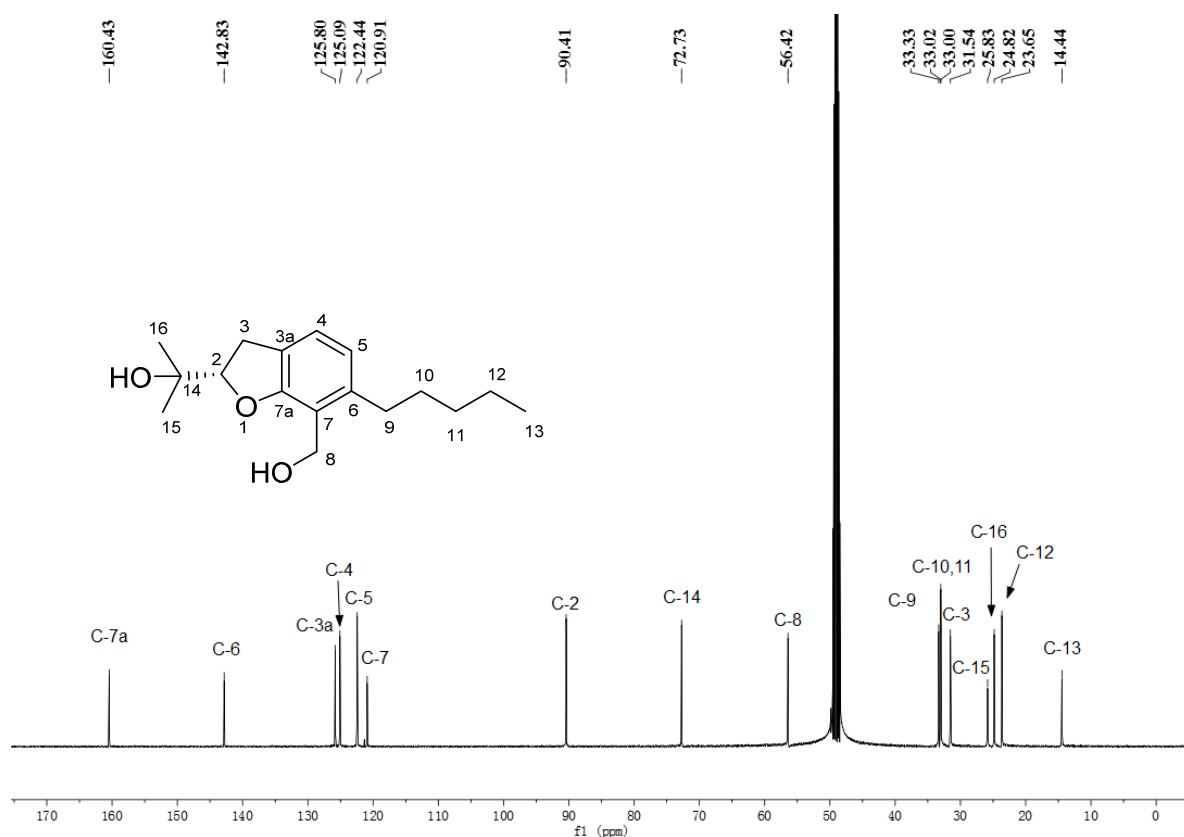
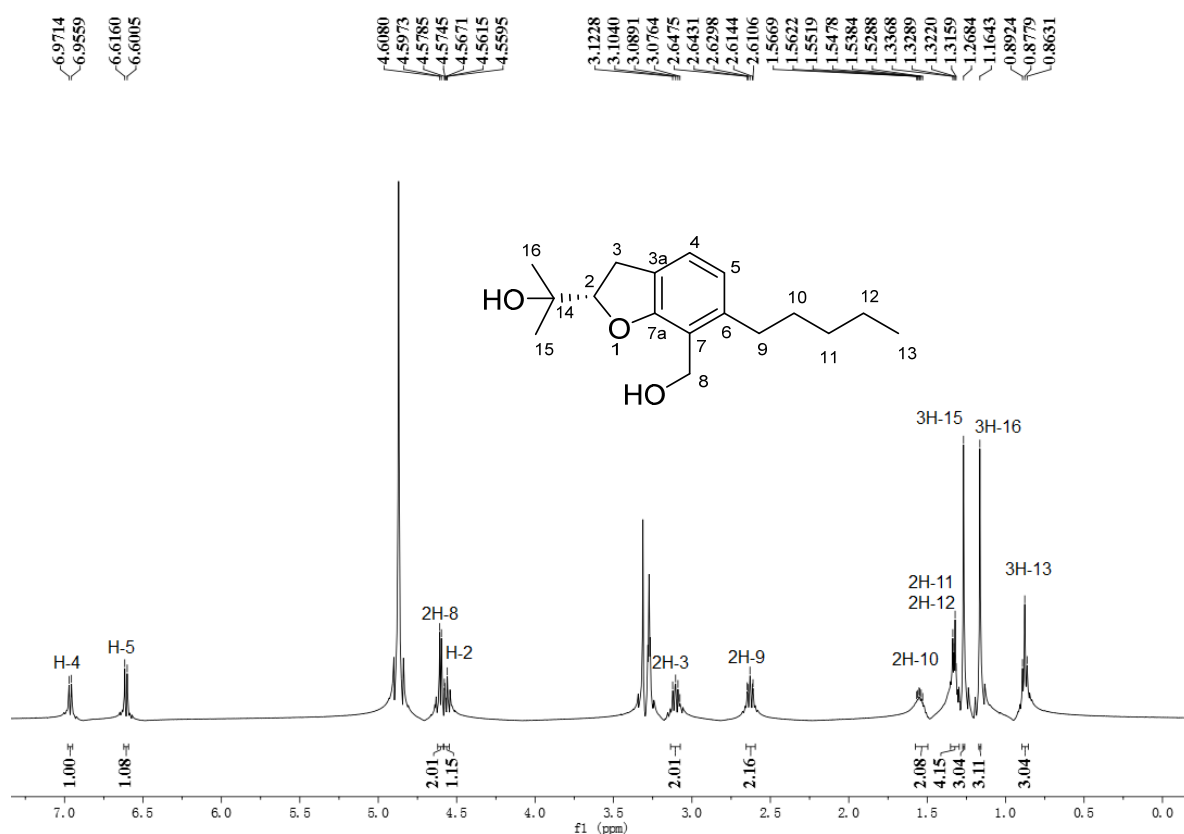
**Figure S53.** HSQC spectrum of (14*S*)-annullatin I (**5**) in  $\text{CD}_3\text{OD}$

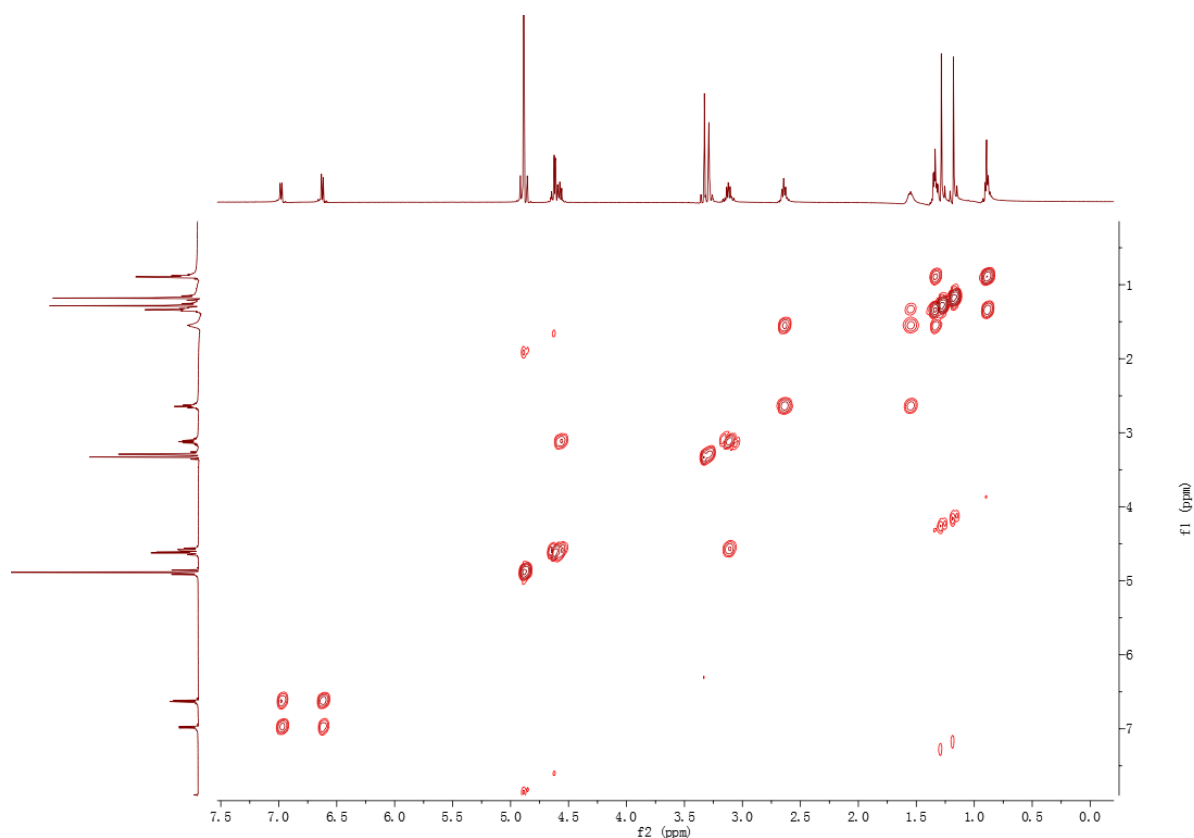


**Figure S54.** HMBC spectrum of (14*S*)-annullatin I (**5**) in CD<sub>3</sub>OD

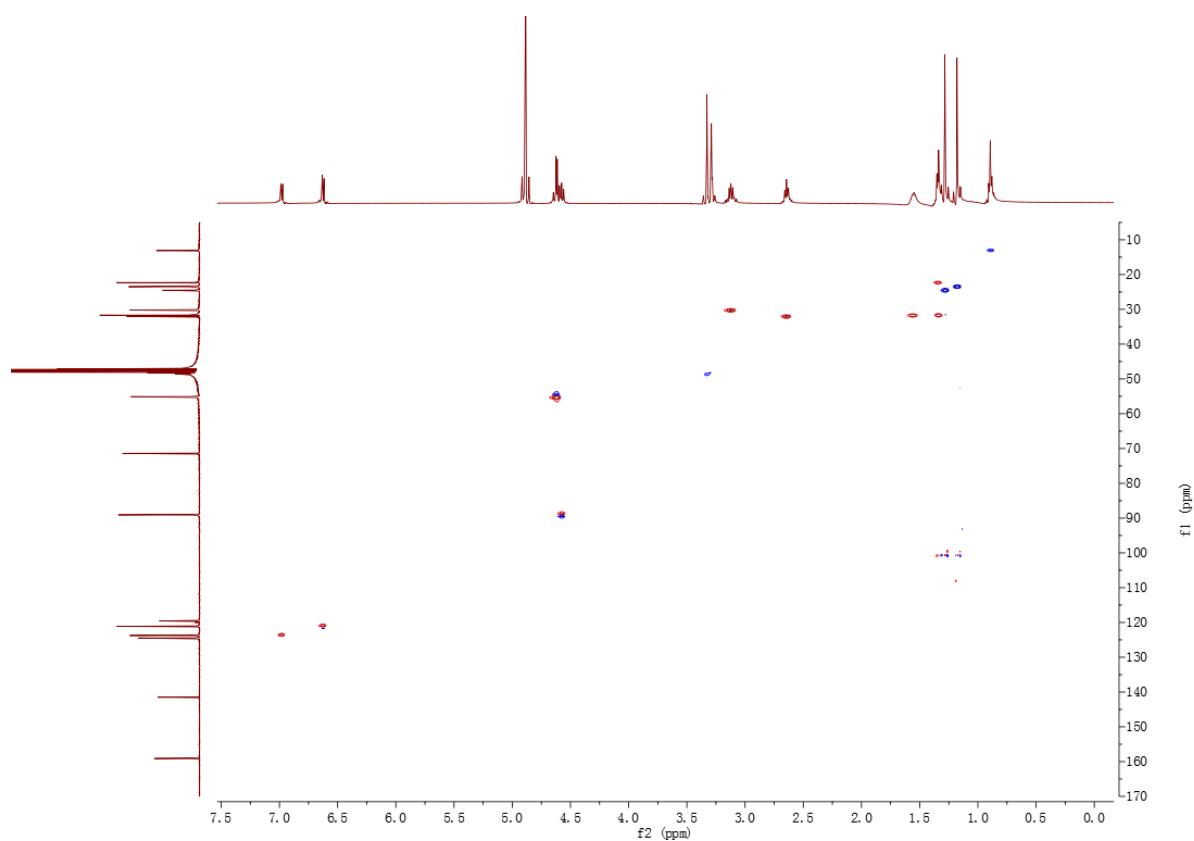


**Figure S55.** <sup>1</sup>H NMR spectrum of 2-hydroxymethyl-3-pentylphenol (**6**) in CD<sub>3</sub>OD (500 MHz)

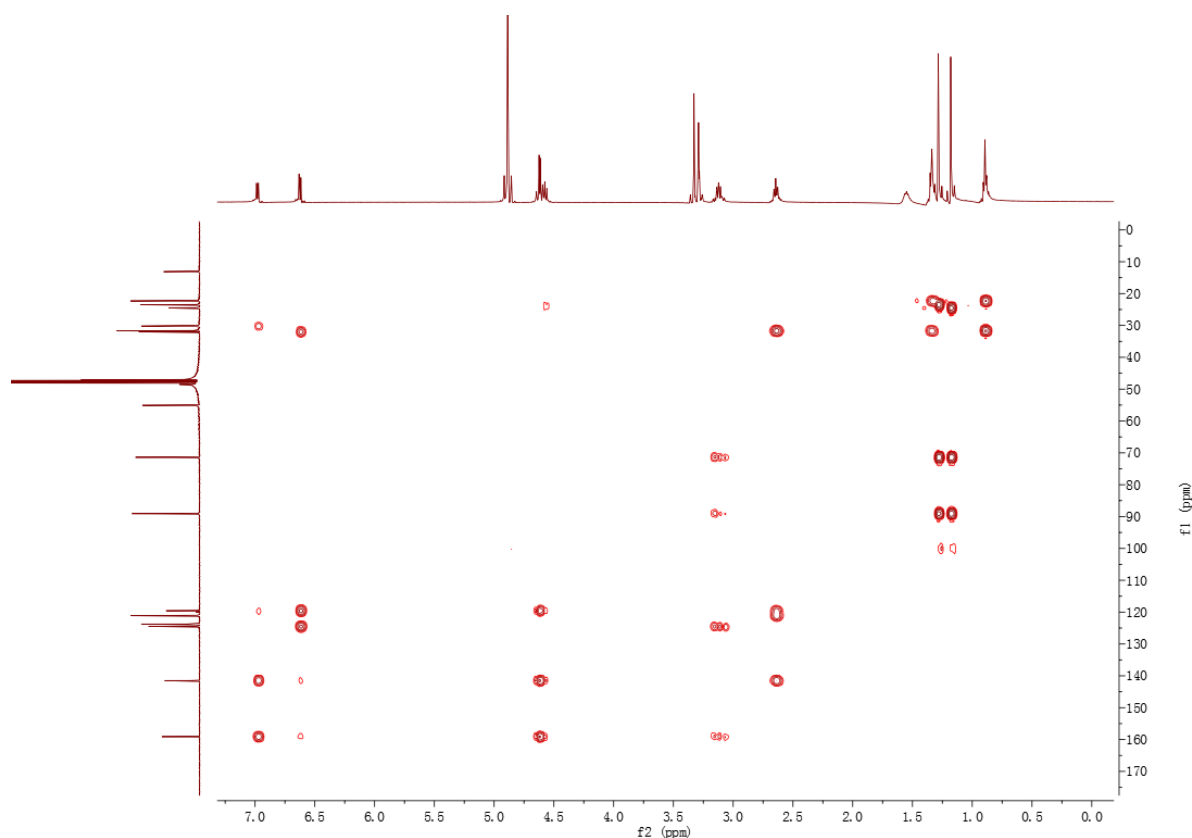




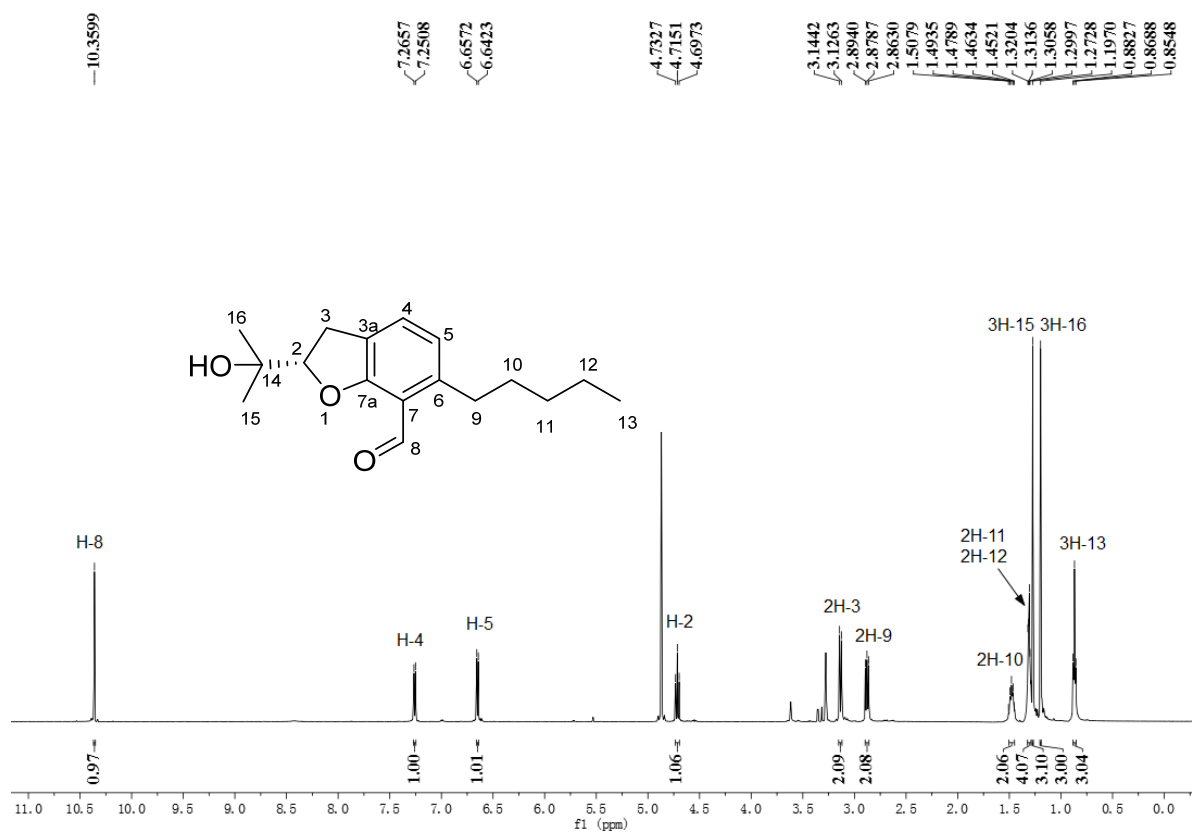
**Figure S58.**  $^1\text{H}$ - $^1\text{H}$  COSY spectrum of (2*S*)-annullatin B (**7**) in  $\text{CD}_3\text{OD}$



**Figure S59.** HSQC spectrum of (2*S*)-annullatin B (**7**) in  $\text{CD}_3\text{OD}$

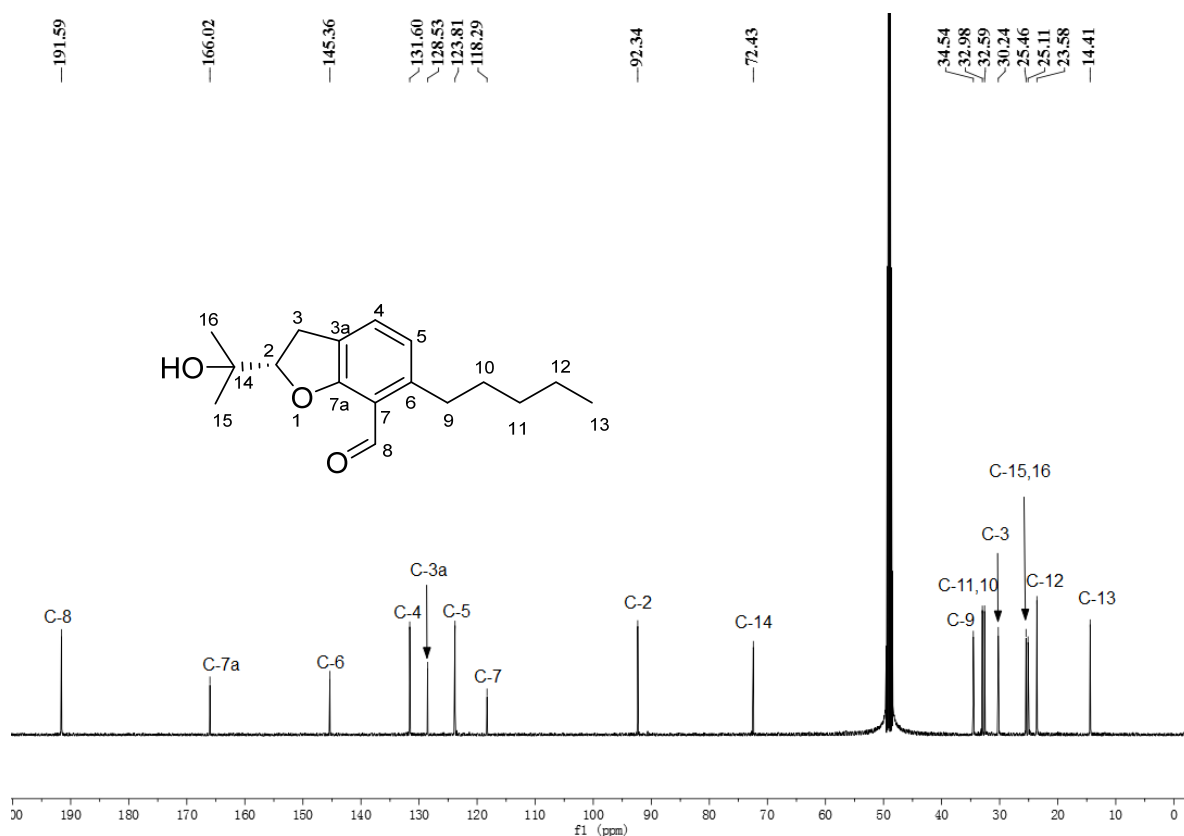


**Figure S60.** HMBC spectrum of (2*S*)-annullatin B (**7**) in CD<sub>3</sub>OD

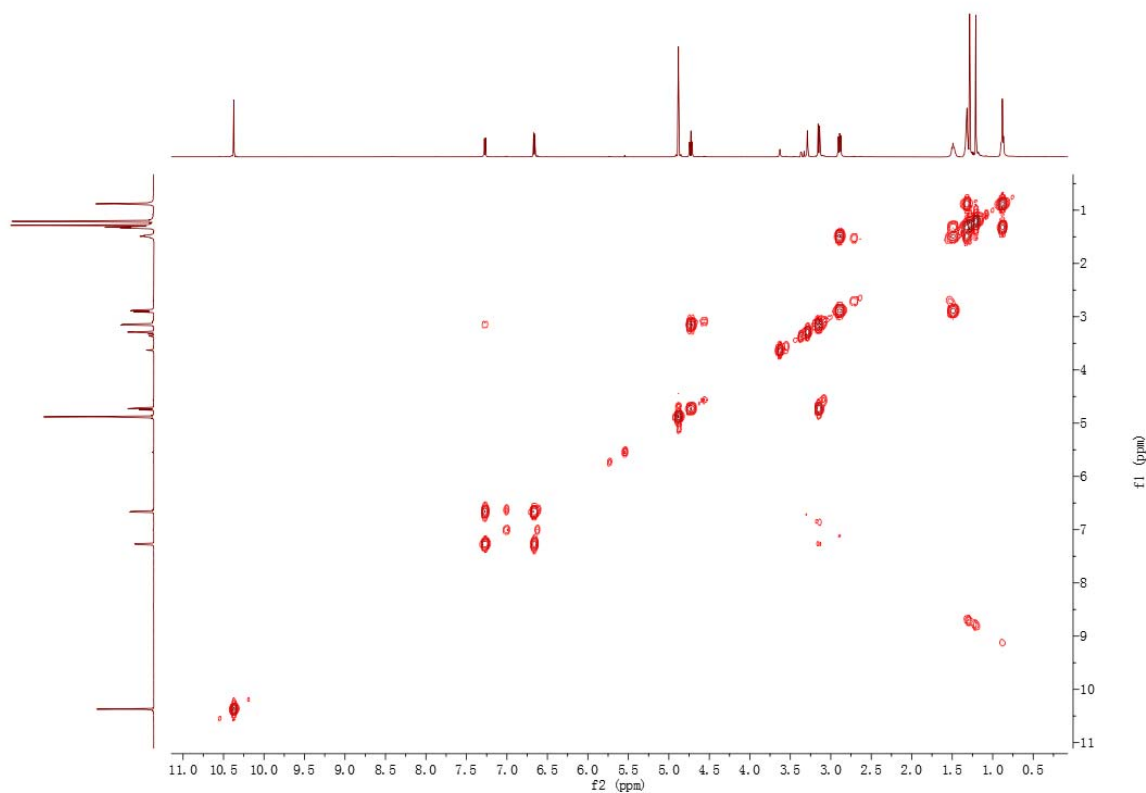


**Figure S61.** <sup>1</sup>H NMR spectrum of (2*S*)-annullatin A (**8**) in CD<sub>3</sub>OD (500 MHz)

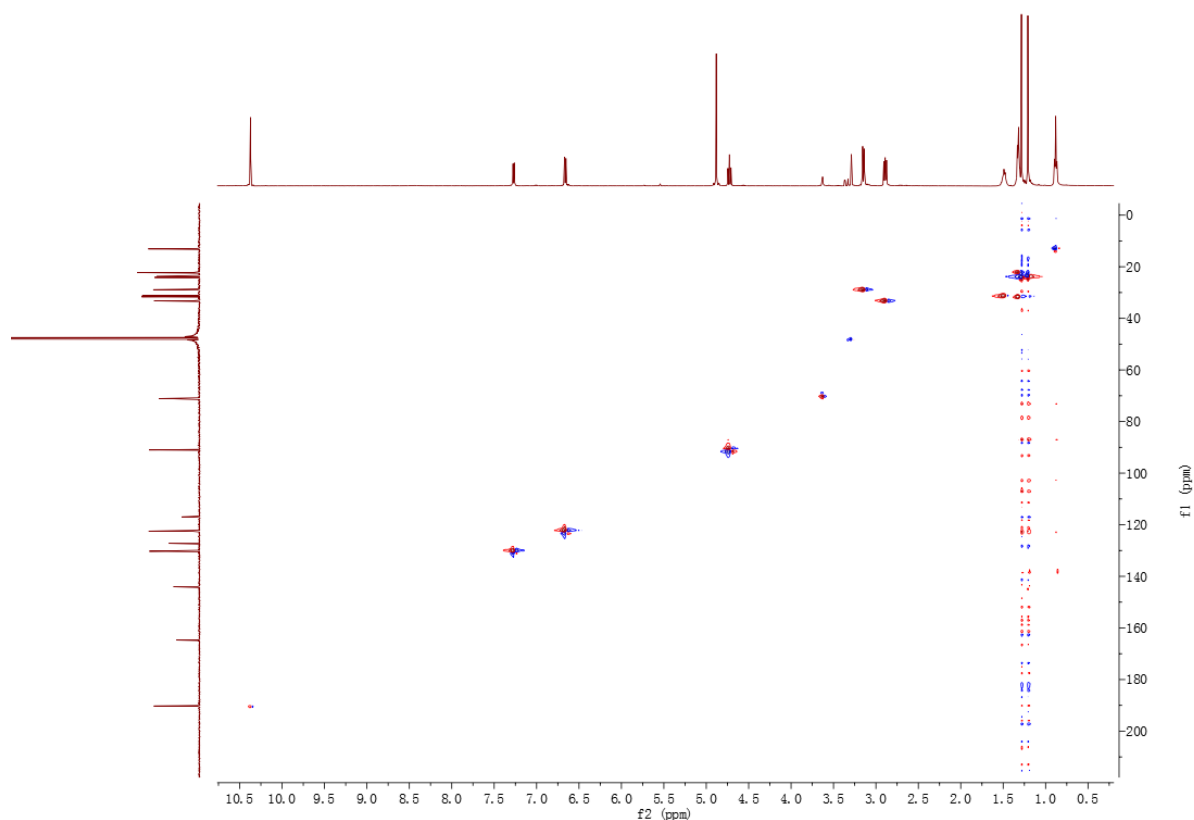




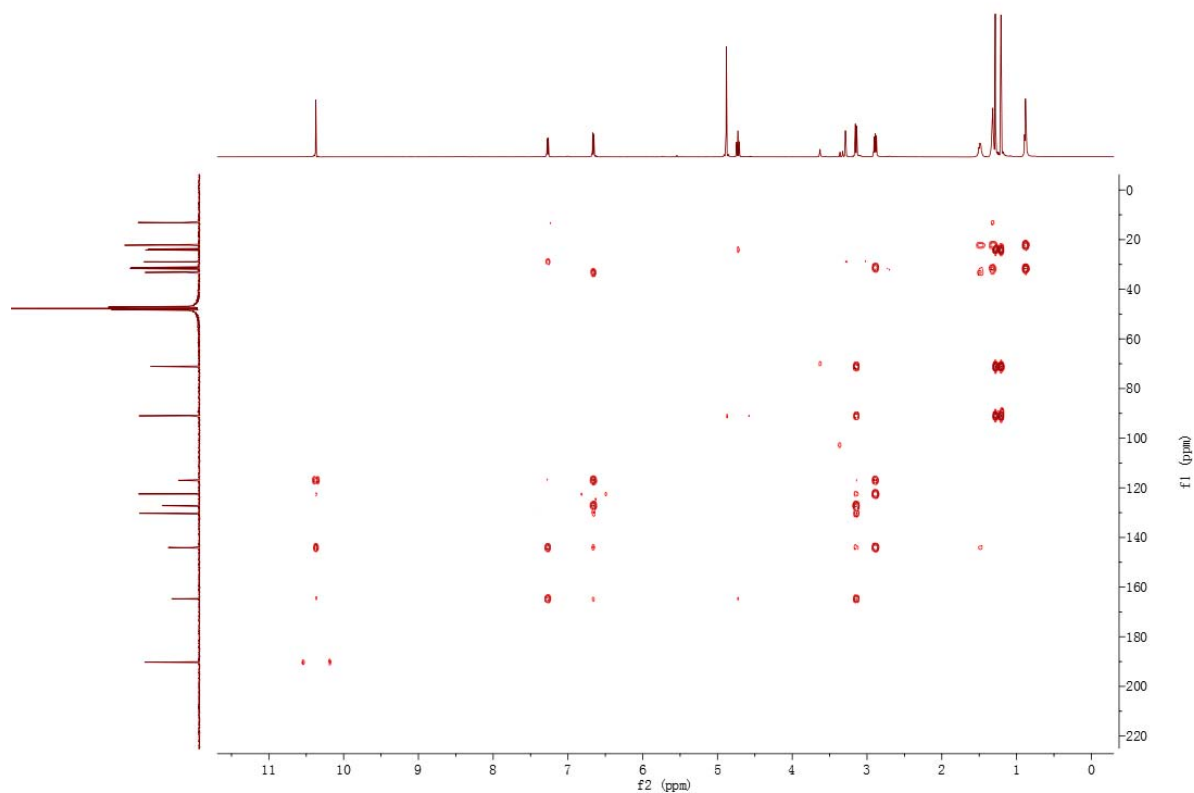
**Figure S62.**  $^{13}\text{C}$  NMR spectrum of (2S)-annullatin A (**8**) in  $\text{CD}_3\text{OD}$  (125 MHz)



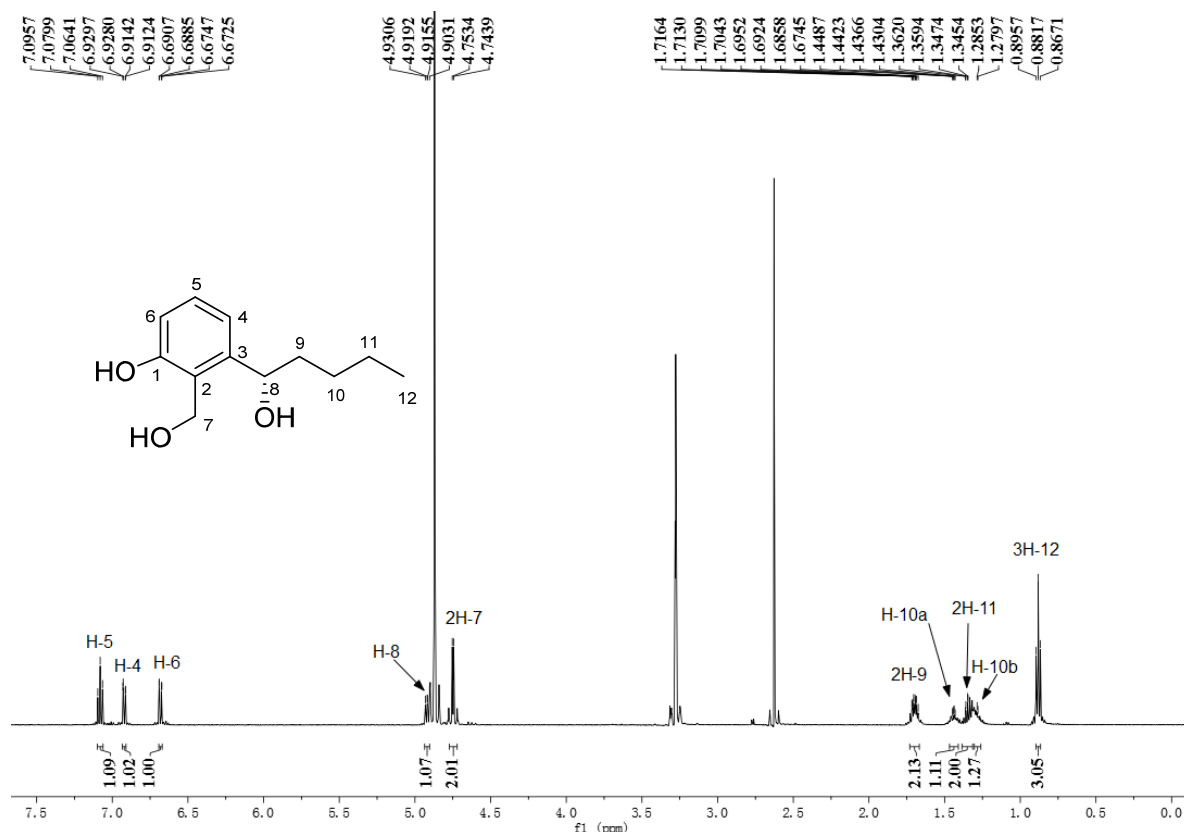
**Figure S63.**  $^1\text{H}$ - $^1\text{H}$  COSY spectrum of (2S)-annullatin A (**8**) in  $\text{CD}_3\text{OD}$



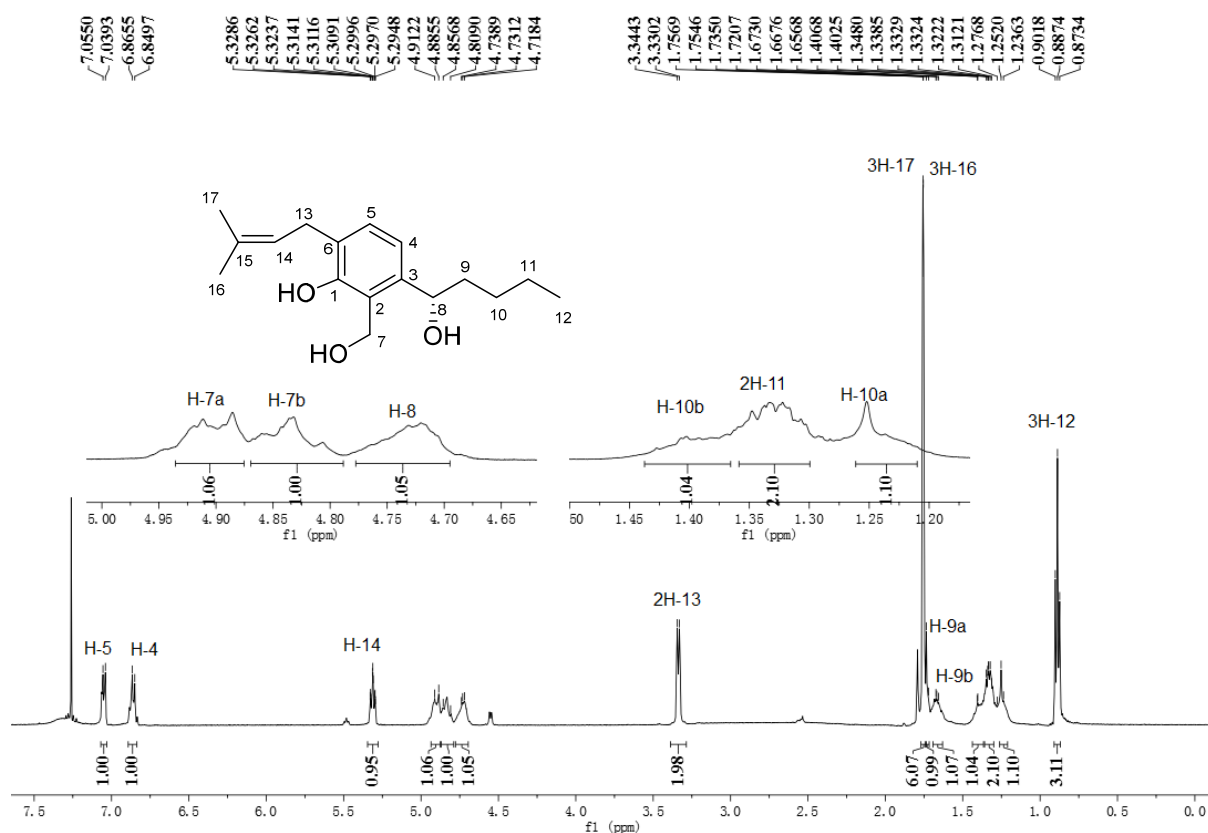
**Figure S64.** HSQC spectrum of (2*S*)-annullatin A (**8**) in CD<sub>3</sub>OD



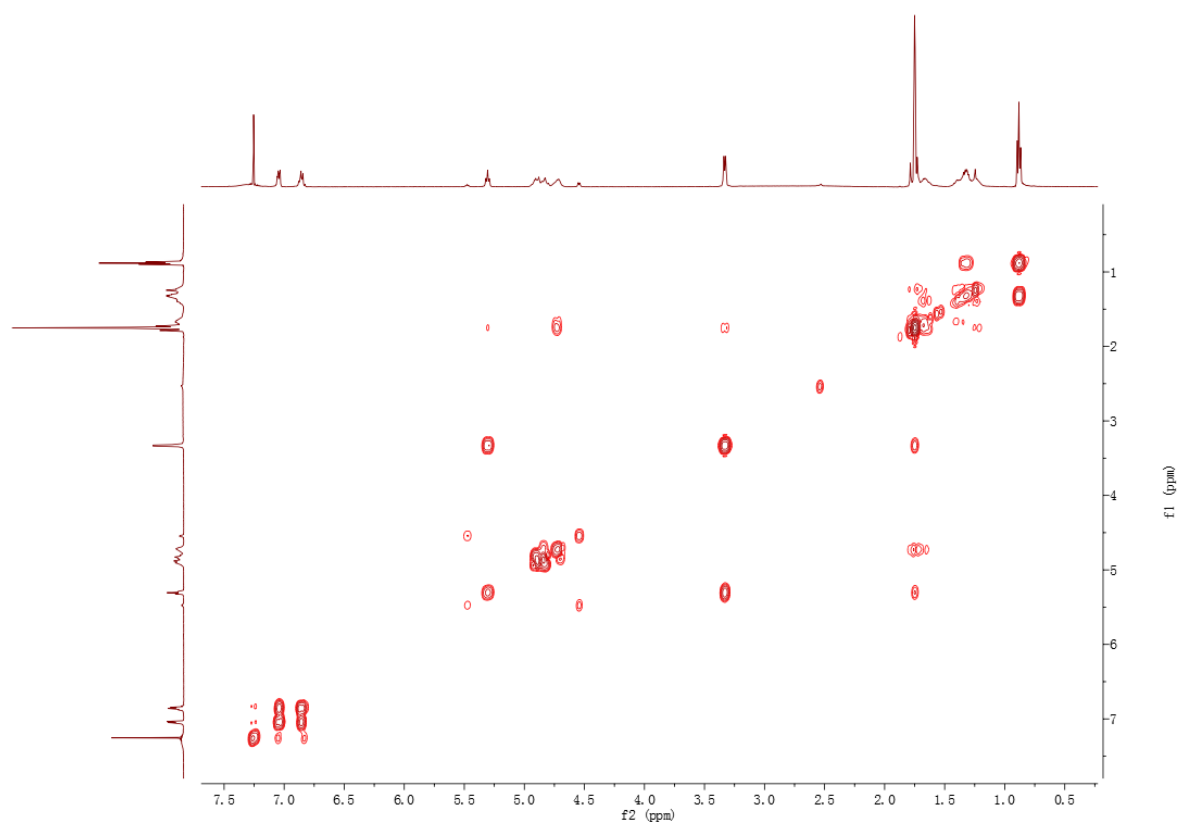
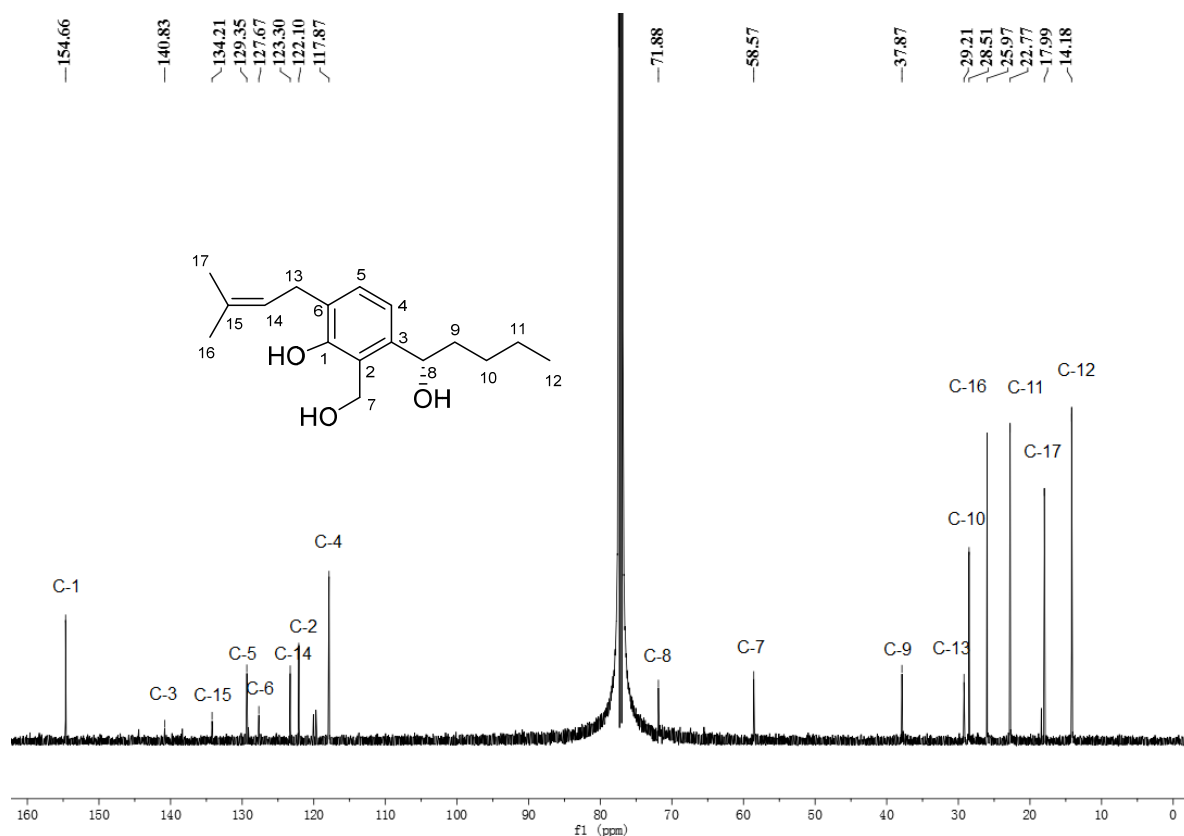
**Figure S65.** HMBC spectrum of (2*S*)-annullatin A (**8**) in CD<sub>3</sub>OD



**Figure S66.** <sup>1</sup>H NMR spectrum of (8S)-annullatin E (**9**) in CD<sub>3</sub>OD (500 MHz)



**Figure S67.** <sup>1</sup>H NMR spectrum of (8S)-annullatin J (**10**) in CDCl<sub>3</sub> (500 MHz)



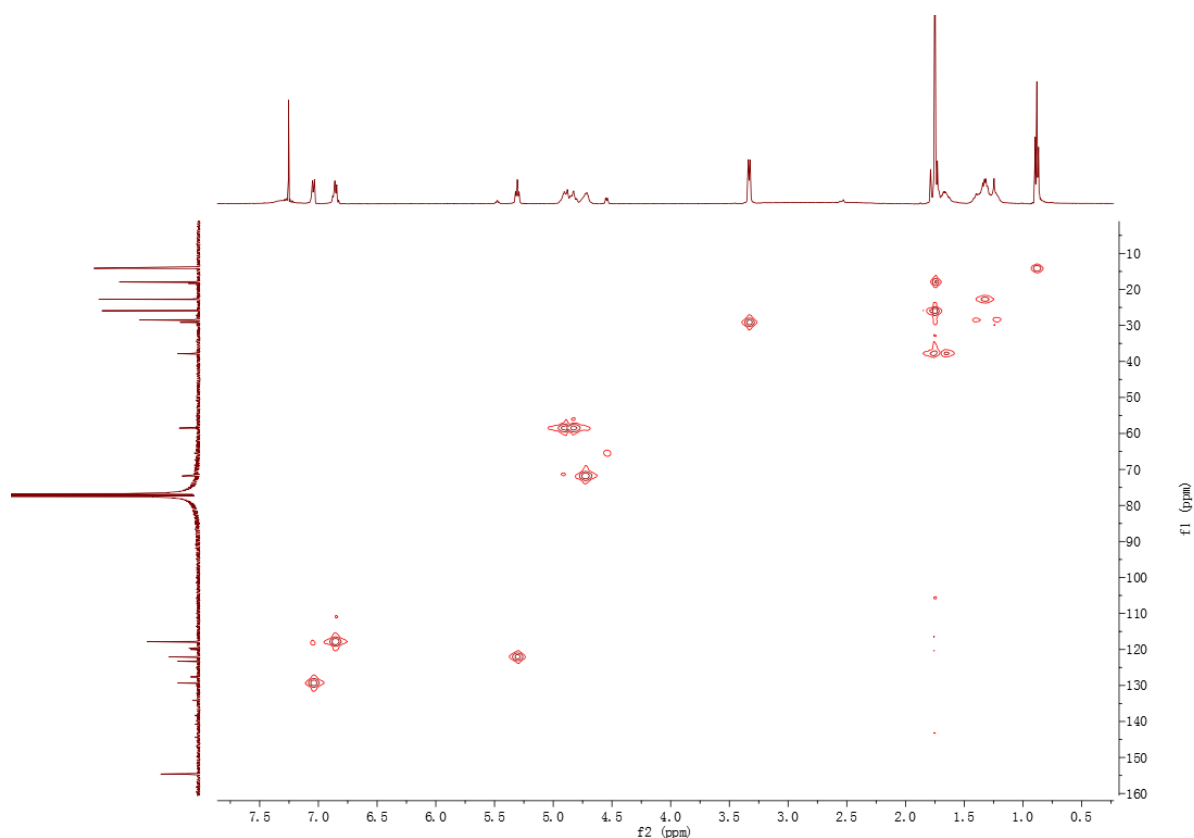


**Figure S70.** HSQC spectrum of (8*S*)-annullatin J (**10**) in CDCl<sub>3</sub>

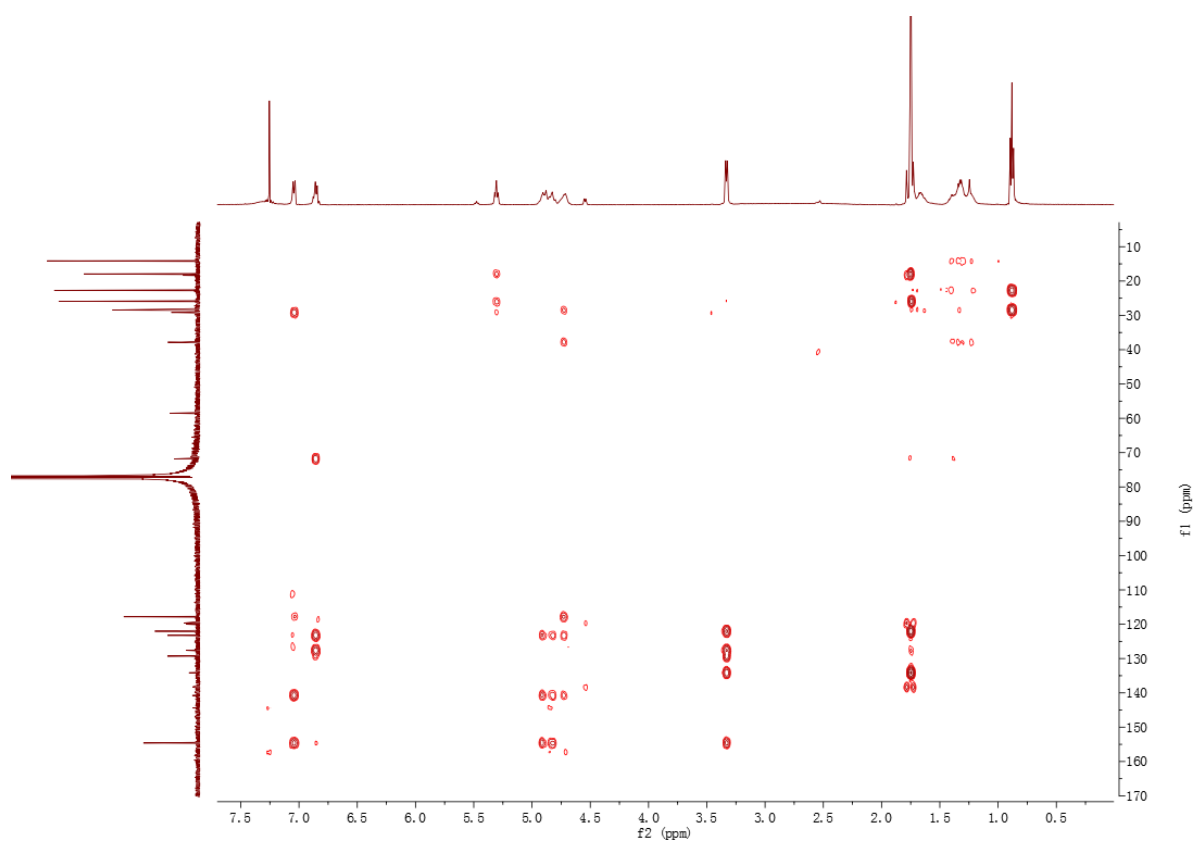


**Figure S71.** HMBC spectrum of (8*S*)-annullatin J (**10**) in CDCl<sub>3</sub>

## Supplementary References

- (1) Li, W.; Fan, A.; Wang, L.; Zhang, P.; Liu, Z.; An, Z.; Yin, W.-B. Asperphenamate biosynthesis reveals a novel two-module NRPS system to synthesize amino acid esters in fungi. *Chem. Sci.* **2018**, *9*, 2589.
- (2) Yin, W. B.; Chooi, Y. H.; Smith, A. R.; Cacho, R. A.; Hu, Y.; White, T. C.; Tang, Y. Discovery of cryptic polyketide metabolites from dermatophytes using heterologous expression in *Aspergillus nidulans*. *ACS Synth. Biol.* **2013**, *2*, 629.
- (3) Chiang, Y. M.; Ahuja, M.; Oakley, C. E.; Entwistle, R.; Asokan, A.; Zutz, C.; Wang, C. C.; Oakley, B. R. Development of genetic dereplication strains in *Aspergillus nidulans* results in the discovery of aspercryptin. *Angew. Chem., Int. Ed. Engl.* **2016**, *55*, 1662.
- (4) Mojardín, L.; Vega, M.; Moreno, F.; Schmitz, H. P.; Heinisch, J. J.; Rodicio, R. Lack of the NAD<sup>+</sup>-dependent glycerol 3-phosphate dehydrogenase impairs the function of transcription factors Sip4 and Cat8 required for ethanol utilization in *Kluyveromyces lactis*. *Fungal. Genet. Biol.* **2018**, *111*, 16.
- (5) Nies, J.; Ran, H.; Wohlgemuth, V.; Yin, W. B.; Li, S.-M. Biosynthesis of the prenylated salicylaldehyde flavoglaucon requires temporary reduction to salicyl alcohol for decoration before reoxidation to the final product. *Org. Lett.* **2020**, *22*, 2256.
- (6) Fan, J.; Liao, G.; Kindinger, F.; Ludwig-Radtke, L.; Yin, W.-B.; Li, S.-M. Peniphenone and penilactone formation in *Penicillium crustosum* via 1,4-Michael additions of *ortho*-quinone methide from hydroxyclovatol to  $\gamma$ -butyrolactones from crustosic acid. *J. Am. Chem. Soc.* **2019**, *141*, 4225.
- (7) Xiang, P.; Ludwig-Radtke, L.; Yin, W.-B.; Li, S.-M. Isocoumarin formation by heterologous gene expression and modification by host enzymes. *Org. Biomol. Chem.* **2020**, *18*, 4946.
- (8) Jacobus, A. P. and Gross, J. Optimal cloning of PCR fragments by homologous recombination in *Escherichia coli*. *PLoS. One.* **2015**, *10*, e0119221.
- (9) Zheng, L.; Yang, Y.; Wang, H.; Fan, A.; Zhang, L.; Li, S.-M. Ustethylin biosynthesis implies phenethyl derivative formation in *Aspergillus ustus*. *Org. Lett.* **2020**, *22*, 7837.
- (10) O'Boyle, N. M.; Banck, M.; James, C. A.; Morley, C.; Vandermeersch, T.; Hutchison, G. R. Open Babel: An open chemical toolbox. *J. Cheminform.* **2011**, *3*, 33.
- (11) Bannwarth, C.; Ehlert, S.; Grimme, S. GFN2-xTB—An accurate and broadly parametrized self-consistent tight-binding quantum chemical method with multipole electrostatics and density-dependent dispersion contributions. *J. Chem. Theory Comput.* **2019**, *15*, 1652.
- (12) Bruhn, T.; Schaumlöffel, A.; Hemberger, Y.; Bringmann, G. SpecDis: Quantifying the comparison of calculated and experimental electronic circular dichroism spectra. *Chirality* **2013**, *25*, 243.
- (13) Gillot, G.; Jany, J. L.; Dominguez-Santos, R.; Poirier, E.; Debaets, S.; Hidalgo, P. I.; Ullan, R. V.; Coton, E.; Coton, M. Genetic basis for mycophenolic acid production and strain-dependent production variability in *Penicillium roqueforti*. *Food Microbiol* **2017**, *62*, 239.
- (14) Asai, T.; Luo, D.; Obara, Y.; Taniguchi, T.; Monde, K.; Yamashita, K.; Oshima, Y. Dihydrobenzofurans as cannabinoid receptor ligands from *Cordyceps annulata*, an entomopathogenic fungus cultivated in the presence of an HDAC inhibitor. *Tetrahedron Lett.* **2012**, *53*, 2239.
- (15) Chang, J. C.; Hsiao, G.; Lin, R. K.; Kuo, Y. H.; Ju, Y. M.; Lee, T. H. Bioactive constituents from the termite nest-derived medicinal fungus *Xylaria nigripes*. *J. Nat. Prod.* **2017**, *80*, 38.

## 5 Conclusions and future prospects

This thesis presented multiple approaches to study the biosynthetic pathways of aromatic fungal SMs. Enzymes involved in the biosynthesis of NPs catalyze an expansive array of chemical transformations for the construction or modification of secondary metabolites. Various bioinformatic tools and genetic manipulation strategies enabled the investigation on the enzymatic assembly lines of different fungal product scaffolds.

In the course of the study in *Penicillium crustosum*, two NRPKS genes were functionally identified by heterologous expression, domain deletion and recombination, as well as feeding experiments. The isocoumarin synthase gene *pcr9304* was successfully heterologously expressed in the established and frequently used host *Aspergillus nidulans* and led to the accumulation of three isocoumarins. Precursor feeding experiments revealed that the initial PKS product can be converted by the host enzymes to its hydroxylated and methylated derivatives. These results provided one additional example that unexpected further modifications of an enzyme product can take place in a heterologous host. Heterologous expression of another PKS gene *oesA* from *P. crustosum* led to the identification of 3-orsellinoxypropanoic acid. Domain deletion and recombination proved that OesA was a bifunctional NRPKS, which catalyzes not only the formation of orsellinic acid but also its transfer to 3-hydroxypropanoic acid. Both ACP domains contribute independently and complementarily to the product formation. Isotopic feeding experiments confirmed the origin of 3-orsellinoxypropanoic acid, in which only the orsellinyl residue is derived from acetate.

Inspired by the flavoglaucon biosynthesis, an eleven-gene (*anu*) cluster containing a HRPKS AnuA was identified to be responsible for the biosynthesis of annullatins in *Penicillium roqueforti*. Annullatins were isolated from the ascomycetous fungus *Cordyceps annullata* and exhibited potent agonistic activities toward the cannabinoid receptors. However, little was known about their biosynthesis, especially on the formation of the lactone ring in annullatin D, and the involved enzymes prior to our study. In the biosynthesis of annullatins, a combination of *in vitro* enzymatic studies and heterologous expression *in vivo*, was used to understand how alkylated aromatic polyketide with a fused dihydrobenzofuran lactone ring system was formed through enzymatic or nonenzymatic reactions. The annullatin backbone is assembled by cooperation of AnuABC and hydroxylated at the C5 alkyl chain by the cytochrome P450 AnuE. The prenyltransferase AnuH subsequently installs one isoprenyl group at the benzene ring to form annullatin J (**15**), which then undergoes a dihydrobenzofuran ring formation between the prenyl and the phenolic hydroxyl groups, resulting in two diastereomers **9** and **17** by enzymatic or non-enzymatic reactions. After that, the alcohol at the C5 side chain of **17** was oxidized to a keto group by the SDR AnuF and further acetylated by the host enzymes. The BBE-like enzyme AnuG-catalyzes a five-member lactone ring formation in **9** to give annullatin D (**7**). As a result, this study demonstrated a highly programmed biosynthetic pathway for annullatins. Particularly, we identified a new BBE-like enzyme for oxidative lactonization between two hydroxyl groups.

## CONCLUSION AND FUTURE PROSPECTS

---

For future prospects, the following works can be performed:

- Although the biosynthetic pathway of annullatin has been identified, the initial aromatization mechanism for the polyketide core structure is still unclear. Biochemical characterization of the two tailoring enzymes AnuB and AnuC may provide new insights into the unique aromatization involved in this pathway
- Obtain recombinant BBE-like enzyme AnuG to understand the detailed catalytic mechanism for the oxidative lactonization
- Further characterization of more BBE-like enzymes to expand the structural diversity by chemoenzymatic strategies
- Targeted protein engineering of the prenyltransferase AnuH can also be performed to expand the substrate specificity and prenyl donor space
- Discover other promising BGCs for interesting natural product biosynthesis in *P. roqueforti*
- Ongoing investigations on the biosynthetic machinery of other alkylated aromatic polyketides from other *Penicillium* strains



## 6 References

1. Walsh, C. T., Tang, Y., *Natural product biosynthesis*. Royal Society of Chemistry, **2017**.
2. Wiemann, P., Keller, N. P., Strategies for mining fungal natural products. *Journal of Industrial Microbiology and Biotechnology* **2014**, *41* (2), 301-313.
3. Dufour, N., Rao, R. P., Secondary metabolites and other small molecules as intercellular pathogenic signals. *FEMS Microbiology Letters* **2011**, *314* (1), 10-17.
4. Yim, G., Huimi Wang, H., Davies FRS, J., Antibiotics as signalling molecules. *Philosophical Transactions of the Royal Society B: Biological Sciences* **2007**, *362* (1483), 1195-1200.
5. Bérdy, J., Thoughts and facts about antibiotics: Where we are now and where we are heading. *The Journal of Antibiotics* **2012**, *65* (8), 385-395.
6. Bérdy, J., Bioactive microbial metabolites. *The Journal of Antibiotics* **2005**, *58* (1), 1-26.
7. Azmir, J., Zaidul, I. S. M., Rahman, M. M., Sharif, K. M., Mohamed, A., Sahena, F., Jahurul, M. H. A., Ghafoor, K., Norulaini, N. A. N., Omar, A. K. M., Techniques for extraction of bioactive compounds from plant materials: a review. *Journal of Food Engineering* **2013**, *117* (4), 426-436.
8. Bennett, R. J., Turgeon, B. G., Fungal sex: the Ascomycota. *Microbiology Spectrum* **2016**, *4* (5), 4.5.20.
9. Webster, J., Weber, R., *Introduction to fungi*. Cambridge University Press, **2007**.
10. Fischer, R., Zekert, N., Takeshita, N., Polarized growth in fungi – interplay between the cytoskeleton, positional markers and membrane domains. *Molecular Microbiology* **2008**, *68* (4), 813-826.
11. Rohlf, M., Churchill, A. C. L., Fungal secondary metabolites as modulators of interactions with insects and other arthropods. *Fungal Genetics and Biology* **2011**, *48* (1), 23-34.
12. Brakhage, A. A., Regulation of fungal secondary metabolism. *Nature Reviews Microbiology* **2013**, *11* (1), 21-32.
13. Fox, E. M., Howlett, B. J., Secondary metabolism: regulation and role in fungal biology. *Current Opinion in Microbiology* **2008**, *11* (6), 481-487.
14. Rodrigues, A. P. D., Carvalho, A. S. C., Santos, A. S., Alves, C. N., do Nascimento, J. L. M., Silva, E. O., Kojic acid, a secondary metabolite from *Aspergillus* sp., acts as an inducer of macrophage activation. *Cell Biology International* **2011**, *35* (4), 335-343.
15. Hoffmeister, D., Keller, N. P., Natural products of filamentous fungi: enzymes, genes, and their regulation. *Natural Product Reports* **2007**, *24* (2), 393-416.
16. Chávez, R., Fierro, F., García-Rico, R. O., Vaca, I., Filamentous fungi from extreme environments as a promising source of novel bioactive secondary metabolites. *Frontiers in Microbiology* **2015**, *6*, 903.
17. Demain, A. L., Sanchez, S., Microbial drug discovery: 80 years of progress. *The Journal of Antibiotics* **2009**, *62* (1), 5-16.
18. Lim, F. Y., Keller, N. P., Spatial and temporal control of fungal natural product synthesis. *Natural Product Reports* **2014**, *31* (10), 1277-1286.
19. Hill, A. M., The biosynthesis, molecular genetics and enzymology of the polyketide-derived metabolites. *Natural Product Reports* **2006**, *23* (2), 256-320.
20. Priest, J. W., Light, R. J., Patulin biosynthesis: epoxidation of toluquinol and gentisyl alcohol by particulate preparations from *Penicillium patulum*. *Biochemistry* **1989**, *28* (23), 9192-9200.
21. Puel, O., Galtier, P., Oswald, I. P., Biosynthesis and toxicological effects of patulin. *Toxins* **2010**, *2* (4), 613-631.

## REFERENCES

---

22. Forrester, P. I., Gaucher, G. M., Conversion of 6-methylsalicylic acid into patulin by *Penicillium urticae*. *Biochemistry* **1972**, 11 (6), 1102-1107.
23. Blanc, P. J., Loret, M. O., Goma, G., Production of citrinin by various species of *Monascus*. *Biotechnology Letters* **1995**, 17 (3), 291-294.
24. He, Y., Cox, R. J., The molecular steps of citrinin biosynthesis in fungi. *Chemical Science* **2016**, 7 (3), 2119-2127.
25. Davison, J., al Fahad, A., Cai, M., Song, Z., Yehia, S. Y., Lazarus, C. M., Bailey, A. M., Simpson, T. J., Cox, R. J., Genetic, molecular, and biochemical basis of fungal tropolone biosynthesis. *Proceedings of the National Academy of Sciences* **2012**, 109 (20), 7642-7647.
26. Tobert, J. A., Lovastatin and beyond: the history of the HMG-CoA reductase inhibitors. *Nature Reviews Drug Discovery* **2003**, 2 (7), 517-526.
27. Hesseltine, C., Shotwell, O. L., Ellis, J., Stubblefield, R., Aflatoxin formation by *Aspergillus flavus*. *Bacteriological Reviews* **1966**, 30 (4), 795-805.
28. Li, F.-Q., Yoshizawa, T., Kawamura, O., Luo, X.-Y., Li, Y.-W., Aflatoxins and fumonisins in corn from the high-incidence area for human hepatocellular carcinoma in Guangxi, China. *Journal of Agricultural and Food Chemistry* **2001**, 49 (8), 4122-4126.
29. Bills, G. F., Gloer, J. B., *Biologically active secondary metabolites from the fungi*. American Society for Microbiology Press, **2017**.
30. Walsh, C. T., Insights into the chemical logic and enzymatic machinery of NRPS assembly lines. *Natural Product Reports* **2016**, 33 (2), 127-135.
31. Wainwright, M., *Miracle cure: the story of penicillin and the golden age of antibiotics*. Blackwell Press, **1990**.
32. Kardos, N., Demain, A. L., Penicillin: the medicine with the greatest impact on therapeutic outcomes. *Applied Microbiology and Biotechnology* **2011**, 92 (4), 677-687.
33. Abraham, E. P., Newton, G. G., The structure of cephalosporin C. *Biochemical Journal* **1961**, 79 (2), 377-393.
34. Scharf, D. H., Heinekamp, T., Remme, N., Hortschansky, P., Brakhage, A. A., Hertweck, C., Biosynthesis and function of gliotoxin in *Aspergillus fumigatus*. *Applied Microbiology and Biotechnology* **2012**, 93 (2), 467-472.
35. Gardiner, D. M., Howlett, B. J., Bioinformatic and expression analysis of the putative gliotoxin biosynthetic gene cluster of *Aspergillus fumigatus*. *FEMS Microbiology Letters* **2005**, 248 (2), 241-248.
36. Denning, D. W., Echinocandins and pneumocandins – a new antifungal class with a novel mode of action. *The Journal of Antimicrobial Chemotherapy* **1997**, 40 (5), 611-614.
37. Matsuda, S., Koyasu, S., Mechanisms of action of cyclosporine. *Immunopharmacology* **2000**, 47 (2), 119-125.
38. Miziorko, H. M., Enzymes of the mevalonate pathway of isoprenoid biosynthesis. *Archives of Biochemistry and Biophysics* **2011**, 505 (2), 131-143.
39. Kellogg, B. A., Poulter, C. D., Chain elongation in the isoprenoid biosynthetic pathway. *Current Opinion in Chemical Biology* **1997**, 1 (4), 570-578.
40. Proctor, R. H., Hohn, T. M., Aristolochene synthase. Isolation, characterization, and bacterial expression of a sesquiterpenoid biosynthetic gene (*Ari1*) from *Penicillium roqueforti*. *Journal of Biological Chemistry* **1993**, 268 (6), 4543-4548.
41. Bömke, C., Tudzynski, B., Diversity, regulation, and evolution of the gibberellin biosynthetic pathway in fungi compared to plants and bacteria. *Phytochemistry* **2009**, 70 (15), 1876-1893.

## REFERENCES

42. Fernandes, P., Fusidic Acid: a bacterial elongation factor inhibitor for the oral treatment of acute and chronic staphylococcal infections. *Cold Spring Harbor Perspectives in Medicine* **2016**, 6 (1), a025437.
43. Gerhards, N., Neubauer, L., Tudzynski, P., Li, S.-M., Biosynthetic pathways of ergot alkaloids. *Toxins* **2014**, 6 (12), 3281-3295.
44. Xu, W., Gavia, D. J., Tang, Y., Biosynthesis of fungal indole alkaloids. *Natural Product Reports* **2014**, 31 (10), 1474-1487.
45. Daley, S.-k., Cordell, G. A., Biologically significant and recently isolated alkaloids from endophytic fungi. *Journal of Natural Products* **2021**, 84 (3), 871-897.
46. Li, Y.-X., Himaya, S. W. A., Dewapriya, P., Zhang, C., Kim, S.-K., Fumigaclavine C from a marine-derived fungus *Aspergillus Fumigatus* induces apoptosis in MCF-7 breast cancer cells. *Marine Drugs* **2013**, 11 (12), 5063-5086.
47. Zhu, Y.-X., Yao, L.-Y., Jiao, R.-H., Lu, Y.-H., Tan, R.-X., Enhanced production of fumigaclavine C in liquid culture of *Aspergillus fumigatus* under a two-stage process. *Bioresource Technology* **2014**, 152, 162-168.
48. Haynes, S. W., Gao, X., Tang, Y., Walsh, C. T., Complexity generation in fungal peptidyl alkaloid biosynthesis: a two-enzyme pathway to the hexacyclic MDR export pump inhibitor ardeemin. *ACS Chemical Biology* **2013**, 8 (4), 741-748.
49. Houbaken, J., Frisvad, J. C., Samson, R. A., Fleming's penicillin producing strain is not *Penicillium chrysogenum* but *P. rubens*. *IMA Fungus* **2011**, 2 (1), 87-95.
50. Larsen, T. O., Frisvad, J. C., Characterization of volatile metabolites from 47 *Penicillium* taxa. *Mycological Research* **1995**, 99 (10), 1153-1166.
51. Kozlovskii, A. G., Zhelifonova, V. P., Antipova, T. V., Fungi of the genus *Penicillium* as producers of physiologically active compounds. *Applied Biochemistry and Microbiology* **2013**, 49 (1), 1-10.
52. Frisvad, J. C., Samson, R. A., Polyphasic taxonomy of *Penicillium* subgenus *Penicillium*. A guide to identification of food and air-borne terverticillate *Penicillia* and their mycotoxin. *Studies in Mycology* **2004**, 49 (1), 1-174.
53. Nelson, J. H., Production of blue cheese flavor via submerged fermentation by *Penicillium roqueforti*. *Journal of Agricultural and Food Chemistry* **1970**, 18 (4), 567-569.
54. Lessard, M.-H., Bélanger, G., St-Gelais, D., Labrie, S., The composition of Camembert cheese-ripening cultures modulates both mycelial growth and appearance. *Applied and Environmental Microbiology* **2012**, 78 (6), 1813-1819.
55. Endo, A., A historical perspective on the discovery of statins. *Proceedings of the Japan Academy, Series B, Physical and Biological Sciences* **2010**, 86 (5), 484-493.
56. Ballester, A.-R., Marcet-Houben, M., Levin, E., Sela, N., Selma-Lázaro, C., Carmona, L., Wisniewski, M., Droby, S., González-Candelas, L., Gabaldón, T., Genome, transcriptome, and functional analyses of *Penicillium expansum* provide new insights into secondary metabolism and pathogenicity. *Molecular Plant-Microbe Interactions* **2015**, 28 (3), 232-248.
57. Li, B., Zong, Y., Du, Z., Chen, Y., Zhang, Z., Qin, G., Zhao, W., Tian, S., Genomic characterization reveals insights into patulin biosynthesis and pathogenicity in *Penicillium* species. *Molecular Plant-Microbe Interactions* **2015**, 28 (6), 635-647.
58. Marcet-Houben, M., Ballester, A.-R., de la Fuente, B., Harries, E., Marcos, J. F., González-Candelas, L., Gabaldón, T., Genome sequence of the necrotrophic fungus *Penicillium digitatum*, the main postharvest pathogen of citrus. *BMC Genomics* **2012**, 13 (1), 646.
59. Frisvad, J. C., *Penicillium/Penicillia in food production*. Elsevier Press, **2014**.
60. Kalinina, S. A., Jagels, A., Cramer, B., Geisen, R., Humpf, H.-U., Influence of environmental factors on the production of penitrems A–F by *Penicillium crustosum*. *Toxins* **2017**, 9 (7), 210.

## REFERENCES

61. Su, S.-S., Song, A.-H., Chen, G., Wang, H.-F., Li, Z.-Q., Pei, Y.-H., Two new indole-diterpenoids from the fungus *Penicillium crustosum* YN-HT-15. *Journal of Asian Natural Products Research* **2014**, *16* (3), 285-289.
62. Wang, H., Chen, G., Liu, Y., Hua, H., Bai, J., Pei, Y.-H., <sup>1</sup>H and <sup>13</sup>C NMR assignments of two new piperazine-trione from the fungus *Penicillium crustosum* YN-HT-15. *Magnetic Resonance in Chemistry* **2015**, *53* (8), 620-623.
63. Wu, G., Ma, H., Zhu, T., Li, J., Gu, Q., Li, D., Penilactones A and B, two novel polyketides from Antarctic deep-sea derived fungus *Penicillium crustosum* PRB-2. *Tetrahedron* **2012**, *68* (47), 9745-9749.
64. Liu, Y.-P., Chen, G., Wang, H.-F., Zhang, X.-L., Pei, Y.-H., Two new compounds from the fungus *Penicillium crustosum* YN-HT-15. *Journal of Asian Natural Products Research* **2014**, *16* (3), 281-284.
65. Feng, D., Tan, L., Qiu, L., Ju, F., Kuang, Q.-X., Chen, J.-F., Li, X.-N., Gu, Y.-C., Guo, D.-L., Deng, Y., Three new polyketides produced by *Penicillium crustosum*, a mycoparasitic fungus from *Ophiocordyceps sinensis*. *Phytochemistry Letters* **2020**, *36*, 150-155.
66. Wu, G., *Studies on secondary metabolites of three different marine environment-derived fungi: structures and bioactivities*. Dissertation, Ocean University of China, **2014**.
67. Fan, J., Liao, G., Kindinger, F., Ludwig-Radtke, L., Yin, W.-B., Li, S.-M., Peniphenone and penilactone formation in *Penicillium crustosum* via 1,4-michael additions of *ortho*-Quinone methide from hydroxyclovatol to  $\gamma$ -butyrolactones from crustosic acid. *Journal of the American Chemical Society* **2019**, *141* (10), 4225-4229.
68. Kindinger, F., Nies, J., Becker, A., Zhu, T., Li, S.-M., Genomic locus of a *Penicillium crustosum* pigment as integration site for secondary metabolite gene expression. *ACS Chemical Biology* **2019**, *14* (6), 1227-1234.
69. Coton, E., Coton, M., Hymery, N., Mounier, J., Jany, J.-L., *Penicillium roqueforti*: an overview of its genetics, physiology, metabolism and biotechnological applications. *Fungal Biology Reviews* **2020**, *34* (2), 59-73.
70. Abbas, A., Dobson, A. D. W., *Yeasts and Molds | Penicillium roqueforti*. Academic Press, **2011**.
71. Gillot, G., Jany, J.-L., Coton, M., Le Floch, G., Debaets, S., Ropars, J., López-Villavicencio, M., Dupont, J., Branca, A., Giraud, T., Coton, E., Insights into *Penicillium roqueforti* morphological and genetic diversity. *PLOS ONE* **2015**, *10* (6), e0129849.
72. Nielsen, K. F., Sumarah, M. W., Frisvad, J. C., Miller, J. D., Production of metabolites from the *Penicillium roqueforti* complex. *Journal of Agricultural and Food Chemistry* **2006**, *54* (10), 3756-3763.
73. Martín, J. F., Coton, M., *Fermented foods in health and disease prevention, chapter 12 - blue cheese: microbiota and fungal metabolites*. Academic Press, **2017**.
74. García-Estrada, C., Martín, J.-F., Biosynthetic gene clusters for relevant secondary metabolites produced by *Penicillium roqueforti* in blue cheeses. *Applied Microbiology and Biotechnology* **2016**, *100* (19), 8303-8313.
75. Cheeseman, K., Ropars, J., Renault, P., Dupont, J., Gouzy, J., Branca, A., Abraham, A.-L., Ceppi, M., Conseiller, E., Debuchy, R., Malagnac, F., Goarin, A., Silar, P., Lacoste, S., Sallet, E., Bensimon, A., Giraud, T., Brygoo, Y., Multiple recent horizontal transfers of a large genomic region in cheese making fungi. *Nature Communications* **2014**, *5* (1), 2876.
76. Keller, N. P., Hohn, T. M., Metabolic pathway gene clusters in filamentous fungi. *Fungal Genetics and Biology* **1997**, *21* (1), 17-29.
77. Skellam, E., Strategies for engineering natural product biosynthesis in fungi. *Trends in Biotechnology* **2019**, *37* (4), 416-427.
78. Keller, N. P., Turner, G., Bennett, J. W., Fungal secondary metabolism – from biochemistry to genomics. *Nature Reviews Microbiology* **2005**, *3* (12), 937-947.

## REFERENCES

79. Shendure, J., Balasubramanian, S., Church, G. M., Gilbert, W., Rogers, J., Schloss, J. A., Waterston, R. H., DNA sequencing at 40: past, present and future. *Nature* **2017**, *550* (7676), 345-353.
80. Rokas, A., Mead, M. E., Steenwyk, J. L., Raja, H. A., Oberlies, N. H., Biosynthetic gene clusters and the evolution of fungal chemodiversity. *Natural Product Reports* **2020**, *37* (7), 868-878.
81. Walton, J. D., Horizontal gene transfer and the evolution of secondary metabolite gene clusters in fungi: an hypothesis. *Fungal Genetics and Biology* **2000**, *30* (3), 167-171.
82. Fisch, K. M., Biosynthesis of natural products by microbial iterative hybrid PKS–NRPS. *RSC Advances* **2013**, *3* (40), 18228-18247.
83. Hawksworth, D. L., Lücking, R., Fungal diversity revisited: 2.2 to 3.8 million species. *Microbiology Spectrum* **2017**, *5* (4), 5.4.10.
84. Medema, M. H., de Rond, T., Moore, B. S., Mining genomes to illuminate the specialized chemistry of life. *Nature Reviews Genetics* **2021**, *22* (9), 553-571.
85. Meng, X., Fang, Y., Ding, M., Zhang, Y., Jia, K., Li, Z., Collemare, J., Liu, W., Developing fungal heterologous expression platforms to explore and improve the production of natural products from fungal biodiversity. *Biotechnology Advances* **2022**, *54*, 107866.
86. Greco, C., Keller, N. P., Rokas, A., Unearthing fungal chemodiversity and prospects for drug discovery. *Current Opinion in Microbiology* **2019**, *51*, 22-29.
87. Romsdahl, J., Wang, C. C. C., Recent advances in the genome mining of *Aspergillus* secondary metabolites (covering 2012 – 2018). *MedChemComm* **2019**, *10* (6), 840-866.
88. Lyu, H.-N., Liu, H.-W., Keller, N. P., Yin, W.-B., Harnessing diverse transcriptional regulators for natural product discovery in fungi. *Natural Product Reports* **2020**, *37* (1), 6-16.
89. Brakhage, A. A., Schroeckh, V., Fungal secondary metabolites – Strategies to activate silent gene clusters. *Fungal Genetics and Biology* **2011**, *48* (1), 15-22.
90. Barkal, L. J., Theberge, A. B., Guo, C.-J., Spraker, J., Rappert, L., Berthier, J., Brakke, K. A., Wang, C. C. C., Beebe, D. J., Keller, N. P., Berthier, E., Microbial metabolomics in open microscale platforms. *Nature Communications* **2016**, *7* (1), 10610.
91. Mosunova, O., Navarro-Muñoz, J. C., Collemare, J., The biosynthesis of fungal secondary metabolites: from fundamentals to biotechnological applications. *Reference Module in Life Sciences* **2021**, *2*, 458-476.
92. Ariantari, N. P., Daletos, G., Mándi, A., Kurtán, T., Müller, W. E. G., Lin, W., Ancheeva, E., Proksch, P., Expanding the chemical diversity of an endophytic fungus *Bulgaria inquinans*, an ascomycete associated with mistletoe, through an OSMAC approach. *RSC Advances* **2019**, *9* (43), 25119-25132.
93. Bode, H. B., Bethe, B., Höfs, R., Zeeck, A., Big effects from small changes: possible ways to explore nature's chemical diversity. *ChemBioChem* **2002**, *3* (7), 619-627.
94. Selegato, D. M., Freire, R. T., Pilon, A. C., Biasetto, C. R., de Oliveira, H. C., de Abreu, L. M., Araujo, A. R., da Silva Bolzani, V., Castro-Gamboa, I., Improvement of bioactive metabolite production in microbial cultures – a systems approach by OSMAC and deconvolution-based <sup>1</sup>HNMR quantification. *Magnetic Resonance in Chemistry* **2019**, *57* (8), 458-471.
95. Fan, A., Mi, W., Liu, Z., Zeng, G., Zhang, P., Hu, Y., Fang, W., Yin, W.-B., Deletion of a histone acetyltransferase leads to the pleiotropic activation of natural products in *Metarhizium robertsii*. *Organic Letters* **2017**, *19* (7), 1686-1689.
96. Szewczyk, E., Chiang, Y.-M., Oakley, C. E., Davidson, A. D., Wang, C. C. C., Oakley, B. R., Identification and characterization of the asperthecin gene cluster of *Aspergillus nidulans*. *Applied and Environmental Microbiology* **2008**, *74* (24), 7607-7612.
97. Cichewicz, R. H., Epigenome manipulation as a pathway to new natural product scaffolds and their congeners. *Natural Product Reports* **2010**, *27* (1), 11-22.

## REFERENCES

98. Yin, W.-B., Baccile, J. A., Bok, J. W., Chen, Y., Keller, N. P., Schroeder, F. C., A nonribosomal peptide synthetase-derived Iron(III) complex from the pathogenic fungus *Aspergillus fumigatus*. *Journal of the American Chemical Society* **2013**, *135* (6), 2064-2067.
99. Lim, F. Y., Hou, Y., Chen, Y., Oh, J.-H., Lee, I., Bugni, T. S., Keller, N. P., Genome-based cluster deletion reveals an endocrocin biosynthetic pathway in *Aspergillus fumigatus*. *Applied and Environmental Microbiology* **2012**, *78* (12), 4117-4125.
100. Bouhired, S., Weber, M., Kempf-Sontag, A., Keller, N. P., Hoffmeister, D., Accurate prediction of the *Aspergillus nidulans* terrequinone gene cluster boundaries using the transcriptional regulator LaeA. *Fungal Genetics and Biology* **2007**, *44* (11), 1134-1145.
101. Baba, S., Kinoshita, H., Nihira, T., Identification and characterization of *Penicillium citrinum* VeA and LaeA as global regulators for ML-236B production. *Current Genetics* **2012**, *58* (1), 1-11.
102. Yang, X.-L., Awakawa, T., Wakimoto, T., Abe, I., Three acyltetronic acid derivatives: noncanonical cryptic polyketides from *Aspergillus niger* identified by genome mining. *ChemBioChem* **2014**, *15* (11), 1578-1583.
103. Sørensen, J. L., Hansen, F. T., Sondergaard, T. E., Staerk, D., Lee, T. V., Wimmer, R., Klitgaard, L. G., Purup, S., Giese, H., Frandsen, R. J. N., Production of novel fusarielins by ectopic activation of the polyketide synthase 9 cluster in *Fusarium graminearum*. *Environmental Microbiology* **2012**, *14* (5), 1159-1170.
104. König, C. C., Scherlach, K., Schroeckh, V., Horn, F., Nietzsche, S., Brakhage, A. A., Hertweck, C., Bacterium induces cryptic meroterpenoid pathway in the pathogenic fungus *Aspergillus fumigatus*. *ChemBioChem* **2013**, *14* (8), 938-942.
105. Chooi, Y.-H., Fang, J., Liu, H., Filler, S. G., Wang, P., Tang, Y., Genome mining of a prenylated and immunosuppressive polyketide from pathogenic fungi. *Organic Letters* **2013**, *15* (4), 780-783.
106. Chiang, Y.-M., Oakley, C. E., Ahuja, M., Entwistle, R., Schultz, A., Chang, S.-L., Sung, C. T., Wang, C. C. C., Oakley, B. R., An efficient system for heterologous expression of secondary metabolite genes in *Aspergillus nidulans*. *Journal of the American Chemical Society* **2013**, *135* (20), 7720-7731.
107. Sakai, K., Kinoshita, H., Shimizu, T., Nihira, T., Construction of a citrinin gene cluster expression system in heterologous *Aspergillus oryzae*. *Journal of Bioscience and Bioengineering* **2008**, *106* (5), 466-472.
108. Bai, T., Quan, Z., Zhai, R., Awakawa, T., Matsuda, Y., Abe, I., Elucidation and heterologous reconstitution of chrodrimanin B biosynthesis. *Organic Letters* **2018**, *20* (23), 7504-7508.
109. Harvey, C. J. B., Tang, M., Schlecht, U., Horecka, J., Fischer, C. R., Lin, H.-C., Li, J., Naughton, B., Cherry, J., Miranda, M., Li, Y. F., Chu, A. M., Hennessy, J. R., Vandova, G. A., Inglis, D., Aiyar, R. S., Steinmetz, L. M., Davis, R. W., Medema, M. H., Sattely, E., Khosla, C., St. Onge, R. P., Tang, Y., Hillenmeyer, M. E., HEx: A heterologous expression platform for the discovery of fungal natural products. *Science Advances* **2018**, *4* (4), eaar5459.
110. Lam, K. N., Spanogiannopoulos, P., Soto-Perez, P., Alexander, M., Nalley, M. J., Bisanz, J. E., Nayak, R. R., Weakley, A. M., Yu, F. B., Turnbaugh, P. J., Phage-delivered CRISPR-Cas9 for strain-specific depletion and genomic deletions in the gut microbiome. *Cell Reports* **2021**, *37* (5), 109930.
111. He, Y., Wang, B., Chen, W., Cox, R. J., He, J., Chen, F., Recent advances in reconstructing microbial secondary metabolites biosynthesis in *Aspergillus* spp. *Biotechnology Advances* **2018**, *36* (3), 739-783.
112. Kjærboelling, I., Mortensen, U. H., Vesth, T., Andersen, M. R., Strategies to establish the link between biosynthetic gene clusters and secondary metabolites. *Fungal Genetics and Biology* **2019**, *130*, 107-121.
113. Ongley, S. E., Bian, X., Neilan, B. A., Müller, R., Recent advances in the heterologous expression of microbial natural product biosynthetic pathways. *Natural Product Reports* **2013**, *30* (8), 1121-1138.

## REFERENCES

---

114. Hannig, G., Makrides, S. C., Strategies for optimizing heterologous protein expression in *Escherichia coli*. *Trends in Biotechnology* **1998**, 16 (2), 54-60.
115. Baltz, R. H., *Streptomyces* and *Saccharopolyspora* hosts for heterologous expression of secondary metabolite gene clusters. *Journal of Industrial Microbiology and Biotechnology* **2010**, 37 (8), 759-772.
116. Lubertozzi, D., Keasling, J. D., Developing *Aspergillus* as a host for heterologous expression. *Biotechnology Advances* **2009**, 27 (1), 53-75.
117. Ikram, N. K. B. K., Zhan, X., Pan, X.-W., King, B. C., Simonsen, H. T., Stable heterologous expression of biologically active terpenoids in green plant cells. *Frontiers in Plant Science* **2015**, 6, 129.
118. Frommer, W. B., Ninnemann, O., Heterologous expression of genes in bacterial, fungal, animal, and plant cells. *Annual Review of Plant Biology* **1995**, 46 (1), 419-444.
119. Lau, J., Tran, C., Licari, P., Galazzo, J., Development of a high cell-density fed-batch bioprocess for the heterologous production of 6-deoxyerythronolide B in *Escherichia coli*. *Journal of Biotechnology* **2004**, 110 (1), 95-103.
120. Kealey, J. T., Liu, L., Santi, D. V., Betlach, M. C., Barr, P. J., Production of a polyketide natural product in nonpolyketide-producing prokaryotic and eukaryotic hosts. *Proceedings of the National Academy of Sciences* **1998**, 95 (2), 505-509.
121. Ma, S. M., Zhan, J., Watanabe, K., Xie, X., Zhang, W., Wang, C. C., Tang, Y., Enzymatic synthesis of aromatic polyketides using PKS4 from *Gibberella fujikuroi*. *Journal of the American Chemical Society* **2007**, 129 (35), 10642-10643.
122. Wawrzyn, G. T., Quin, M. B., Choudhary, S., López-Gallego, F., Schmidt-Dannert, C., Draft genome of *Omphalotus olearius* provides a predictive framework for sesquiterpenoid natural product biosynthesis in basidiomycota. *Chemistry and Biology* **2012**, 19 (6), 772-783.
123. Zabala, A. O., Xu, W., Chooi, Y.-H., Tang, Y., Characterization of a silent azaphilone gene cluster from *Aspergillus niger* ATCC 1015 reveals a hydroxylation-mediated pyran-ring formation. *Chemistry and Biology* **2012**, 19 (8), 1049-1059.
124. Wang, M., Beissner, M., Zhao, H., Aryl-aldehyde formation in fungal polyketides: discovery and characterization of a distinct biosynthetic mechanism. *Chemistry and Biology* **2014**, 21 (2), 257-263.
125. Lazarus, C. M., Williams, K., Bailey, A. M., Reconstructing fungal natural product biosynthetic pathways. *Natural Product Reports* **2014**, 31 (10), 1339-1347.
126. Ishiuchi, K. i., Nakazawa, T., Ookuma, T., Sugimoto, S., Sato, M., Tsunematsu, Y., Ishikawa, N., Noguchi, H., Hotta, K., Moriya, H., Watanabe, K., Establishing a new methodology for genome mining and biosynthesis of polyketides and peptides through yeast molecular genetics. *ChemBioChem* **2012**, 13 (6), 846-854.
127. Wattanachaisaereekul, S., Lantz, A. E., Nielsen, M. L., Andrésón, Ó. S., Nielsen, J., Optimization of heterologous production of the polyketide 6-MSA in *Saccharomyces cerevisiae*. *Biotechnology and Bioengineering* **2007**, 97 (4), 893-900.
128. Rugbjerg, P., Naesby, M., Mortensen, U. H., Frandsen, R. J. N., Reconstruction of the biosynthetic pathway for the core fungal polyketide scaffold rubrofusarin in *Saccharomyces cerevisiae*. *Microbial Cell Factories* **2013**, 12 (1), 31.
129. Hashimoto, M., Wakana, D., Ueda, M., Kobayashi, D., Goda, Y., Fujii, I., Product identification of non-reducing polyketide synthases with C-terminus methyltransferase domain from *Talaromyces stipitatus* using *Aspergillus oryzae* heterologous expression. *Bioorganic and Medicinal Chemistry Letters* **2015**, 25 (7), 1381-1384.
130. Liu, T., Chiang, Y.-M., Somoza, A. D., Oakley, B. R., Wang, C. C. C., Engineering of an "unnatural" natural product by swapping polyketide synthase domains in *Aspergillus nidulans*. *Journal of the American Chemical Society* **2011**, 133 (34), 13314-13316.

## REFERENCES

---

131. Frisvad, J. C., Møller, L. L. H., Larsen, T. O., Kumar, R., Arnau, J., Safety of the fungal workhorses of industrial biotechnology: update on the mycotoxin and secondary metabolite potential of *Aspergillus niger*, *Aspergillus oryzae*, and *Trichoderma reesei*. *Applied Microbiology and Biotechnology* **2018**, 102 (22), 9481-9515.
132. Chiang, Y.-M., Ahuja, M., Oakley, C. E., Entwistle, R., Asokan, A., Zutz, C., Wang, C. C. C., Oakley, B. R., Development of genetic dereplication strains in *Aspergillus nidulans* results in the discovery of aspercryptin. *Angewandte Chemie International Edition* **2016**, 55 (5), 1662-1665.
133. A. K. Pahirulzaman, K., Williams, K., Lazarus, C. M., *Methods in enzymology, chapter twelve - a toolkit for heterologous expression of metabolic pathways in Aspergillus oryzae*. Academic Press, **2012**.
134. Matsuda, Y., Abe, I., Biosynthesis of fungal meroterpenoids. *Natural Product Reports* **2016**, 33 (1), 26-53.
135. Dao, T. T., de Mattos-Shipley, K. M. J., Prosser, I. M., Williams, K., Zacharova, M. K., Lazarus, C. M., Willis, C. L., Bailey, A. M., Cleaning the cellular factory-deletion of McrA in *Aspergillus oryzae* NSAR1 and the generation of a novel kojic acid deficient strain for cleaner heterologous production of secondary metabolites. *Frontiers in Fungal Biology* **2021**, 2, 632542.
136. Clevenger, K. D., Bok, J. W., Ye, R., Miley, G. P., Verdan, M. H., Velk, T., Chen, C., Yang, K., Robey, M. T., Gao, P., Lamprecht, M., Thomas, P. M., Islam, M. N., Palmer, J. M., Wu, C. C., Keller, N. P., Kelleher, N. L., A scalable platform to identify fungal secondary metabolites and their gene clusters. *Nature Chemical Biology* **2017**, 13 (8), 895-901.
137. Andersson, R., Sandelin, A., Determinants of enhancer and promoter activities of regulatory elements. *Nature Reviews Genetics* **2020**, 21 (2), 71-87.
138. Fleißner, A., Dersch, P., Expression and export: recombinant protein production systems for *Aspergillus*. *Applied Microbiology and Biotechnology* **2010**, 87 (4), 1255-1270.
139. Meyer, V., Wanka, F., Gent, J. v., Arentshorst, M., Hondel, C. A. M. J. J. v. d., Ram, A. F. J., Fungal gene expression on demand: an inducible, tunable, and metabolism-independent expression system for *Aspergillus niger*. *Applied and Environmental Microbiology* **2011**, 77 (9), 2975-2983.
140. Miyanaga, A., Structure and function of polyketide biosynthetic enzymes: various strategies for production of structurally diverse polyketides. *Bioscience, Biotechnology, and Biochemistry* **2017**, 81 (12), 2227-2236.
141. Moore, B. S., Hertweck, C., Biosynthesis and attachment of novel bacterial polyketide synthase starter units. *Natural Product Reports* **2002**, 19 (1), 70-99.
142. Chan, Y. A., Podevels, A. M., Kevany, B. M., Thomas, M. G., Biosynthesis of polyketide synthase extender units. *Natural Product Reports* **2009**, 26 (1), 90-114.
143. Schor, R., Cox, R., Classic fungal natural products in the genomic age: the molecular legacy of Harold Raistrick. *Natural Product Reports* **2018**, 35 (3), 230-256.
144. Zheng, L., Yang, Y., Wang, H., Fan, A., Zhang, L., Li, S. M., Ustethylin biosynthesis implies phenethyl derivative formation in *Aspergillus ustus*. *Organic Letters* **2020**, 22 (20), 7837-7841.
145. Shen, B., Polyketide biosynthesis beyond the type I, II and III polyketide synthase paradigms. *Current Opinion in Chemical Biology* **2003**, 7 (2), 285-295.
146. Chooi, Y.-H., Tang, Y., Navigating the fungal polyketide chemical space: from genes to molecules. *The Journal of Organic Chemistry* **2012**, 77 (22), 9933-9953.
147. Staunton, J., Wilkinson, B., Combinatorial biosynthesis of polyketides and nonribosomal peptides. *Current Opinion in Chemical Biology* **2001**, 5 (2), 159-164.
148. Sundaram, S., Hertweck, C., On-line enzymatic tailoring of polyketides and peptides in thiotemplate systems. *Current Opinion in Chemical Biology* **2016**, 31, 82-94.



## REFERENCES

---

149. Cox, R. J., Simpson, T. J., *Methods in enzymology, chapter 3 fungal type I polyketide synthases*. Academic Press, **2009**.
150. Du, L., Lou, L., PKS and NRPS release mechanisms. *Natural Product Reports* **2010**, 27 (2), 255-278.
151. Herbst, D. A., Townsend, C. A., Maier, T., The architectures of iterative type I PKS and FAS. *Natural Product Reports* **2018**, 35 (10), 1046-1069.
152. Hertweck, C., Luzhetskyy, A., Rebets, Y., Bechthold, A., Type II polyketide synthases: gaining a deeper insight into enzymatic teamwork. *Natural Product Reports* **2007**, 24 (1), 162-190.
153. Austin, M. B., Noel, J. P., The chalcone synthase superfamily of type III polyketide synthases. *Natural Product Reports* **2003**, 20 (1), 79-110.
154. Keatinge-Clay, A. T., The structures of type I polyketide synthases. *Natural Product Reports* **2012**, 29 (10), 1050-1073.
155. Fischbach, M. A., Walsh, C. T., Assembly-line enzymology for polyketide and nonribosomal peptide antibiotics: logic, machinery, and mechanisms. *Chemical Reviews* **2006**, 106 (8), 3468-3496.
156. Rawlings, B. J., Type I polyketide biosynthesis in bacteria (part A-erythromycin biosynthesis). *Natural Product Reports* **2001**, 18 (2), 190-227.
157. Keatinge-Clay, A. T., The uncommon enzymology of *cis*-acyltransferase assembly lines. *Chemical Reviews* **2017**, 117 (8), 5334-5366.
158. Helfrich, E. J. N., Piel, J., Biosynthesis of polyketides by *trans*-AT polyketide synthases. *Natural Product Reports* **2016**, 33 (2), 231-316.
159. Cox, R. J., Polyketides, proteins and genes in fungi: programmed nano-machines begin to reveal their secrets. *Organic and Biomolecular Chemistry* **2007**, 5 (13), 2010-2026.
160. Zhou, H., Li, Y., Tang, Y., Cyclization of aromatic polyketides from bacteria and fungi. *Natural Product Reports* **2010**, 27 (6), 839-868.
161. Keller, N. P., Fungal secondary metabolism: regulation, function and drug discovery. *Nature Reviews Microbiology* **2019**, 17 (3), 167-180.
162. Minto, R. E., Townsend, C. A., Enzymology and molecular biology of aflatoxin biosynthesis. *Chemical Reviews* **1997**, 97 (7), 2537-2556.
163. Sanchez, J. F., Chiang, Y.-M., Szewczyk, E., Davidson, A. D., Ahuja, M., Elizabeth Oakley, C., Woo Bok, J., Keller, N., Oakley, B. R., Wang, C. C. C., Molecular genetic analysis of the orsellinic acid/F9775 gene cluster of *Aspergillus nidulans*. *Molecular BioSystems* **2010**, 6 (3), 587-593.
164. Bailey, A. M., Cox, R. J., Harley, K., Lazarus, C. M., Simpson, T. J., Skellam, E., Characterisation of 3-methylorcinolaldehyde synthase (MOS) in *Acremonium strictum*: first observation of a reductive release mechanism during polyketide biosynthesis. *Chemical Communications* **2007**, 39, 4053-4055.
165. Cox, R. J., Skellam, E., Williams, K., Biosynthesis of fungal polyketides. *Physiology and Genetics* **2018**, 15, 385-412.
166. Campbell, C. D., Vederas, J. C., Biosynthesis of lovastatin and related metabolites formed by fungal iterative PKS enzymes. *Biopolymers* **2010**, 93 (9), 755-763.
167. Xie, X., Watanabe, K., Wojcicki, W. A., Wang, C. C. C., Tang, Y., Biosynthesis of lovastatin analogs with a broadly specific acyltransferase. *Chemistry and Biology* **2006**, 13 (11), 1161-1169.
168. Sun, H., Ho, C. L., Ding, F., Soehano, I., Liu, X.-W., Liang, Z.-X., Synthesis of (*R*)-mellein by a partially reducing iterative polyketide synthase. *Journal of the American Chemical Society* **2012**, 134 (29), 11924-11927.
169. Wang, J., Zhang, R., Chen, X., Sun, X., Yan, Y., Shen, X., Yuan, Q., Biosynthesis of aromatic polyketides in microorganisms using type II polyketide synthases. *Microbial Cell Factories* **2020**, 19 (1), 110.

## REFERENCES

---

170. Kim, J., Yi, G. S., PKMiner: a database for exploring type II polyketide synthases. *BMC Microbiol* **2012**, 12 (1), 169.
171. Rix, U., Fischer, C., Remsing, L. L., Rohr, J., Modification of post-PKS tailoring steps through combinatorial biosynthesis. *Natural Product Reports* **2002**, 19 (5), 542-580.
172. Hutchinson, C. R., Biosynthetic studies of daunorubicin and tetracenomycin C. *Chemical Reviews* **1997**, 97 (7), 2525-2536.
173. Funo, N., Ohnishi, Y., Fujii, I., Shibuya, M., Ebizuka, Y., Horinouchi, S., A new pathway for polyketide synthesis in microorganisms. *Nature* **1999**, 400 (6747), 897-899.
174. Hashimoto, M., Nonaka, T., Fujii, I., Fungal type III polyketide synthases. *Natural Product Reports* **2014**, 31 (10), 1306-1317.
175. Flores-Sanchez, I. J., Verpoorte, R., Plant polyketide synthases: a fascinating group of enzymes. *Plant Physiology and Biochemistry* **2009**, 47 (3), 167-174.
176. Hertweck, C., The biosynthetic logic of polyketide diversity. *Angewandte Chemie International Edition* **2009**, 48 (26), 4688-4716.
177. Lim, Y. P., Go, M. K., Yew, W. S., Exploiting the biosynthetic potential of type III polyketide synthases. *Molecules* **2016**, 21 (6), 806.
178. Olano, C., Méndez, C., Salas, J. A., Post-PKS tailoring steps in natural product-producing actinomycetes from the perspective of combinatorial biosynthesis. *Natural Product Reports* **2010**, 27 (4), 571-616.
179. Sattely, E. S., Fischbach, M. A., Walsh, C. T., Total biosynthesis: *in vitro* reconstitution of polyketide and nonribosomal peptide pathways. *Natural Product Reports* **2008**, 25 (4), 757-793.
180. Walsh, C. T., The chemical versatility of natural product assembly lines. *Accounts of Chemical Research* **2008**, 41 (1), 4-10.
181. Alhassan, A. M., Abdullahi, M. I., Uba, A., Umar, A., Prenylation of aromatic secondary metabolites: a new frontier for development of novel drugs. *Tropical Journal of Pharmaceutical Research* **2014**, 13 (2), 307-314.
182. Heide, L., Prenyl transfer to aromatic substrates: genetics and enzymology. *Current Opinion in Chemical Biology* **2009**, 13 (2), 171-179.
183. Winkelblech, J., Fan, A., Li, S.-M., Prenyltransferases as key enzymes in primary and secondary metabolism. *Applied Microbiology and Biotechnology* **2015**, 99 (18), 7379-7397.
184. Mori, T., Enzymatic studies on aromatic prenyltransferases. *Journal of Natural Medicines* **2020**, 74 (3), 501-512.
185. Li, S.-M., Prenylated indole derivatives from fungi: structure diversity, biological activities, biosynthesis and chemoenzymatic synthesis. *Natural Product Reports* **2010**, 27 (1), 57-78.
186. Fan, A., Winkelblech, J., Li, S.-M., Impacts and perspectives of prenyltransferases of the DMATS superfamily for use in biotechnology. *Applied Microbiology and Biotechnology* **2015**, 99 (18), 7399-7415.
187. Liao, G., Mai, P., Fan, J., Zocher, G., Stehle, T., Li, S.-M., Complete decoration of the indolyl residue in *cyclo*-L-Trp-L-Trp with geranyl moieties by using engineered dimethylallyl transferases. *Organic Letters* **2018**, 20 (22), 7201-7205.
188. Metzger, U., Schall, C., Zocher, G., Unsöld, I., Stec, E., Li, S.-M., Heide, L., Stehle, T., The structure of dimethylallyl tryptophan synthase reveals a common architecture of aromatic prenyltransferases in fungi and bacteria. *Proceedings of the National Academy of Sciences* **2009**, 106 (34), 14309-14314.
189. Rittle, J., Green, M. T., Cytochrome P450 compound I: capture, characterization, and C-H bond activation kinetics. *Science* **2010**, 330 (6006), 933-937.

## REFERENCES

---

190. Guengerich, F. P., Mechanisms of cytochrome P450-catalyzed oxidations. *ACS Catalysis* **2018**, *8* (12), 10964-10976.
191. Bakkes, P. J., Riehm, J. L., Sagadin, T., Rühlmann, A., Schubert, P., Biemann, S., Girhard, M., Hutter, M. C., Bernhardt, R., Urlacher, V. B., Engineering of versatile redox partner fusions that support monooxygenase activity of functionally diverse cytochrome P450s. *Scientific Reports* **2017**, *7* (1), 9570.
192. Zhang, X., Li, S., Expansion of chemical space for natural products by uncommon P450 reactions. *Natural Product Reports* **2017**, *34* (9), 1061-1089.
193. van den Brink, H. M., van Gorcom, R. F. M., van den Hondel, C. A. M. J. J., Punt, P. J., Cytochrome P450 enzyme systems in fungi. *Fungal Genetics and Biology* **1998**, *23* (1), 1-17.
194. Durairaj, P., Hur, J.-S., Yun, H., Versatile biocatalysis of fungal cytochrome P450 monooxygenases. *Microbial Cell Factories* **2016**, *15* (1), 125.
195. Pratiwi, R. A., Yahya, N. S. W., Chi, Y., Bio function of cytochrome P450 on fungus: a review. *IOP Conference Series: Earth and Environmental Science* **2022**, *959* (1), 012023.
196. Zhang, Z.-X., Li, Z.-H., Yin, W.-B., Li, S.-M., Biosynthesis of viridicatol in *Penicillium palitans* implies a cytochrome P450-mediated *meta* hydroxylation at a monoalkylated benzene ring. *Organic Letters* **2022**, *24* (1), 262-267.
197. Mazzaferro, L. S., Hüttel, W., Fries, A., Müller, M., Cytochrome P450-catalyzed regio- and stereoselective phenol coupling of fungal natural products. *Journal of the American Chemical Society* **2015**, *137* (38), 12289-12295.
198. Wallner, S., Dully, C., Daniel, B., Macheroux, P., *Handbook of flavoproteins, Berberine bridge enzyme and the family of bicovalent flavoenzymes*. De Gruyter, **2012**.
199. Leferink, N. G. H., Heuts, D. P. H. M., Fraaije, M. W., van Berkel, W. J. H., The growing VAO flavoprotein family. *Archives of Biochemistry and Biophysics* **2008**, *474* (2), 292-301.
200. Daniel, B., Wallner, S., Steiner, B., Oberdorfer, G., Kumar, P., van der Graaff, E., Roitsch, T., Sensen, C. W., Gruber, K., Macheroux, P., Structure of a berberine bridge enzyme-like enzyme with an active site specific to the plant family Brassicaceae. *PLOS ONE* **2016**, *11* (6), e0156892.
201. Daniel, B., Konrad, B., Toplak, M., Lahham, M., Messenlehner, J., Winkler, A., Macheroux, P., The family of berberine bridge enzyme-like enzymes: a treasure-trove of oxidative reactions. *Archives of Biochemistry and Biophysics* **2017**, *632*, 88-103.
202. Finn, R. D., Coghill, P., Eberhardt, R. Y., Eddy, S. R., Mistry, J., Mitchell, A. L., Potter, S. C., Punta, M., Qureshi, M., Sangrador-Vegas, A., Salazar, G. A., Tate, J., Bateman, A., The Pfam protein families database: towards a more sustainable future. *Nucleic Acids Research* **2015**, *44* (D1), D279-D285.
203. Facchini, P. J., Penzes, C., Johnson, A. G., Bull, D., Molecular characterization of berberine bridge enzyme genes from opium poppy. *Plant Physiology* **1996**, *112* (4), 1669-1677.
204. Daniel, B., Pavkov-Keller, T., Steiner, B., Dordic, A., Gutmann, A., Nidetzky, B., Sensen, C. W., van der Graaff, E., Wallner, S., Gruber, K., Macheroux, P., Oxidation of monolignols by members of the berberine bridge enzyme family suggests a role in plant cell wall metabolism. *Journal of Biological Chemistry* **2015**, *290* (30), 18770-18781.
205. Liu, Y.-C., Li, Y.-S., Lyu, S.-Y., Hsu, L.-J., Chen, Y.-H., Huang, Y.-T., Chan, H.-C., Huang, C.-J., Chen, G.-H., Chou, C.-C., Tsai, M.-D., Li, T.-L., Interception of teicoplanin oxidation intermediates yields new antimicrobial scaffolds. *Nature Chemical Biology* **2011**, *7* (5), 304-309.
206. Nielsen, C. A. F., Folly, C., Hatsch, A., Molt, A., Schröder, H., O'Connor, S. E., Naesby, M., The important ergot alkaloid intermediate chanoclavine-I produced in the yeast *Saccharomyces cerevisiae* by the combined action of EasC and EasE from *Aspergillus japonicus*. *Microbial Cell Factories* **2014**, *13* (1), 95.

## REFERENCES

207. Lin, H.-C., Chiou, G., Chooi, Y.-H., McMahon, T. C., Xu, W., Garg, N. K., Tang, Y., Elucidation of the concise biosynthetic pathway of the communesin indole alkaloids. *Angewandte Chemie International Edition* **2015**, *54* (10), 3004-3007.
208. Liu, S. H., Wei, Y. Y., Xing, Y. N., Chen, Y., Wang, W., Wang, K. B., Liang, Y., Jiao, R. H., Zhang, B., Ge, H. M., A BBE-like oxidase, AsmF, dictates the formation of naphthalenic hydroxyl groups in ansaseomycin biosynthesis. *Organic Letters* **2021**, *23* (9), 3724-3728.
209. Zhang, J.-M., Liu, X., Wei, Q., Ma, C., Li, D., Zou, Y., Berberine bridge enzyme-like oxidase-catalysed double bond isomerization acts as the pathway switch in cytochalasin synthesis. *Nature Communications* **2022**, *13* (1), 225.
210. Persson, B., Kallberg, Y., Classification and nomenclature of the superfamily of short-chain dehydrogenases/reductases (SDRs). *Chemico-Biological Interactions* **2013**, *202* (1), 111-115.
211. Moummou, H., Kallberg, Y., Tonfack, L. B., Persson, B., van der Rest, B., The plant short-chain dehydrogenase (SDR) superfamily: genome-wide inventory and diversification patterns. *BMC Plant Biology* **2012**, *12* (1), 219.
212. Kallberg, Y., Oppermann, U., Jörnvall, H., Persson, B., Short-chain dehydrogenases/reductases (SDRs). *European Journal of Biochemistry* **2002**, *269* (18), 4409-4417.
213. Filling, C., Berndt, K. D., Benach, J., Knapp, S., Prozorovski, T., Nordling, E., Ladenstein, R., Jörnvall, H., Oppermann, U., Critical residues for structure and catalysis in short-chain dehydrogenases/reductases. *Journal of Biological Chemistry* **2002**, *277* (28), 25677-25684.
214. Kavanagh, K., Jörnvall, H., Persson, B., Oppermann, U., The SDR superfamily: functional and structural diversity within a family of metabolic and regulatory enzymes. *Cellular and Molecular Life Sciences* **2008**, *65* (24), 3895-3906.
215. Liu, C., Liu, K., Zhao, C., Gong, P., Yu, Y., The characterization of a short chain dehydrogenase/reductase (SDRx) in *Comamonas testosteroni*. *Toxicology Reports* **2020**, *7*, 460-467.
216. Mo, X., Zhang, H., Du, F., Yang, S., Short-chain dehydrogenase NcmD is responsible for the C-10 oxidation of nocamycin F in nocamycin biosynthesis. *Frontiers in Microbiology* **2020**, *11*, 610827.
217. Sonawane, P. D., Heinig, U., Panda, S., Gilboa, N. S., Yona, M., Kumar, S. P., Alkan, N., Unger, T., Bocobza, S., Pliner, M., Malitsky, S., Tkachev, M., Meir, S., Rogachev, I., Aharoni, A., Short-chain dehydrogenase/reductase governs steroidal specialized metabolites structural diversity and toxicity in the genus *Solanum*. *Proceedings of the National Academy of Sciences* **2018**, *115* (23), E5419-E5428.
218. Ahmed Laskar, A., Younus, H., Aldehyde toxicity and metabolism: the role of aldehyde dehydrogenases in detoxification, drug resistance and carcinogenesis. *Drug Metabolism Reviews* **2019**, *51* (1), 42-64.
219. Newman, D. J., Natural product based antibody drug conjugates: clinical status as of November 9, 2020. *Journal of Natural Products* **2021**, *84* (3), 917-931.
220. Brakhage, A. A., Spröte, P., Al-Abdallah, Q., Gehrke, A., Plattner, H., Tüncher, A., *Regulation of penicillin biosynthesis in filamentous fungi*. Springer Press, **2004**.
221. Fan, J., Liao, G., Ludwig-Radtke, L., Yin, W.-B., Li, S.-M., Formation of terrestric acid in *Penicillium crustosum* requires redox-assisted decarboxylation and stereoisomerization. *Organic Letters* **2020**, *22* (1), 88-92.
222. Wei, Q., Bai, J., Yan, D., Bao, X., Li, W., Liu, B., Zhang, D., Qi, X., Yu, D., Hu, Y., Genome mining combined metabolic shunting and OSMAC strategy of an endophytic fungus leads to the production of diverse natural products. *Acta Pharmaceutica Sinica B* **2021**, *11* (2), 572-587.
223. Laursen, J. B., Nielsen, J., Phenazine natural products: biosynthesis, synthetic analogues, and biological activity. *Chemical Reviews* **2004**, *104* (3), 1663-1686.

## REFERENCES

224. Gaucher, G. M., Shepherd, M. G., Isolation of orsellinic acid synthase. *Biochemical and Biophysical Research Communications* **1968**, 32 (4), 664-671.
225. Nies, J., Ran, H., Wohlgemuth, V., Yin, W.-B., Li, S.-M., Biosynthesis of the prenylated salicylaldehyde flavoglaucon requires temporary reduction to salicyl alcohol for decoration before reoxidation to the final product. *Organic Letters* **2020**, 22 (6), 2256-2260.
226. Barka, E. A., Vatsa, P., Sanchez, L., Gaveau-Vaillant, N., Jacquard, C., Klenk, H.-P., Clément, C., Ouhdouch, Y., Wezel, G. P. v., Taxonomy, physiology, and natural products of actinobacteria. *Microbiology and Molecular Biology Reviews* **2016**, 80 (1), 1-43.
227. O'Brien, M., Nielsen, K. F., O'Kiely, P., Forristal, P. D., Fuller, H. T., Frisvad, J. C., Mycotoxins and other secondary metabolites produced *in vitro* by *Penicillium paneum* Frisvad and *Penicillium roqueforti* Thom isolated from baled grass silage in Ireland. *Journal of Agricultural and Food Chemistry* **2006**, 54 (24), 9268-9276.
228. Nielsen, K. F., Mogensen, J. M., Johansen, M., Larsen, T. O., Frisvad, J. C., Review of secondary metabolites and mycotoxins from the *Aspergillus niger* group. *Analytical and Bioanalytical Chemistry* **2009**, 395 (5), 1225-1242.
229. Sanchez, J. F., Somoza, A. D., Keller, N. P., Wang, C. C. C., Advances in *Aspergillus* secondary metabolite research in the post-genomic era. *Natural Product Reports* **2012**, 29 (3), 351-371.
230. Chen, H., Du, L., Iterative polyketide biosynthesis by modular polyketide synthases in bacteria. *Applied Microbiology and Biotechnology* **2016**, 100 (2), 541-557.
231. Chiang, Y.-M., Oakley, B. R., Keller, N. P., Wang, C. C. C., Unraveling polyketide synthesis in members of the genus *Aspergillus*. *Applied Microbiology and Biotechnology* **2010**, 86 (6), 1719-1736.
232. Yin, W.-B., Chooi, Y. H., Smith, A. R., Cacho, R. A., Hu, Y., White, T. C., Tang, Y., Discovery of cryptic polyketide metabolites from dermatophytes using heterologous expression in *Aspergillus nidulans*. *ACS Synthetic Biology* **2013**, 2 (11), 629-634.
233. Zaehle, C., Gressler, M., Shelest, E., Geib, E., Hertweck, C., Brock, M., Terrein biosynthesis in *Aspergillus terreus* and its impact on phytotoxicity. *Chemistry and Biology* **2014**, 21 (6), 719-731.
234. Wu, C., Zhu, H., van Wezel, G. P., Choi, Y. H., Metabolomics-guided analysis of isocoumarin production by *Streptomyces* species MBT76 and biotransformation of flavonoids and phenylpropanoids. *Metabolomics* **2016**, 12 (5), 90.
235. Nomoto, S., Mori, K., Synthesis of acetophthalidin, a fungal metabolite which inhibits the progression of the mammalian cell cycle. *Liebigs Annalen* **1997**, 1997 (4), 721-723.
236. Kumagai, H., Amemiya, M., Naganawa, H., Sawa, T., Ishizuka, M., Takeuchi, T., Biosynthesis of antitumor antibiotic, cytogenin. *The Journal of Antibiotics* **1994**, 47 (4), 440-446.
237. Chen, G.-D., Hu, D., Huang, M.-J., Tang, J., Wang, X.-X., Zou, J., Xie, J., Zhang, W.-G., Guo, L.-D., Yao, X.-S., Abe, I., Gao, H., Sporormielones A–E, bioactive novel C–C coupled orsellinic acid derivative dimers, and their biosynthetic origin. *Chemical Communications* **2020**, 56 (33), 4607-4610.
238. Schroeckh, V., Scherlach, K., Nützmann, H.-W., Shelest, E., Schmidt-Heck, W., Schuemann, J., Martin, K., Hertweck, C., Brakhage, A. A., Intimate bacterial–fungal interaction triggers biosynthesis of archetypal polyketides in *Aspergillus nidulans*. *Proceedings of the National Academy of Sciences* **2009**, 106 (34), 14558-14563.
239. Calcul, L., Chow, R., Oliver, A. G., Tenney, K., White, K. N., Wood, A. W., Fiorilla, C., Crews, P., NMR strategy for unraveling structures of bioactive sponge-derived oxy-polyhalogenated diphenyl ethers. *Journal of Natural Products* **2009**, 72 (3), 443-449.
240. Bashyal, B. P., Wijeratne, E. M. K., Faeth, S. H., Gunatilaka, A. A. L., Globosumones A–C, cytotoxic orsellinic acid esters from the Sonoran desert endophytic fungus *Chaetomium globosum*. *Journal of Natural Products* **2005**, 68 (5), 724-728.

## REFERENCES

---

241. Lünne, F., Niehaus, E.-M., Lipinski, S., Kunigkeit, J., Kalinina, S. A., Humpf, H.-U., Identification of the polyketide synthase PKS7 responsible for the production of lecanoric acid and ethyl lecanorate in *Claviceps purpurea*. *Fungal Genetics and Biology* **2020**, *145*, 103481.
242. Feng, C., Wei, Q., Hu, C., Zou, Y., Biosynthesis of diphenyl ethers in fungi. *Organic Letters* **2019**, *21* (9), 3114-3118.
243. Zheng, L., Li, S.-M., Benzoyl ester formation in *Aspergillus ustus* by hijacking the polyketide acyl intermediates with alcohols. *Archives of Microbiology* **2021**, *203* (4), 1795-1800.
244. Little, R. F., Hertweck, C., Chain release mechanisms in polyketide and non-ribosomal peptide biosynthesis. *Natural Product Reports* **2022**, *39* (1), 163-205.
245. Kahlert, L., Villanueva, M., Cox, R. J., Skellam, E. J., Biosynthesis of 6-hydroxymellein requires a collaborating polyketide synthase-like enzyme. *Angewandte Chemie International Edition* **2021**, *60* (20), 11423-11429.
246. Braesel, J., Fricke, J., Schwenk, D., Hoffmeister, D., Biochemical and genetic basis of orsellinic acid biosynthesis and prenylation in a stercaceous basidiomycete. *Fungal Genetics and Biology* **2017**, *98*, 12-19.
247. Kumar, V., Ashok, S., Park, S., Recent advances in biological production of 3-hydroxypropionic acid. *Biotechnology Advances* **2013**, *31* (6), 945-961.
248. Chen, Y., Nielsen, J., Biobased organic acids production by metabolically engineered microorganisms. *Current Opinion in Biotechnology* **2016**, *37*, 165-172.
249. Skellam, E., Biosynthesis of fungal polyketides by collaborating and *trans*-acting enzymes. *Natural Product Reports* **2022**, *39* (4), 754-783.
250. Kennedy, J., Auclair, K., Kendrew, S. G., Park, C., Vederas, J. C., Richard Hutchinson, C., Modulation of polyketide synthase activity by accessory proteins during lovastatin biosynthesis. *Science* **1999**, *284* (5418), 1368-1372.
251. Atanasov, A. G., Zotchev, S. B., Dirsch, V. M., the International Natural Product Sciences Taskforce, Supuran, C. T., Natural products in drug discovery: advances and opportunities. *Nature Reviews Drug Discovery* **2021**, *20* (3), 200-216.
252. Jacob, S., Grötsch, T., Foster, A. J., Schöffler, A., Rieger, P. H., Sandjo, L. P., Liermann, J. C., Opatz, T., Thines, E., Unravelling the biosynthesis of pyriculol in the rice blast fungus *Magnaporthe oryzae*. *Microbiology* **2017**, *163* (4), 541-553.
253. Zhao, Z., Ying, Y., Hung, Y.-S., Tang, Y., Genome mining reveals *Neurospora crassa* can produce the salicylaldehyde sordarial. *Journal of Natural Products* **2019**, *82* (4), 1029-1033.
254. Liu, L., Tang, M.-C., Tang, Y., Fungal highly reducing polyketide synthases biosynthesize salicylaldehydes that are precursors to epoxycyclohexenol natural products. *Journal of the American Chemical Society* **2019**, *141* (50), 19538-19541.
255. Boysen, M. E., Jacobsson, K.-G., Schnürer, J., Molecular identification of species from the *Penicillium roqueforti* group associated with spoiled animal feed. *Applied and Environmental Microbiology* **2000**, *66* (4), 1523-1526.
256. Fernández-Bodega, Á., Álvarez-Álvarez, R., Liras, P., Martín, J. F., Silencing of a second dimethylallyltryptophan synthase of *Penicillium roqueforti* reveals a novel clavine alkaloid gene cluster. *Applied Microbiology and Biotechnology* **2017**, *101* (15), 6111-6121.
257. Blin, K., Shaw, S., Kloosterman, A. M., Charlop-Powers, Z., van Wezel, G. P., Medema, Marnix H., Weber, T., antiSMASH 6.0: improving cluster detection and comparison capabilities. *Nucleic Acids Research* **2021**, *49* (W1), W29-W35.
258. Xiang, P., Ludwig-Radtke, L., Yin, W.-B., Li, S.-M., Isocoumarin formation by heterologous gene expression and modification by host enzymes. *Organic and Biomolecular Chemistry* **2020**, *18* (26), 4946-4948.

## REFERENCES

---

259. Winkler, A., Motz, K., Riedl, S., Puhl, M., Macheroux, P., Gruber, K., Structural and mechanistic studies reveal the functional role of bicovalent flavinylation in berberine bridge enzyme. *Journal of Biological Chemistry* **2009**, 284 (30), 19993-20001.
260. Toplak, M., Wiedemann, G., Ulićević, J., Daniel, B., Hoernstein, S. N. W., Kothe, J., Niederhauser, J., Reski, R., Winkler, A., Macheroux, P., The single berberine bridge enzyme homolog of *Physcomitrella patens* is a cellobiose oxidase. *The FEBS Journal* **2018**, 285 (10), 1923-1943.
261. Ran, H., Li, S.-M., Fungal benzene carbaldehydes: occurrence, structural diversity, activities and biosynthesis. *Natural Product Reports* **2021**, 38 (1), 240-263.





## **Statutory Declaration**

Ich, Pan Xiang, versichere, dass ich meine Dissertation

„Investigation on the biosynthesis of polyketides in two *Penicillium* strains“

selbständig ohne unerlaubte Hilfe angefertigt und mich dabei keiner anderen als der von mir ausdrücklich bezeichneten Quellen bedient habe. Alle vollständig oder sinngemäß übernommenen Zitate sind als solche gekennzeichnet.

Die Dissertation wurde in der jetzigen oder einer ähnlichen Form noch bei keiner anderen Hochschule eingereicht und hat noch keinen sonstigen Prüfungszwecken gedient.

Marburg, den.....

.....  
Pan Xiang



### **Acknowledgements**

I would like to take this opportunity to express my thanks to the people who guided and supported me during my PhD study.

Firstly, I would like to give my sincere appreciations to my advisor Prof. Dr. Shu-Ming Li for giving me the chance to study as a PhD student in his research group. I'm very grateful for his excellent supervision and guidance on my biological and chemical research. It is of great value for his scientific advices on the projects, his meticulous on the manuscripts, and his assistance in my daily life. All I have learned and trained during the past five years will benefit me greatly in my future life.

I am very grateful to Prof. Dr. Michael Keusgen for his agreement to be my second supervisor and examiner. I sincerely thank Bastian Kemmerich for his work and his help in the cooperation of the third project. Many thanks to Lena Ludwig-Radtke and Rixa Kraut for measuring LCMS samples, Dr. Stefan Newel for taking NMR spectra. I also really appreciate the efforts made by Sina Stierle for translating the summary part and together with Jenny Zhou for proof reading the dissertation.

Special thanks must go to Dr. Ge Liao and Dr. Jing Liu who accompanied me and gave me generous help during my life in Germany. I also want to thank Dr. Florian Kindinger, Dr. Jonas Nies and Dr. Jie Fan for their help and useful suggestions at the beginning of my first project. Also great thanks to Dr. Huili Yu, Dr. Jinglin Wang, Yiling Yang, Yu Dai, Jenny Zhou, Sina Stierle, Lauritz Harken, Dr. Lindsay Coby, Johanna Schäfer for the wonderful time we have spent together.

I also want to express my sincere gratitude to all my current and former colleagues, Wen Li, Dr. Liujuan Zheng, Haowen Wang, Zhanghai Li, Xuping Zhang, Jing Zhou, Wei Li, Marlies Peter, Daniel Jonathan Janzen, Daniel Ostendorff, Andreas Martin, David Breyer, Hendrik Sostmann, Philipp Mann, Dr. Elisabeth Hühner, Linus Naumann, Lena Mikulski, Kristin Öqvist, Sonja Hiemenz and Dr. Dieter Kreusch.

I wish to thank the constant encouragement from my friends outside of the laboratory.

I would like to acknowledge the China Scholarship Council (CSC) for financial supports.

Finally, I must extend my heartfelt thanks to my parents for their unconditional love and supports as always.



## Curriculum Vitae

### Personal Information

---

**Name:** Pan Xiang

**Date of Birth:** 24.09.1992

**Place of Birth:** Taoyuan, Hunan Province, P. R. China

**Nationality:** Chinese

**Address:** Robert-Koch-Str. 4, 35032, Marburg

**Email:** pan.xiang@pharmazie.uni-marburg.de

### Education & Research

---

**PhD candidate:** 10.2017 – now

Philipps-University Marburg, Germany

Institute for Pharmaceutical Biology and Biotechnology

Thesis title: "Investigation on the biosynthesis of polyketides in two *Penicillium* strains"

Supervisor: Prof. Dr. Shu-Ming Li

**Master of Medical:** 09.2014 – 06.2017

Dali University, China

College of Pharmacy

Thesis title: "Isolation, identification and bioactivities of 2-(2-phenylethyl) chromone polymer derivatives mediated by UPLC-MS in artificial holing agarwood"

Supervisor: Prof. Dr. Haofu Dai

**Bachelor of Science:** 09.2010 – 06.2014

Hunan University of Chinese Medicine, China

School of Pharmacy

Thesis title: "Study on preparation and *in vitro* dissolution of liensinine solid dispersion"

Supervisor: Prof. Dr. Hui Gui

**High School:** 09.2007 – 06.2010

The Ninth Middle School of Taoyuan, China